



**National Library  
of Canada**

**Bibliothèque nationale  
du Canada**

**Canadian Theses Service**

**Service des thèses canadiennes**

**Ottawa, Canada  
K1A 0N4**

## **NOTICE**

The quality of this microform is heavily dependent upon the quality of the original thesis submitted for microfilming. Every effort has been made to ensure the highest quality of reproduction possible.

If pages are missing, contact the university which granted the degree.

Some pages may have indistinct print especially if the original pages were typed with a poor typewriter ribbon or if the university sent us an inferior photocopy.

Reproduction in full or in part of this microform is governed by the Canadian Copyright Act, R.S.C. 1970, c. C-30, and subsequent amendments.

## **AVIS**

La qualité de cette microforme dépend grandement de la qualité de la thèse soumise au microfilmage. Nous avons tout fait pour assurer une qualité supérieure de reproduction.

S'il manque des pages, veuillez communiquer avec l'université qui a conféré le grade.

La qualité d'impression de certaines pages peut laisser à désirer, surtout si les pages originales ont été dactylographiées à l'aide d'un ruban usé ou si l'université nous a fait parvenir une photocopie de qualité inférieure.

La reproduction, même partielle, de cette microforme est soumise à la Loi canadienne sur le droit d'auteur, SRC 1970, c. C-30, et ses amendements subséquents.

**THE UNIVERSITY OF ALBERTA**

**THE REACTIVITY OF SOLVATED ELECTRONS IN  
METHANOL / WATER AND ETHANOL / WATER MIXTURES**

**CHARLES WING - CHIU LAI**

**A THESIS**

**SUBMITTED TO THE FACULTY OF GRADUATE STUDIES AND RESEARCH  
IN PARTIAL FULFILMENT OF THE REQUIREMENTS FOR THE DEGREE  
OF  
DOCTOR OF PHILOSOPHY**

**DEPARTMENT OF CHEMISTRY**

**EDMONTON, ALBERTA**

**SPRING, 1989**

Permission has been granted to the National Library of Canada to microfilm this thesis and to lend or sell copies of the film.

The author (copyright owner) has reserved other publication rights, and neither the thesis nor extensive extracts from it may be printed or otherwise reproduced without his/her written permission.

L'autorisation a été accordée à la Bibliothèque nationale du Canada de microfilmer cette thèse et de prêter ou de vendre des exemplaires du film.

L'auteur (titulaire du droit d'auteur) se réserve les autres droits de publication; ni la thèse ni de longs extraits de celle-ci ne doivent être imprimés ou autrement reproduits sans son autorisation écrite.

ISBN 0-315-52848-6

THE UNIVERSITY OF ALBERTA  
RELEASE FORM

NAME OF AUTHOR: Charles Wing-Chiu Lai  
TITLE OF THESIS: The reactivity of solvated electrons in methanol / water and ethanol / water mixtures  
DEGREE FOR WHICH THESIS WAS PRESENTED: Doctor of Philosophy  
YEAR THIS DEGREE GRANTED: 1989

Permission is hereby granted to THE UNIVERSITY OF ALBERTA LIBRARY to reproduce single copies of this thesis and to lend or sell such copies for private, scholarly or scientific research purposes only.

The author reserves other publication rights, and neither the thesis nor extensive extracts from it may be printed or otherwise reproduced without the author's written permission.

  
.....  
(signed)

PERMANENT ADDRESS:

1807 Galbraith House  
Michener Park  
Edmonton, Alberta

Date: *22nd Dec, '88*

**THE UNIVERSITY OF ALBERTA**  
**FACULTY OF GRADUATE STUDIES AND RESEARCH**

The undersigned certify that they have read, and recommend to the Faculty of Graduate Studies and Research for acceptance, a thesis entitled

" The reactivity of solvated electrons in methanol / water and ethanol / water mixtures "

submitted by Charles Wing-Chiu Lai in partial fulfillment of the requirements for the degree of Doctor of Philosophy.

*J. R. Freeman*  
.....  
Supervisor

*H. S. G. ...*  
.....

*George R. Hule*  
.....

*A. Trujillo*  
.....

*.....*  
.....

*G. N. Patey*  
.....  
External examiner

Date: *22 Dec / 88*  
.....

**To Wai-Chue and Garlog**

## **ABSTRACT**

The kinetics of the reactions of solvated electrons with a number of organic (nitrobenzene, acetone, phenol and toluene) and inorganic (silver perchlorate, copper (II) perchlorate, lithium nitrate and lithium chromate) solutes were studied in the water mixtures of methanol and ethanol as a function of solvent composition and temperature.

The effects of solvent viscosity ( $\eta$ ) and static dielectric constant ( $\epsilon$ ) on the composition dependence of the nearly diffusion controlled rate constants ( $k_2$ ) at 298K were analyzed according to the Stokes-Smoluchowski and Debye models.

In the water-rich solvents, the rate constants for the reactions with nitrobenzene and silver (I) are almost identical, and are inversely related to the solvent viscosity,  $k_2 \propto \eta^{-1}$ , as predicted from the simplified models. In the alcohol-rich solvents, the smaller dependence of the rate constants on solvent viscosity is due to an increase in diffusion radii of the reactants and a decrease in solvation of the transition state. The influence of the solvation of the transition state on the viscosity normalized rate constants  $\eta k_2$  for the reactions with nitrobenzene and acetone was illustrated by the linear correlations of  $\ln \eta k_2$  with  $\epsilon^{-1}$ .

The diffusion radii of the ionic scavengers decrease as the alcohol content of the mixtures increases. The diffusion radii of the cationic scavengers in the methanol/water mixtures are similar to that of the ethanol/water mixtures. The size of the alkyl group on the alcohol molecule has a steric effect on the diffusion of the anions.

The encounter efficiencies for the reactions with the inefficient electron scavengers (phenol, toluene) were correlated with the optical absorption energy  $E_r$  of the solvated electron. In the water-rich solvents, the activation energies for the reactions with the inefficient scavengers are similar to those of the efficient scavengers. The differences in reactivity between the efficient and the inefficient electron scavengers are due to entropies of activation rather than energies of activation.

## **ACKNOWLEDGEMENTS**

The author wishes to express his sincerest thanks to Professor G. R. Freeman for his guidance during the time this thesis was researched and written.

The author is deeply indebted to his wife Wai-Chue for her assistance, patience and encouragement during the course of the work.

Special thanks go to my sister Kam Shue-yee who had travelled around the world to Edmonton to type part of this thesis.

Appreciation is extended to the Natural Sciences and Engineering Research Council of Canada for financial assistance.



## **TABLE OF CONTENTS**

	<b><u>Page</u></b>
<b>CHAPTER ONE : INTRODUCTION</b>	<b>1</b>
<b>I Solvated Electrons</b>	<b>1</b>
<b>II Pulse Radiolysis and Solvated Electrons</b>	<b>1</b>
<b>III Properties of Solvated Electrons</b>	<b>2</b>
1. Mobility	3
2. Optical Absorption Spectrum	3
A. Nature of the Absorption Band	4
(a) Band-Broadening	4
(b) Transitions	4
B. Models	5
C. Optical Absorption Spectrum in Hydroxylic Solvents	6
<b>IV Structure and Properties of Hydroxylic Solvents</b>	<b>7</b>
1. Structure of Hydroxylic Solvents	7
A. Water	7
B. Alcohols	9
2. Structure and Properties of Water / Alcohol Mixtures	10
A. Static Dielectric Properties	10
B. Thermodynamic Properties	10
C. Viscosity	11
<b>V Reactivity of Solvated Electrons</b>	<b>12</b>
<b>VI Present Work</b>	<b>16</b>

	<b>Page</b>
<b>CHAPTER TWO : EXPERIMENTAL</b>	<b>17</b>
<b>I Materials</b>	<b>17</b>
<b>II Apparatus for Kinetic Measurements</b>	<b>18</b>
1. Sample Cells	18
2. Argon - Bubbling System	18
3. Irradiation, Detection and Control Systems	18
A. The van de Graaff Accelerator	18
B. Secondary Emission Monitor	20
C. Optical Detection System	21
(a) The Analyzing Light	21
(b) Monochromator Grating and Filters	21
(c) Digital Voltmeter, Oscilloscope and Plotter	24
D. Temperature Control System	24
(a) Cooling and Heating Systems	24
(b) Cell Holder Box	25
<b>III Apparatus for Conductivity Measurements</b>	<b>25</b>
1. Impedance Bridge	25
2. Conductance Cells	26
3. Constant Temperature Bath	26
<b>IV Techniques</b>	<b>28</b>
1. Sample Preparations	28
2. Kinetic Measurements	31
3. Conductivity Measurements	34

	<b>Page</b>
<b>CHAPTER THREE : RESULTS</b>	<b>35</b>
<b>I Reaction Kinetics of Solvated Electrons with Organic Compounds</b>	<b>35</b>
<b>1. Reactions of Solvated Electrons in Methanol/Water Mixtures</b>	<b>35</b>
<b>A. Reaction of Solvated Electrons with Nitrobenzene</b>	<b>35</b>
<b>B. Reaction of Solvated Electrons with Acetone</b>	<b>46</b>
<b>C. Reaction of Solvated Electrons with Phenol</b>	<b>55</b>
<b>D. Reaction of Solvated Electrons with Toluene</b>	<b>64</b>
<b>2. Reactions of Solvated Electrons in Ethanol/Water Mixtures</b>	<b>72</b>
<b>A. Reaction of Solvated Electrons with Nitrobenzene</b>	<b>72</b>
<b>B. Reaction of Solvated Electrons with Acetone</b>	<b>82</b>
<b>C. Reaction of Solvated Electrons with Phenol</b>	<b>91</b>
<b>D. Reaction of Solvated Electrons with Toluene</b>	<b>100</b>
<b>II Reaction Kinetics of Solvated Electrons with Inorganic Ions</b>	<b>108</b>
<b>1. Reactions of Solvated Electrons in Methanol/Water Mixtures</b>	<b>108</b>
<b>A. Reaction of Solvated Electrons with Nitrate Ion</b>	<b>108</b>
<b>B. Reaction of Solvated Electrons with Silver Ion</b>	<b>118</b>
<b>C. Reaction of Solvated Electrons with Chromate Ion</b>	<b>127</b>
<b>D. Reaction of Solvated Electrons with Copper (II) Ion</b>	<b>136</b>
<b>2. Reactions of Solvated Electrons in Ethanol/Water Mixtures</b>	<b>146</b>
<b>A. Reaction of Solvated Electrons with Nitrate Ion</b>	<b>146</b>
<b>B. Reaction of Solvated Electrons with Silver Ion</b>	<b>157</b>
<b>C. Reaction of Solvated Electrons with Chromate Ion</b>	<b>166</b>
<b>D. Reaction of Solvated Electrons with Copper (II) Ion</b>	<b>174</b>
<b>III Conductivities of Inorganic Electrolytes in Alcohol/Water Mixtures</b>	<b>183</b>
<b>1. Methanol/Water Mixtures</b>	<b>183</b>
<b>2. Ethanol/Water Mixtures</b>	<b>183</b>

	<b>Page</b>
<b>CHAPTER FOUR : DISCUSSION</b>	<b>225</b>
<b>I    Reactions with Organic Electron Scavengers</b>	<b>225</b>
1. <b>Efficient Organic Electron Scavengers</b>	<b>225</b>
A. <b>Solvent Viscosity Effects</b>	<b>225</b>
B. <b>Solvent Dielectric Effects</b>	<b>237</b>
(a) <b>The Debye Model</b>	<b>237</b>
(b) <b>Effects of Dielectric Constant</b>	<b>242</b>
2. <b>Inefficient Organic Electron Scavengers</b>	<b>248</b>
3. <b>Energies and Entropies of Activation</b>	<b>260</b>
<b>II    Reactions with Inorganic Electron Scavengers</b>	<b>268</b>
1. <b>Positively Charged Scavengers</b>	<b>269</b>
2. <b>Negatively Charged Scavengers</b>	<b>278</b>
3. <b>Energies and Entropies of Activation</b>	<b>281</b>
<b>III   Conclusion</b>	<b>287</b>
<b>REFERENCES</b>	<b>289</b>

## LIST OF TABLES

<u>Table</u>	<u>Page</u>
3-1 Second-order rate constants for the reaction of solvated electrons with nitrobenzene in methanol / water mixtures at various temperatures	44
3-2 Rate parameters for the reaction of solvated electrons with nitrobenzene in methanol / water mixtures	45
3-3 Second-order rate constants for the reaction of solvated electrons with acetone in methanol / water mixtures at various temperatures	53
3-4 Rate parameters for the reaction of solvated electrons with acetone in methanol / water mixtures	54
3-5 Second-order rate constants for the reaction of solvated electrons with phenol in methanol / water mixtures at various temperatures	62
3-6 Rate parameters for the reaction of solvated electrons with phenol in methanol / water mixtures	63
3-7 Second-order rate constants for the reaction of solvated electrons with toluene in methanol / water mixtures at various temperatures	69
3-8 Rate parameters for the reaction of solvated electrons with toluene in methanol / water mixtures	70
3-9 Second-order rate constants for the reaction of solvated electrons with nitrobenzene in ethanol / water mixtures at various temperatures	80
3-10 Rate parameters for the reaction of solvated electrons with nitrobenzene in ethanol / water mixtures	81
3-11 Second-order rate constants for the reaction of solvated electrons with acetone in ethanol / water mixtures at various temperatures	89
3-12 Rate parameters for the reaction of solvated electrons with acetone in ethanol / water mixtures	90

<b><u>Table</u></b>	<b><u>Page</u></b>
3-13 Second-order rate constants for the reaction of solvated electrons with phenol in ethanol / water mixtures at various temperatures	98
3-14 Rate parameters for the reaction of solvated electrons with phenol in ethanol / water mixtures	99
3-15 Second-order rate constants for the reaction of solvated electrons with toluene in ethanol / water mixtures at various temperatures	106
3-16 Rate parameters for the reaction of solvated electrons with toluene in ethanol / water mixtures	107
3-17 Second-order rate constants for the reaction of solvated electrons with lithium nitrate in methanol / water mixtures at various temperatures	116
3-18 Rate parameters for the reaction of solvated electrons with lithium nitrate in methanol / water mixtures	117
3-19 Second-order rate constants for the reaction of solvated electrons with silver perchlorate in methanol/water mixtures at various temperatures	125
3-20 Rate parameters for the reaction of solvated electrons with silver perchlorate in methanol / water mixtures	126
3-21 Second-order rate constants for the reaction of solvated electrons with lithium chromate in methanol/water mixtures at various temperatures	134
3-22 Rate parameters for the reaction of solvated electrons with lithium chromate in methanol / water mixtures	135
3-23 Second-order rate constants for the reaction of solvated electrons with copper perchlorate in methanol/water mixtures at various temperatures	144
3-24 Rate parameters for the reaction of solvated electrons with copper perchlorate in methanol / water mixtures	145
3-25 Second-order rate constants for the reaction of solvated electrons with lithium nitrate in ethanol / water mixtures at various temperatures	155

<b>Table</b>		<b>Page</b>
3-26	Rate parameters for the reaction of solvated electrons with lithium nitrate in ethanol / water mixtures	156
3-27	Second-order rate constants for the reaction of solvated electrons with silver perchlorate in ethanol / water mixtures at various temperatures	164
3-28	Rate parameters for the reaction of solvated electrons with silver perchlorate in ethanol / water mixtures	165
3-29	Second-order rate constants for the reaction of solvated electrons with lithium chromate in ethanol / water mixtures at various temperatures	172
3-30	Rate parameters for the reaction of solvated electrons with lithium chromate in ethanol / water mixtures	173
3-31	Second-order rate constants for the reaction of solvated electrons with copper perchlorate in ethanol / water mixtures at various temperatures	181
3-32	Rate parameters for the reaction of solvated electrons with copper perchlorate in ethanol / water mixtures	182
3-33	Temperature and composition dependence of molar conductance of inorganic electrolytes in methanol / water mixtures	202
3-34	Temperature and composition dependence of molar conductance of inorganic electrolytes in ethanol / water mixtures	224

## LIST OF FIGURES

<u>Figure</u>	<u>Page</u>
1-1    Composition dependence of optical absorption maximum energy ( $E_{Amax}$ ) for alcohol / water mixtures at 298 K	8
2-1    The bubbling system	19
2-2    The secondary emission monitor	21
2-3    The path of the analyzing light	23
2-4    Temperature control of the water bath	27
2-5    Temperature regulating system	27
2-6    The sample sealing procedure	30
2-7    Typical solvated electron kinetic trace	32
3-1    Temperature and concentration dependence of the first-order (A-L) rate constant for the reaction of solvated electrons with nitrobenzene in methanol / water mixtures	36
3-2    Arrhenius plots for the reaction of solvated electrons with nitrobenzene in methanol / water mixtures	42
3-3    Composition dependence of $k_{292}$ for the reaction of solvated electrons with nitrobenzene in methanol / water mixtures	43
3-4    Temperature and concentration dependence of the first-order (A-J) rate constant for the reaction of solvated electrons with acetone in methanol / water mixtures	46
3-5    Arrhenius plots for the reaction of solvated electrons with acetone in methanol / water mixtures	52



<b>Figure</b>	<b>Page</b>
3-6 (A-L) Temperature and concentration dependence of the first-order rate constant for the reaction of solvated electrons with phenol in methanol / water mixtures	55
3-7 Arrhenius plots for the reaction of solvated electrons with phenol in methanol / water mixtures	61
3-8 (A-H) Temperature and concentration dependence of the first-order rate constant for the reaction of solvated electrons with toluene in methanol / water mixtures	64
3-9 Arrhenius plots for the reaction of solvated electrons with toluene in methanol / water mixtures	69
3-10 (A-J) Temperature and concentration dependence of the first-order rate constant for the reaction of solvated electrons with nitrobenzene in ethanol / water mixtures	72
3-11 Arrhenius plots for the reaction of solvated electrons with nitrobenzene in ethanol / water mixtures	78
3-12 Composition dependence of $k_{298}$ for the reaction of solvated electrons with nitrobenzene in ethanol / water mixtures	79
3-13 (A-J) Temperature and concentration dependence of the first-order rate constant for the reaction of solvated electrons with acetone in ethanol / water mixtures	82
3-14 Arrhenius plots for the reaction of solvated electrons with acetone in ethanol / water mixtures	88
3-15 (A-J) Temperature and concentration dependence of the first-order rate constant for the reaction of solvated electrons with phenol in ethanol / water mixtures	91
3-16 Arrhenius plots for the reaction of solvated electrons with phenol in ethanol / water mixtures	97

<b>Figure</b>	<b>Page</b>
3-17    Temperature and concentration dependence of the first-order (A-H)    rate constant for the reaction of solvated electrons with toluene in ethanol / water mixtures	100
3-18    Arrhenius plots for the reaction of solvated electrons with toluene in ethanol / water mixtures	105
3-19    Temperature and concentration dependence of the first-order (A-K)    rate constant for the reaction of solvated electrons with lithium nitrate in methanol / water mixtures	109
3-20    Arrhenius plots for the reaction of solvated electrons with lithium nitrate in methanol / water mixtures	115
3-21    Temperature and concentration dependence of the first-order (A-J)    rate constant for the reaction of solvated electrons with silver perchlorate in methanol / water mixtures	118
3-22    Arrhenius plots for the reaction of solvated electrons with silver perchlorate in methanol / water mixtures	124
3-23    Temperature and concentration dependence of the first-order (A-K)    rate constant for the reaction of solvated electrons with lithium chromate in methanol / water mixtures	127
3-24    Arrhenius plots for the reaction of solvated electrons with lithium chromate in methanol / water mixtures	133
3-25    Temperature and concentration dependence of the first-order (A-J)    rate constant for the reaction of solvated electrons with copper (II) perchlorate in methanol / water mixtures	137
3-26    Arrhenius plots for the reaction of solvated electrons with copper (II) perchlorate in methanol / water mixtures	143

<b>Figure</b>	<b>Page</b>
3-27 (A-L) Temperature and concentration dependence of the first-order rate constant for the reaction of solvated electrons with lithium nitrate in ethanol / water mixtures	146
3-28 Arrhenius plots for the reaction of solvated electrons with lithium nitrate in ethanol / water mixtures	153
3-29 Composition dependence of $k_{298}$ for the reaction of solvated electrons with lithium nitrate in ethanol / water mixtures	154
3-30 (A-K) Temperature and concentration dependence of the first-order rate constant for the reaction of solvated electrons with silver perchlorate in ethanol / water mixtures	157
3-31 Arrhenius plots for the reaction of solvated electrons with silver perchlorate in ethanol / water mixtures	163
3-32 (A-I) Temperature and concentration dependence of the first-order rate constant for the reaction of solvated electrons with lithium chromate in ethanol / water mixtures	166
3-33 Arrhenius plots for the reaction of solvated electrons with lithium chromate in methanol / water mixtures	171
3-34 (A-J) Temperature and concentration dependence of the first-order rate constant for the reaction of solvated electrons with copper (II) perchlorate in ethanol / water mixtures	174
3-35 Arrhenius plots for the reaction of solvated electrons with copper (II) perchlorate in ethanol / water mixtures	180
3-36 (A-F) Temperature and concentration dependence of the conductance of lithium nitrate in methanol / water mixtures	184
3-37 (A-F) Temperature and concentration dependence of the conductance of silver perchlorate in methanol / water mixtures	187

<b>Figure</b>	<b>Page</b>
3-38 Temperature and concentration dependence of the conductance of (A-F) lithium chromate in methanol / water mixtures	190
3-39 Temperature and concentration dependence of the conductance of (A-F) copper (II) perchlorate in methanol / water mixtures	193
3-40 Arrhenius plots of molar conductance of lithium nitrate in methanol / water mixtures	197
3-41 Arrhenius plots of molar conductance of silver perchlorate in methanol / water mixtures	198
3-42 Arrhenius plots of molar conductance of lithium chromate in methanol / water mixtures	199
3-43 Arrhenius plots of molar conductance of copper (II) perchlorate in methanol / water mixtures	200
3-44 Composition dependence of the activation energy of conductance of some inorganic electrolytes in methanol / water mixtures	201
3-45 Temperature and concentration dependence of the conductance of (A-G) lithium nitrate in ethanol / water mixtures	203
3-46 Temperature and concentration dependence of the conductance of (A-G) silver perchlorate in ethanol / water mixtures	207
3-47 Temperature and concentration dependence of the conductance of (A-G) lithium chromate in ethanol / water mixtures	211
3-48 Temperature and concentration dependence of the conductance of (A-G) copper (II) perchlorate in ethanol / water mixtures	214
3-49 Arrhenius plots of molar conductance of lithium nitrate in ethanol / water mixtures	218
3-50 Arrhenius plots of molar conductance of silver perchlorate in ethanol / water mixtures	219

<b>Figure</b>	<b>Page</b>
3-51 Arrhenius plots of molar conductance of lithium chromate in ethanol / water mixtures	220
3-52 Arrhenius plots of molar conductance of copper (II) perchlorate in ethanol / water mixtures	221
3-53 Composition dependence of the activation energy of conductance of some inorganic electrolytes in ethanol / water mixtures	222
3-54 Composition dependence of the molar conductance of some inorganic electrolytes in methanol / water and ethanol / water mixtures	223
4-1 The composition dependence of the second-order rate constants for the reaction of solvated electrons with organic electron-scavengers in methanol/water mixtures at 298 K	226
4-2 The composition dependence of the second-order rate constants for the reaction of solvated electrons with organic electron-scavengers in ethanol/water mixtures at 298 K	227
4-3 The composition dependence of solvent viscosity in methanol/water and ethanol/water mixtures at 298 K	230
4-4 The viscosity dependence of the second-order rate constants for the reaction of solvated electrons with nitrobenzene in methanol/water mixtures at 298 K	231
4-5 The viscosity dependence of the second-order rate constants for the reaction of solvated electrons with nitrobenzene in ethanol/water mixtures at 298 K	232
4-6 The composition dependence of the diffusion coefficients of solvated electrons and nitrobenzene in methanol/water and ethanol/water mixtures at 298 K	235

<b>Figure</b>	<b>Page</b>
4-7 The composition dependence of the reaction radii for the reaction of solvated electrons with nitrobenzene in methanol/water mixtures at 298 K	236
4-8 The viscosity dependence of the normalized $k_2/f$ values for the reaction of solvated electrons with nitrobenzene in methanol/water mixtures at 298 K	240
4-9 The composition dependence of the relative effective diffusion radii ( $r_w/r$ ) for the reaction of solvated electrons with nitrobenzene in methanol/water and ethanol/water mixtures at 298 K	241
4-10 The composition dependence of the static dielectric constants of solvated electrons in methanol/water and ethanol/water mixtures at 298K	243
4-11 The viscosity normalized rate constants for the reaction of solvated electrons with nitrobenzene and acetone as a function of $\epsilon^{-1}$ in methanol/water and ethanol/water mixtures at 298 K	244
4-12 The viscosity normalized rate constants for the reaction of solvated electrons with nitrobenzene as a function of $\epsilon^{-1}$ in alcohol at 298 K	247
4-13 The viscosity normalized limiting molar conductance of some ions as a function of $\epsilon^{-1}$ in ethanol/water mixtures at 298 K	249
4-14 The viscosity dependence of the second-order rate constants for the reaction of solvated electrons with phenol and toluene in methanol/water mixtures at 298 K	250
4-15 The viscosity dependence of the second-order rate constants for the reaction of solvated electrons with phenol and toluene in ethanol/water mixtures at 298 K	251
4-16 The relationship between $E_{Amax}$ and $E_r$ in the optical absorption spectrum of solvated electrons	253

<b>Figure</b>	<b>Page</b>
4-17 The composition dependence of the optical absorption energies of solvated electrons in methanol/water mixtures at 298K	254
4-18 The composition dependence of the optical absorption energies of solvated electrons in ethanol/water mixtures at 298K	255
4-19 Encounter efficiency for inefficient scavenger against solvated electron trap depth in ethanol/water mixtures at 298K	258
4-20 Encounter efficiency for inefficient scavenger against solvated electron trap depth in methanol/water mixtures at 298K	259
4-21 The composition dependence of the activation energies for the reaction of solvated electrons with organic electron-scavengers in methanol/water mixtures	261
4-22 The composition dependence of the activation energies for the reaction of solvated electrons with organic electron-scavengers in ethanol/water mixtures	262
4-23 The composition dependence of the energies of viscous flow in methanol/water and ethanol/water mixtures at 298K	263
4-24 The composition dependence of the entropy of activation for the reaction of solvated electrons with organic electron-scavengers in methanol/water mixtures	266
4-25 The composition dependence of the entropy of activation for the reaction of solvated electrons with organic electron-scavengers in ethanol/water mixtures	267
4-26 The composition dependence of the second-order rate constants for the reaction of solvated electrons with inorganic electron-scavengers in methanol/water mixtures at 298 K	270

<b>Figure</b>	<b>Page</b>
4-27 The composition dependence of the second-order rate constants for the reaction of solvated electrons with inorganic electron scavengers in ethanol/water mixtures at 298 K	271
4-28 The viscosity dependence of the second-order rate constants for the reaction of solvated electrons with silver ions and nitrobenzene in methanol/water mixtures at 298 K	272
4-29 The viscosity dependence of the second-order rate constants for the reaction of solvated electrons with silver ions and nitrobenzene in ethanol/water mixtures at 298 K	273
4-30 The composition dependence of the relative effective diffusion radii ( $r_w/r$ ) for the reaction of solvated electrons with nitrobenzene and silver ions in methanol/water mixtures at 298 K	274
4-31 The composition dependence of the relative effective diffusion radii ( $r_w/r$ ) for the reaction of solvated electrons with nitrobenzene and silver ions in ethanol/water mixtures at 298 K	275
4-32 The composition dependence of the relative effective diffusion radii ( $r_w/r$ ) for the reaction of solvated electrons with silver ions in methanol/water and ethanol/water mixtures at 298 K	276
4-33 The composition dependence of the relative effective diffusion radii ( $r_w/r$ ) for the reaction of solvated electrons with copper (II) ions in methanol/water and ethanol/water mixtures at 298 K	277
4-34 The composition dependence of the relative effective diffusion radii ( $r_w/r$ ) for the reaction of solvated electrons with chromate ions in methanol/water and ethanol/water mixtures at 298 K	279
4-35 The composition dependence of the relative effective diffusion radii ( $r_w/r$ ) for the reaction of solvated electrons with nitrate ions in methanol/water and ethanol/water mixtures at 298 K	280



<b>Figure</b>		<b>Page</b>
4-36	The composition dependence of the activation energies for the reaction of solvated electrons with inorganic electron-scavengers in methanol/water mixtures	282
4-37	The composition dependence of the activation energies for the reaction of solvated electrons with inorganic electron-scavengers in ethanol/water mixtures	283
4-38	The composition dependence of the entropy of activation for the reaction of solvated electrons with inorganic electron-scavengers in methanol/water mixtures	284
4-39	The composition dependence of the entropy of activation for the reaction of solvated electrons with inorganic electron-scavengers in ethanol/water mixtures	285

# CHAPTER ONE

## INTRODUCTION

### I Solvated Electrons

It was the German chemist W. Weyl who discovered in 1864 that a deep blue solution can be formed by dissolving either sodium or potassium in ammonia (1). It was not until 1922 that it was demonstrated by conductance measurements that this blue solution contained solvated electrons (2).

Solvated electrons can convert a wide range of chemical substances (S) to their reduced forms (S<sup>-</sup>), which may then undergo further reaction to yield other products (3).



### II Pulse Radiolysis and Solvated Electrons

The most convenient method to produce electrons in a liquid for physical measurements is to generate them with a pulse of high energy radiation (equation [1-3]).



Upon the absorption of ionizing energy, an electron is ejected from a molecule and travels a certain distance away from its "parent ion" before losing all its excess energy in collisions. Thus the electron is thrust into the body of the liquid. It loses its excess energy by ionizing and exciting the medium. If the solvent is electrophilic in nature, the slowed-down electron becomes attached to the solvent molecule to form a negative ion. If the electron does not attach to a molecule, it ultimately reaches a state of thermal equilibrium with the medium, the solvated state.

In a polar liquid, the thermalized electron is localized in a coulombic potential well created by several suitably oriented solvent dipoles (4-7). In a non-polar liquid, localization occurs due to the anisotropic polarizability of the molecules (8). If the molecules of the medium are isotropically polarizable, the potential well will be shallow, and the electron can not be localized to any large extent. Such delocalized electrons are called "quasi-free" electrons (5).

Since electronic polarization of molecules occurs in about  $10^{-15}$  second, the trapped electron initially finds itself in an electronically polarized potential well. The electric field of the electron causes the neighboring solvent molecules to reorient along the axes of permanent dipoles or that of the maximum polarizability. The potential well of the cavity deepens as this reorientation occurs. The trapped electron relaxes into the solvated state in about a picosecond in water (9).

### III Properties of Solvated Electrons

The interactions between the electron and the neighboring solvent molecules manifest themselves in a number of physico-chemical properties, which allow the behavior of solvated electrons to be elucidated.

The paramagnetic nature of the solvated electron has been confirmed by the electron spin resonance (ESR) spectrum (10).

The thermodynamic properties of solvated electrons, such as the standard potential (11), the solvation energy and entropy (12) of solvated electrons in water, are still not accurately known, and therefore must be used with reservation (11).

The mobility and the optical absorption spectrum of solvated electrons have been useful in providing information about their behavior.

## 1. Mobility

Data on the mobility of solvated electrons can be obtained from the conductivity studies of their solutions (13). The mobilities of solvated electrons in water (14) and in liquid ammonia (8) are three to five times higher than those of sodium and chloride (15,16) ions. In water, the mobility of solvated electrons is equal to that of hydroxide ions and smaller than that of protons (15). In non-polar liquids, the mobilities of solvated electrons depend strongly on the structure of the solvent molecules (8,17-20).

## 2. Optical Absorption Spectrum

Solvated electrons absorb light of energies ranging from infrared to ultraviolet. The absorption band is structureless, broad and asymmetric, with a long tail extending to the ultraviolet region.

The energy at the absorption maximum,  $E_{Amax}$ , and the width of the band depend on the polarity of the solvent. Electrons in protic solvents such as ammonia (22), water and alcohols (23) have an absorption maximum in the visible to near infrared region. In aliphatic hydrocarbons (24,25), the maximum is in the infrared region. This suggests that the interaction of the electron with the permanent dipoles is stronger than that with the electron-induced dipoles. In the polar aprotic solvents such as ethers (26) and substituted amines (27), the absorption maxima are located in between those for protic and non-polar solvents. For a given category of organic solvents, it has been observed that the  $E_{Amax}$  values of solvated electrons are affected not only by the types and number of functional groups on the solvent molecules, but also by the degree of alkyl substitution at the  $\alpha$ -carbon (24). This is probably due to the combined result of steric and inductive effects.

The absorption spectra of solvated electrons are temperature dependent. Values of  $E_{Amax}$  decrease with increasing temperature, which indicates that thermal agitation of the solvent molecules produces shallower potential wells (23).

## **A. Nature of the Absorption Band**

### **(a) Band-Broadening**

The shape of the optical absorption spectrum of solvated electrons is similar in any solvent; it is broad and asymmetric, skewed to the higher energy side. Different theories have been suggested to interpret the band broadening of the solvated electron spectrum. The theory of homogeneous broadening involves bandwidth that originates from the optical absorption of only one type of absorbing species (28,29) and broadening is due to phonon coupling in the excited state. But in a liquid where randomness persists, the probability that all the potential wells of the solvated electron are of the same depth seems negligible. Another theory has attributed the broadening to the excitations from traps of various depths (heterogeneous band broadening), and each transition gives rise to a spectrum slightly different from another (30,31). Broadening is no doubt caused by both of these factors and may be called nonhomogeneous broadening.

### **(b) Transitions**

Two types of transitions have been suggested to be responsible for the absorption spectrum of solvated electrons :

- (i) from the ground state discrete energy level to an excited state discrete energy level (bound to bound transition) (32),
- (ii) from the ground state discrete energy level to the higher energy continuum (bound to continuum) (33),
- (iii) Both (i) and (ii) might occur (34-36).

If the transitions are of the bound to bound type, one expects the absorption spectrum to be symmetrical in energy. Thus the other transition mechanisms appear to be more adequate to account for the asymmetry of the band. The skewing of the absorption band to the high energy side is usually explained by bound to continuum transitions. Studies of photoconductivity spectra of solvated electrons give additional insight to the nature of

excitation in the optical absorption process. The measurement of the photoconductivity spectra corresponds to the bound ground level to continuum transitions. Comparison of the optical absorption spectrum with the photoconductivity spectrum gives an estimate of threshold energy ( $E_{th}$ ) for photoconductivity and also the extent of bound to continuum transitions in the absorption spectrum (37-40). The threshold energy is the minimum energy required for the bound to continuum transition, that is, the energy difference between the ground state energy level and the bottom of the conduction band. If the photoconductivity and the optical absorption spectra overlapped completely, the optical transition would be solely due to bound to continuum transitions.

Comparisons of the photoconductivity and optical absorption spectra indicate that in all systems, the optical absorption band consists of both bound to bound and bound to continuum transitions (31,37-43). In most solvent systems,  $E_{th}$  is less than  $E_{Amax}$ , suggesting that a major contribution of the optical absorption spectra is due to the bound to continuum transitions.

It has been suggested that a distribution of potential wells is possible for electrons in solution, and the depth limits of the traps have been estimated (31). Photoconductivity spectral data for polar/non-polar solvent mixtures (40-43) indicate that as the non-polar component in the mixture decreases, the potential wells become deeper, and the extent of bound to bound transitions increases.

## B. Models

A number of models have been developed to analyse the optical absorption spectra of solvated electrons. The simplest cavity model (44) of solvated electrons consists of a spherical potential well. The electron is localized in a physical cavity, with the positive ends of the solvent dipoles aligned around it.

In the continuum model (45), the electron is considered to be located in a cavity of a polarized dielectric continuum. In the semi-continuum models (46,47), the electron is assumed to be in a spherical cavity which is surrounded by a solvation shell of a fixed number of solvent molecules. The solvent beyond the solvation shell is regarded as a dielectric continuum.

The calculations done according to these models have been successful in reproducing the  $E_{Amax}$  value. The calculated line shape, however, is more narrow and symmetrical than observed. Statistical mechanical models that consider the molecular properties of the solvent are being developed (7,48,49).

The ESR studies of solvated electrons in aqueous glasses (50) has suggested that the electron is solvated in the centre of an octahedron that made up of six water molecules, with the -OH groups point towards the electron. In methanol, the ESR spectrum indicates that there are four methanol molecules in the corners of a tetrahedral structure (50).

### C. Optical Absorption Spectrum in Hydroxylic Solvents

The optical absorption energies of solvated electrons are critically dependent on the interaction between the electron and the solvent molecules. The absorption energies in water, alcohols and their mixtures are higher than those in ammonia and amines (37,51). This means that there are stronger electron-solvent interactions in the hydroxylic solvents.

Electron solvation in alcohols affected by the alkyl substitution on the  $\alpha$ -carbon atom. The  $E_{Amax}$  values of solvated electrons in alcohols are in the order of : primary > secondary > tertiary (23,52). In the primary alcohol series, for alcohols other than ethanol, the  $E_{Amax}$  values are almost independent of chain length (53) and branching (23) of the alkyl group. This indicates that configuration of the -OH group in the solvation shells of the electrons are of the similar type, and the alkyl group beyond the  $\alpha$ -carbon has only slight effect on the interaction between the electron and the solvent (53,54). The value of  $E_{Amax}$  in ethanol is about 8% lower than those in the other primary alcohols at the same

temperature (52). This must be connected with the structure of the liquid, but the specific reason is not known.

The lower values of  $E_{Amax}$  in secondary and tertiary alcohols probably result from the weaker alignment of solvent dipoles around the electron. This indicates that the combined effects of electronic induction and steric hindrance of the alkyl substituent hinder alignment of the O-H dipoles with the field of the electron.

The widths of the solvated electron absorption band at half height ( $W_{1/2}$ ) in alcohols are about twice that in water (55). The  $W_{1/2}$  values in amines are also about twice that in ammonia (56). The bound to continuum transition mode has been considered as a major contributor in the absorption spectra of solvated electron in alcohols, and the extent of the bound to bound transition may vary with the type of alcohol (39,55).

Spectral parameters of solvated electrons in alcohol/water mixtures display strong composition dependence (23). The variation of  $E_{Amax}$  as a function of mole % of water in alcohol is shown in Fig. 1-1. The minimum of  $E_{Amax}$  values in primary alcohol/water mixtures is attributed to a water nucleated solvent structure at that composition region. The similarities of trends in the water-rich region among alcohol/water mixtures indicate the liquid structures change in the same way. The near constant values in the central region are probably due to selective solvation of the electron in similar environments. This may indicate the existence of clusters of alcohol-water complexes in this composition region (23). Hence optical absorption spectroscopy of solvated electrons provides valuable information about the microscopic solvent structure changes.

#### IV Structure and Properties of Hydroxylic Solvents

##### 1. Structure of Hydroxylic Solvents

###### A. Water

The earliest model of the structure of water was based on radial distribution functions which had a pattern similar to that of a "broken down" ice structure (57). In ice, each



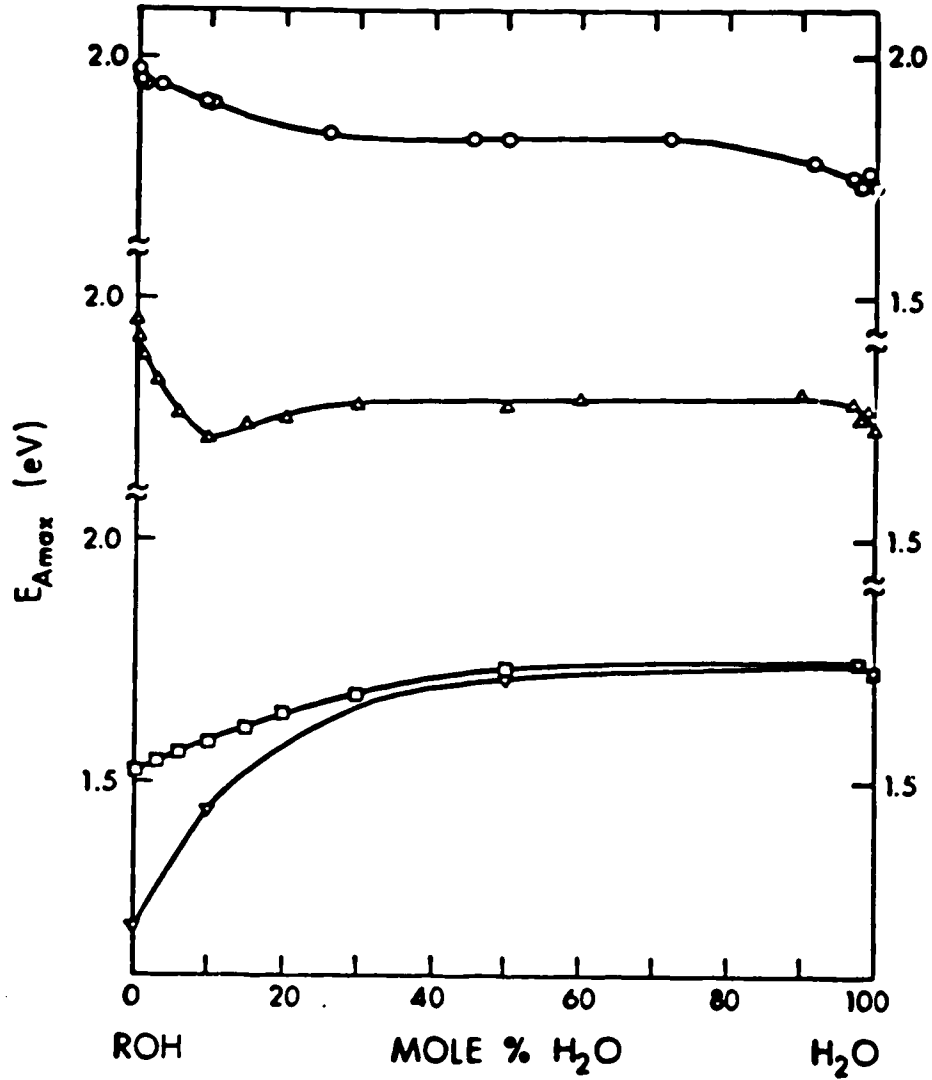


Fig. 1-1 Composition dependence of optical absorption maximum energy ( $E_{Amax}$ )  
for alcohol / water mixtures at 298 K (ref.23)

○, methanol; ▲, 1-propanol; □, 2-propanol; ▼, t-butyl alcohol. Shapes for other primary and secondary alcohols are similar to that for ▲ and □, respectively

water molecule is hydrogen-bonded tetrahedrally to four other molecules. The distribution functions of water (58,59) indicate slightly more than four nearest neighbors. Numerous models have been proposed for the structure of water, they fall into two broad categories: (a) uniformist models (60-64); (b) mixture models (65-69).

The uniformist models assume water to consist of a single type of three-dimensional random hydrogen bond network. There are no significant amounts of monomer water (molecules without hydrogen bonds). There is an equilibrium between free and bonded -OH groups. The structure can be visualized as a network of cavities with structural order that is only short range and approximately tetrahedral.

The mixture models assume water to consist of a mixture of two or more species. These are water molecules with no hydrogen bonds (monomers), or with up to four hydrogen bonds. The hydrogen bonded water molecules form an open network full of cavities or clusters of water molecules. These exist in equilibrium with monomer water which forms a dense medium. Cluster size and concentration change with temperature.

None of these models is able to explain all properties of water. Experimental results are usually explained with one model or the other. Simulations of water structure are being done in order to develop a better model for water (70, 71).

## B. Alcohols

In contrast to water, the structures of alcohols are simpler because there is only one hydroxyl group per molecule. Alcohols can form up to three hydrogen-bonds per molecule, while water can form four hydrogen-bonds. The presence of monomers, dimers and polymers has been suggested in various spectroscopic studies (72-74). There are linear or ring polymers where approximately two hydrogen bonds per alcohol molecules are formed. A higher proportion of monomer and ring-like polymers exists in alcohols with larger alkyl groups due to steric hindrance (75). About 5-10% of the lower alcohol

molecules participate in a third hydrogen-bond which leads to a three-dimensional linkage of polymer chains (76, 77).

## 2. Structure and Properties of Water/Alcohol Mixtures

### A. Static Dielectric Properties

Dielectric properties give information about the short-range order in a liquid. The Kirkwood structure factor,  $g_k$ , which is calculated from the dielectric constant, dipole moment and density, is a measure of the short-range order (78). For highly associated liquids,  $g_k > 1$ , molecular dipoles are oriented in series and are greater than that measured in the gas phase. For head-to-tail interaction between molecular dipoles (contra-associated),  $g_k < 1$ , the liquid phase dipole moment is less than that in the gas-phase. Random orientation gives  $g_k = 1$ .

The Kirkwood structure factors of water and primary alcohols are greater than unity (79-81), indicating short range order. For primary alcohols, the value of  $g_k$  increases with increasing chain length, suggesting that alcohols with longer chains are better aligned. In lower alcohols where the degree of cross-linkage between polymer chains is higher, linear arrangement of dipoles are more difficult. This leads to lower  $g_k$  values. Among alcohols with the same number of carbon atoms, tertiary alcohols have the lowest  $g_k$  values, which can be explained by the the ring-like polymeric structure (82).

When water is added to methanol or tertiary alcohols (80, 82), the structure factors increase slightly. Water hydrogen bonds with these alcohol molecules to attain a better linear arrangement of dipoles. Thus water has a structure building effect. The  $g_k$  values decrease when water is added to other alcohols, and reach a minimum in the mid-composition range (80). Water has a structure breaking effect on secondary alcohols.

### B. Thermodynamic Properties

The thermodynamic functions of mixing alcohol and water are used to suggest the first properties employed to suggest a structure for alcohol/water mixtures. The extent of change depends on the alkyl group (83-85).

In associated systems, negative enthalpy of mixing implies hydrogen bond formation and a positive value implies hydrogen bond rupture. Dissolution of a small amount of alcohol or other non-electrolyte in water is accompanied by loss of enthalpy (exothermicity) and loss of entropy. This has been interpreted by (a) the non-electrolyte molecule promotes water-water hydrogen bonding, in clusters that form small domains (86-88) or (b) water molecules order around the non-electrolyte and form oligomers similar to clathrates (89-90). The second effect has been referred as "hydrophobic effect" or called "ice-berg" formation.

The alcohol molecules thus strengthen the water structure. The composition at which the maximum strengthening occurs, depends on the alcohol. The mole fraction of alcohol at this composition is lower when the alkyl group of the alcohol is larger (85-89).

When water is added to the lower alcohols such as methanol and ethanol some of these alcohol molecules make hydrogen bonds with water. The enthalpy of mixing of higher alcohols with water is positive (endothermic); water acts as a structure breaker (83, 84).

### C. Viscosity

Diffusion in a liquid is inversely related to its viscosity. Viscosities of pure alcohols are either close to or higher than that of water at the same temperature. The viscosity is higher in alcohols with longer (and more branched) alkyl groups. Such alcohols flow less easily because of the bulkiness (and relative rigidity) of the molecules.

Viscosities are strongly composition dependent in mixtures of alcohol and water. The composition dependence is characterized by (69, 92):

- (a) a maximum in viscosity at compositions ranging from 0.65 to 0.75 mole fraction of water;
- (b) a sharp increase in viscosity when a few mole percent of alcohol is added to water;
- (c) small changes in viscosity when a few mole percent of water is added to alcohol.

Addition of alcohol to water increases the viscous resistance to flow. This perhaps is due to the clathrate-like structure formation (89,90). In the lower alcohols, water acts as a structure maker, indicated by an increase in viscosity. The addition of water to larger alcohols is accompanied by a decrease in viscosity, which can be explained by the formation of water nucleated alcohol complexes (23, 84), or the breakdown of alcohol structure by water (93).

#### V Reactivity of Solvated Electrons

In addition to the optical properties, another useful way to gain understanding of solvated electrons is through their reactivities with different types of solute. An enormous amount of kinetic data has been reported. Several hundred rate constants have been determined for the reaction of electrons solvated in water (94), alcohols (95-101), alcohol mixtures (102-105) and alcohol/water mixtures (106-118).

Water/alcohol solvent mixtures offer the possibility of changing the three-dimensional hydrogen-bond network of water by gradually increasing the amount of the alcoholic component. When the change in free energy associated with the change of the microenvironment of the reactants (induced by the alcoholic cosolvent) is different from that of the transition state, the activation and rate parameters of the reaction change. The change in microenvironment of the reactants by gradual modification of the solvent structure (change of water content) therefore offers a powerful tool to assess the nature of solvent effects on solvated electron reactions.

The complex dependence of the physical properties of alcohol/water systems upon composition (67,119-121) also makes them valuable solvents to probe the behavior of solvated electrons. Examples of the physical properties include (i) excess enthalpy of mixing, which is always negative in the water-rich region, but in the alcohol-rich region is negative for methyl and ethyl alcohols, and positive for higher alcohols (67,85,119-121); (ii) viscosity, where a maximum always occurs at 70-80 mole % water (93,120); (iii)

mutual diffusion coefficients, which have a minimum at 70-80 mole % water (123-124); (iv) dielectric relaxation, where the relaxation time of alcohols increases with addition of a small amount of water, and the relaxation time of water increases with addition of a small amount of alcohol (125-128); (v) acoustics, where excess absorption occurs due to bulk viscosity (129).

The kinetic studies of solvated electrons with solutes in alcohol/water mixtures have been reported for the methanol (106-108), ethanol (106-110), 1-propanol (112), 2-propanol (117), 1-butanol (113), 2-butanol (116), isobutyl alcohol (116) and t-butyl alcohol (115,116,118) systems.

The majority of kinetic investigations of solvated electrons in the alcohol /water mixed systems involve electron-scavengers of high electron affinity, so that the rates of reaction are limited mainly by the rate at which the reactants diffuse together. The rate constants for such fast reaction are of the order of  $10^7 \text{m}^3/\text{mol.s}$ . The composition dependence of the nearly diffusion controlled rate constants has been analyzed using the Stokes - Smoluchowski (130) and Debye (131) models. The rate constants for the reactions with inefficient electron-scavengers are explained in terms of the energy of solvation of electrons in the different solvents, rather than in terms of solvent transport properties (115,116).

In the Stokes-Smoluchowski model, the diffusion controlled rate constant ( $k_d$ ) for the reaction between species x and y is related to the viscosity ( $\eta$ ) of the medium, and the diffusion radii ( $r$ ) and reaction radii ( $R$ ) of the reactants.

$$k_d = \frac{N_A k_B T}{1.5 \eta} \left( \frac{1}{r_x} + \frac{1}{r_y} \right) (R_x + R_y) \quad [1-4]$$

where  $N_A$  is the Avogadro's constant,  $k_B$  is the Boltzmann's constant and  $T$  is the temperature.

For a number of alcohol/water mixture systems, the experimental second-order rate constants ( $k_2$ ) for the reaction between nitrobenzene and solvated electrons are inversely proportional to the viscosity of the solvents in the composition range of  $\chi_{\eta_{\max}} \leq \chi_w \leq 1$  (where  $\chi_w$  is the mole fraction of water in alcohol and  $\chi_{\eta_{\max}}$  is the mole fraction of water in alcohol at the maximum viscosity), which indicate that the factors  $(1/r_x + 1/r_y)(R_x + R_y)$  in equation [1-4] do not vary much in this region (112,115). For solvent composition of  $\chi_w < \chi_{\eta_{\max}}$ , the viscosity dependence of the rate constant is more complex. For example, in the 1-propanol/water mixture system, the  $k_2$  value in the composition region of  $0.1 \leq \chi_w \leq 0.7$  decreases as the viscosity decreases, whereas in the  $0 \leq \chi_w \leq 0.1$  region, there is a sharp increase in  $k_2$  regardless of the slight increase in viscosity (112). These results have been explained by consideration of the microscopic structures of the alcohol/waters, that was suggested in the studies of the optical absorption spectra of solvated electrons (23). Since the diffusion coefficients of the reacting species depend on the microscopic structures of the liquid, the nearly diffusion controlled reaction rate constants are affected by the microscopic structures of the medium (112-118).

The Debye modification (131) of the Smoluchowski relation (equation [1-5]) has been used to analyze the solvent effects on the reaction kinetics of solvated electrons with charged and polar scavengers in tert-butyl alcohol/water mixtures (118). In the Debye model a factor  $f$ , which considers the coulombic interaction potential  $U(R)$  between the electron and a dipolar or ionic solute, is applied to account for the enhancement (or retardation) of the diffusion rate constant due to electrostatic attraction (or repulsion) at the encounter distance  $R = R_x + R_y$ .

$$k_d = \frac{N_A k_B T}{1.5 \eta} \left( \frac{1}{r_x} + \frac{1}{r_y} \right) (R_x + R_y) f \quad [1-5]$$

where  $f = (U(R) / k_B T) [ \exp ( U(R) / k_B T ) - 1 ]^{-1}$  [1-6]

Both the Smoluchowski and Debye relations consider the bulk (macroscopic) viscosity of the solvent. This may be different from the microscopic viscosity experienced by the diffusing reactants. The local viscosity around a polar solute is related to the bulk viscosity and to other dynamic dielectric properties of the medium, which may also influence the effective diffusion radii of the reactants (132). The effect of static dielectric constant on the viscosity normalized rate constants ( $\eta k_2$ ) for a number of electron-organic solute reactions was found to be similar to that on the Walden product ( $\eta \lambda_0$ , where  $\lambda_0$  is the limiting molar conductance) for ions in ethanol/water mixtures (113). This suggests that the diffusion coefficients for both organic solutes and inorganic ions decline towards the pure alcohol. However, as the water content of the medium increases, the  $k_2/\lambda_0$  ratio decreases. This reflects the smaller diffusion coefficient of ions than of organic solutes in the alcohol-rich solvents. The larger effective radii of diffusion and reaction in alcohol than in water may be explained by considering the solvation structure of the solutes. In alcohol, the solutes are solvated by the hydroxy ends of the molecules, and when the two solvated species diffuse together, they are buffered by the alkyl groups (113).

Solutes that have low electron affinities have low reaction rate constants. The composition dependence of such rate constants has been attributed to the variation of solvated electron trap depth (98,112-113,115-116), which is related to the optical absorption energy (12). Electrons in the shallower traps have a greater probability of reaction than those of the deeper traps, so the optical absorption energy ( $E_T$ ) half way up the low energy side of the band was used to correlate  $k_2$  with the electron trap depth.

The effects of temperature on reaction kinetics can also provide valuable data for postulating mechanisms. Changes in reaction rates due to temperature change are generally expressed in terms of the activation energy ( $E_a$ ) and the frequency factor ( $A$ ) of the Arrhenius equation [1-7]:

$$k = A e^{-E_a/RT} \quad [1-7]$$



Information about solvent effects on reaction rate parameters  $A$  and  $E_a$  of solvated electrons assists in achieving a better understanding of the nature of the reaction.

There is a correlation between the activation energy of reaction and the activation energy of viscous flow ( $E_\eta$ ) (115,116). Organic reactants that are less soluble in water seem to have higher activation energies (115). This may suggest that electrons are preferentially solvated by water and the organic solute is preferentially solvated by alcohol, which raises the energy required for the close approach of the reactant.

Entropies of activation are more negative for less efficient scavengers. The difference of reactivity between efficient and inefficient scavengers is due mainly to changes of entropy rather than of energy (115).

## VI Present Work

When this work began, few data were available concerning the pulse radiolysis of alcohol/water mixtures. Information was especially lacking about temperature effects on the reactions of solvated electrons in water mixed with the two smallest alcohols, methanol and ethanol. The objective of the present work is to learn more about the behavior of solvated electrons in methanol and ethanol/water mixed solvents, by studying the kinetics of their reactions with a number of organic and inorganic solutes.

## CHAPTER TWO

### EXPERIMENTAL

#### I Materials

Methanol (spectrophotometric grade, gold label, 99.9%) was obtained from Aldrich Chemical Company. It was treated for three hours under argon (Linde, ultra-high purity grade, 99.999%) with sodium borohydride (Fisher Scientific, reagent grade) (one gram per liter of methanol) at 328K. It was then fractionally distilled under argon, through a 52 x 2.5 cm column packed with 0.6 cm glass beads, discarding the first 20% and last 35%. The middle fraction was collected and kept in an argon-pressurized syphon system. The water content measured by Karl-Fisher titration was 0.04 mol. %.

Absolute-reagent grade ethanol was obtained from the U.S. Industrial Chemical Company. Experience had shown this to be the best available (133) having reported maximum impurity levels of 50 ppm water, 5 ppm methanol, and less than 1 ppm benzene, halogen compounds or carbonyl compounds. Treatment by the purification method used with methanol resulted in no improvement in purity. The water content measured by Karl-Fisher titration was 0.04 mol. %.

The solvated electron half-life after a 100 ns pulse of 1.9 MeV electrons ( $2 \times 10^{16}$  eV/g) at 298K was 4  $\mu$ s for methanol, and 6.5  $\mu$ s for ethanol.

Toluene (Aldrich, gold label) was distilled over sodium under argon. Phenol (Aldrich, 99+%) was sublimed three times under reduced pressure (0.75 torr) at 308K. Lithium chromate (K and K, reagent grade) was dried overnight using an Abderhalden drying pistol under reduced pressure (0.1 torr) at 328K with phosphorus pentoxide powder (American, reagent grade). Nitrobenzene (Aldrich, 99+%, gold label), acetone (Aldrich, 99+%, spectrophotometric grade, gold label), lithium nitrate (Aldrich, 99.999%, gold label), silver perchlorate (Strem, reagent grade) and copper (II) perchlorate (Aldrich, reagent grade) were used as received.

Water from two sources was used. Laboratory distilled water supply (from a Bransted continuous distillation apparatus that produce distilled water at a rate of 15 gallons/hr.) was used as the starter in both cases. In one method this water was first distilled from a Coring AG-1b distillation apparatus, then re-distilled from alkaline permanganate through a one-meter glass-packed column in a stream of ultra high pure argon. In the other method distilled water was passed through a Barnstead Nanopure II ion exchange system. The solvated electron half-life in either case was 20  $\mu$ s.

## II Apparatus for Kinetic Measurements

### 1. Sample Cells

Cells of Suprasil Quartz from Terochem Laboratories were used at atmospheric pressure for temperatures varying from 223K to 283K. The optical path length was 1 cm, and the inside dimensions were 1 x 1 x 4.5 cm. The cell was topped by a grade seal so that it could be attached to a Pyrex tube.

### 2. Argon-Bubbling System

Samples in quartz cells were argon bubbled prior to irradiation. The argon bubbling system (Fig. 2-1) was made by attaching 1 cm<sup>3</sup> syringes to a Pyrex tube. Pyrex/Teflon stopcocks (No. 7282, Canadian Laboratory Supplies Ltd.) were used to control the rate of gas flow through the stainless steel needles (30 cm long, 0.625 mm i.d.). The rate of bubbling was 20 cm<sup>3</sup>/minute.

### 3. Irradiation, Detection and Control Systems

#### A. The van de Graaff Accelerator

The source of high energy electrons was a type AK-60 2MeV van de Graaff Accelerator (VDGA) manufactured by High Voltage Engineering Corporation. The maximum peak current delivered during a pulsed operation was 150 mA. Pulse durations

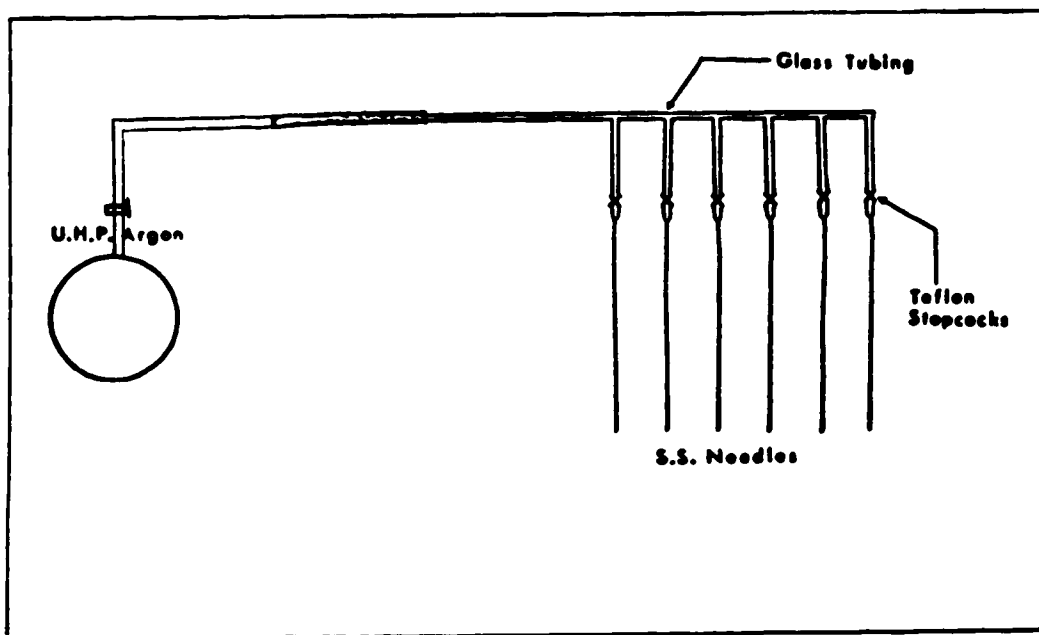


Fig. 2-1 The Bubbling System

of 3, 10, 30, 100 nanoseconds (ns) and 1 microsecond ( $\mu$ s) were available. The 30 and 100 ns pulse durations were used to obtain an appropriate pulse dose.

The entrance from the control room to the accelerator and target room was shielded by a concrete maze. Closing and locking the iron-gate at the control room end of the maze sounded a warning buzzer for 15 seconds. Accelerator operations was possible only after cessation of the buzzer. Opening of the iron-gate resulted in immediate shutdown of the accelerator.

The method commonly used to monitor the steering and focussing of the electron beam was to fix a piece of phosphorescent paper to the end of the accelerator beam pipe. The paper could be viewed by a closed circuit television. Each pulse of electrons caused a visible glow where it struck the phosphor, enabling accurate steering and focussing by adjustment of the current in the electromagnets. When equipment blocked visual observation, the beam could be steered by maximizing either the secondary emission monitor's (SEM) dose or the optical absorption of solvated electrons in a water sample.

Typical beam diameter at the electron window was 2.5 cm, with the most intense portion confined to an area of about 1 cm<sup>2</sup>.

#### B. Secondary Emission Monitor

The relative dose for each electron pulse was indicated by a secondary emission monitor (SEM). It consisted of three thin metal foils placed inside the accelerator beam pipe close to the electron window (Fig. 2-2). These metal foils were cobalt based high strength alloy sheets (0.0025 mm), and were obtained from the Hamilton Watch Company, Precision Metal Division. The low average atomic number (approx. 27) of this material made it superior to gold (atomic number 79) because of less beam attenuation by electron scattering.

The 5 cm diameter foils were separated by 0.5 cm. The outer two were maintained at a potential of 50 V. Passage of an electron pulse generated secondary electrons at the foils.

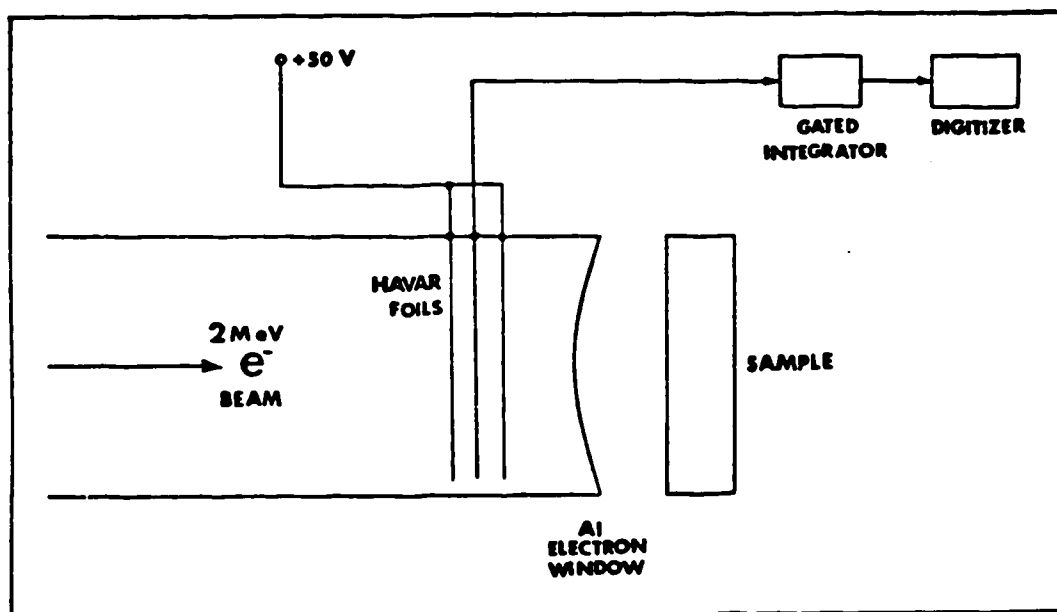


Fig. 2-2 The Secondary Emission Monitor

The electrons ejected from the centre foil were collected by outer foils, the net result being a current flow from the centre foil. Current flow occurred only during a high energy electron pulse and was measured by a gated integrator, digitized and displayed on a digital readout.

### C. Optical Detection System

#### (a) The Analyzing Light

A schematic diagram of the path of the analyzing light is shown in Fig.2-3.

The light source was a high pressure Xenon arc lamp (Optical Radiation Corporation, model XLN 1000 W) contained in a lamp housing (Photochemical Research Associates, model PRA ALH 220). A rhodium coated off axis paraboloid mirror (Melles Griot-02 POH 015) placed in the beam path absorbed the UV light with wavelength shorter than 320 nm. This prevented excess ozone formation in the room. The lamp was run at 1 kW and pulsed to 9.75 kW for 500  $\mu$ s when a decay signal was desired.

A light shutter protected the sample from unnecessary exposure by opening for only 55 ms. The above mentioned mirror was used to focus the light beam at the center of the irradiation cell. Front surface aluminized mirrors coated with silicone monoxide were used to reflect the light beam from the irradiation room to the control room through a hole in the 1.2m thick concrete wall. Finally a concave mirror was used to focus the light into the monochromator housing.

#### (b) Monochromator Grating and Filters

The monochromator was Bauch and Lomb type 33-86-25. The two gratings used were type 33-86-02 for light from 350 nm to 800 nm and 33-86-03 for light from 700 to 1000 nm. The two Corning filters used were type CS-2-64 for wavelengths between 700 to 1000 nm, and CS-3-73 for wavelengths between 480 to 700 nm. The front and back slit widths of the monochromator were 2.5 mm and 1.4 mm, respectively.

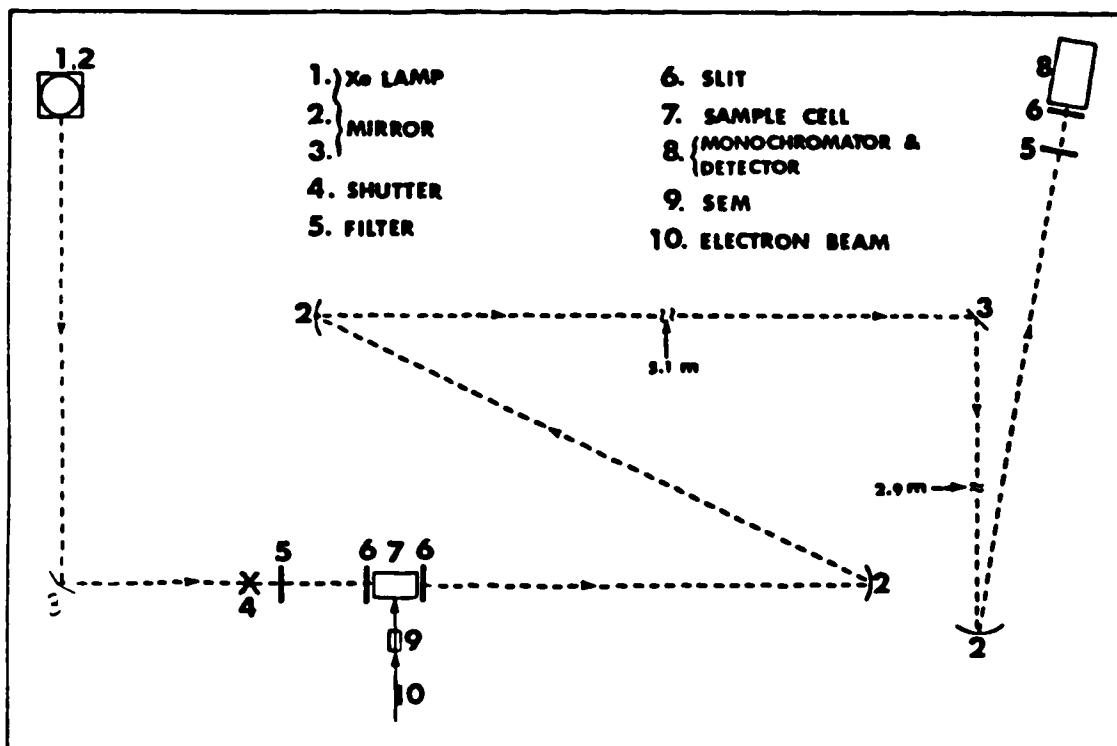


Fig. 2-3 The Path of the Analyzing Light



(c) Digital voltmeter, Oscilloscope and Plotter

The incident light intensity at the detector was recorded as a voltage on a digital multimeter (Fluke 8810A), displayed on an oscilloscope (Tektronix R7623) and plotted on a digital plotter (Zeta 1200). The signals were displayed as plots of voltage against time. All the information related to the particular signal (total light, dose, temperature, sensitivity, time scale, signal starting point, half-life curve and cell holder number) were also printed on the chart.

D. Temperature Control System

(a) Cooling and Heating Systems

Temperatures from 223K to 298K were achieved by boiling liquid nitrogen and regulating the temperature of the resulting nitrogen gas by using another heater. Liquid nitrogen was boiled at a controlled rate from a 50 L, Narrow necked aluminum Dewar vessel (Lakeshore Cryotonics Inc.). A stainless steel pipe (5 cm diameter) extended to the bottom of the Dewar. It was fixed to a lid which fitted snugly into the neck of the Dewar. A 600 W nichrome heating coil was attached to the inside of the steel pipe to about 7 cm from the bottom. When being used, only 190 W was applied to this heating coil.

Cold nitrogen gas was transported to the sample box through one meter of Rubatex foam-rubber pipe. Both ends had glass inserts to which a leather seal was connected. Cold air that came from this pipe flowed through another stainless steel pipe (2.5 cm diam.) that had a Nichrome heating wire (0.024 cm diam. x 4 m Long) inserted inside it, before entering the cell box. This heating coil regulated the nitrogen gas to the required temperature.

Temperatures from 296K to 373K were obtained using air from a laboratory heat gun (Master Appliance Corporation, model AH 0751). The nichrome wire heated the air to the required temperature.

**(b) Cell Holder Box**

Eight cell holders were mounted on a circular (7 cm diam.) aluminium base, which was connected to a motor. This system was fixed inside a box insulated with foam glass (Pittsburg Corning Corporation). When the cells were not being pulse irradiated, the cell holder made continuous clockwise and counterclockwise full cycle rotations. Just before a pulse was given, the pre-selected cell stopped in front of the electron window. The gas entered the cell box (40 cm high, 8cm i.d.) below the aluminum base and was stirred by the rotating cell holder before leaving a 2.5 cm diameter hole in the lid.

The temperature of the system was monitored using a thermocouple mounted in a cell filled with solvent. A temperature sensor used by the temperature controller (Taylor Microscan 1300) was also fixed to one of the cell holders. The temperature of the thermocouple cell was measured by a Fluke Digital Thermometer (model 2100A). Thermal equilibrium in the system was established when the thermocouple cell indicated a steady temperature for a period of 15 minutes. Once the thermal equilibrium was reached, the temperature of the thermocouple cell varied only 0.1 K.

**III Apparatus for Conductivity Measurements****1. Impedance Bridge**

The type 1608-A Impedance Bridge (General Radio Co.) was a self-contained impedance-measuring system, which included six bridges for the measurement of conductance, capacitance, resistance, and inductance, as well as the generators and detectors necessary for DC and AC measurements. To obtain the conductance reading, the bridge was set to the conductance mode and the variable resistor and capacitor were adjusted until null balance was achieved. An oscillator frequency of 1 kHz was used for the AC measurements.

## 2. Conductance Cells

Pyrex conductivity cells (YSI 3403) from Yellow Springs Instrument Co., Inc. were used for temperatures varying from 283K to 358K. The cell chamber was 5 cm deep, overall length was 20 cm, o.d. 1.2 cm.

Graduated cylinders (25-cm<sup>3</sup>, 16 cm long, 1.4 cm i.d.) were used to contain the electrolyte solutions. A rubber adaptor made from a size no.2 stopper was used to provide a tight seal between the cell and the solution container. The wrapping of 2 to 4 layers of parafilm (American Can Company) around the adaptor-container junction was essential to secure a tight seal at elevated temperatures.

Calibration of cells were performed at 298.15K using a secondary standard solution (YSI 3161) available from Yellow Springs Instrument Co., Inc.. This calibration solution contained water, 0.0002% iodine as an anti-microbial, and sufficient ACS reagent grade potassium chloride to attain a specific conductance of  $1000 \pm 5 \mu\text{S/cm}$ .

The electrodes of the cells were coated with platinum black. This coating was very important to cell operation. When the coating appeared to be wearing off the electrodes, the cells were cleaned using a solution of equal parts of isopropyl alcohol and 10 molar HCl, then replatinized using a replatinizing solution (YSI 3140) on a platinizing instrument (YSI 3139) at a current of 50 milliamp.

## 3. Constant Temperature Bath

Conductivity measurements at various temperatures were done in a 10 L glass Dewar vessel filled with distilled water (Fig. 2-4). The Dewar was equipped with a motor controlled stirrer, a refrigeration unit (Tecumseh model AE 1343AA) and a heating coil. The output of the heating coil was manually controlled by a variac (Ohmite, mode VT). A knife-heater (Cenco, 53 ohm, 350W) was controlled by a temperature regulating system (Fig. 2-5). The temperature was measured with a platinum resistance digital thermometer (Fluke, mode 2189A) to 0.01K. Temperature variations in the bath were recorded by a

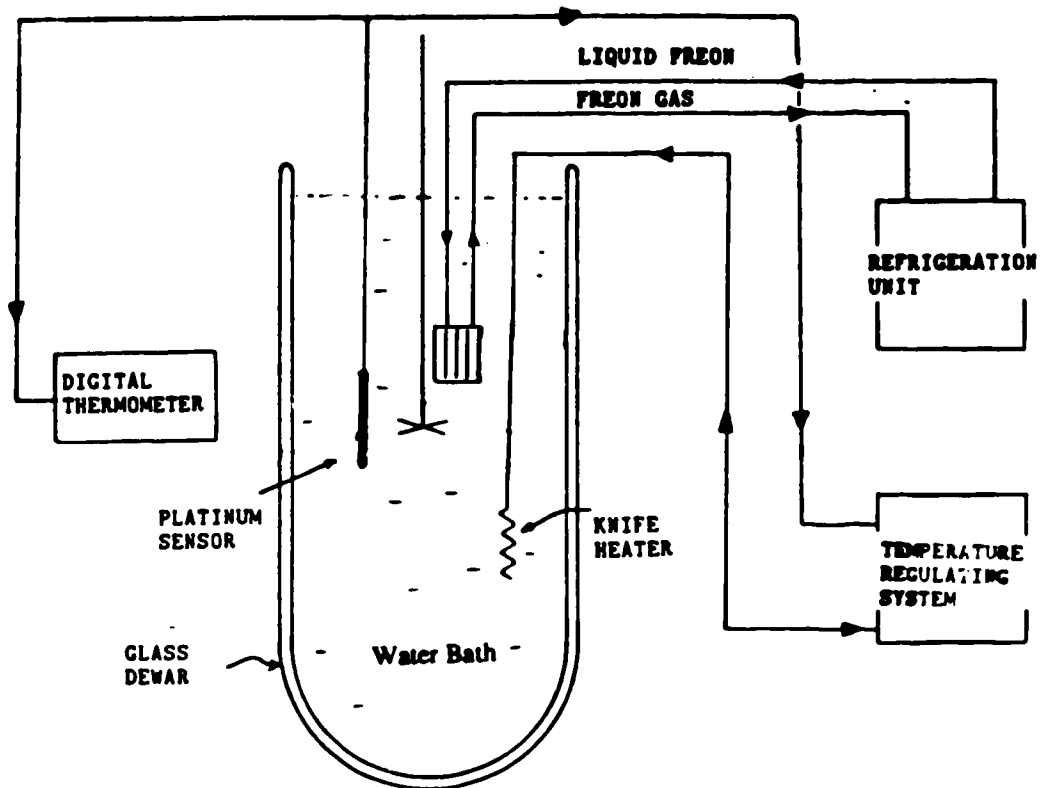


Fig2-4 Temperature Control of the Water Bath

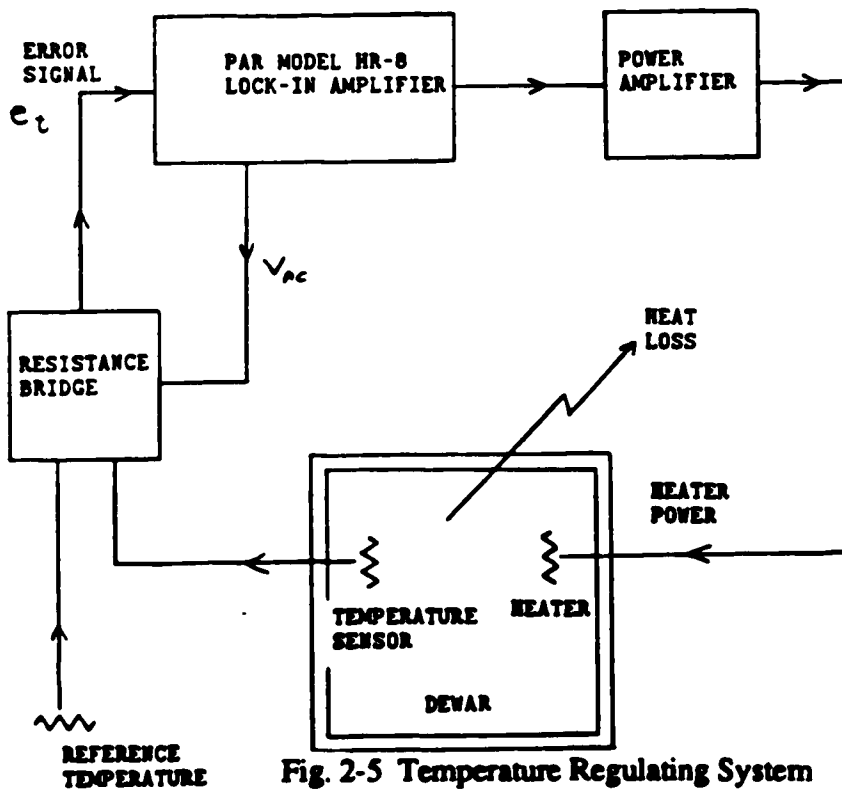


Fig. 2-5 Temperature Regulating System

chart recorder (Sargent, model SR), using a platinum resistance detector (Omega, model TFD). Thermal equilibrium in the system was established when the chart recorder showed a temperature variation of  $\leq 0.01\text{K}$  for 20 minutes.

#### IV Techniques

##### 1. Sample Preparations

Quartz cells and other glassware were cleaned by performing the following sequence of operations. First the vessel was rinsed twice with ethanol. While the surface was still alcohol wetted (with approx. 5 drops of alcohol in cell), a few drops of concentrated nitric acid were added. The resulting exothermic reaction caused the acid to boil vigorously. The acid was then removed by rinsing many times with distilled water, followed by dilute potassium hydroxide. Finally the vessel was rinsed many times with distilled water. The glassware and quartz cells were dried at 390K in a clean oven reserved for that purpose. New stainless steel syringe needles were washed first with hexane to remove oil and grease, then rinsed twice with methanol. They were finally rinsed many times with distilled water and oven dried. Before use they were rinsed several times with the solvent or the solution being used.

Solvent mixtures were prepared in volumetric flasks by volume measurements. Stock solutions were prepared in 10, 25 or 50 ml volumetric flasks. Liquid solutes were added by microlitre syringe (10, 50 or 100ul). Solid solutes were weighed in the volumetric flask on an analytical balance (August Sauter, model Monopan). The balance is readable to 0.1 mg with a precision of 0.1 mg, determined by repeated weighings of a constant weight. Aliquots of the stock solutions were transferred using syringes or volumetric pipets, then were diluted to make up a set of four to six different concentrations of sample solutions. For the conductance measurements, because the electrolyte containers were rinsed twice with the sample solutions before use, 25 ml of each of the electrolyte solutions were prepared.

For the pulsed radiolysis kinetic measurements, the sample solutions were de-aerated by bubbling with UHP argon at room temperature at a rate of approx. 20 cm<sup>3</sup> per minute for 30 minutes, and then sealed as illustrated in Fig. 2-6. Step 1 took place at room temperature. The syringe needle was then withdrawn to just above the liquid as shown in step 2. The argon flow rate was increased somewhat. The area around the sealing position was heated with a low flame to vaporize and flush out the volatile substances from the tube wall. The syringe needle was then further withdrawn as illustrated in step 3, and the seal was made as rapidly as possible.

The argon-bubbling method minimizes the dissolved gaseous impurities such as oxygen and carbon dioxide, it also, however, can easily evaporate the more volatile solutes (acetone and toluene) out of solution. This was a problem especially when the solute concentrations were low. Under these circumstances, the solute was injected into the solvent that had been argon-deaerated (30 minutes), and the solution was bubbled again with argon for two minutes, and then sealed.

The concentration of the organic solutes in solution was determined spectrophotometrically. For phenol and the more concentrated toluene solutions, after the kinetic runs, the samples were diluted 10, 25 or 50 times with solvent, and the absorbance was measured at the wavelength of the absorption maximum, using a 1 cm quartz cell. The absorbance of the solute was obtained from the correction of a solvent blank. For samples which contained low concentration of solute (nitrobenzene, acetone and toluene), the absorbance readings were taken directly in the reaction quartz cells. The absorbance of the solvent blank (i.e. before the solute was added to the same reaction quartz cell) was subtracted from the solution's absorbance to obtain the absorbance of the solute. The concentration of the organic solutes was then calculated using the Lambert-Beer law. The analytical wavelengths for the concentration measurements were chosen at the absorption maximum of the solutes. The molar extinction coefficients and absorption maxima of the organic solutes in the water-alcohol mixtures were also determined spectrophotometrically,

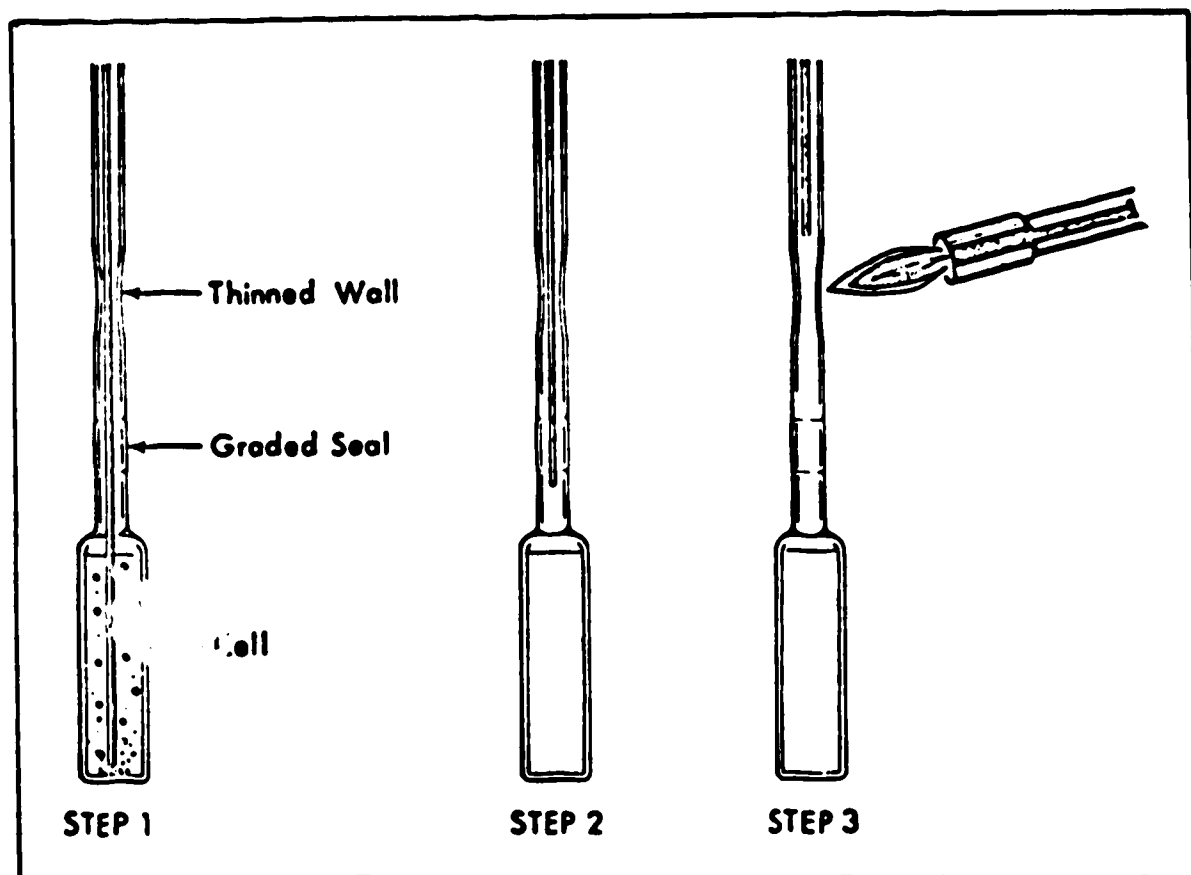
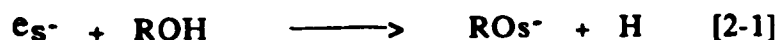


Fig. 2-6 The Sample Sealing Procedure

as described, using standard solutions of known concentration. The absorption maximum and the molar extinction coefficient varied slightly with solvent composition.

## 2. Kinetic Measurements

Solvated electrons can react with the hydroxylic solvent and the solute to yield a number of products (equations [2-1] and [2-2]).



Since the concentration of the solvent and the solute (scavenger) are much greater than of the solvated electrons, the kinetics of these reactions are first-order, and the observed first-order rate constant ( $k_{obs}$ ) is given by equation [2-3] :

$$k_{obs} = k_1 + k_2 [S] \quad [2-3]$$

$$\text{where } k_1 = k_s [ROH] \quad [2-4]$$

The decay kinetics of the solvated electrons was monitored at the wavelength of absorption maximum of the solvated electrons. A typical decay curve of the solvated electrons is shown in Fig. 2-7. The picture shows the first-order decay of the solvated electrons in the presence of  $2.31 \times 10^{-2} \text{ mol/m}^3$  of nitrobenzene in 60 mole % water-ethanol at 295.8K. It was recorded after a 100 ns pulse of 1.9 MeV electron, at a time sweep of  $1.0 \mu\text{s/cm}$ . The vertical scale is in millivolt/cm and is proportional to the absorbance at 690nm of the solvated electron.

The half-life of the solvated electrons,  $t_{1/2}$ , which is the time required for the concentration of solvated electrons to decrease by 50%, was measured from the picture. When the half-lives were measured from the decay curve, the first centimeter or so of the trace was usually ignored, because the beginning of the trace was sometimes not first-order. This could be due to the delayed response and noise of the electronic detector, or a contribution from geminate reaction, or both. In another method, the half-lives were



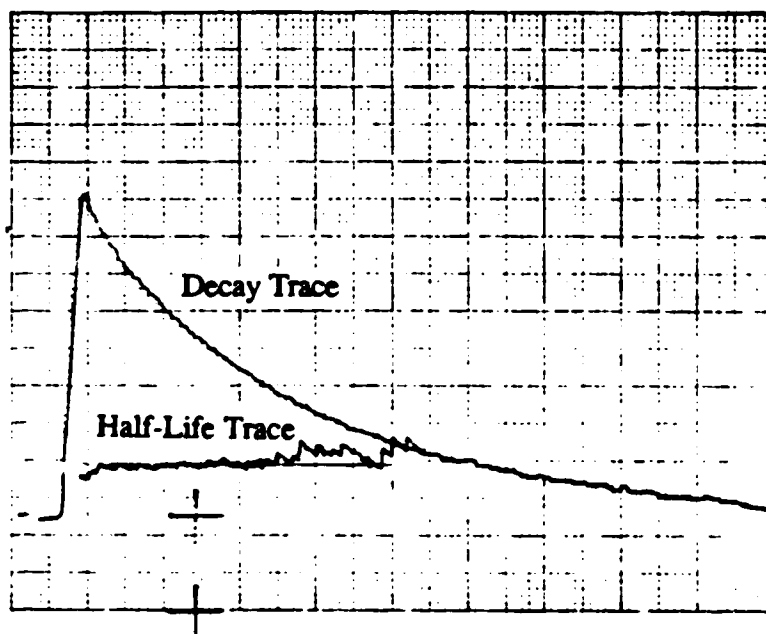


Fig. 2-7 Typical Solvated Electron Kinetic Trace

measured from a half-life curve generated by the computer. The computer calculated a large set of half-life values along the decay trace at a frequency of 51 points/centimeter, and plotted this set of half-life trace together with the decay trace onto the plotter. When the decay kinetic was first-order, the half-life trace was a horizontal line. The half-life was then obtained by measuring the vertical distance between the reference point (the lower "+" mark) and the horizontal line. Although the two methods for the half-life measurements were equivalent, the second method was preferred, because it not only allowed a more direct and rapid measurement of  $t_{1/2}$  but also provided a quick and easy way of indicating the region where the kinetics were first-order.

The  $k_{obs}$  of the system was calculated using the average half-life from at least two pictures, according to equation [2-5] :

$$k_{obs} = \ln 2 / t_{1/2} \quad [2-5]$$

Plots of the  $k_{obs}$  against at least four scavenger concentrations had a slope equal to the second-order scavenging rate constant,  $k_2$ . The error in the second-order rate constants was  $\pm 4\%$ . In water-rich/alcohol mixtures, the error of the toluene results may be  $\pm 10\%$ . The second-order rate constants obtained at different temperature were used to determine the Arrhenius activation energy parameters. Activation energies ( $E_a$ ) were calculated from the slope of a plot of the log of the second-order rate constant against the reciprocal of the absolute temperature (equation [2-6]), and entropies of activation at 298K were calculated from equation [2-7]. The errors in the calculated  $E_a$  and  $\Delta S^\ddagger$  values were  $\pm 1\text{kJ/mole}$  and  $\pm 3\text{J/mol.K}$ .

$$\ln k_2 = \ln A - E_a / RT \quad [2-6]$$

$$\Delta S^\ddagger = 19 (\text{Log } A - 9.8) \quad [2-7]$$

where A is in units of  $\text{m}^3/\text{mol.s}$

### 3. Conductivity measurements

The specific conductance ( $\kappa$ , in siemen/meter) was calculated from the conductance measured ( $L$ , in siemen) according to equation [2-9] :

$$\kappa = C \times L \quad [2-29]$$

where  $C$  is the cell constant in meter<sup>-1</sup>

The molar conductance,  $\Lambda$ , in units of Sm<sup>2</sup>/mol, was obtained as the slope from a plot of the specific conductance against at least four electrolyte concentrations. The error was  $\pm 1\%$ . When the molar conductance was independence of the concentrations within the concentration range studied, it is also equivalent to the limiting molar conductance. The activation energies of the conducting process ( $E_A$ ), were calculated from the slope of a plot the log of the molar conductance against the reciprocal of the absolute temperature near 298K. The error in the calculated  $E_A$  values was  $\pm 1$ kJ/mole.

## CHAPTER THREE

### RESULTS

#### I Reaction kinetics of solvated electrons with organic compounds

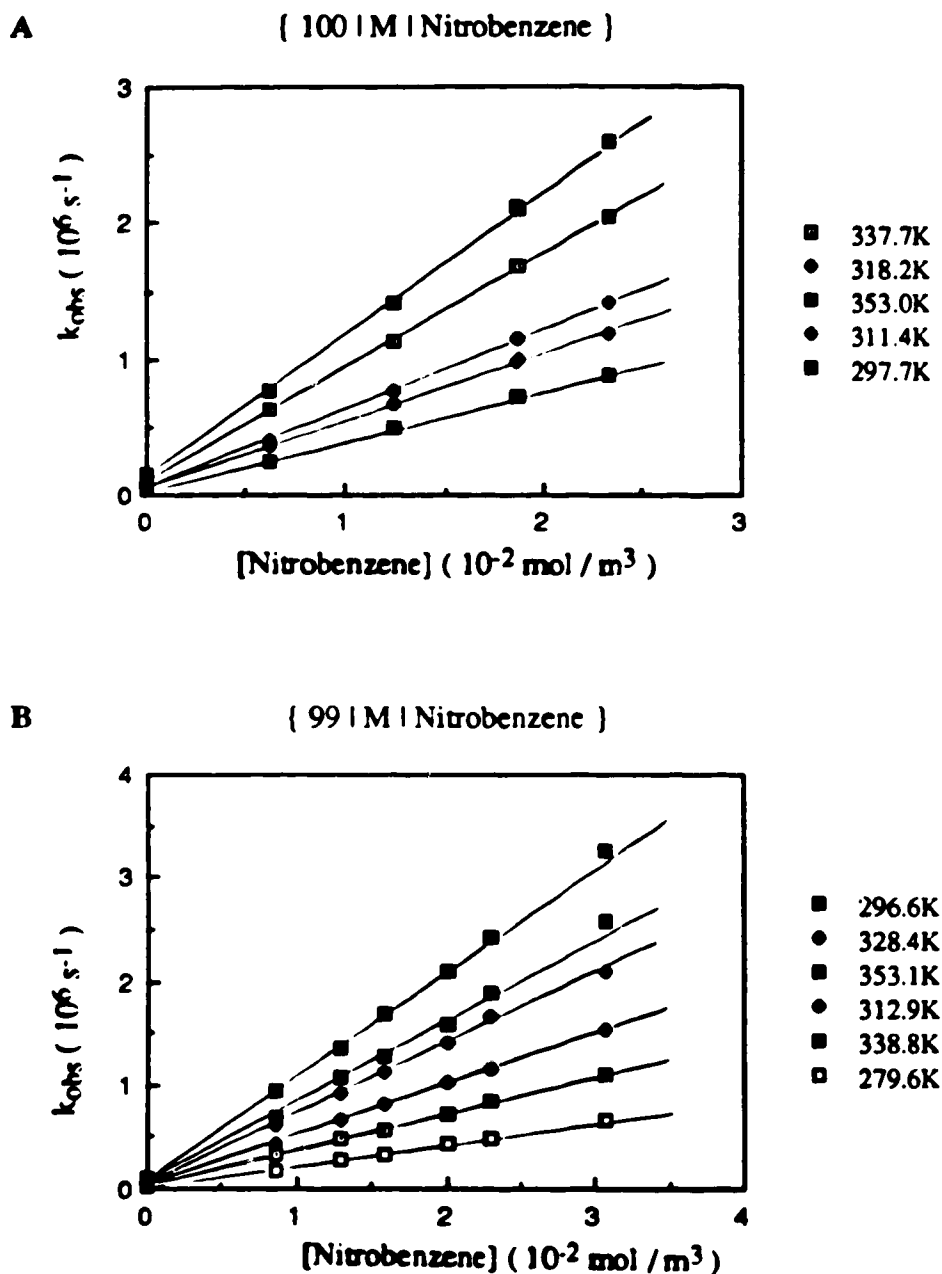
The kinetics of the reaction for solvated electrons with nitrobenzene, acetone, phenol and toluene were studied in methanol / water and ethanol / water mixed solvents of compositions ranging from pure alcohol to pure water.

##### 1. Reactions of solvated electrons in methanol / water mixtures

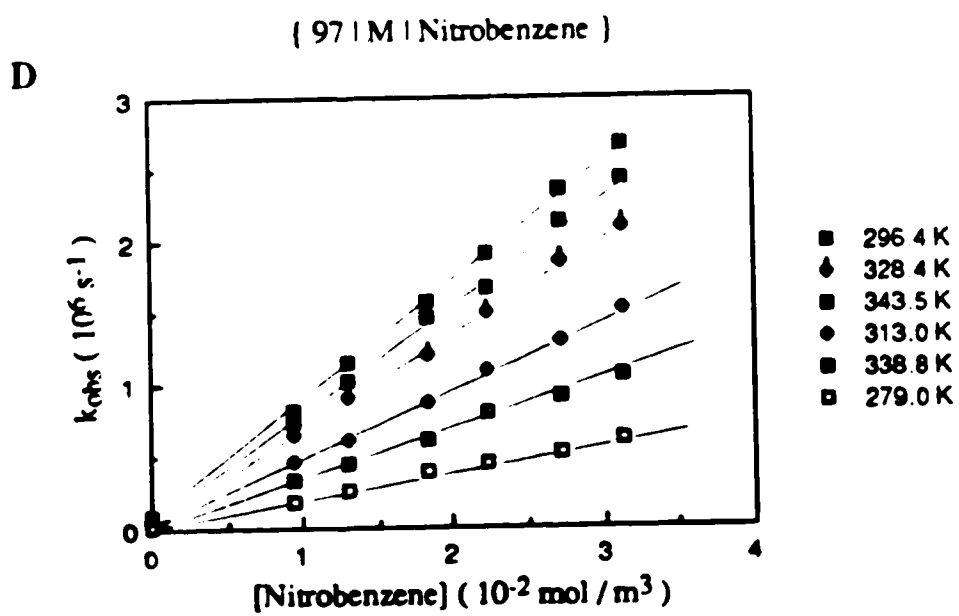
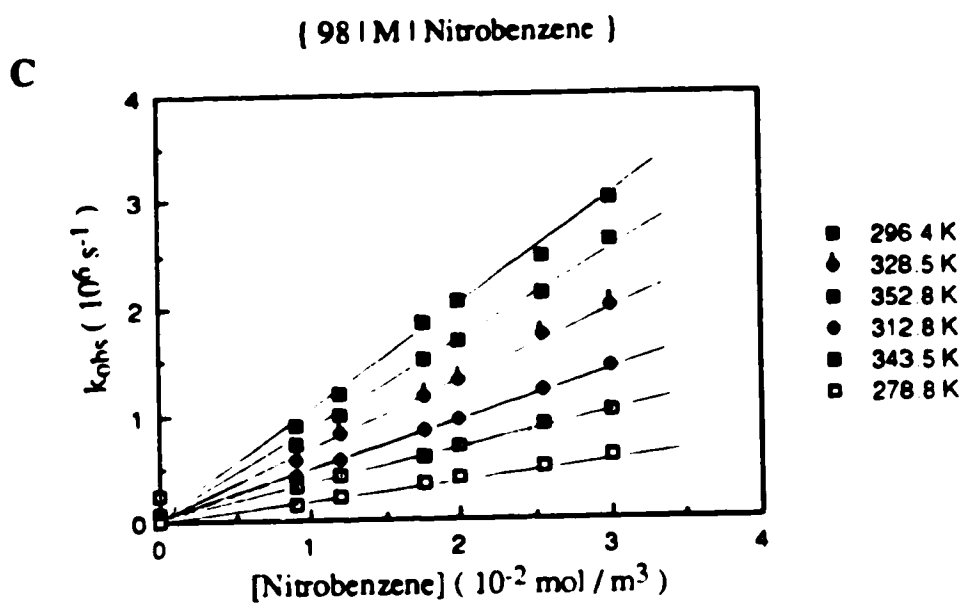
##### A. Reaction of solvated electrons with nitrobenzene

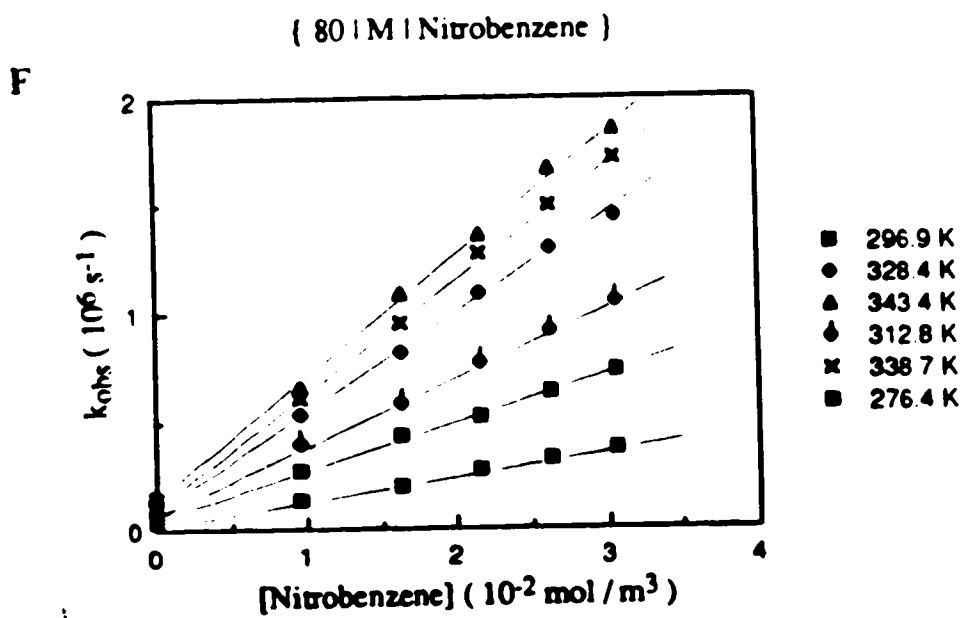
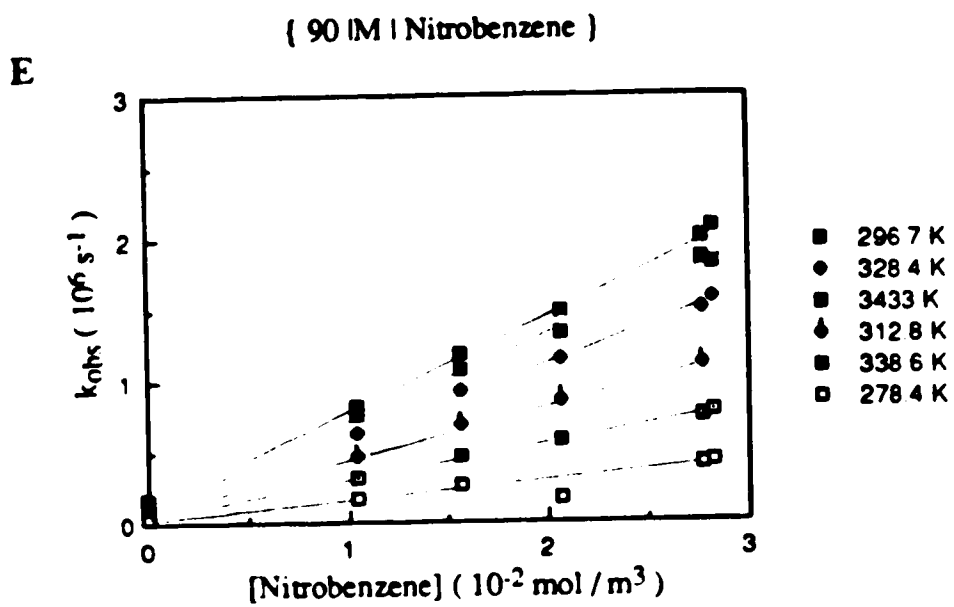
The temperature and concentration dependence of the first-order rate constant for the reaction of solvated electrons with nitrobenzene are shown in Figs.3-1(A-L). The concentration range of nitrobenzene was 6 - 42 mmol/m<sup>3</sup>. The second-order rate constants at various temperatures are given in Table 3-1. The rate constants  $k_{298}$  (at 298K) were obtained from the Arrhenius plots (Fig.3-2). The rate constant at 298K is  $3.7 \times 10^7$  m<sup>3</sup>/mol.s in water and  $2.4 \times 10^7$  m<sup>3</sup>/mol.s in methanol. The literature results are  $3.8 \times 10^7$  m<sup>3</sup>/mol.s (112,115) and  $4.2 \times 10^7$  m<sup>3</sup>/mol.s (100) in water and  $2.3 \times 10^7$  m<sup>3</sup>/mol.s (98,100) in methanol. The rate constants at 292K show similar composition dependence to those obtained by Milosavljević and Mičić (106), who conducted experiments at only one temperature. The comparison is shown in Fig.3-3. The composition dependences of  $k_{298}$ , activation energy and entropy of activation for the reaction of solvated electrons with nitrobenzene are summarized in Table 3-2. Graphic representation of these results is presented in the Discussion (Chapter Four), together with other organic electron-scavengers for comparison.

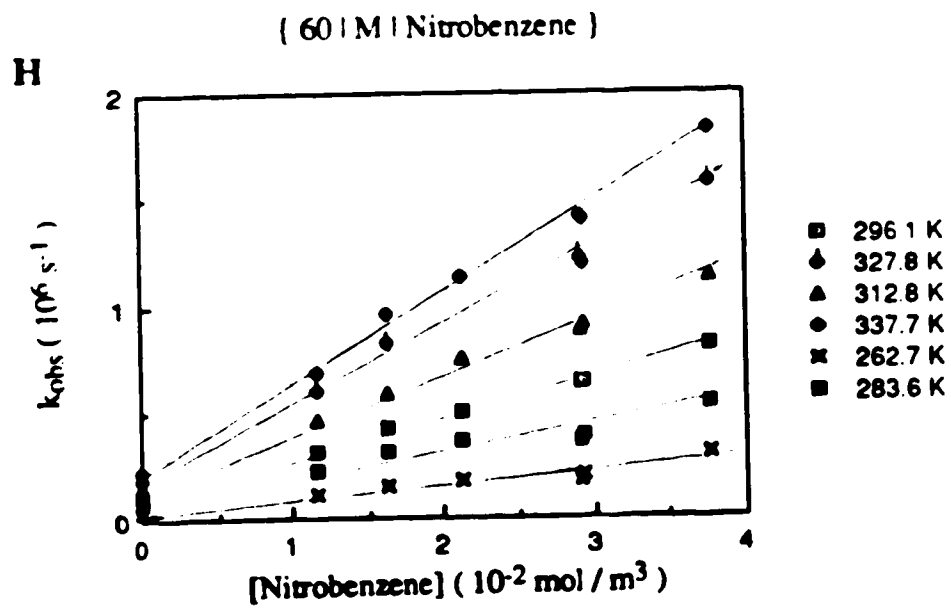
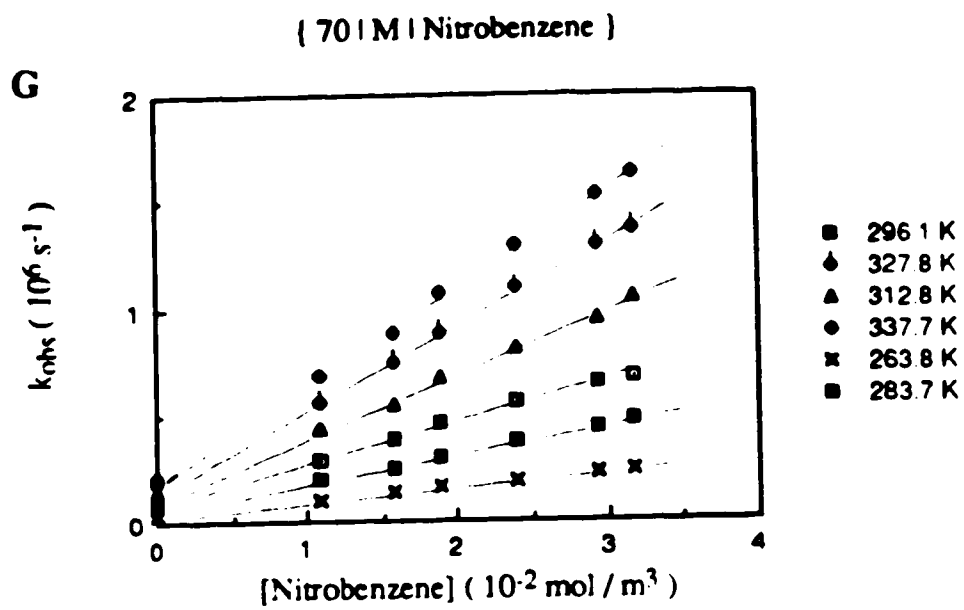
Fig. 3-1 (A-L) Temperature and concentration dependence of the first order rate constants for the reaction of solvated electrons with nitrobenzene in methanol / water mixtures.



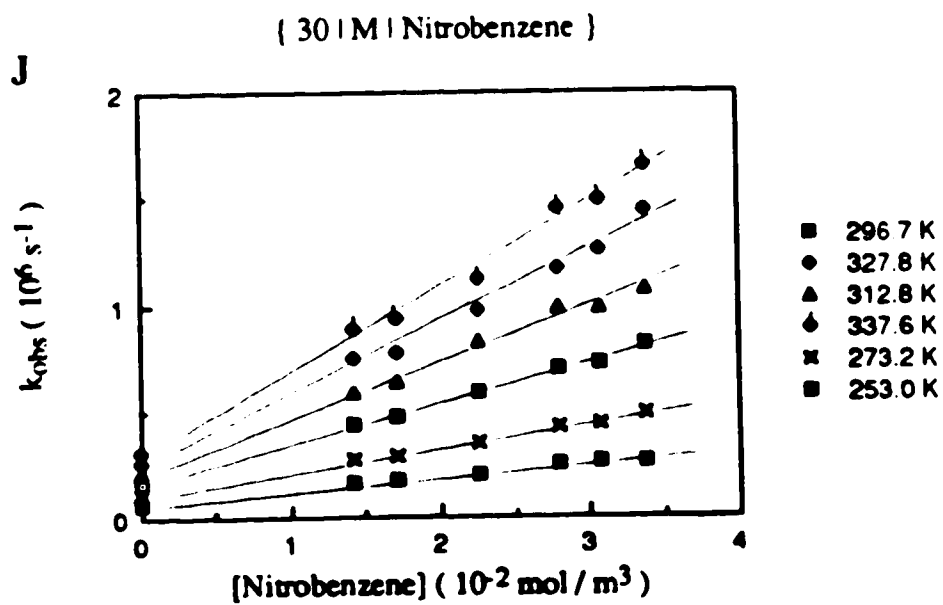
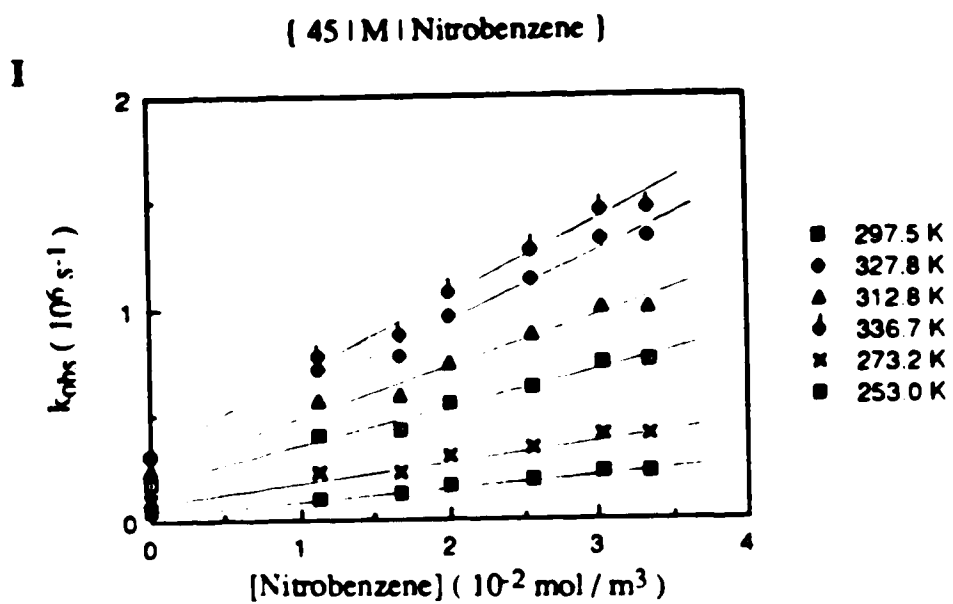
In the graph code { C | A | S }, C represents the mole % of water in the solvent mixture, A represents the alcohols and S the electron scavenger. The alcohols are represented by M for methanol and E for ethanol.











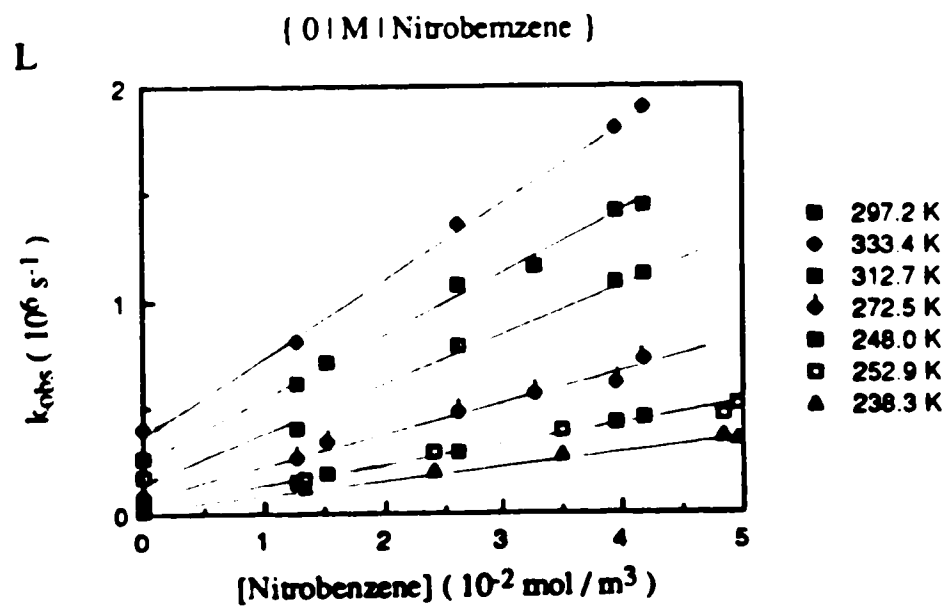
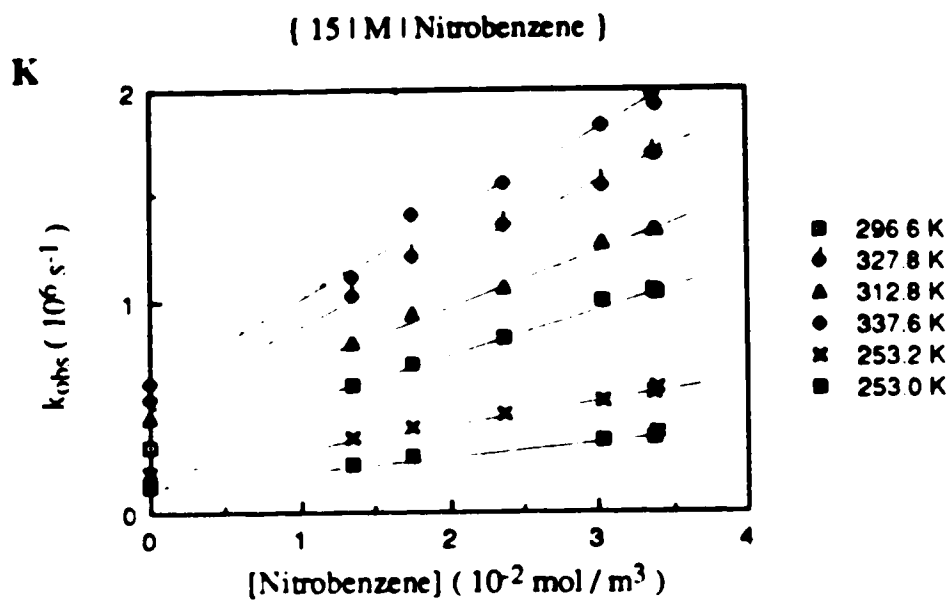


Fig. 3-2 Arrhenius plots for the reaction of solvated electrons with nitrobenzene in methanol / water mixtures

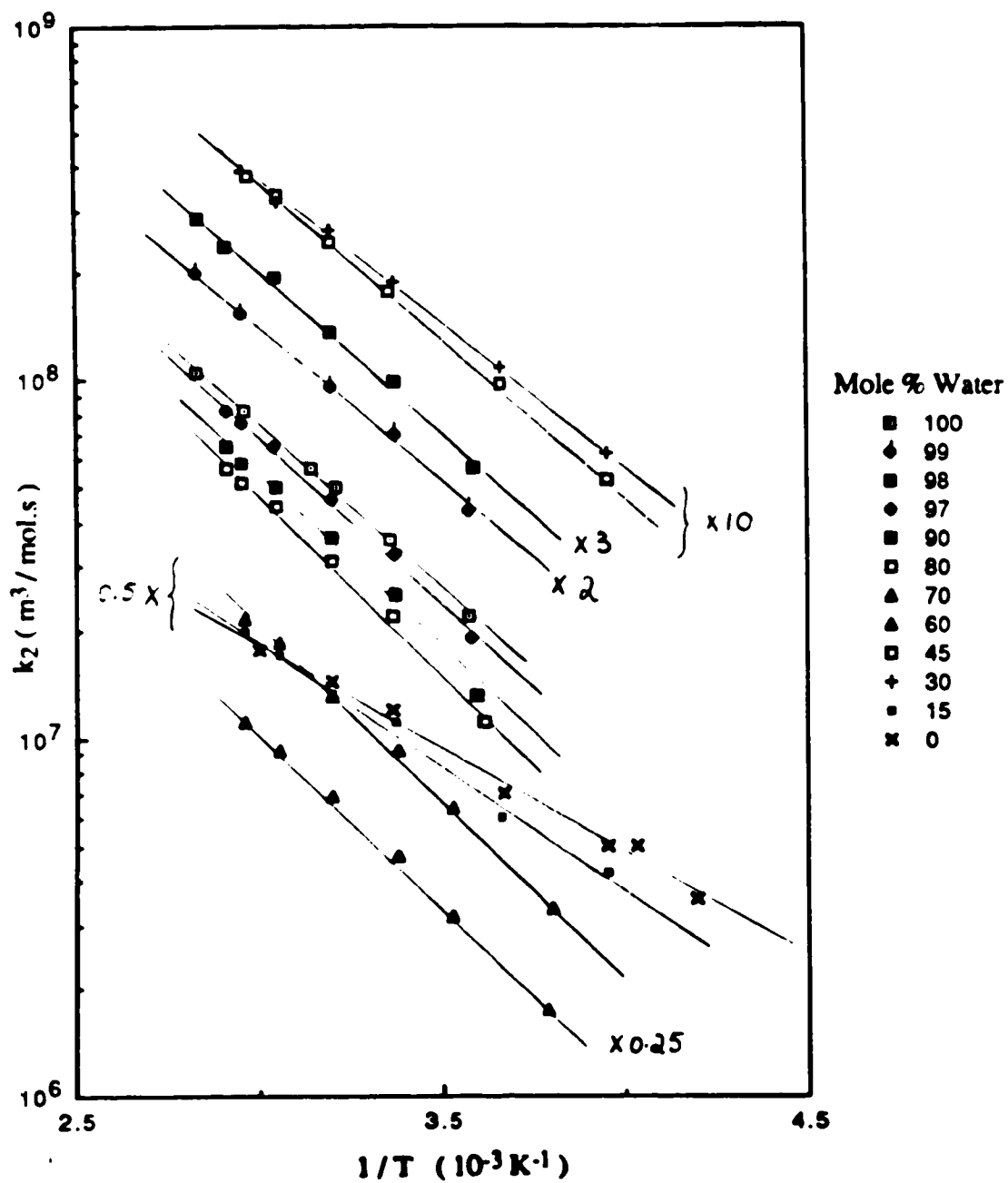
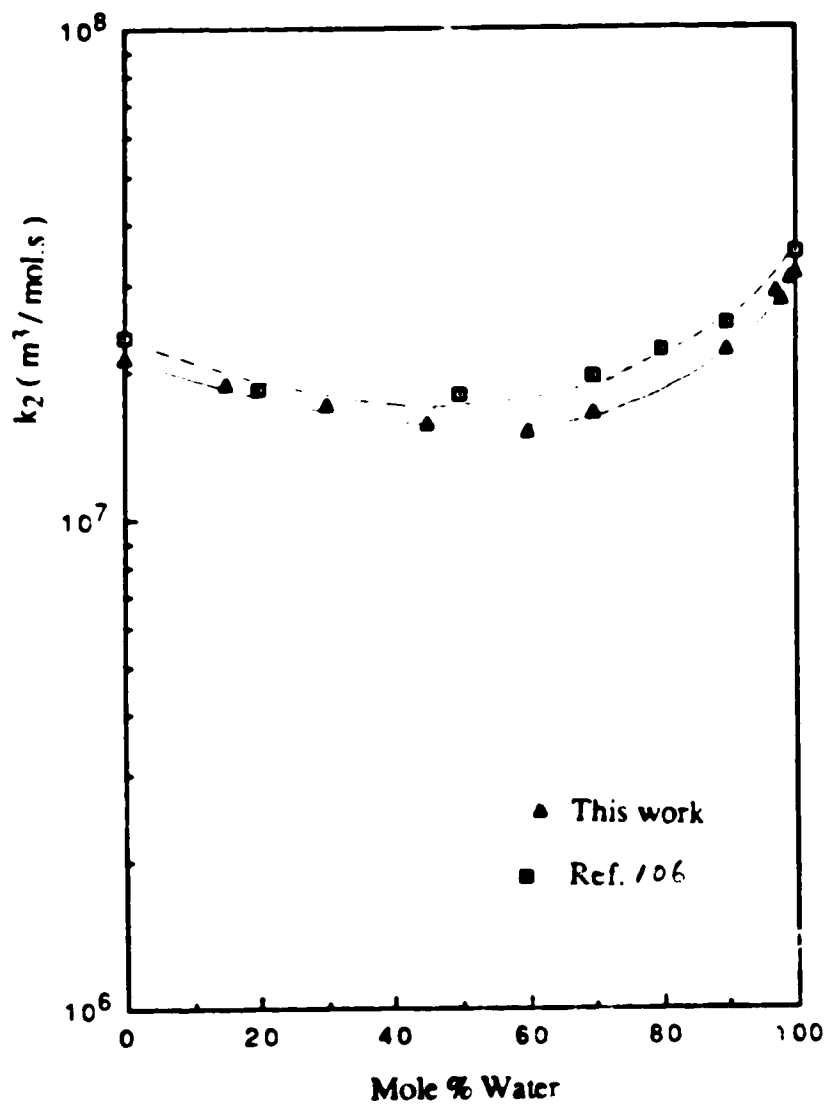


Fig. 3-3 Composition dependence of  $k_{292}$  for the reaction of solvated electrons with nitrobenzene in methanol / water mixtures



**Table 3-1 Second-order rate constants for the reaction of solvated electrons with nitrobenzene in methanol / water mixtures at various temperatures**

$\chi_w$	Temp.	$k_2$	$\chi_w$	Temp.	$k_2$	$\chi_w$	Temp.	$k_2$
	(K)	( $10^7 \text{ m}^3/\text{mol}\cdot\text{s}$ )		(K)	( $10^7 \text{ m}^3/\text{mol}\cdot\text{s}$ )		(K)	( $10^7 \text{ m}^3/\text{mol}\cdot\text{s}$ )
1.00	279.9	2.2	0.90	278.4	1.3	0.45	253.0	0.53
	297.7	3.6		296.7	2.5		273.2	0.98
	311.4	5.0		312.8	3.6		297.5	1.8
	318.2	5.7		328.4	5.0		312.8	2.5
	337.7	8.3		338.6	5.8		327.8	3.3
353.0	10.6	343.3	6.5	336.7	3.8			
0.99	279.6	2.1	0.80	276.4	1.1	0.30	253.0	0.62
	296.6	3.5		296.9	2.2		273.2	1.1
	312.9	4.8		312.8	3.1		296.7	1.9
	338.8	7.8		328.4	4.4		312.8	2.7
	353.1	10		338.7	5.1		327.8	3.2
			343.4	5.7	337.6	3.9		
0.98	278.8	1.9	0.70	263.8	6.9	0.15	253.0	0.84
	296.4	3.3		283.7	1.3		273.2	1.2
	312.8	4.6		296.1	1.9		296.6	2.2
	328.5	6.6		312.8	2.8		312.8	2.7
	343.5	8.0		327.8	2.8		312.8	3.4
352.8	9.6	337.7	4.4	337.6	4.0			
0.97	279.0	1.9	0.60	262.7	0.67	0.00	238.3	0.71
	296.4	3.3		283.6	1.3		248.0	1.0
	313.0	4.7		296.1	1.9		272.9	1.0
	328.4	6.5		312.8	2.6		272.8	1.4
	338.8	7.7		327.8	3.7		297.2	2.4
343.5	8.3	337.7	4.3	312.7	2.9			
						333.4	3.5	

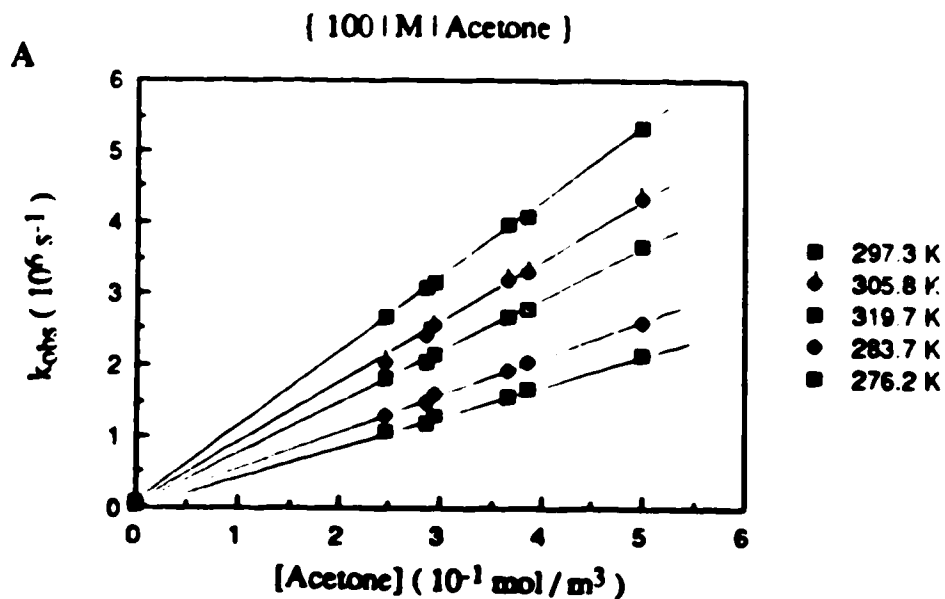
**Table 3-2** Rate parameters for the reaction of solvated electrons with nitrobenzene in methanol / water mixtures

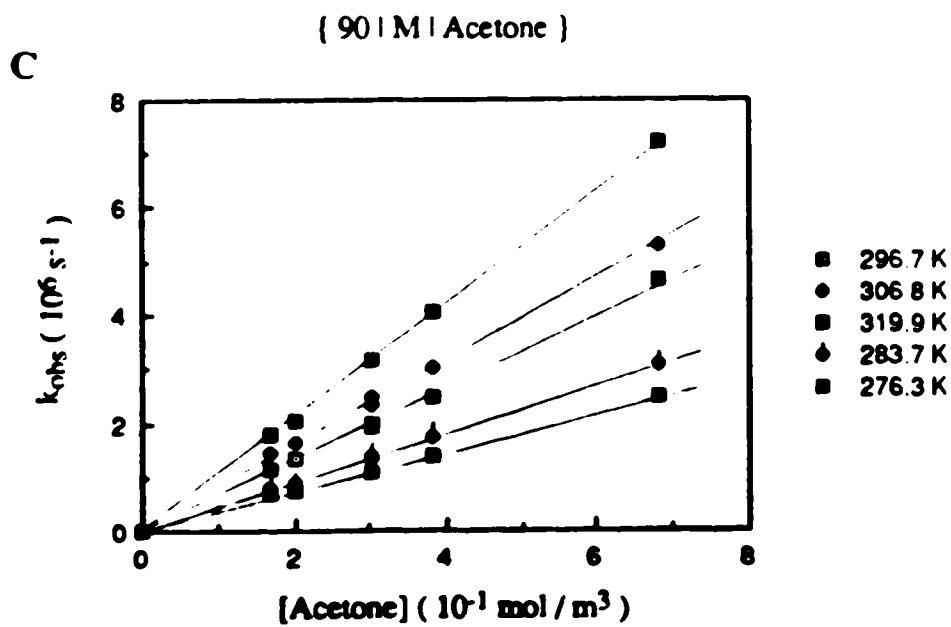
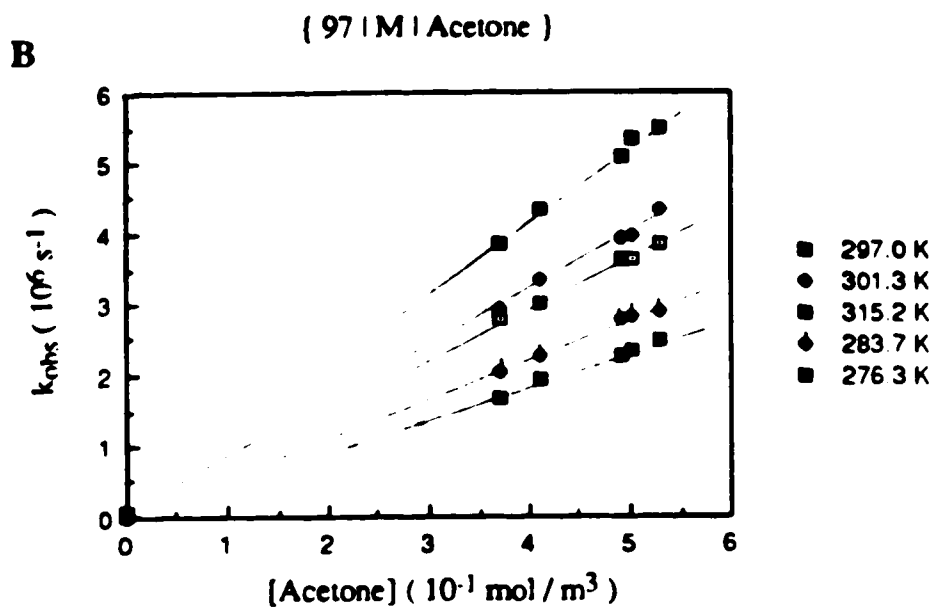
$\chi_w$	$k_{298}$ ( $10^7$ m <sup>3</sup> /mol.s)	$E_a$ (kJ/mol.)	LogA	$\Delta S^\ddagger$ (J/mol.K)
1.00	3.7	16	13.42	12
0.99	3.5	17	13.47	13
0.98	3.3	17	13.55	14
0.97	3.3	18	13.59	15
0.90	2.5	18	13.51	14
0.80	2.2	18	13.50	13
0.70	1.9	18	11.50	13
0.60	1.9	18	13.41	12
0.45	1.8	17	13.17	7
0.30	1.9	15	12.92	2
0.15	2.1	13	12.66	-3
0.00	2.3	11	12.30	-10

### B. Reaction of solvated electrons with acetone

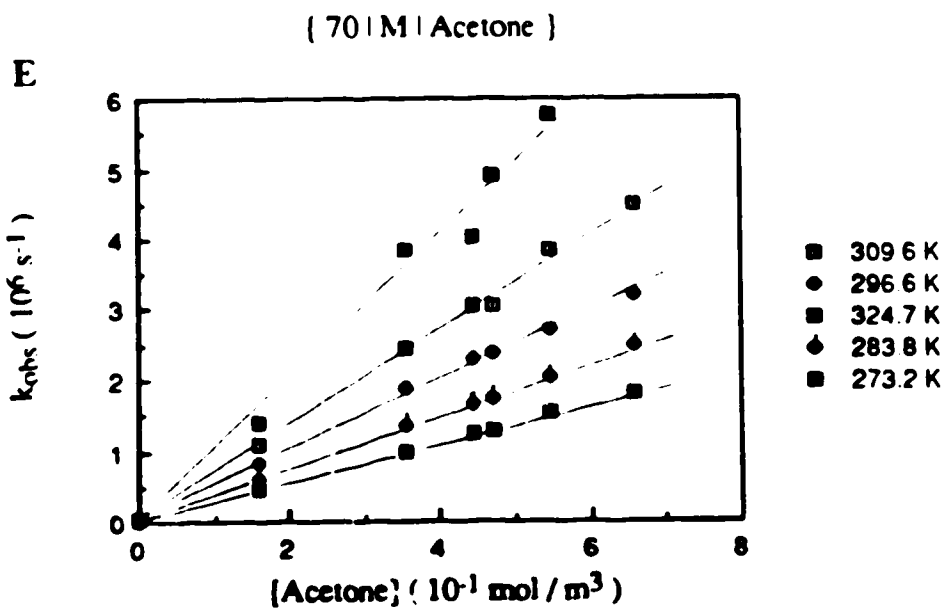
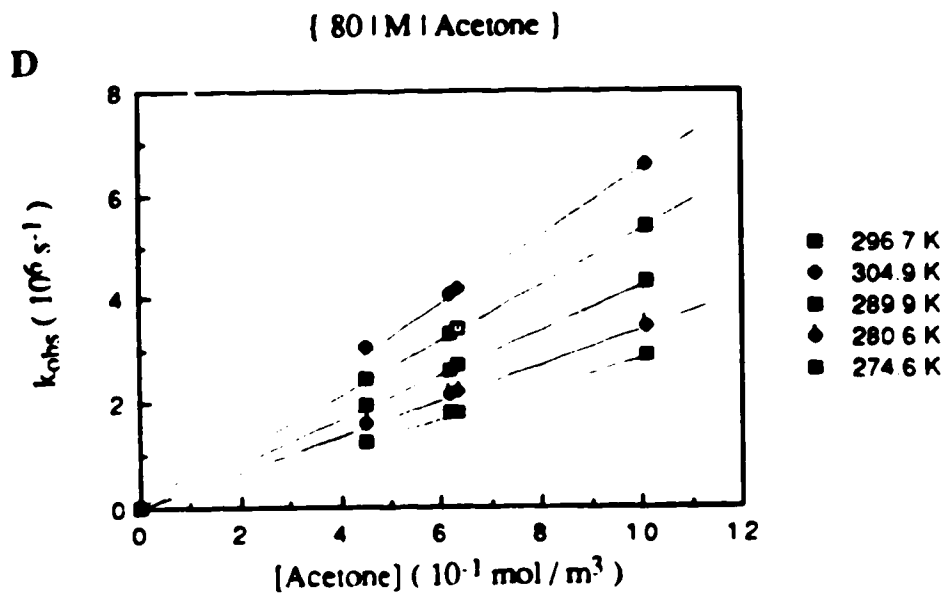
The temperature and concentration dependence of the first-order rate constant for the reaction of solvated electrons with acetone are shown in Figs.3-4(A-J). The concentration range of acetone was 0.17-1.2 mol/m<sup>3</sup>. The second-order rate constants at various temperatures are listed in Table 3-3. The rate parameters are obtained from the Arrhenius plots in Fig.3-5. They are summarized in Table 3-4. The rate constant at 298K is  $7.7 \times 10^6$  m<sup>3</sup>/mol.s in water and  $4.9 \times 10^6$  m<sup>3</sup>/mol.s in methanol. The literature results are  $6.8 \times 10^6$  m<sup>3</sup>/mol.s (100),  $7.7 \times 10^6$  m<sup>3</sup>/mol.s (115) and  $8.0 \times 10^6$  m<sup>3</sup>/mol.s (112) in water and  $4.3 \times 10^6$  m<sup>3</sup>/mol.s (98) in methanol.

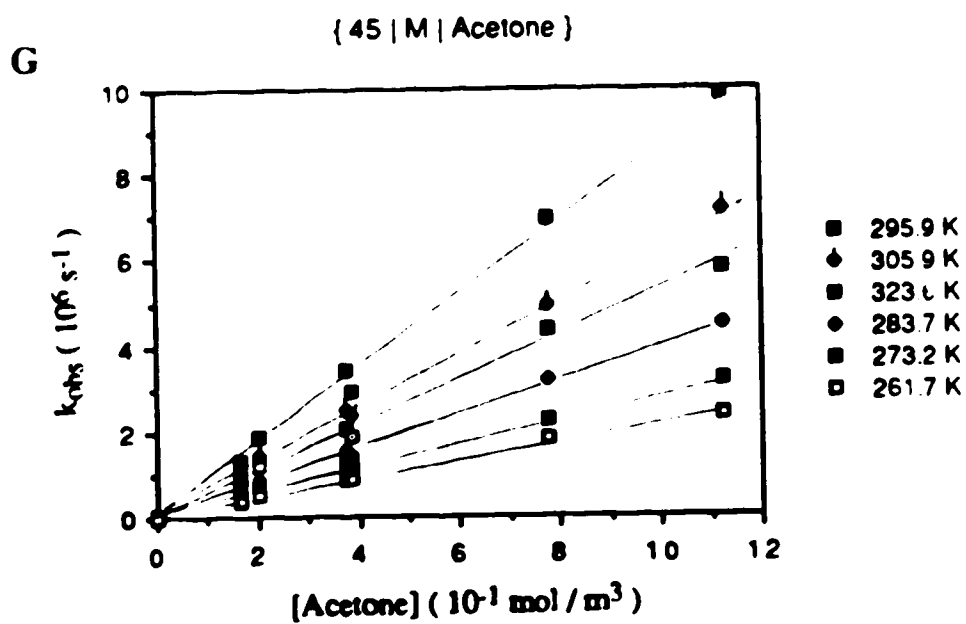
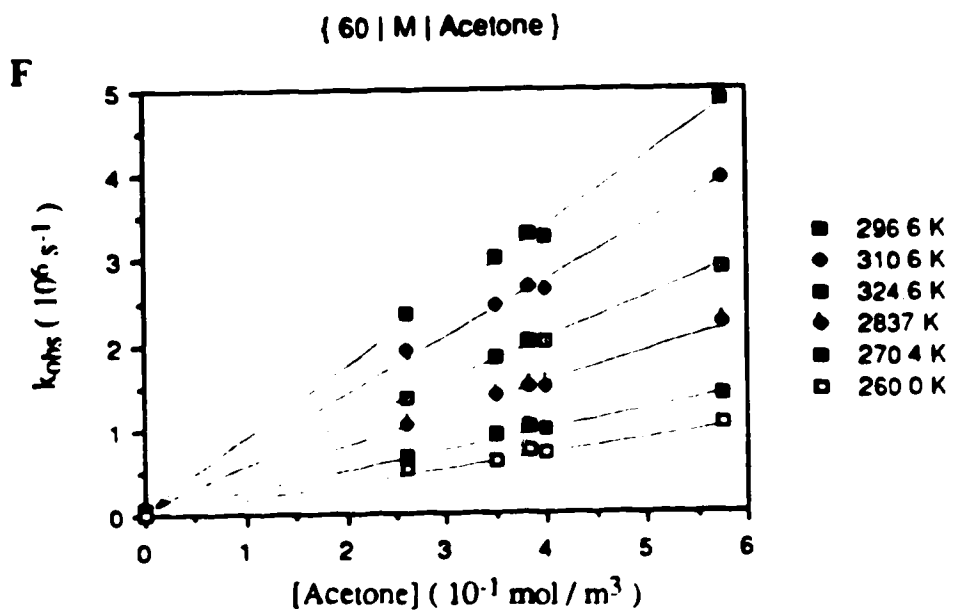
Fig. 3-4 Temperature and concentration dependence of the first-order rate constant for the reaction of solvated electrons with acetone in methanol / water mixtures

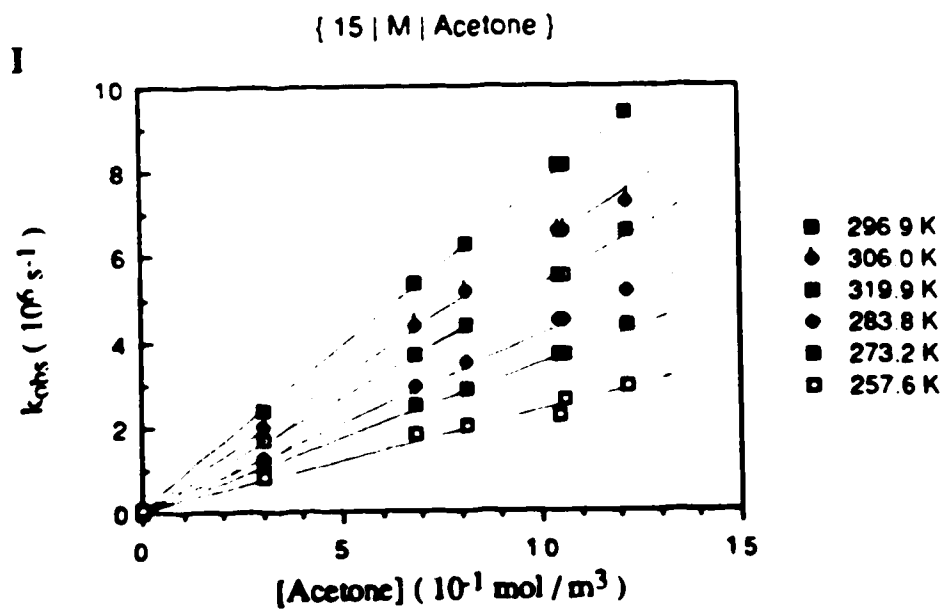
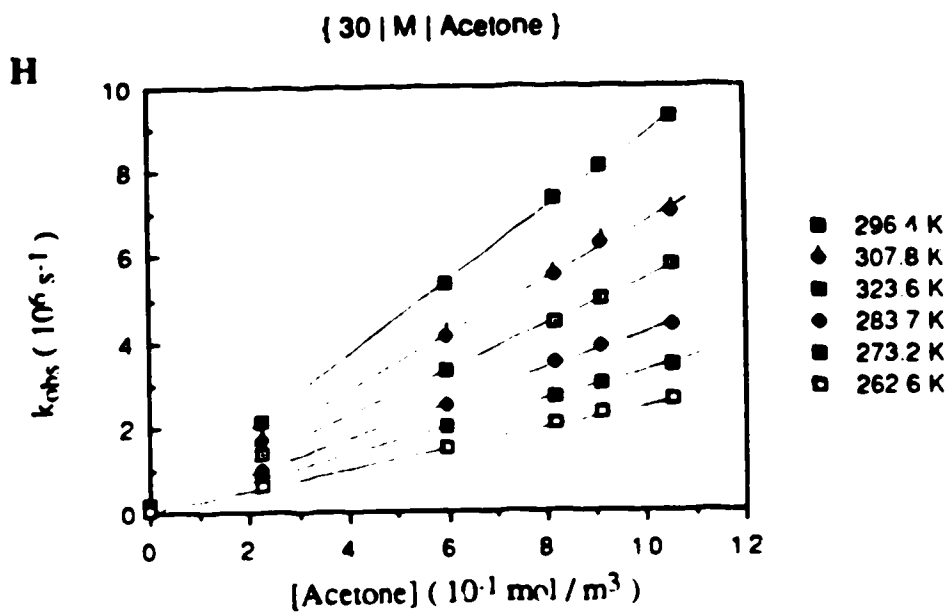












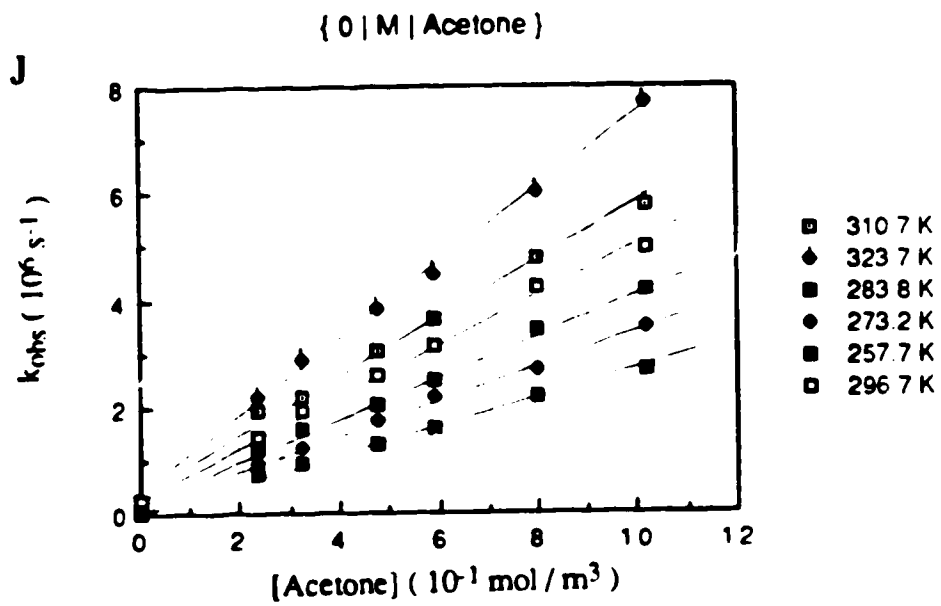
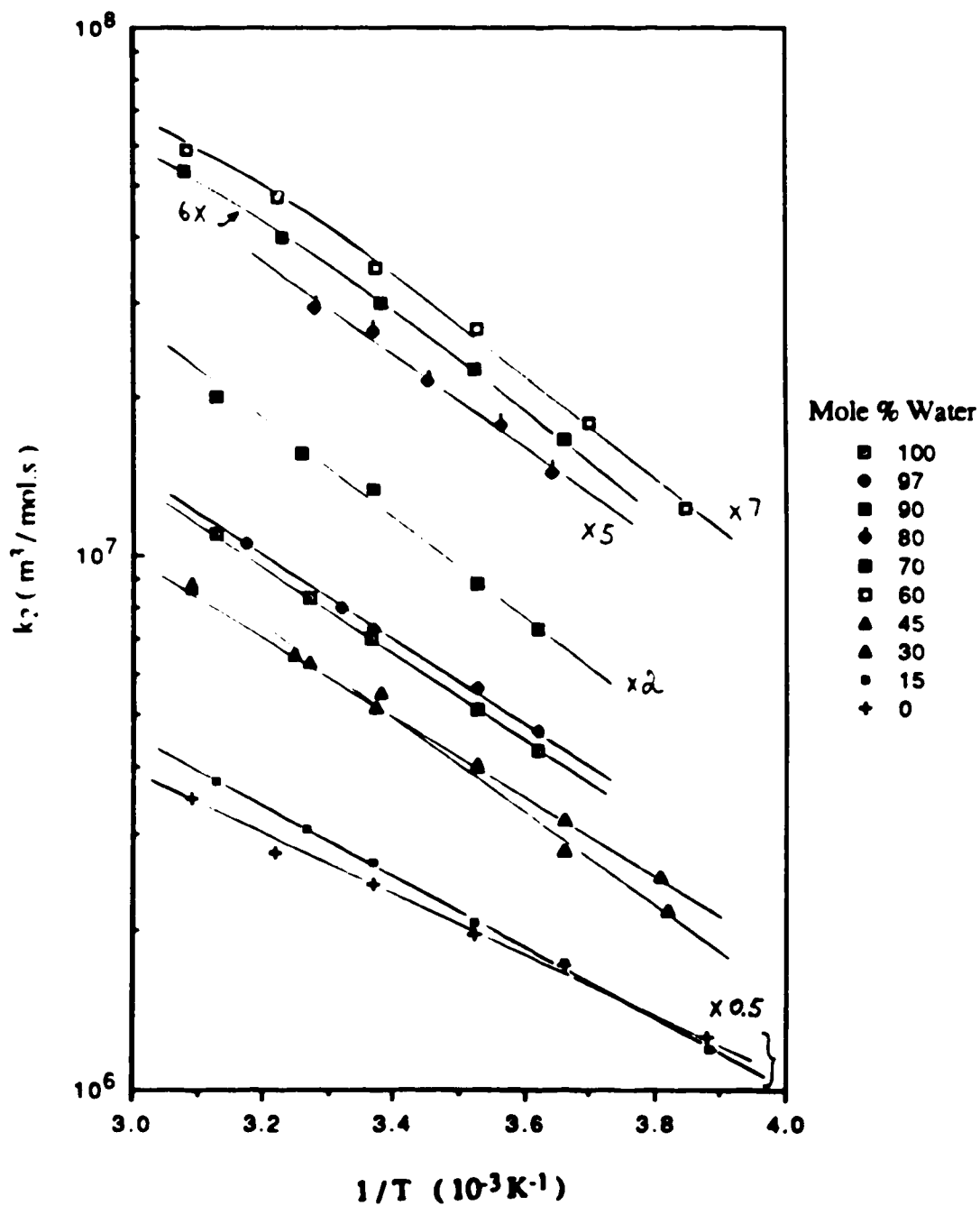


Fig. 3-5 Arrhenius plots for the reaction of solvated electrons with acetone in methanol / water mixtures



**Table 3-3 Second-order rate constants for the reaction of solvated electrons with acetone in methanol / water mixtures at various temperatures**

$\chi_w$	Temp.	$k_2$	$\chi_w$	Temp.	$k_2$	$\chi_w$	Temp.	$k_2$
	(K)	( $10^6 \text{ m}^3/\text{mol.s}$ )		(K)	( $10^6 \text{ m}^3/\text{mol.s}$ )		(K)	( $10^6 \text{ m}^3/\text{mol.s}$ )
1.00	276.2	4.3	0.70	273.2	2.8	0.30	262.6	2.5
	283.7	5.1		283.8	3.8		273.2	3.2
	297.3	7.0		296.0	5.0		283.7	4.1
	305.8	8.3		309.6	6.7		296.4	5.2
	319.7	11		324.7	8.9		307.8	6.5
						323.6	8.7	
0.97	276.3	4.7	0.6	260.0	1.8	0.15	257.6	2.4
	283.7	5.6		270.4	2.5		273.2	3.5
	297.0	7.3		283.7	3.9		283.8	4.1
	301.3	8.0		296.6	5.0		296.9	5.3
	315.2	11		310.6	6.8		306.0	6.1
			324.6	8.4	319.9	7.5		
0.90	276.3	3.6	0.45	261.7	2.2	0.00	257.7	2.5
	283.7	4.4		273.2	2.8		273.2	3.4
	296.7	6.7		283.7	4.0		283.8	3.9
	306.8	7.8		295.9	5.5		296.7	4.8
	319.9	10		305.9	6.3		310.7	5.6
			323.6	8.8	323.7	7.0		
0.80	274.6	2.9						
	280.6	3.5						
	289.9	4.3						
	296.7	5.3						
	304.9	5.9						

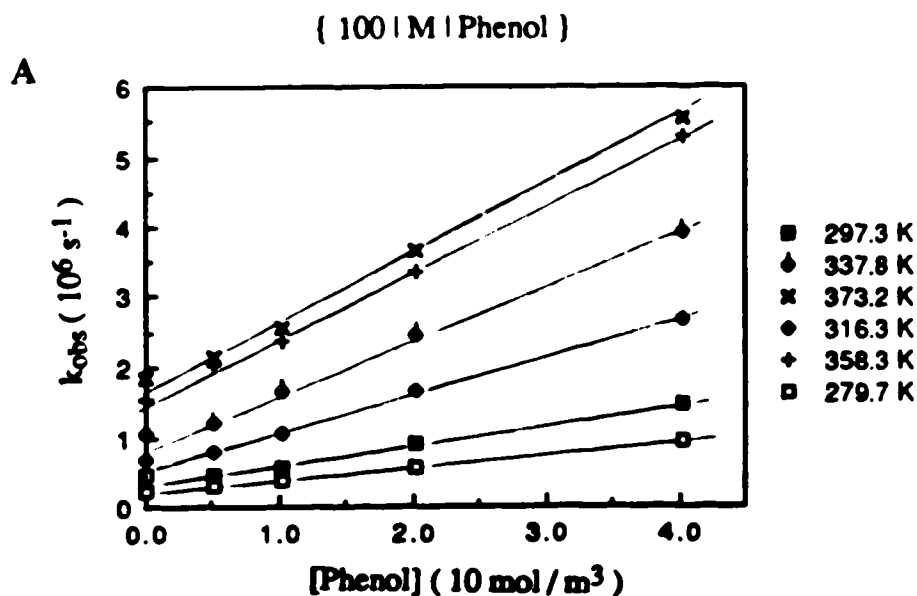
**Table 3-4** Rate parameters for the reaction of solvated electrons with acetone in methanol / water mixtures

$\chi_w$	$k_{298}$ ( $10^6 \text{ m}^3/\text{mol}\cdot\text{s}$ )	$E_a$ (kJ/mol.)	LogA	$\Delta S^\ddagger$ (J/mol.K)
1.00	7.7	15	12.45	-7
0.97	7.6	16	12.62	-3
0.90	6.4	17	12.83	1
0.80	5.3	17	12.76	-1
0.70	5.2	17	12.74	-1
0.60	5.2	17	12.74	-1
0.45	5.3	17	12.62	-3
0.30	5.2	14	12.22	-11
0.15	5.3	12	11.93	-16
0.00	4.9	11	11.57	-23

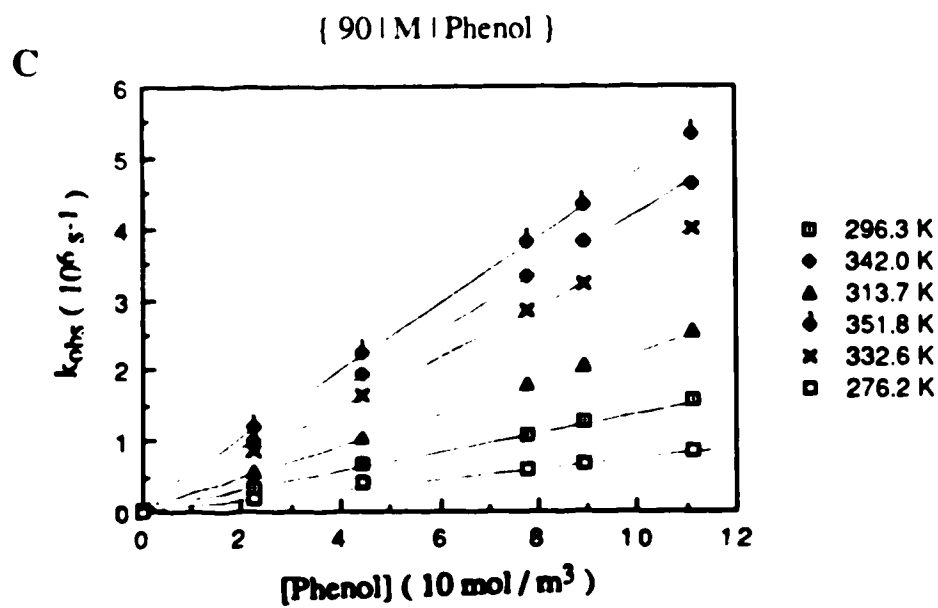
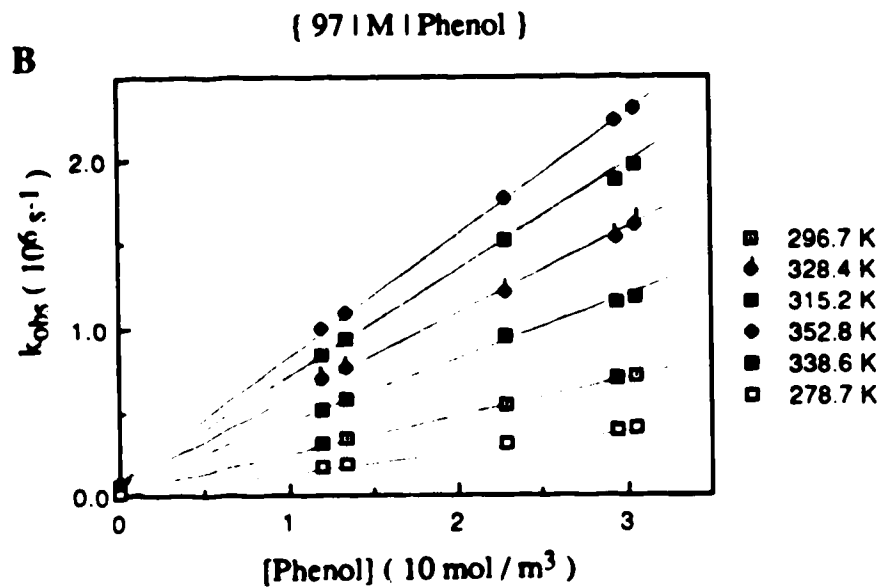
### C. Reaction of solvated electrons with phenol

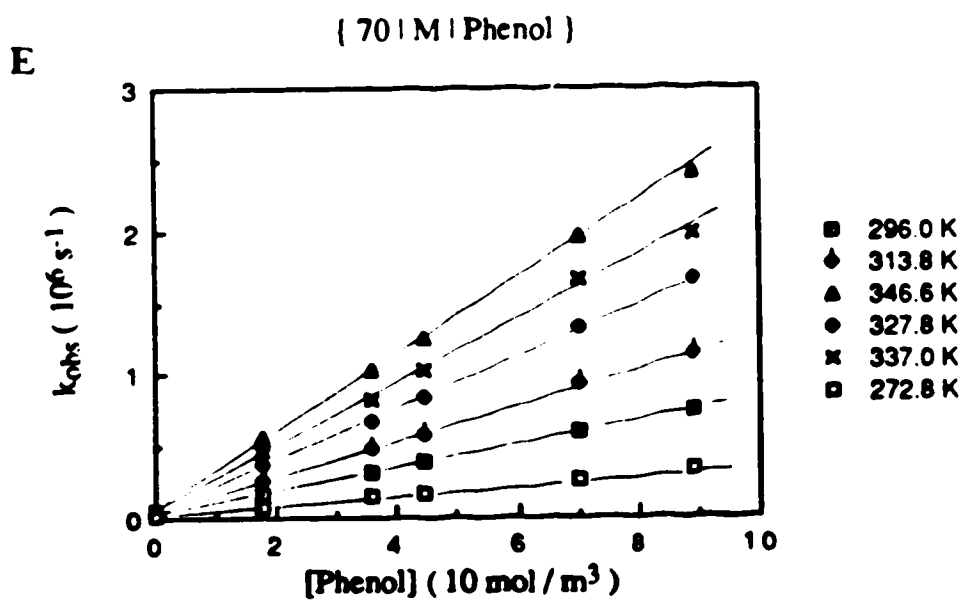
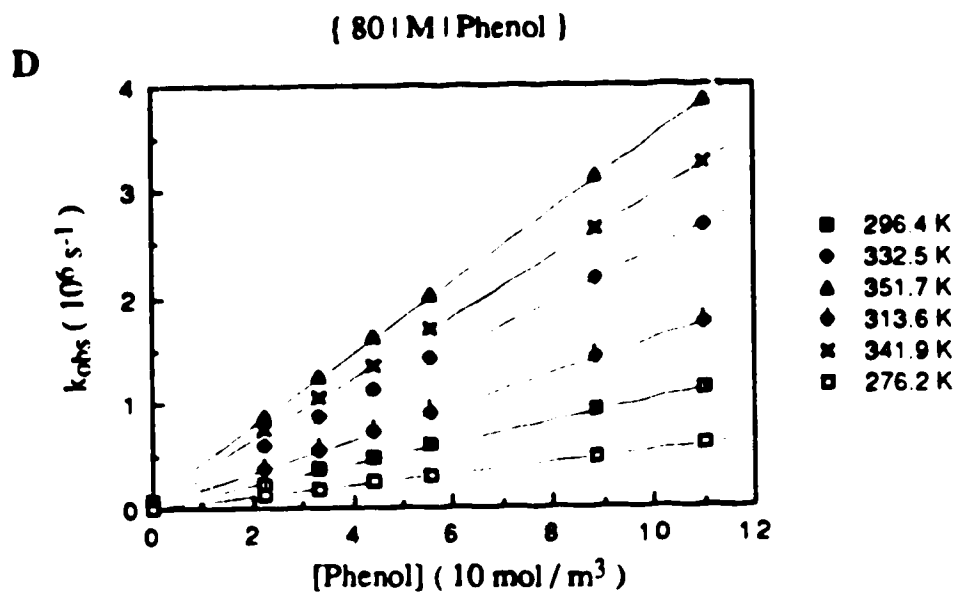
The temperature and concentration dependence of the first-order rate constant for the reaction of solvated electrons with phenol are shown in Figs.3-6(A-J). The concentration range of phenol was 5 -30 mol/m<sup>3</sup>. The second-order rate constants at various temperatures are listed in Table 3-5. The rate parameters are obtained from the Arrhenius plots in Fig.3-7. In water and 97 mole% water - methanol, the Arrhenius plots show a slight downward curvature at the high temperature region, therefore the rate parameters are obtained from the temperature range of 276-323K. The rate parameters are summarized in Table 3-6. The rate constant at 298K is  $3.0 \times 10^4$  m<sup>3</sup>/mol.s in water and  $1.1 \times 10^4$  m<sup>3</sup>/mol.s in methanol. The literature results are  $2.1 \times 10^4$  m<sup>3</sup>/mol.s (112),  $2.7 \times 10^4$  m<sup>3</sup>/mol.s (115) in water and  $1.0 \times 10^4$  m<sup>3</sup>/mol.s (100) in methanol.

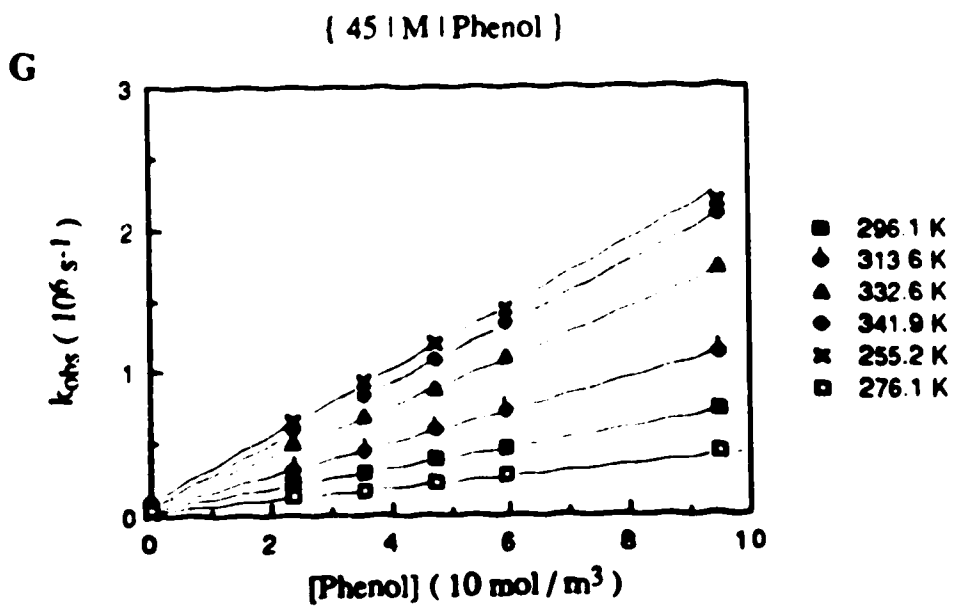
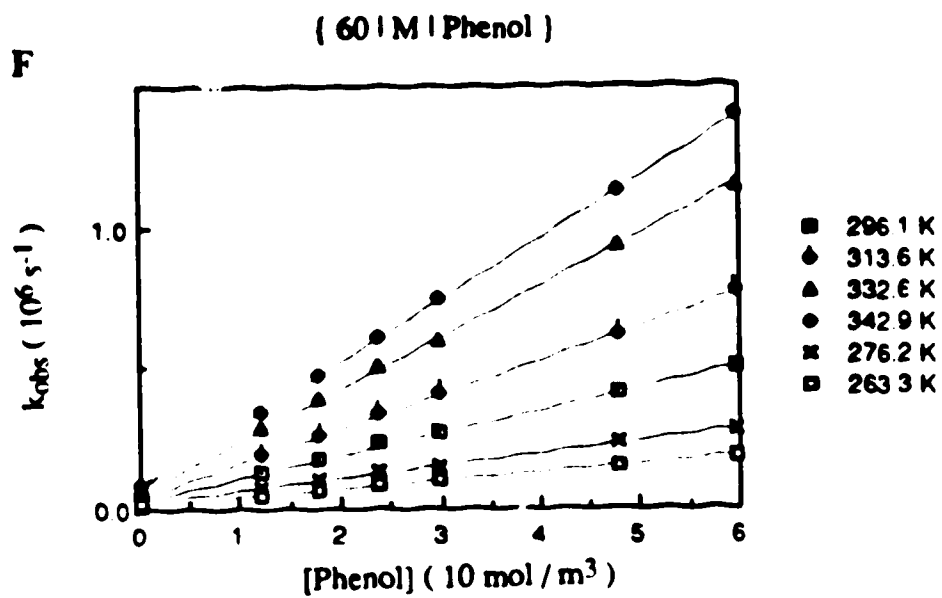
Fig. 3-6 (A-L) Temperature and concentration dependence of the first-order rate constant for the reaction of solvated electrons with phenol in methanol / water mixtures

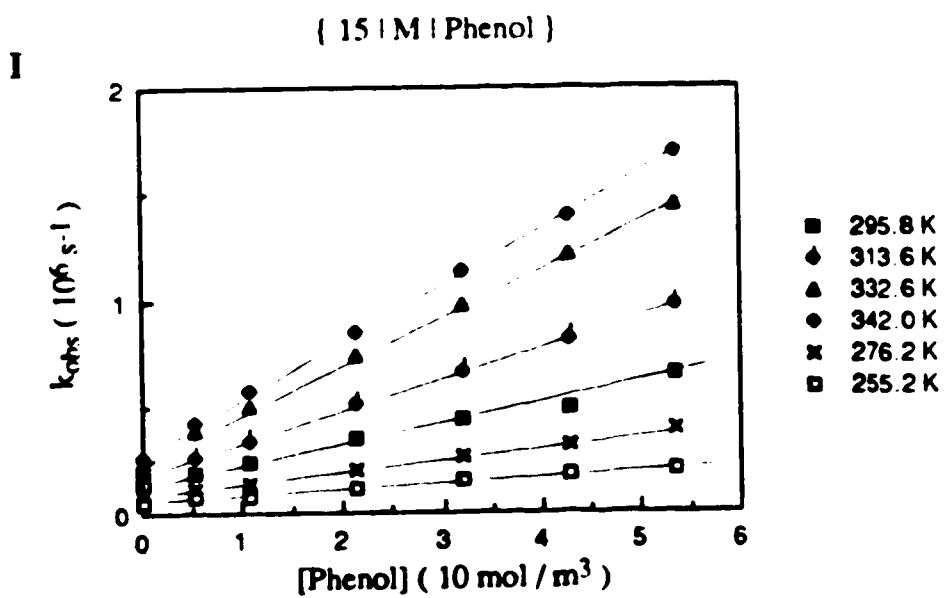
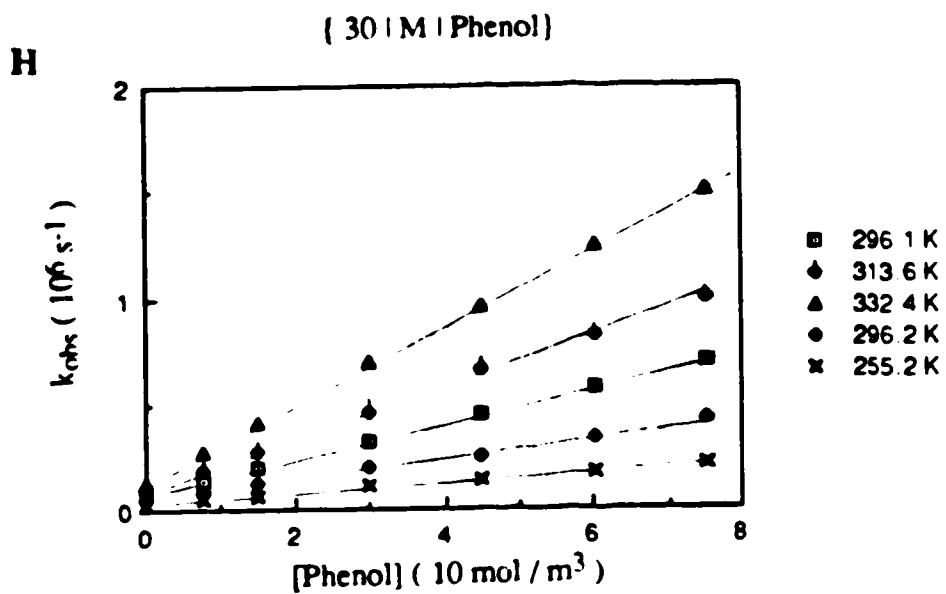












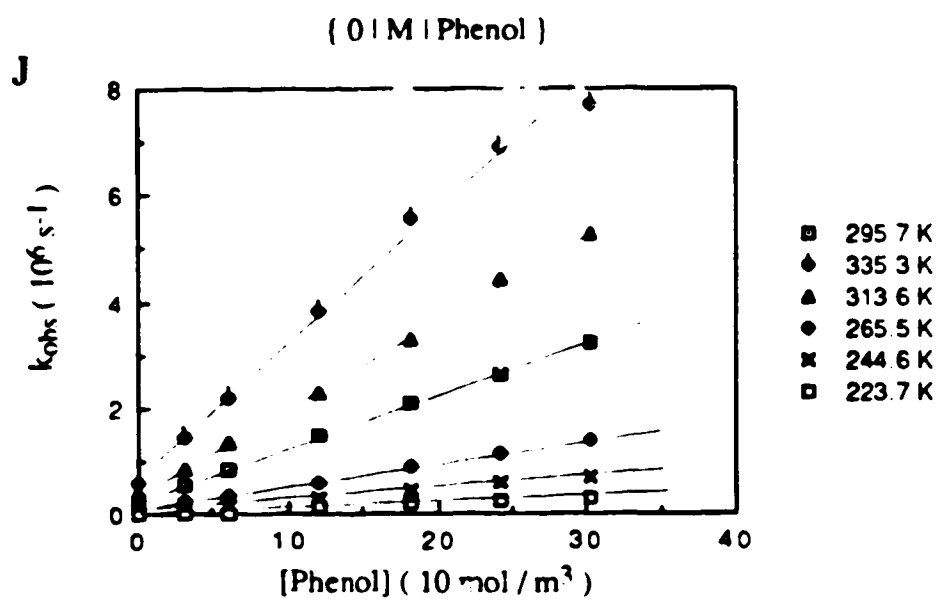
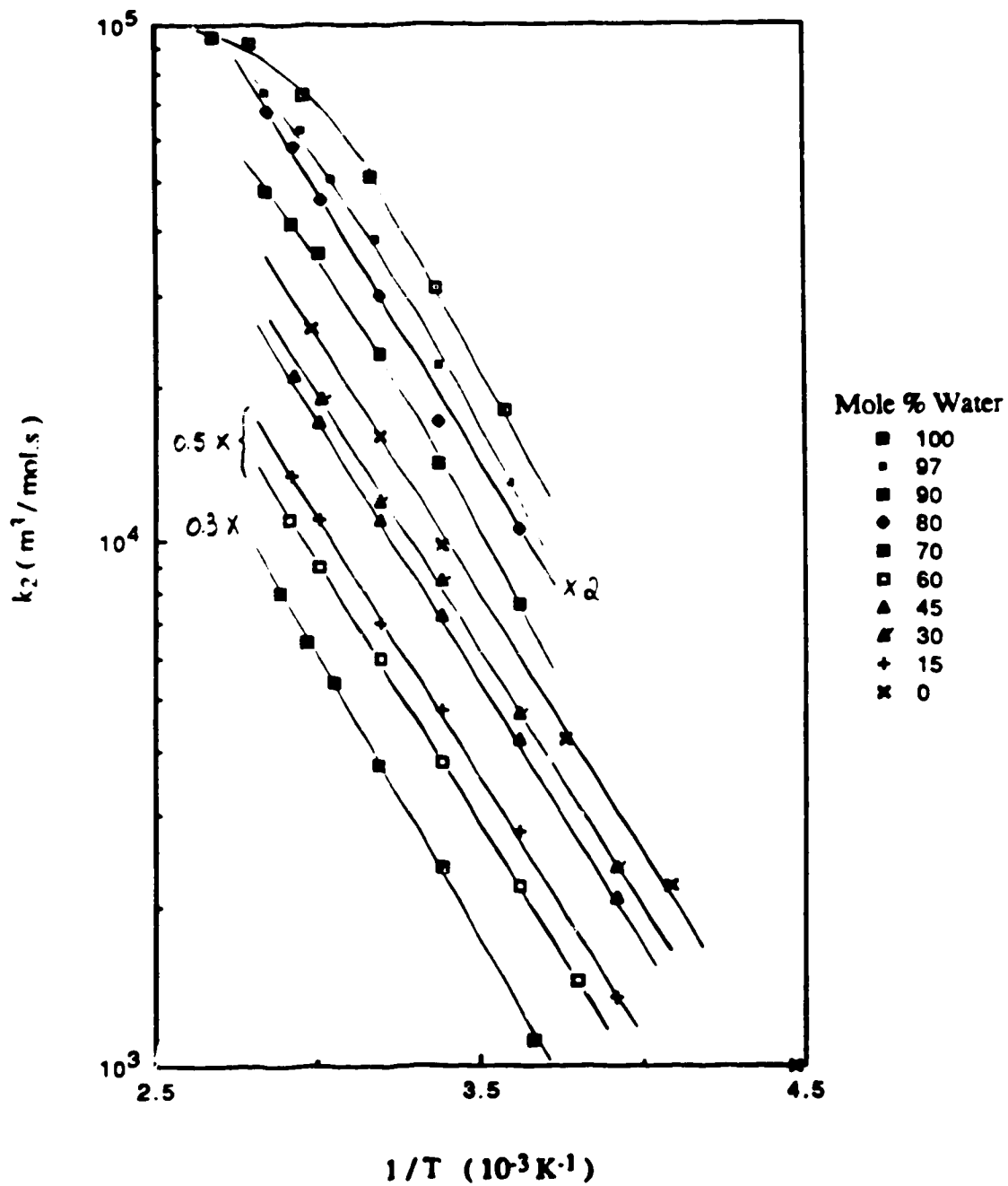


Fig. 3-7 Arrhenius plots for the reaction of solvated electrons with phenol in methanol / water mixtures



**Table 3-5 Second-order rate constants for the reaction of solvated electrons with phenol in methanol / water mixtures at various temperatures**

$\chi_w$	Temp. (K)	$k_2$ ( $10^4 \text{ m}^3/\text{mol.s}$ )	$\chi_w$	Temp. (K)	$k_2$ ( $10^4 \text{ m}^3/\text{mol.s}$ )	$\chi_w$	Temp. (K)	$k_2$ ( $10^4 \text{ m}^3/\text{mol.s}$ )
1.00	279.7	1.8	0.80	276.2	0.53	0.45	255.2	0.21
	297.3	3.1		296.4	0.95		276.1	0.42
	316.3	5.1		313.6	1.5		296.1	0.72
	337.8	7.3		332.5	2.3		313.6	1.1
	358.3	9.2		341.9	2.9		332.6	1.7
	373.2	9.5		351.7	3.4		341.9	2.1
0.97	278.7	1.3	0.70	272.8	0.37	0.30	255.2	0.24
	296.7	2.2		296.0	0.8		276.2	0.47
	315.2	3.9		313.8	1.3		296.1	0.84
	328.4	5.1		327.8	1.8		313.6	1.2
	338.6	6.3		337.0	2.2		332.4	1.9
	352.8	7.4		346.6	2.7			
0.90	276.2	0.76	0.6	263.3	0.29	0.15	255.2	0.27
	296.3	1.4		276.2	0.44		276.2	0.56
	313.7	2.3		296.1	0.76		295.8	0.95
	332.6	3.6		313.6	1.2		313.6	1.4
	342.6	4.1		332.6	1.8		332.6	2.2
	351.8	4.8		342.9	2.2	342.0	2.7	
								0.00
							244.6	0.22
							265.5	0.42
							295.7	0.98
							313.6	1.6
							335.3	2.6

**Table 3-6** Rate parameters for the reaction of solvated electrons with phenol in methanol / water mixtures

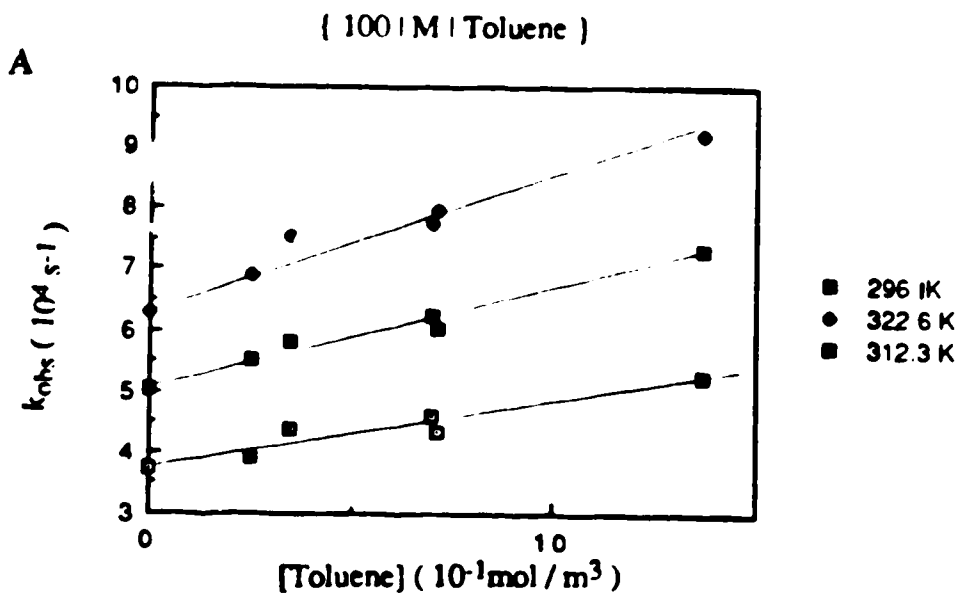
$\chi_w$	$k_{298}$ ( $10^4 \text{ m}^3/\text{mol}\cdot\text{s}$ )	$E_a$ (kJ/mol.)	LogA	$\Delta S^\ddagger$ (J/mol.K)
1.00	3.0	18	10.58	-42
0.97	2.3	20	10.69	-40
0.90	1.4	20	10.72	-40
0.80	1.1	20	10.48	-44
0.70	0.86	20	10.38	-46
0.60	0.80	19	10.24	-49
0.45	0.77	19	10.17	-50
0.30	0.85	18	10.15	-50
0.15	1.0	19	10.23	-49
0.00	1.1	19	10.25	-48

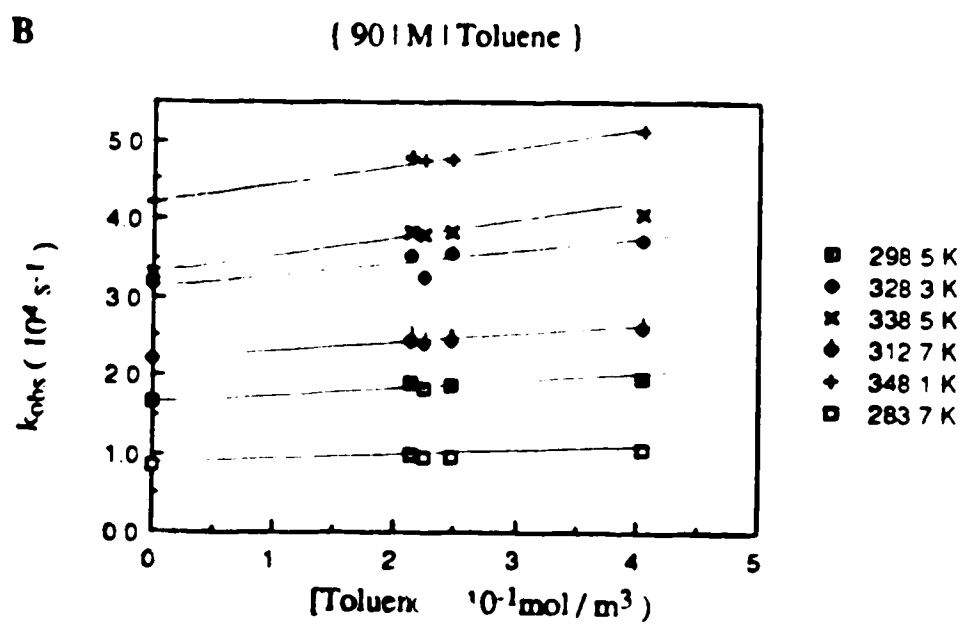


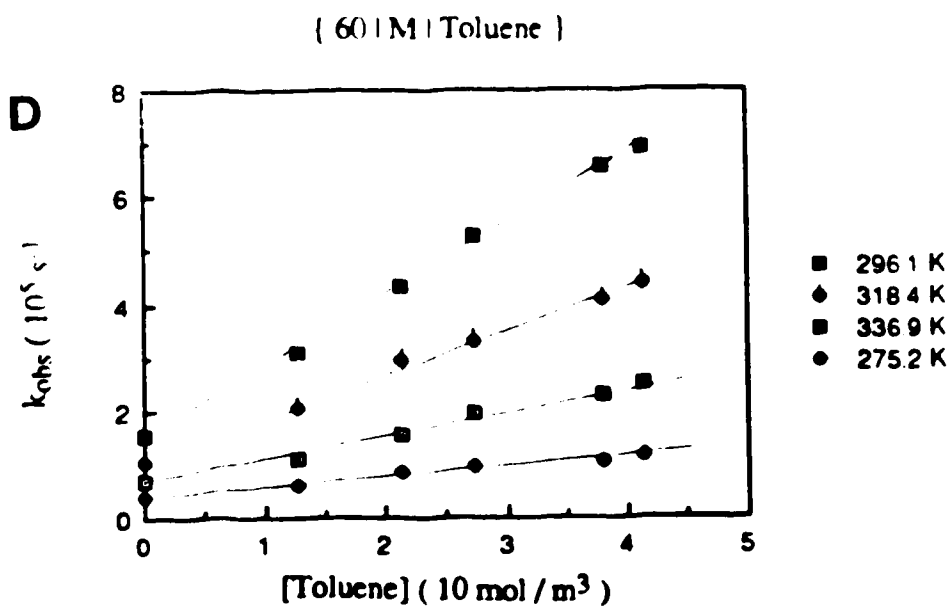
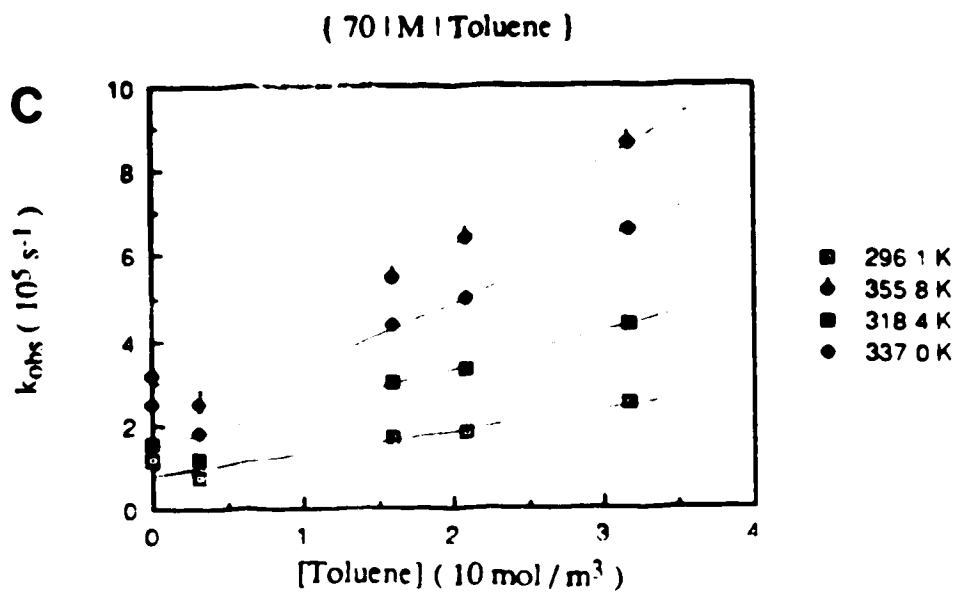
#### D. Reaction of solvated electrons with toluene

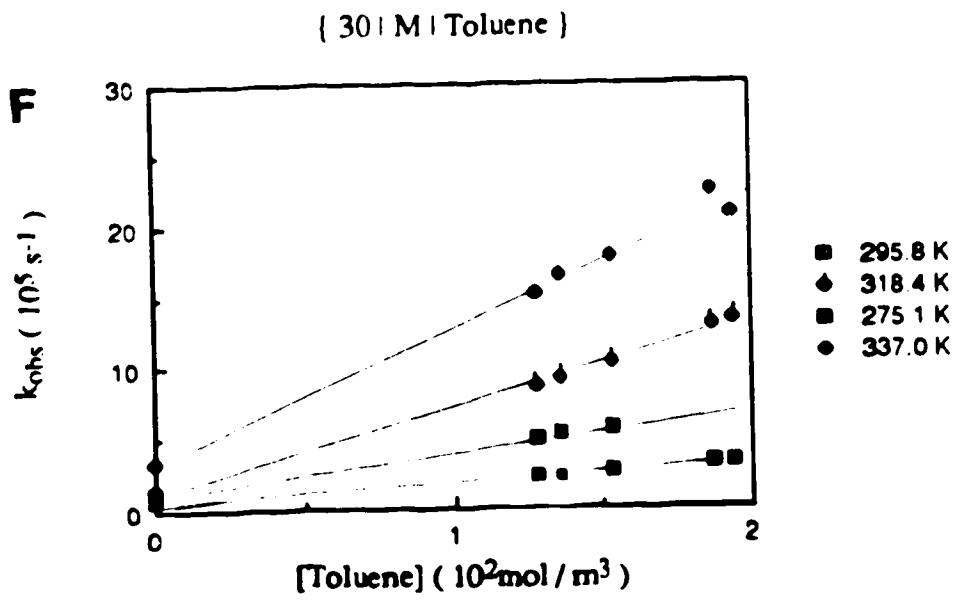
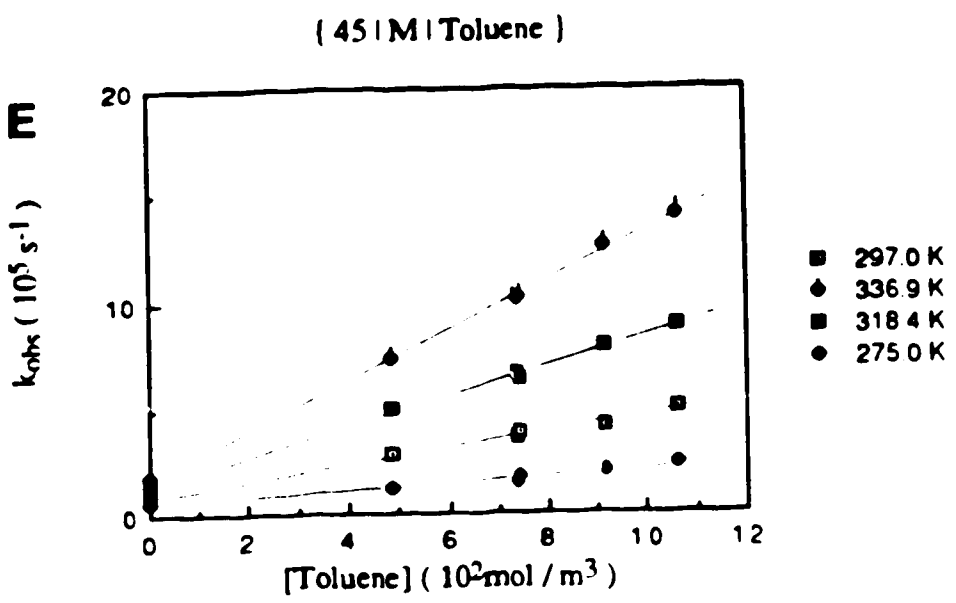
The temperature and concentration dependence of the first-order rate constant for the reaction of solvated electrons with toluene are shown in Figs.3-8(A-D). The concentration range of toluene was 0.2-370 mol/m<sup>3</sup>. The second-order rate constants at various temperatures are listed in Table 3-7. The rate parameters are obtained from the Arrhenius plots in Fig.3-9. They are summarized in Table 3-8. The rate constant at 298K is  $1.1 \times 10^4$  m<sup>3</sup>/mol.s in water and  $2.0 \times 10^3$  m<sup>3</sup>/mol.s in methanol. The literature results are  $1.3 \times 10^4$  m<sup>3</sup>/mol.s (115) and  $1.4 \times 10^4$  m<sup>3</sup>/mol.s (112) in water and  $1.6 \times 10^3$  m<sup>3</sup>/mol.s (99) in methanol.

Fig. 3-8 Temperature and concentration dependence of the first-order rate constant for the reaction of solvated electrons with toluene in methanol / water mixtures









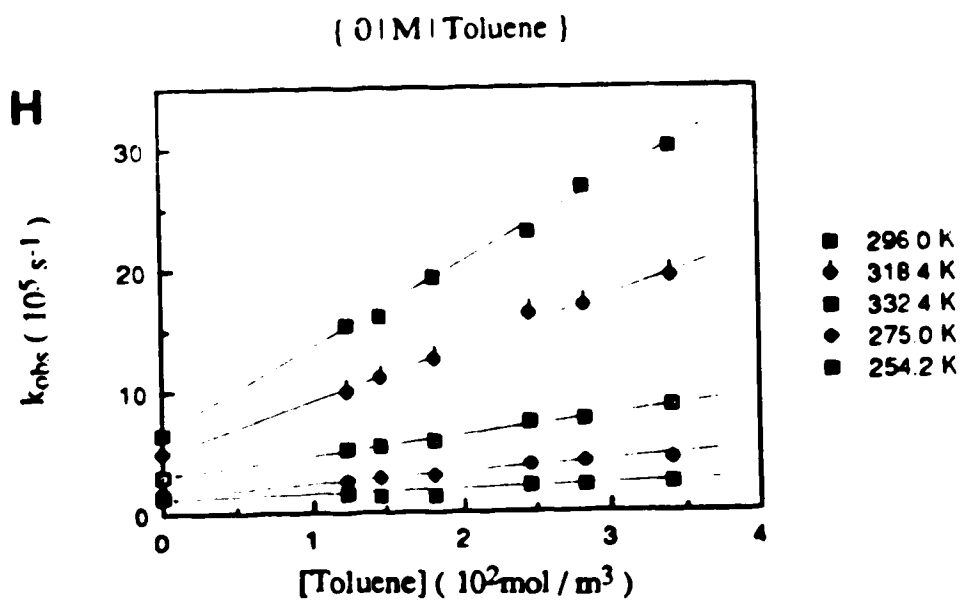
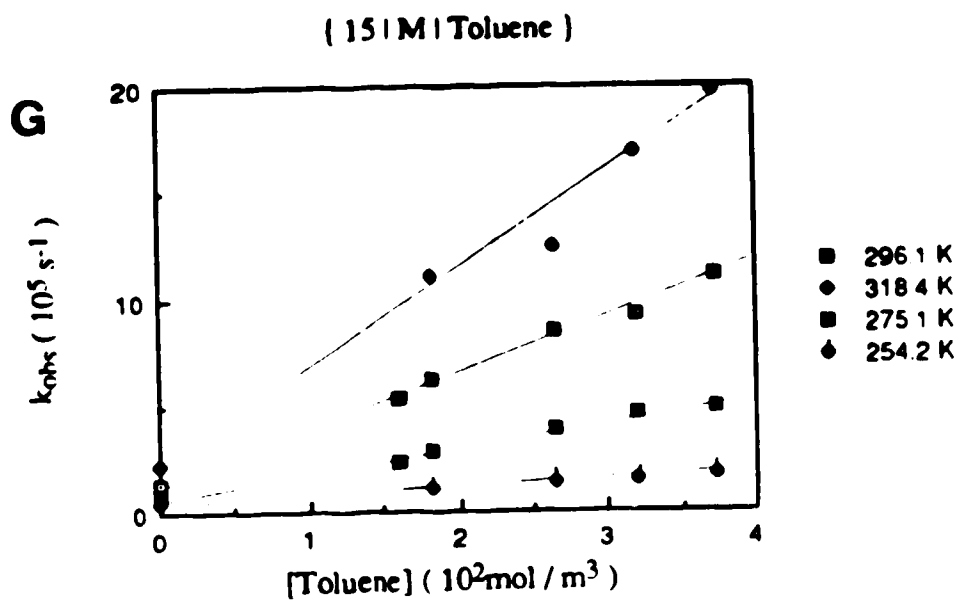


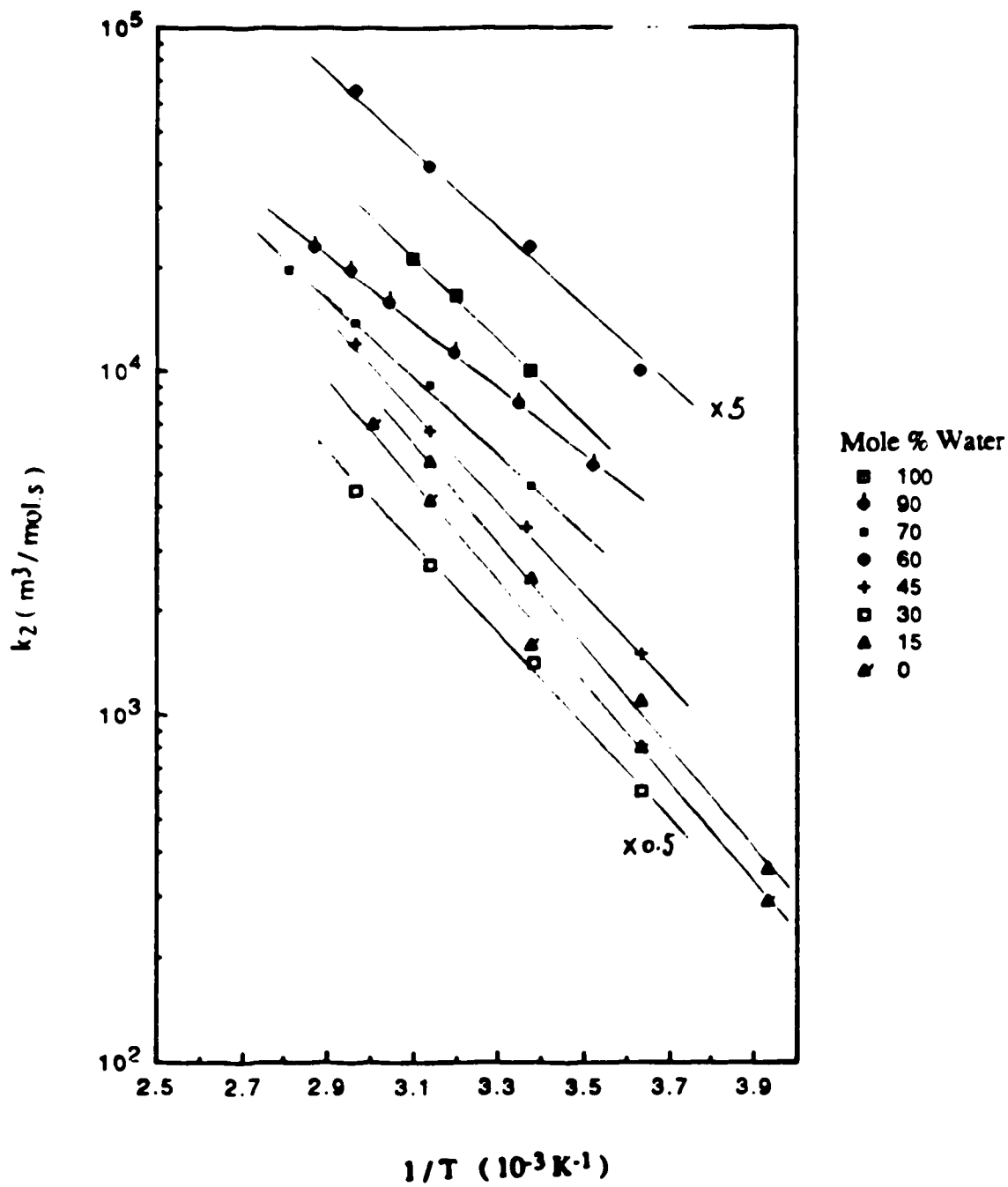
**Table 3-7** Second-order rate constants for the reaction of solvated electrons with toluene in ethanol / water mixtures at various temperatures

$\chi_w$	Temp (K)	$k_2$ ( $10^4 \text{ m}^3/\text{mol}\cdot\text{s}$ )	$\chi_w$	Temp. (K)	$k_2$ ( $10^4 \text{ m}^3/\text{mol}\cdot\text{s}$ )	$\chi_w$	Temp. (K)	$k_2$ ( $10^4 \text{ m}^3/\text{mol}\cdot\text{s}$ )
1.00	296.1	1.0	0.70	296.1	0.46	0.30	275.1	0.12
	312.7	1.7		318.4	0.91		295.8	0.28
	322.6	2.1		337.0	1.4		318.4	0.55
				355.8	2.0		337.0	0.90
0.90	283.7	0.53	0.60	275.2	0.20	0.15	254.2	0.036
	298.5	0.80		296.1	0.46		275.1	0.11
	312.7	1.1		318.4	0.79		296.1	0.25
	328.3	1.6		336.9	1.3		318.4	0.55
	338.5	2.0	0.45	275.0	0.15	0.00	254.2	0.029
	348.1	2.3		297.0	0.35		275.0	0.080
		318.4	0.67	296.0	0.16			
		336.9	1.2	318.4	0.42			
				332.4	0.70			

Table 3-8 Rate parameters for the reaction of solvated electrons with toluene in methanol / water mixtures

$\chi_w$	$k_{298}$ ( $10^4 \text{ m}^3/\text{mol.s}$ )	$E_a$ (kJ/mol.)	LogA	$\Delta S^\ddagger$ (J/mol.K)
1.00	1.1	18	10.14	-51
0.90	0.79	19	10.22	-49
0.70	0.52	21	10.41	-45
0.60	0.53	23	10.68	-40
0.45	0.36	24	10.72	-39
0.30	0.28	26	11.00	-34
0.15	0.27	27	11.21	-30
0.00	0.21	28	11.26	-29

Fig. 3-9 Arrhenius plots for the reaction of solvated electrons with toluene in methanol / water mixtures



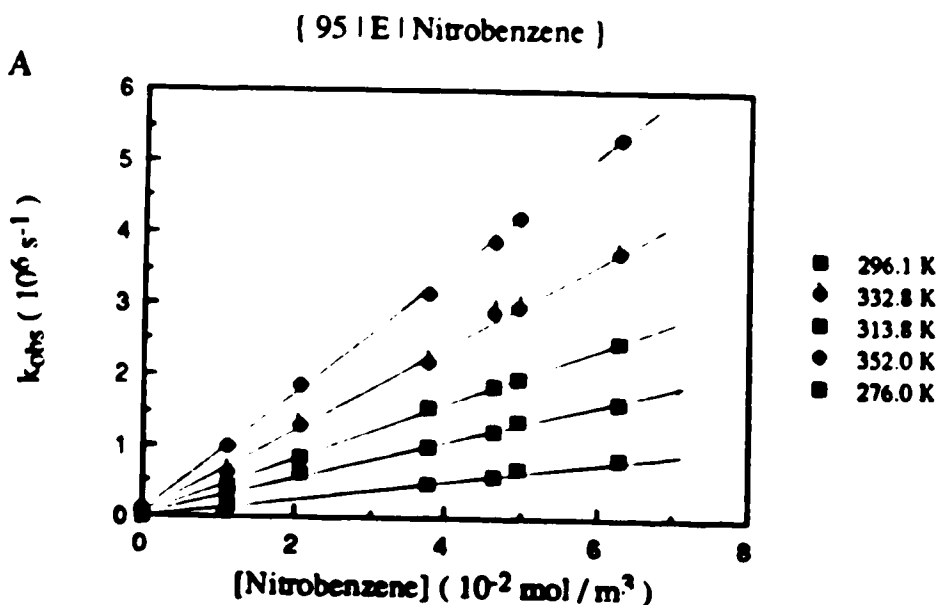


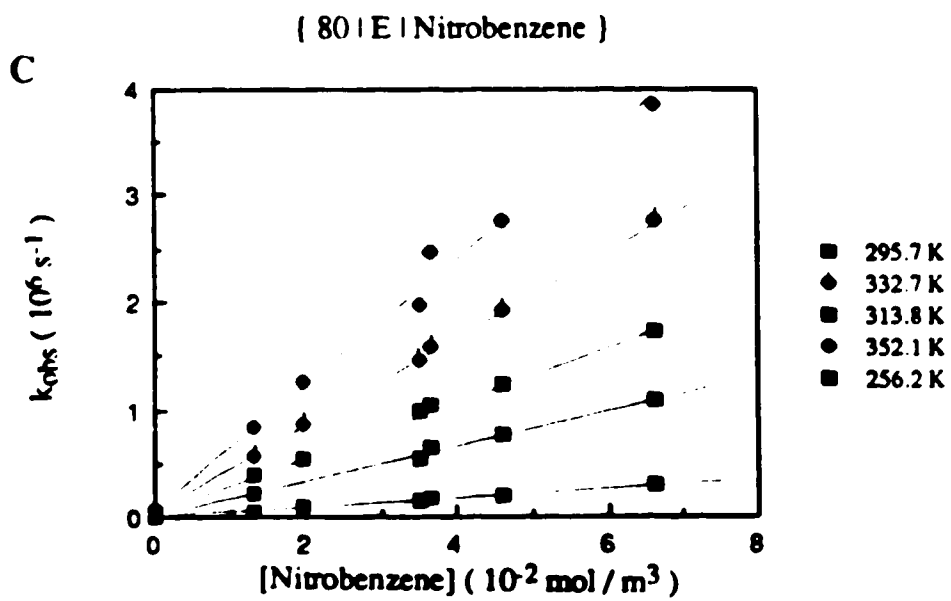
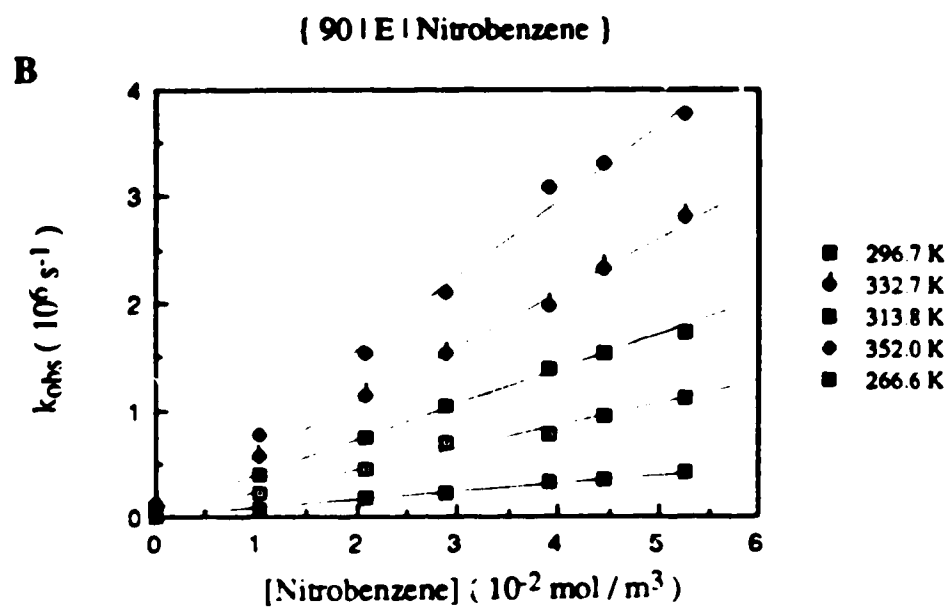
## 2. Reactions of solvated electrons in ethanol / water mixed solvents

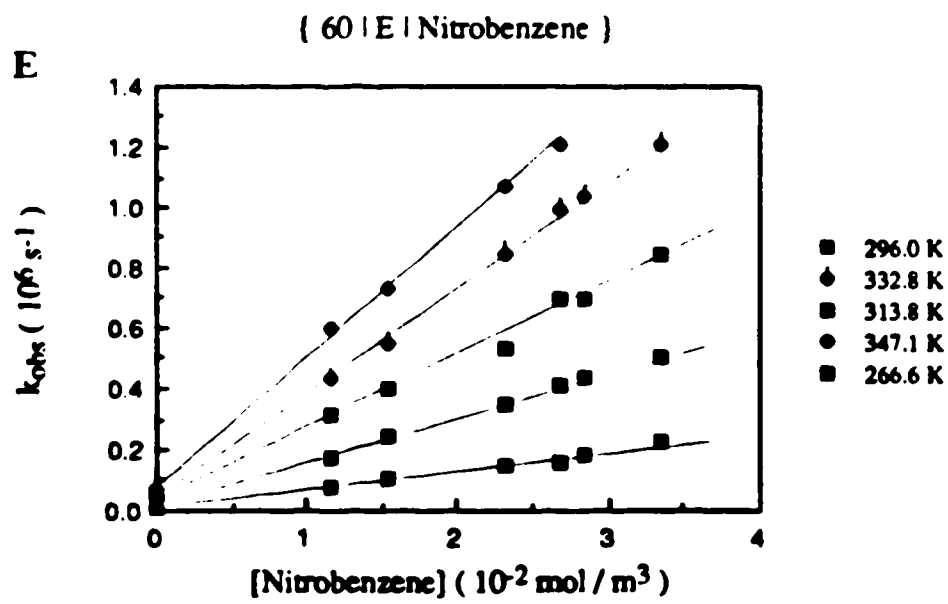
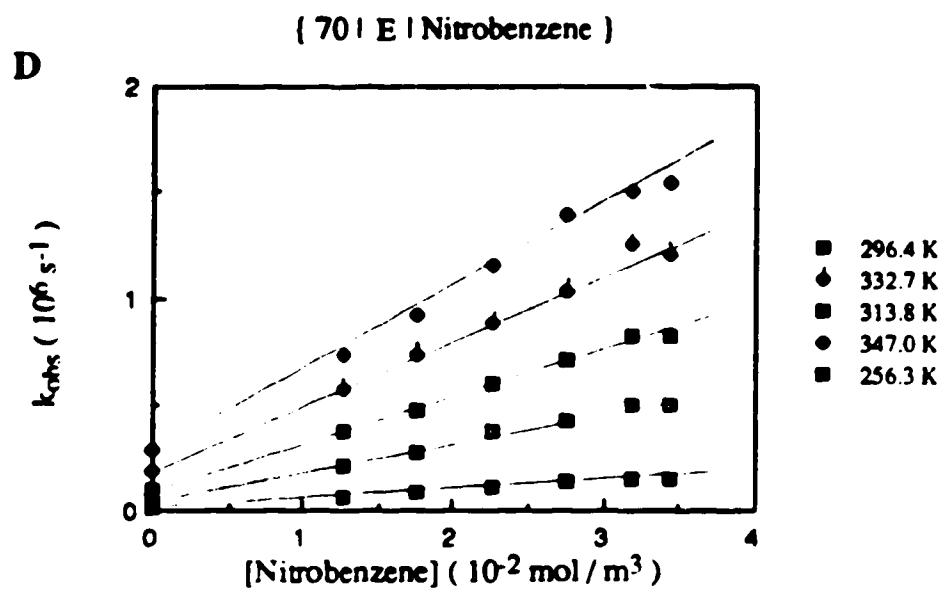
### A. Reaction of solvated electrons with nitrobenzene

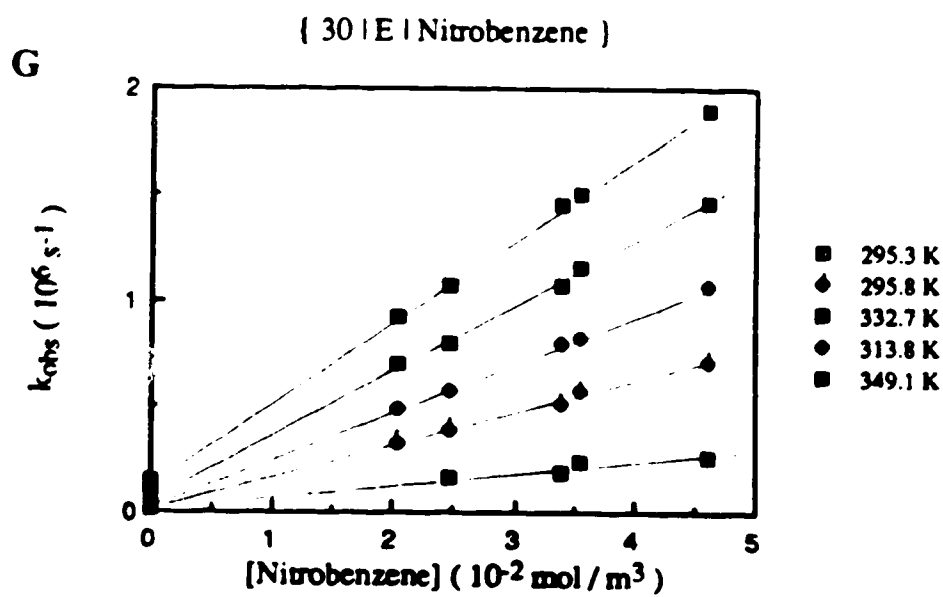
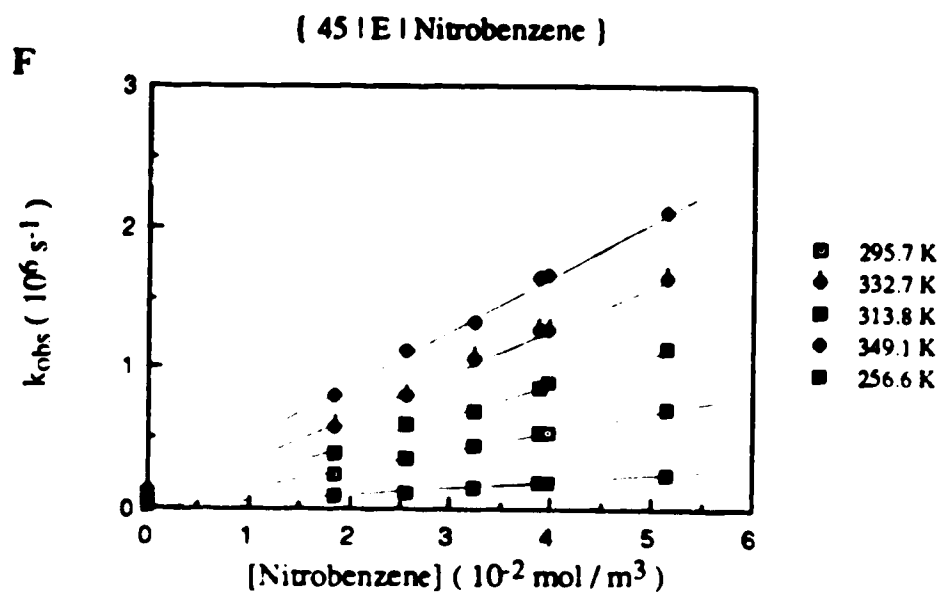
The temperature and concentration dependence of the first-order rate constant for the reaction of solvated electrons with nitrobenzene are shown in Figs.3-10(A-J). The concentration range of nitrobenzene was 10-62 mmol/m<sup>3</sup>. The second-order rate constants at various temperatures are listed in Table 3-9. The rate parameters are obtained from the Arrhenius plots in Fig.3-11. They are summarized in Table 3-10. The rate constant in ethanol at 298K is  $1.6 \times 10^7$  m<sup>3</sup>/mol.s . The literature results are  $1.5 \times 10^7$  m<sup>3</sup>/mol.s (98,100,109). The composition dependence of  $k_{298}$  is similar to those obtained by Hickel and coworkers (109). The comparison is shown in Fig.3-12.

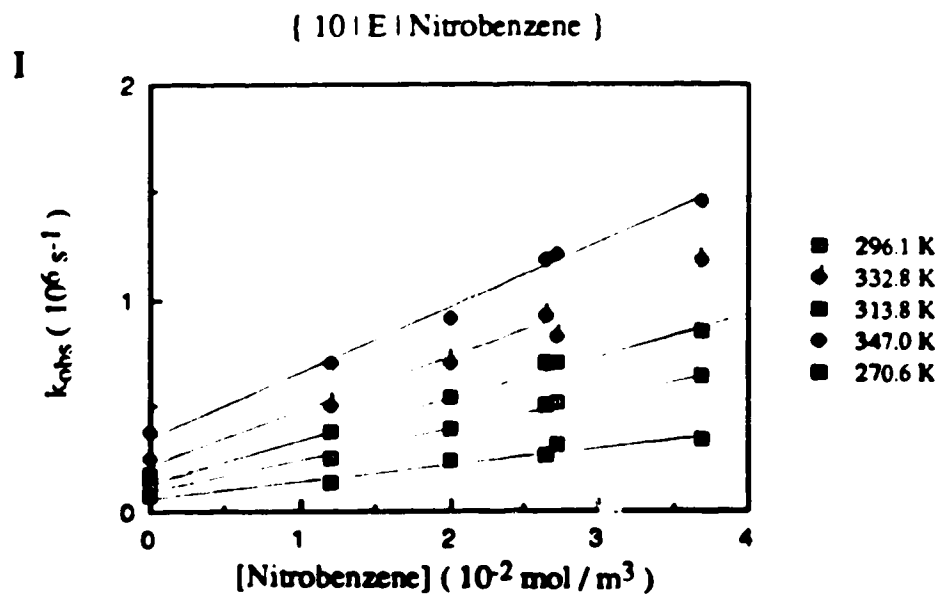
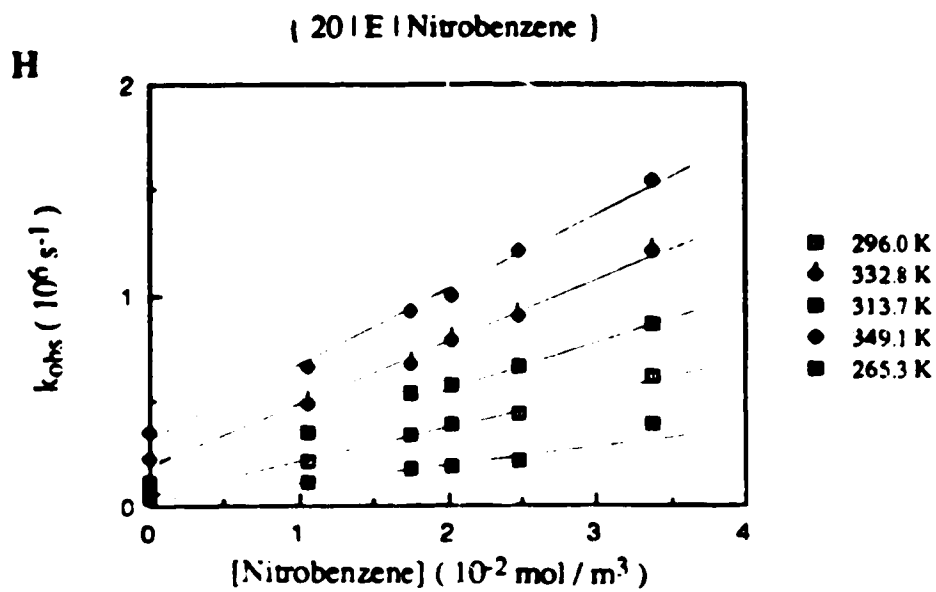
Fig. 3-10 Temperature and concentration dependence of the first-order rate constant for the reaction of solvated electrons with nitrobenzene in ethanol / water mixtures











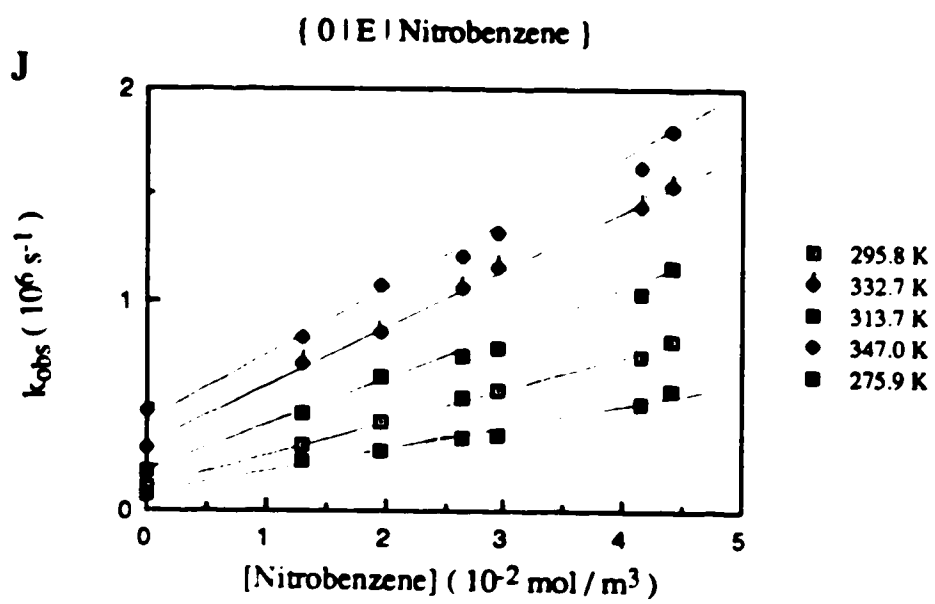


Fig. 3-11 Arrhenius plots for the reaction of solvated electrons with nitrobenzene in ethanol / water mixtures

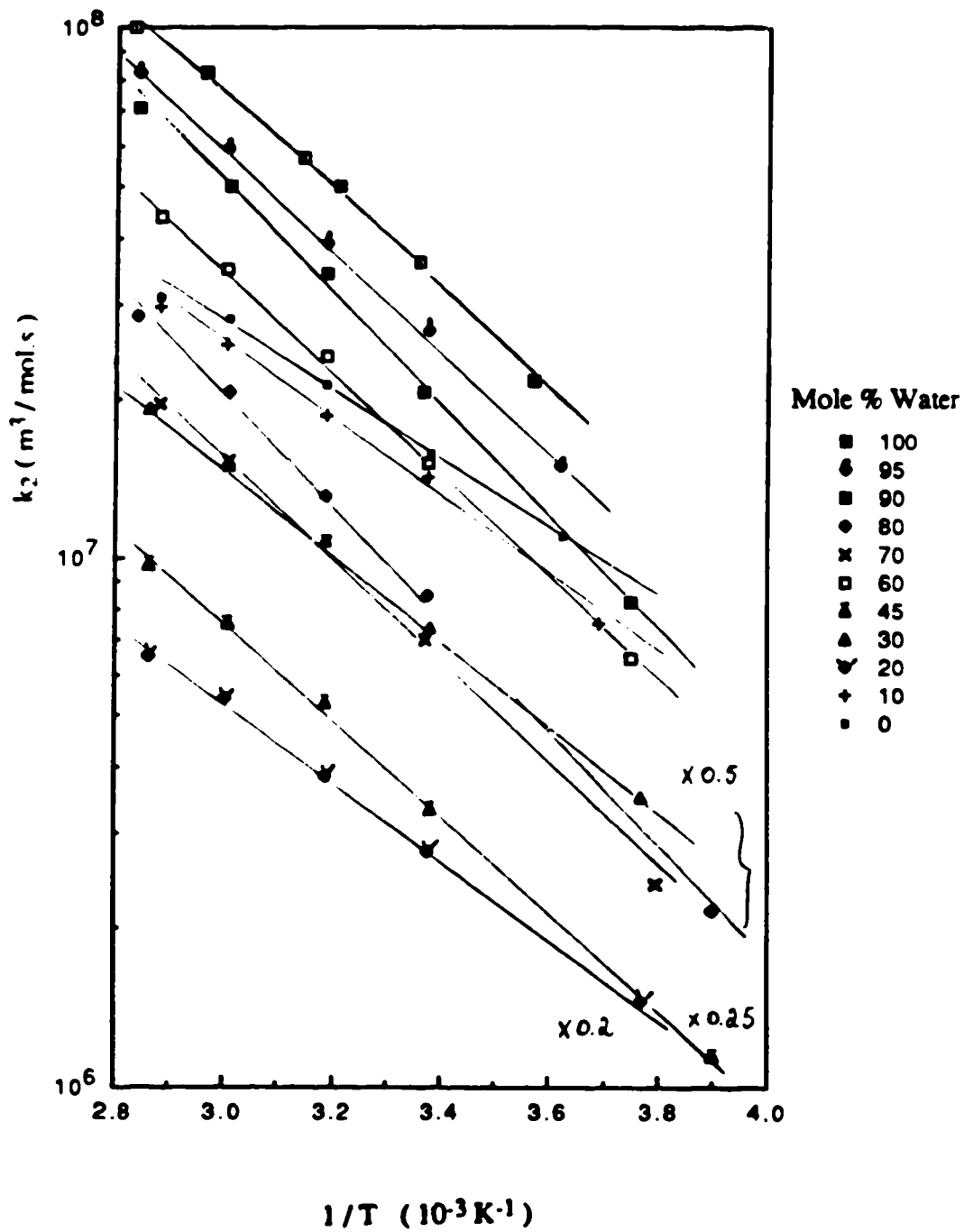
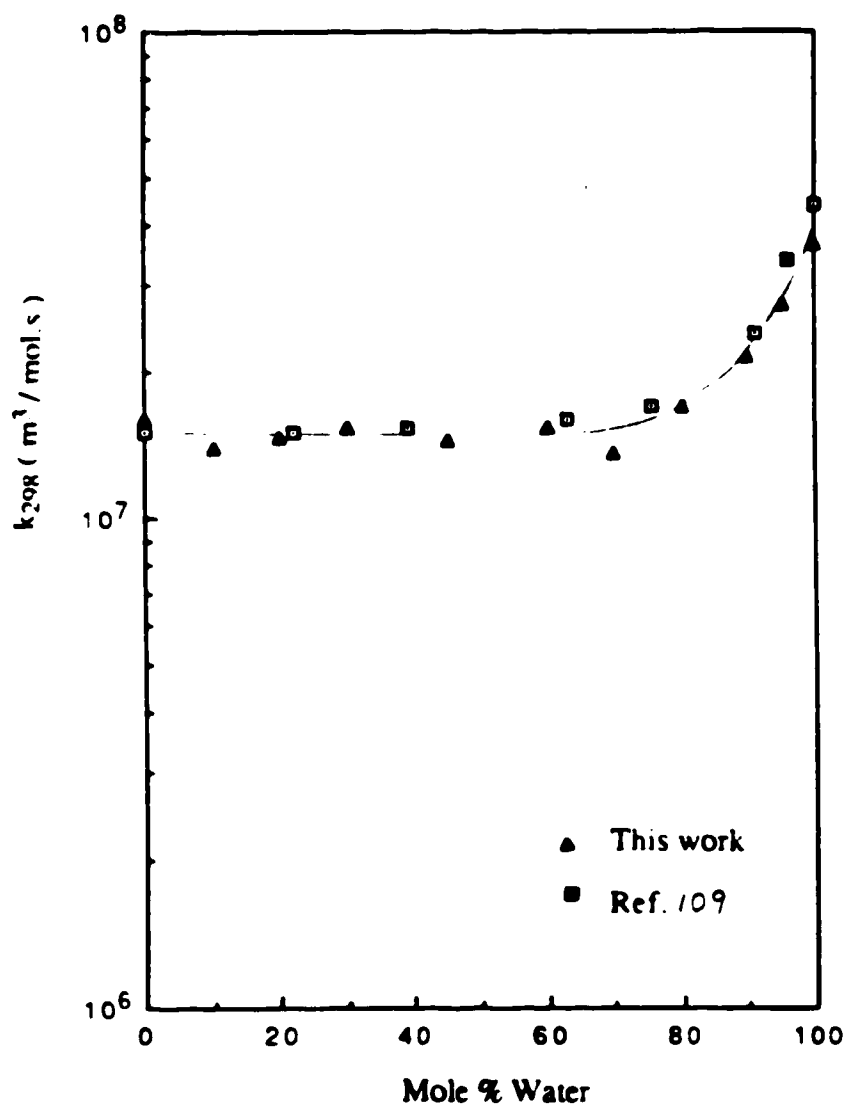


Fig. 3-12 Composition dependence of  $k_{298}$  for the reaction of solvated electrons with nitrobenzene in ethanol / water mixtures





**Table 3-9 Second-order rate constants for the reaction of solvated electrons with nitrobenzene in ethanol / water mixtures at various temperatures**

$\chi_w$	Temp. (K)	$k_2$ ( $10^7 \text{ m}^3/\text{mol.s}$ )	$\chi_w$	Temp. (K)	$k_2$ ( $10^7 \text{ m}^3/\text{mol.s}$ )	$\chi_w$	Temp. (K)	$k_2$ ( $10^7 \text{ m}^3/\text{mol.s}$ )
1.00	279.9	2.2	0.70	263.3	0.48	0.20	265.3	0.72
	297.7	3.6		296.4	1.4		296.0	1.4
	311.4	5.0		313.8	2.1		313.7	1.9
	318.2	5.7		332.7	3.1		332.8	2.7
	337.7	8.3		347.0	3.9		349.1	3.3
	353.0	11						
0.95	276.0	1.5	0.60	266.6	0.64	0.10	270.6	0.75
	296.1	2.7		296.0	1.4		296.1	1.4
	313.8	3.9		313.8	2.4		313.8	1.9
	332.8	5.9		332.8	3.5		332.8	2.5
	352.0	8.3		347.1	4.4		347.0	3.0
0.90	266.6	0.82	0.45	256.4	0.46	0.00	275.9	1.1
	296.7	2.1		295.7	1.3		295.8	1.6
	313.8	3.4		313.8	2.1		313.7	2.1
	332.7	5.0		332.7	3.0		332.7	2.8
	352.0	2.1		349.1	3.9		347.0	3.1
0.80	256.2	0.43	0.30	265.3	0.70			
	295.9	1.7		295.8	1.5			
	313.8	2.6		313.8	2.2			
	332.7	4.1		332.7	3.0			
	352.1	5.7		349.1	3.8			

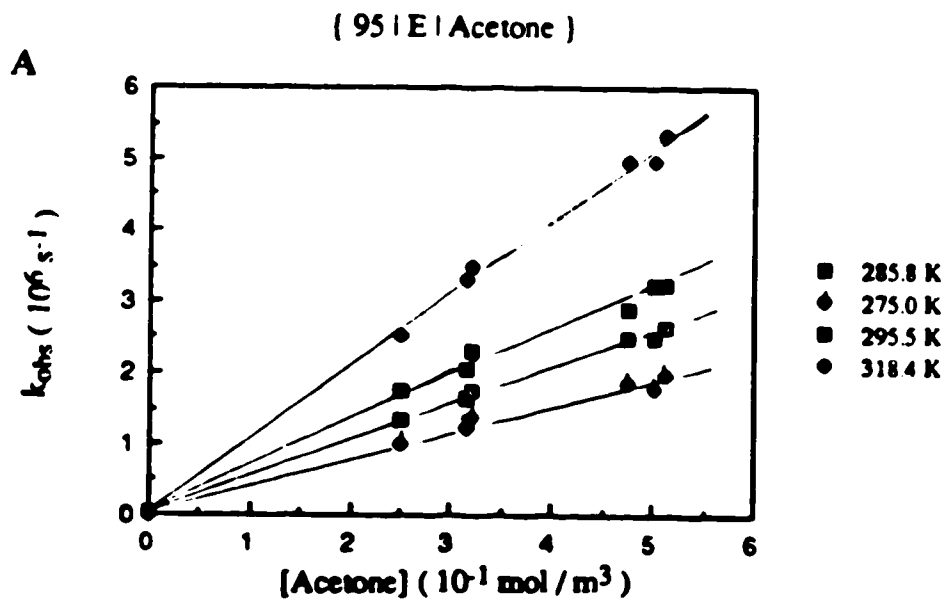
**Table 3-10** Rate parameters for the reaction of solvated electrons with nitrobenzene in ethanol / water mixtures

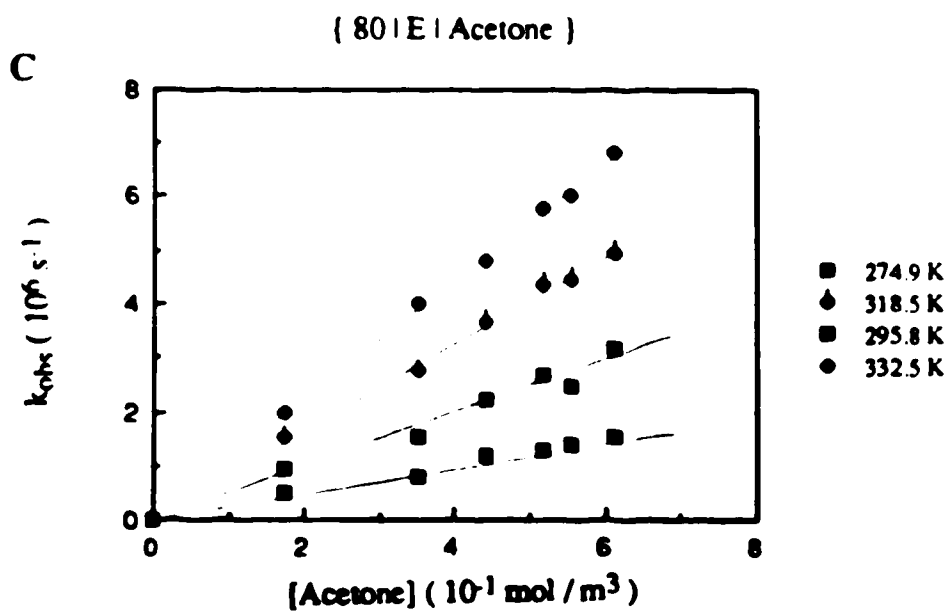
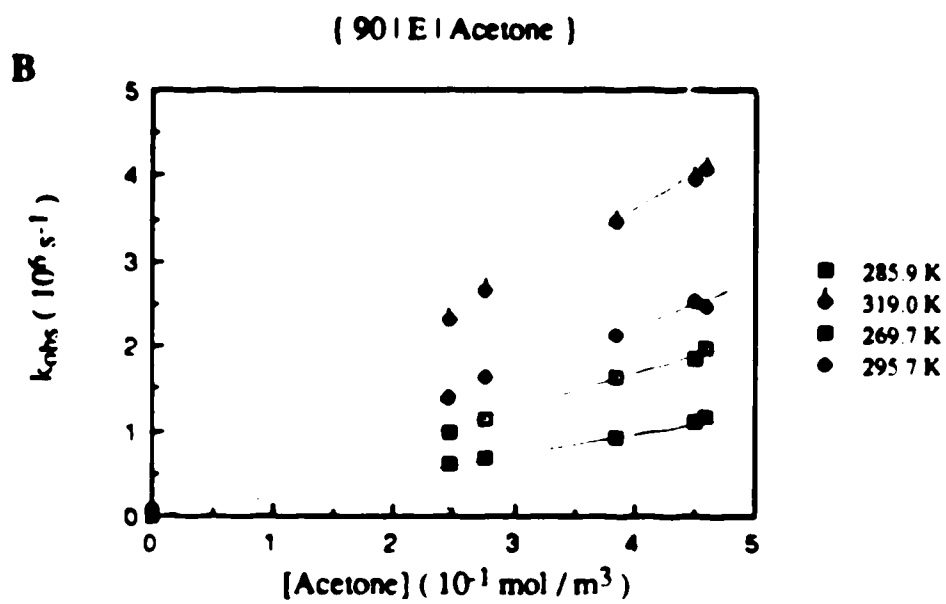
$\chi_w$	$k_{298}$ ( $10^7 \text{ m}^3/\text{mol.s}$ )	$E_a$ (kJ/mol.)	LogA	$\Delta S^\ddagger$ (J/mol.K)
1.00	3.7	17	13.42	12
0.95	2.8	18	13.62	16
0.90	2.2	20	13.78	19
0.80	1.7	21	13.87	20
0.70	1.4	20	13.62	16
0.60	1.6	18	13.40	11
0.45	1.5	17	13.11	6
0.30	1.6	15	12.88	2
0.20	1.5	15	12.78	0
0.10	1.4	14	12.52	-5
0.00	1.6	13	12.40	-8

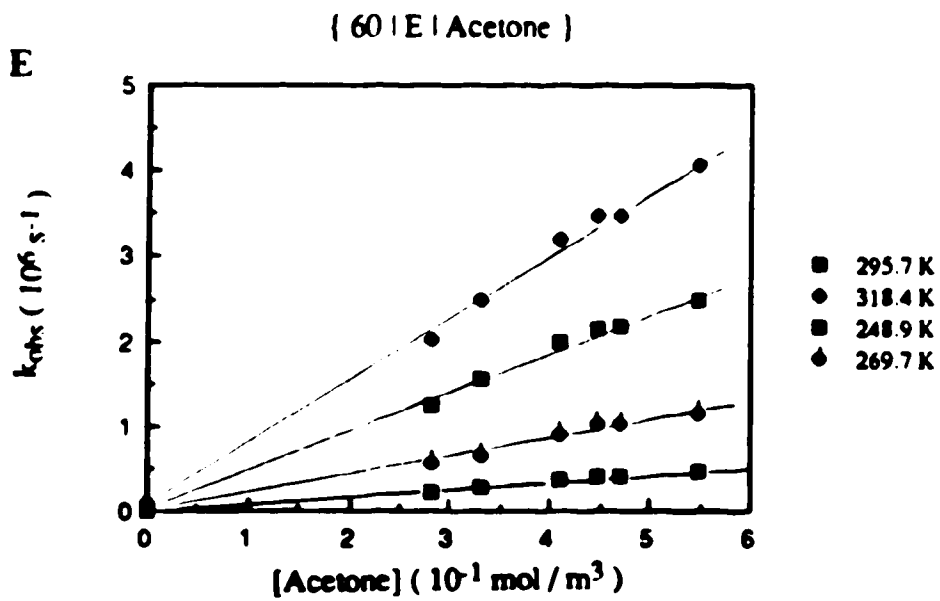
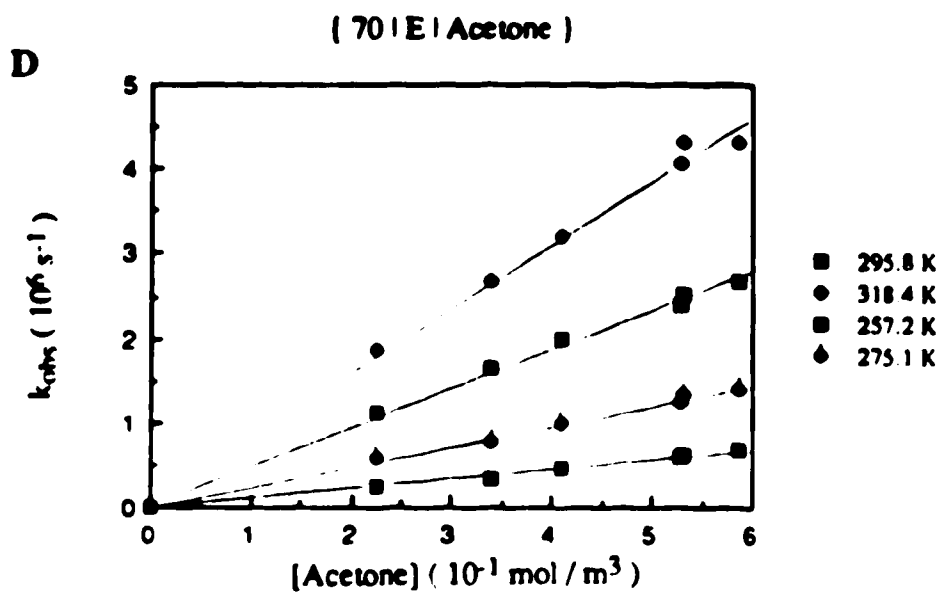
### B. Reaction of solvated electrons with acetone

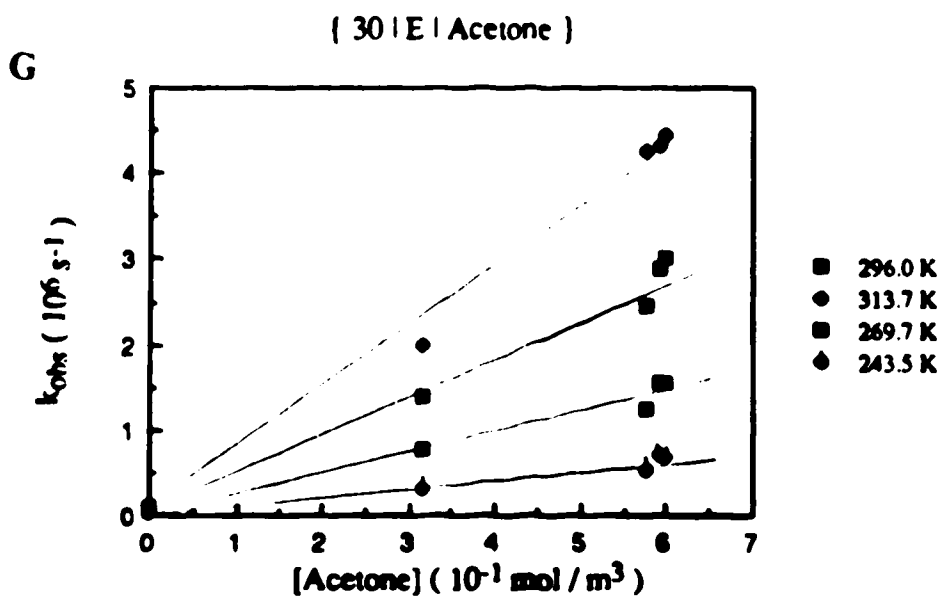
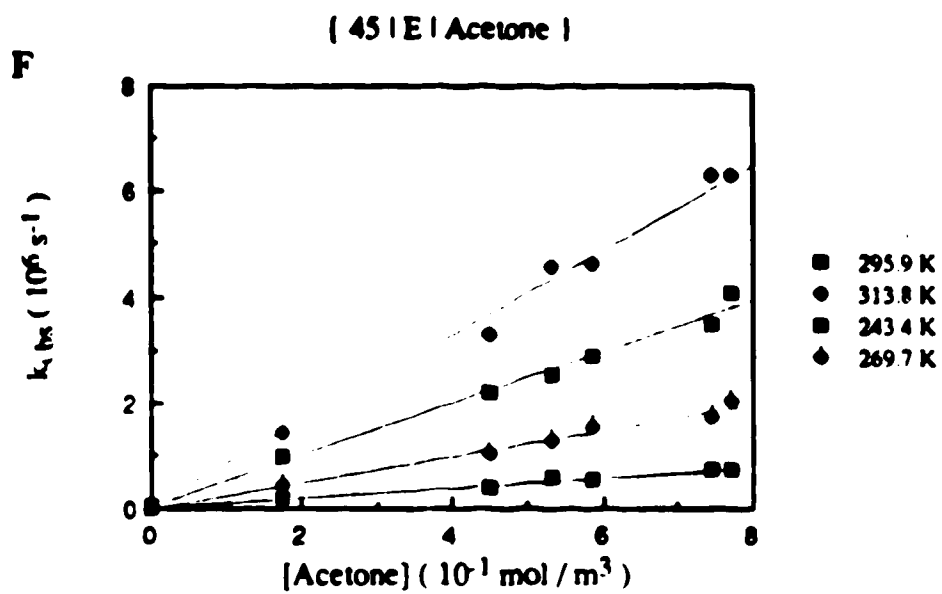
The temperature and concentration dependence of the first-order rate constant for the reaction of solvated electrons with acetone are shown in Figs.3-13(A-J). The concentration range of acetone was 100-930 mmol/m<sup>3</sup>. The second-order rate constants at various temperatures are listed in Table 3-11. The rate parameters are obtained from the Arrhenius plots in Fig.3-14. They are summarized in Table 3-12. The rate constant in ethanol at 298K is  $6.3 \times 10^6 \text{ m}^3/\text{mol}\cdot\text{s}$ . The literature value is  $4.7 \times 10^6 \text{ m}^3/\text{mol}\cdot\text{s}$  (100).

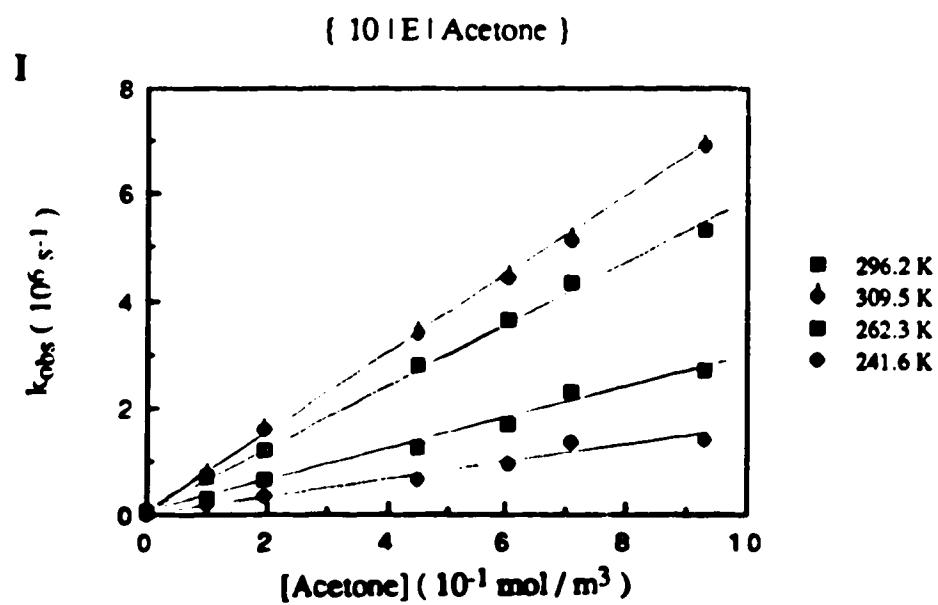
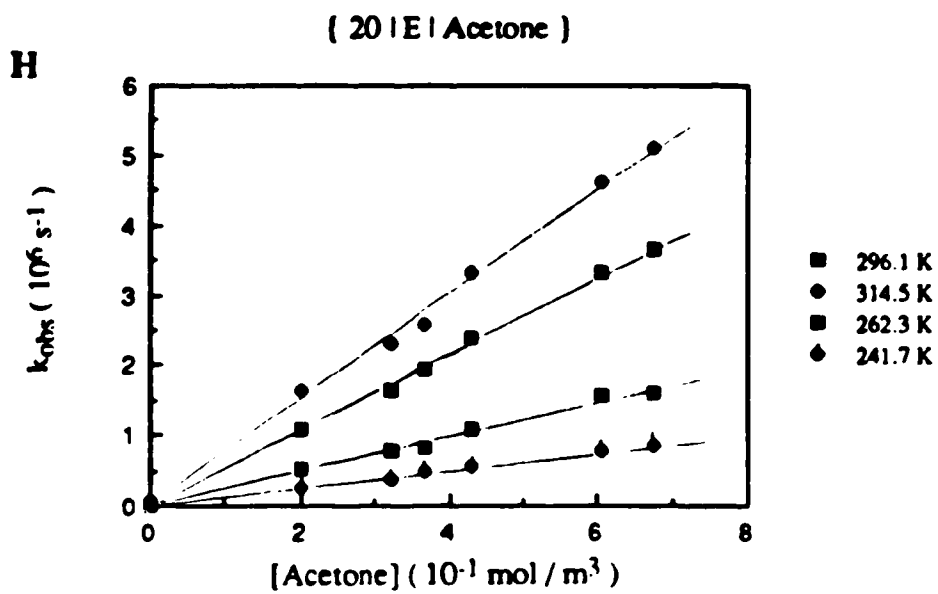
Fig. 3-13 Temperature and concentration dependence of the first-order rate constant for the reaction of solvated electrons with acetone in ethanol / water mixtures (A-J)











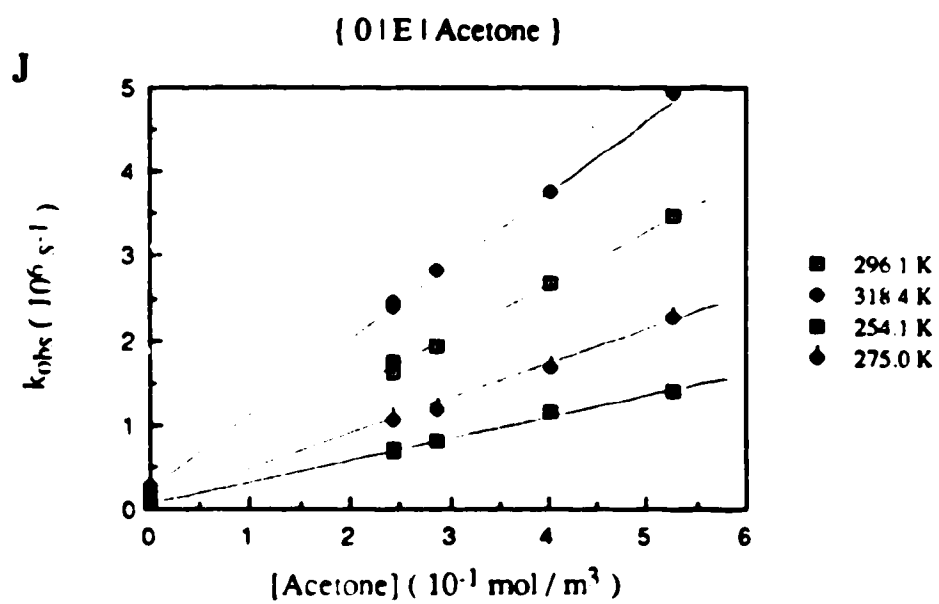




Fig. 3-14 Arrhenius plots for the reaction of solvated electrons with acetone in ethanol / water mixtures

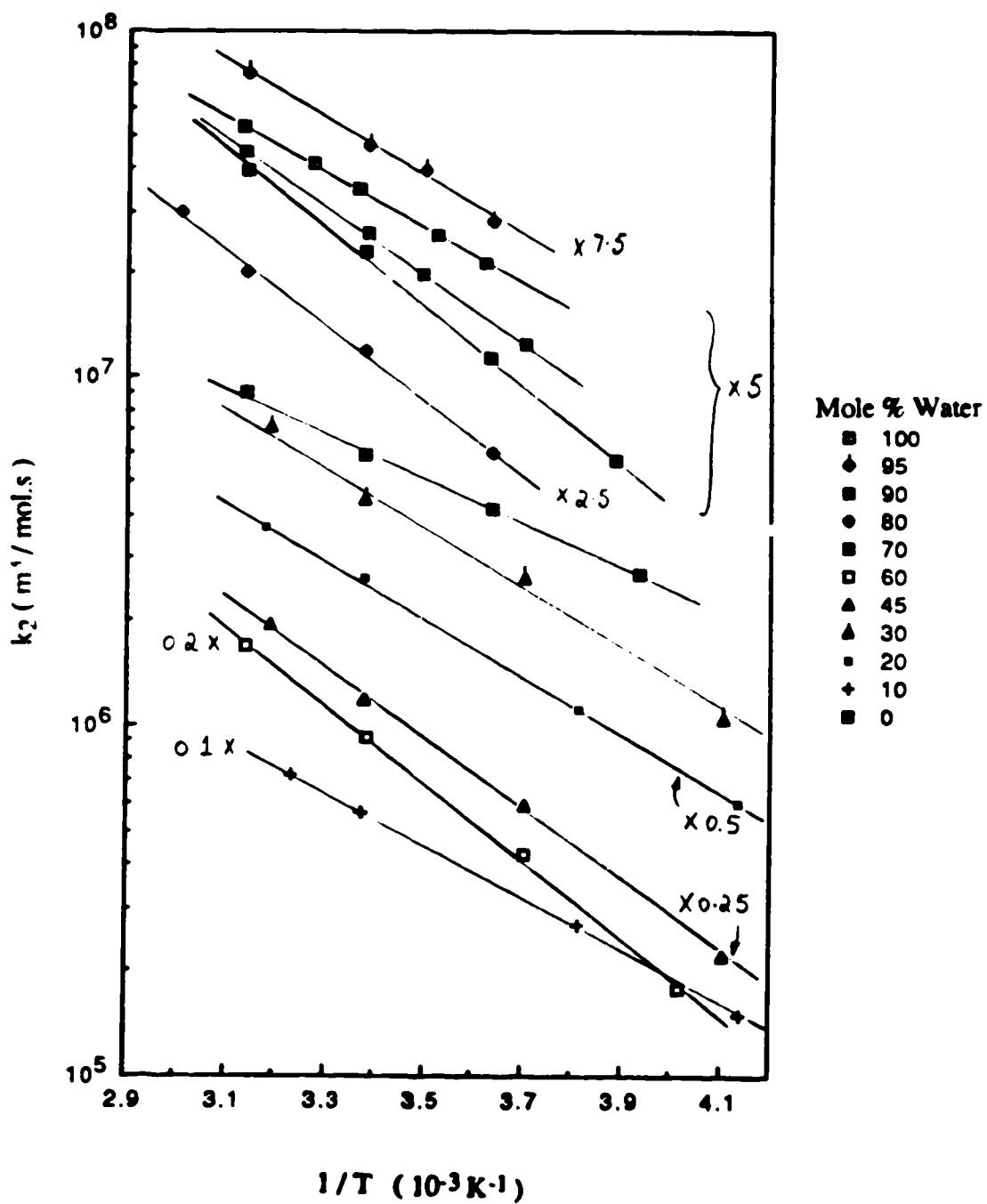




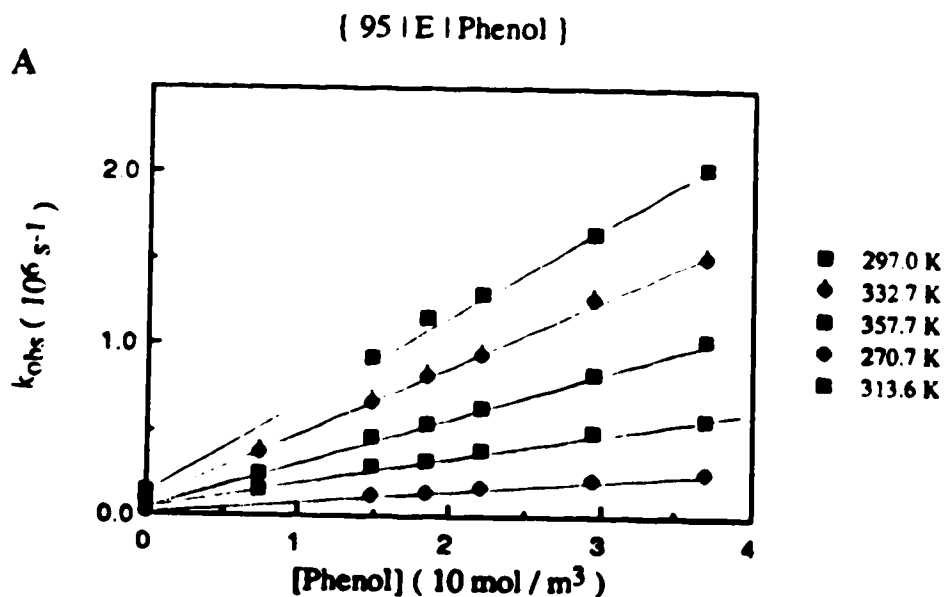
Table 3-12 Rate parameters for the reaction of solvated electrons with  
acetone in ethanol / water mixtures

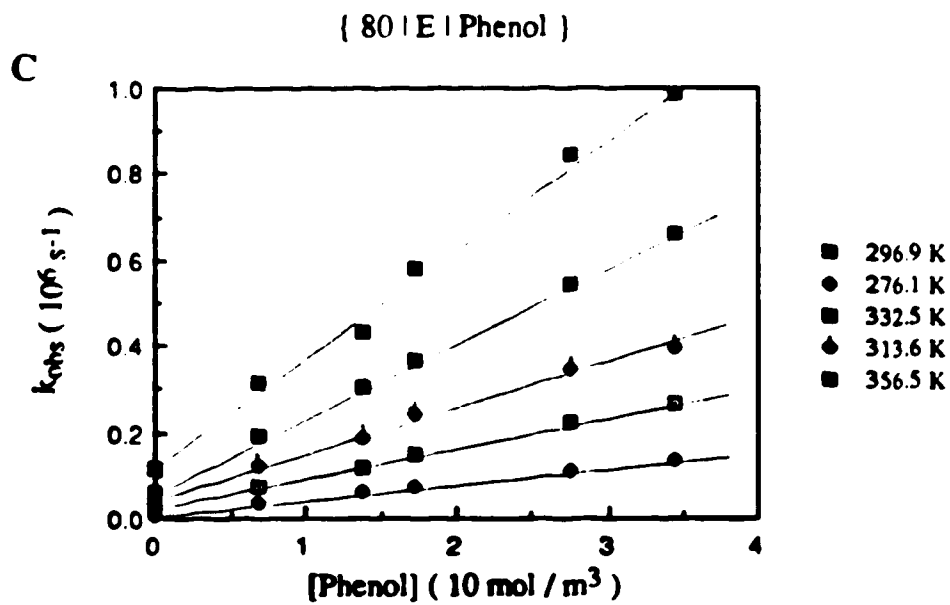
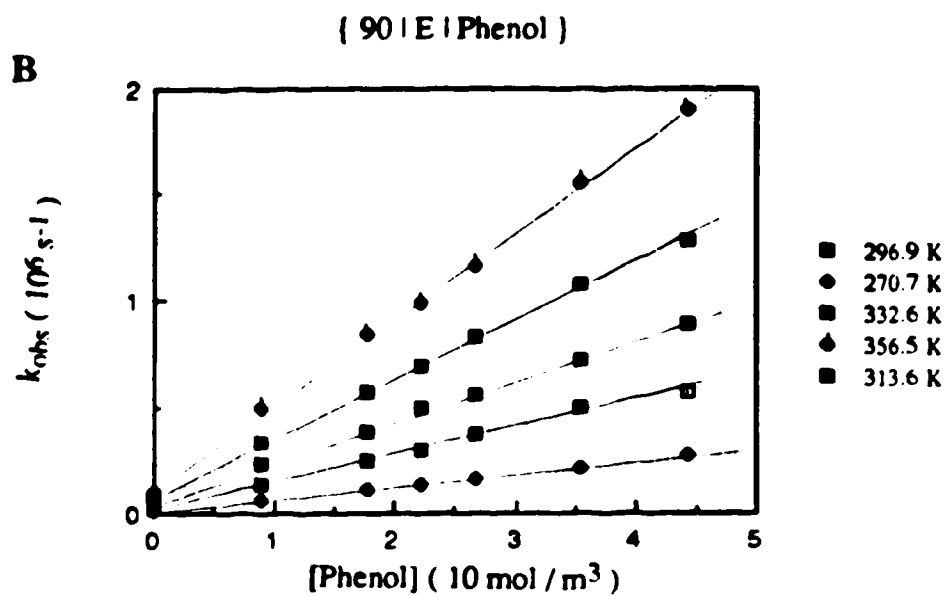
$\chi_w$	$k_{298}$ ( $10^6 \text{ m}^3/\text{mol.s}$ )	$E_a$ (kJ/mol.)	LogA	$\Delta S^\ddagger$ (J/mol.K)
1.00	7.7	15	12.45	-7
0.95	6.6	17	12.72	-2
0.90	5.5	19	13.00	4
0.80	4.9	21	13.36	11
0.70	4.7	22	13.47	13
0.60	5.0	21	13.43	12
0.45	5.0	19	13.08	5
0.30	5.0	17	12.74	-1
0.20	5.2	16	12.44	-8
0.10	5.8	14	12.27	-10
0.00	6.3	13	12.00	-15

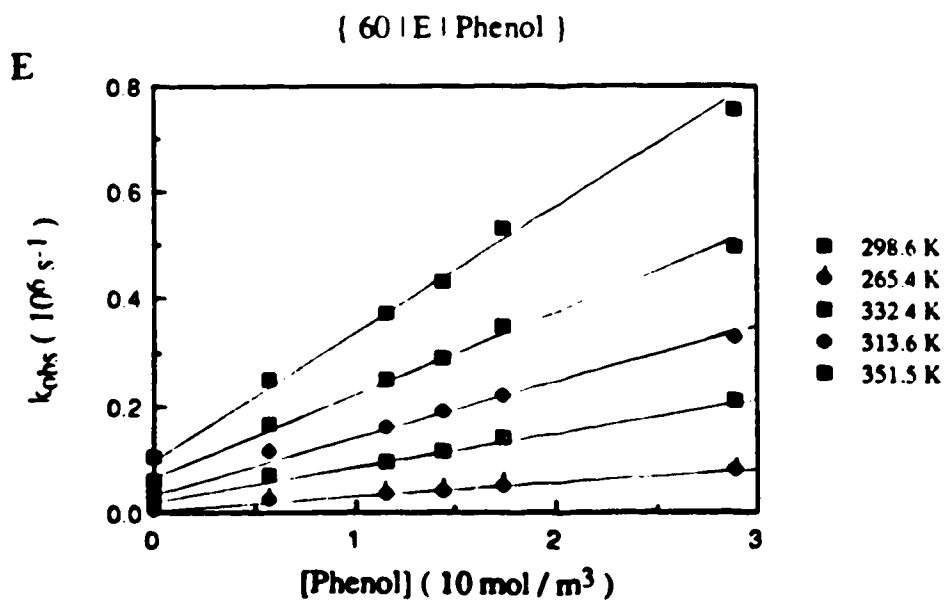
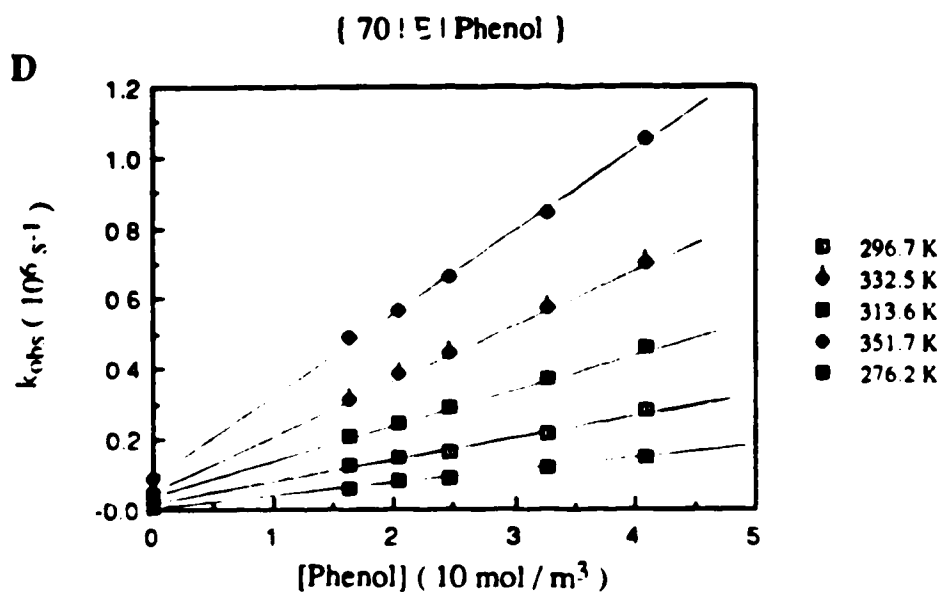
C. Reaction of solvated electrons with phenol

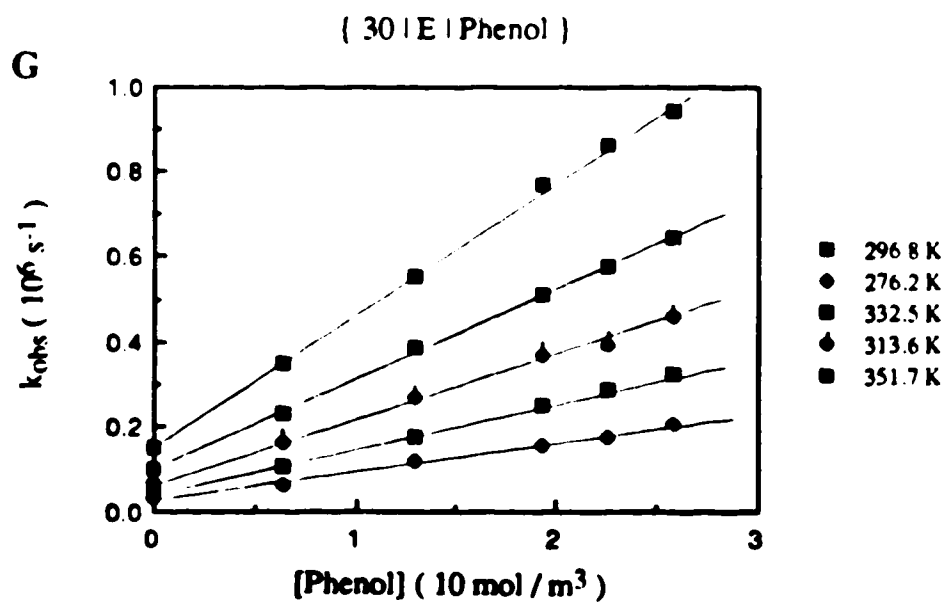
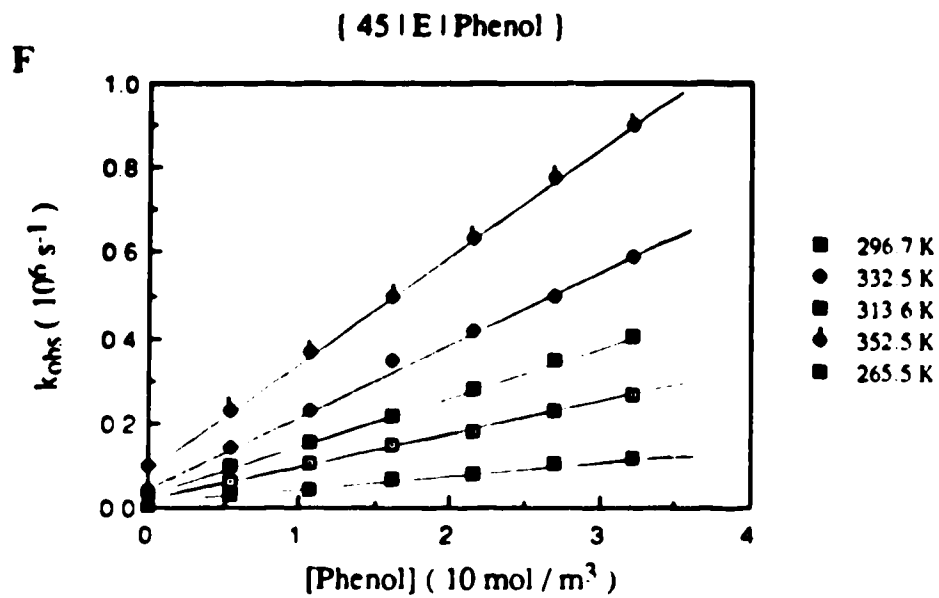
The temperature and concentration dependence of the first-order rate constant for the reaction of solvated electrons with phenol are shown in Figs.3-15(A-J). The concentration range of phenol was 5-57 mol/m<sup>3</sup>. The second-order rate constants at various temperatures are listed in Table 3-13. In contrast to the reaction of solvated electrons with the same scavenger in the methanol / water mixtures, the Arrhenius plots (Fig.3-16) of the water-rich ethanol mixtures do not show any significant curvature (Fig.3-16). The rate parameters are summarized in Table 3-14. The rate constant in ethanol at 298K is  $5.9 \times 10^4$  m<sup>3</sup>/mol.s. The literature value is  $5.0 \times 10^4$  m<sup>3</sup>/mol.s (98).

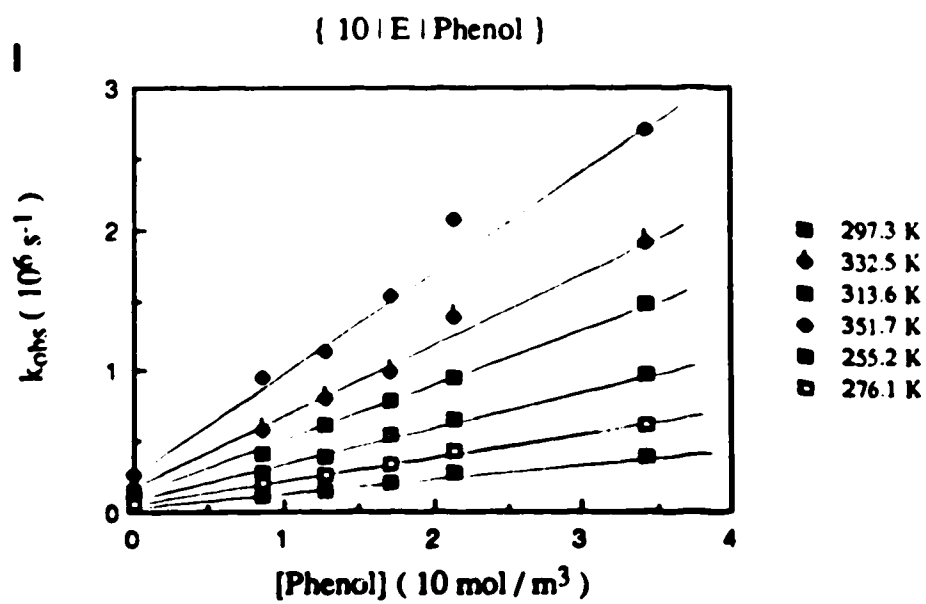
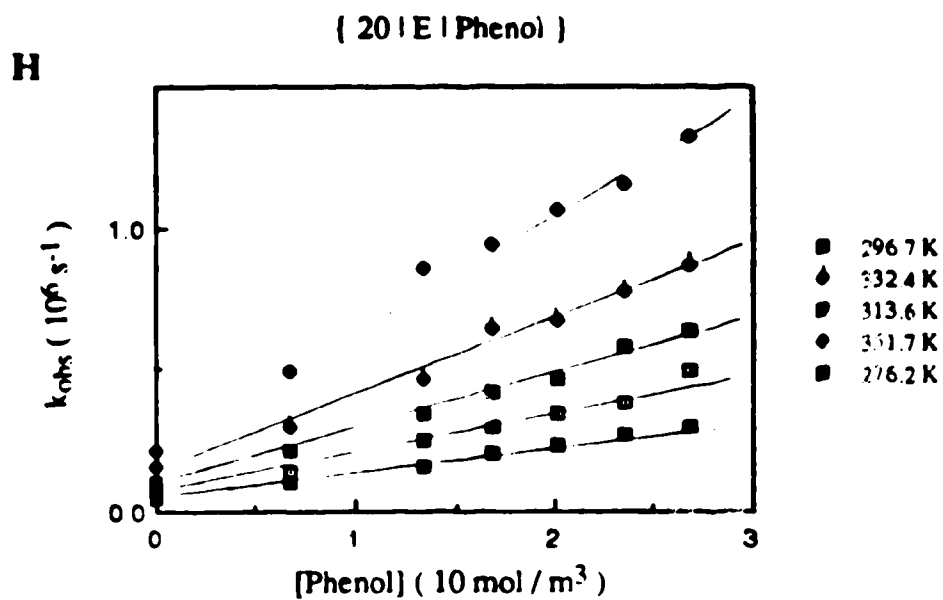
Fig. 3-15 Temperature and concentration dependence of the first-order rate constant for the reaction of solvated electrons with phenol in ethanol / water mixtures (A-J)













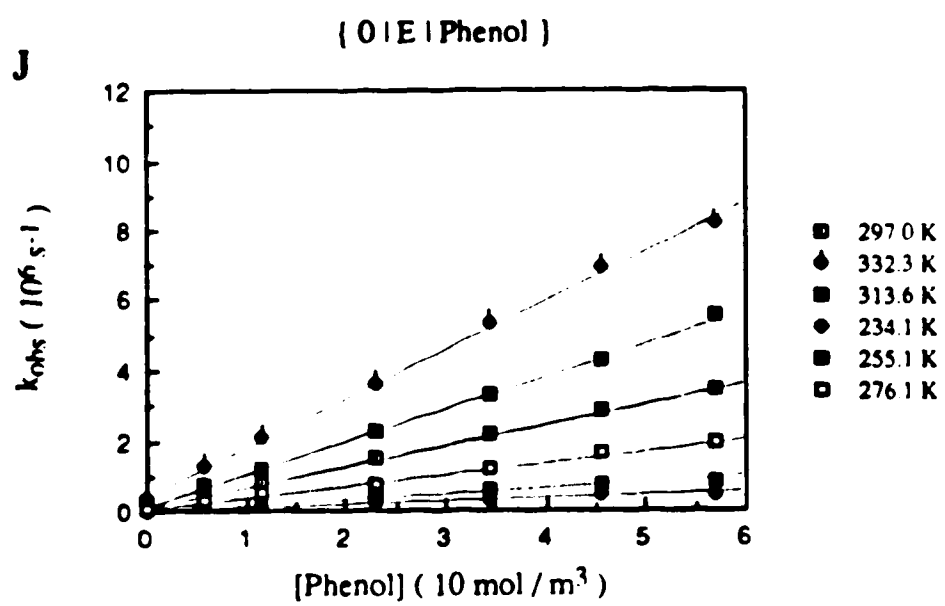
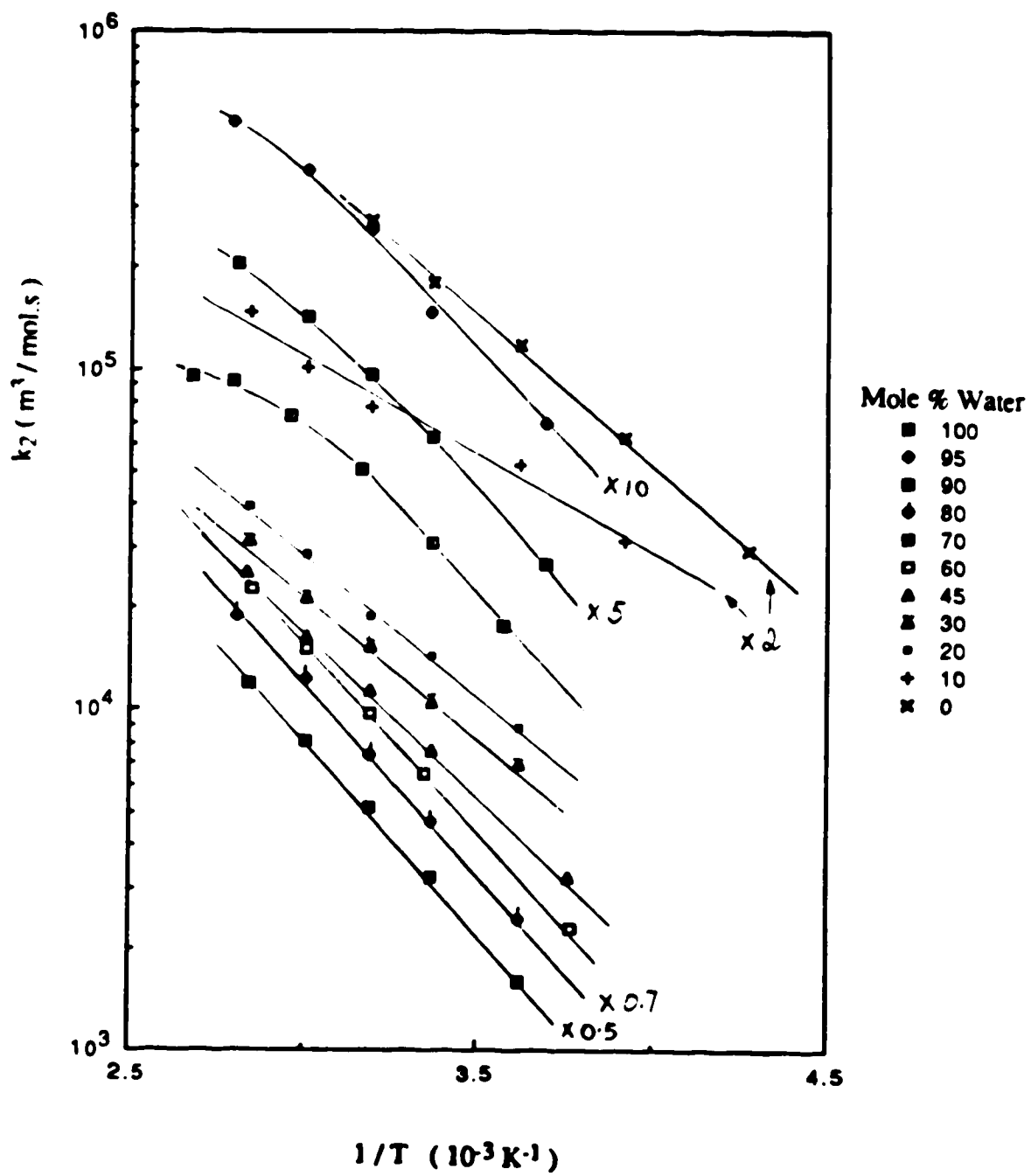


Fig. 3-16 Arrhenius plots for the reaction of solvated electrons with phenol in ethanol / water mixtures





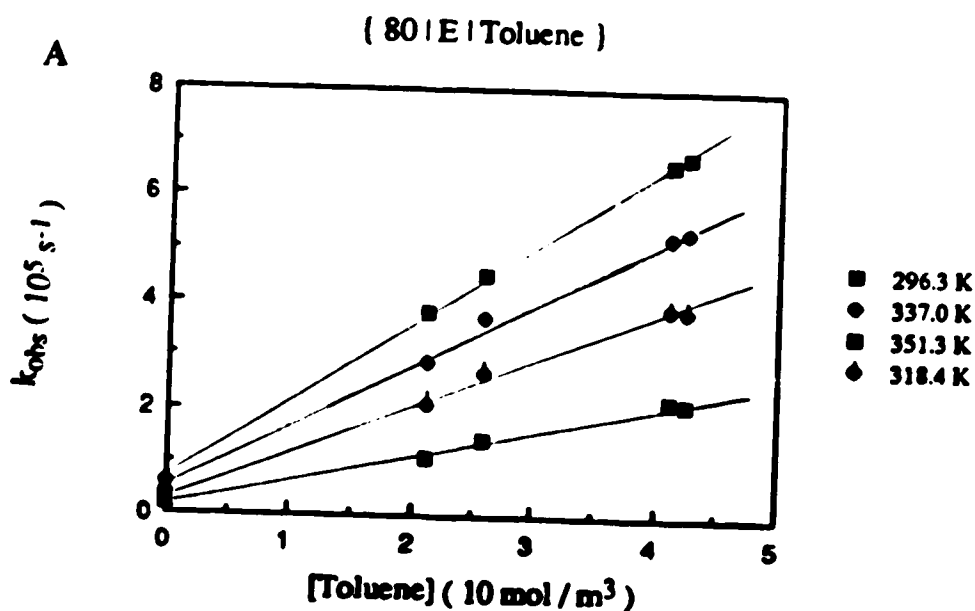
**Table 3-14 Rate parameters for the reaction of solvated electrons with phenol in ethanol / water mixtures**

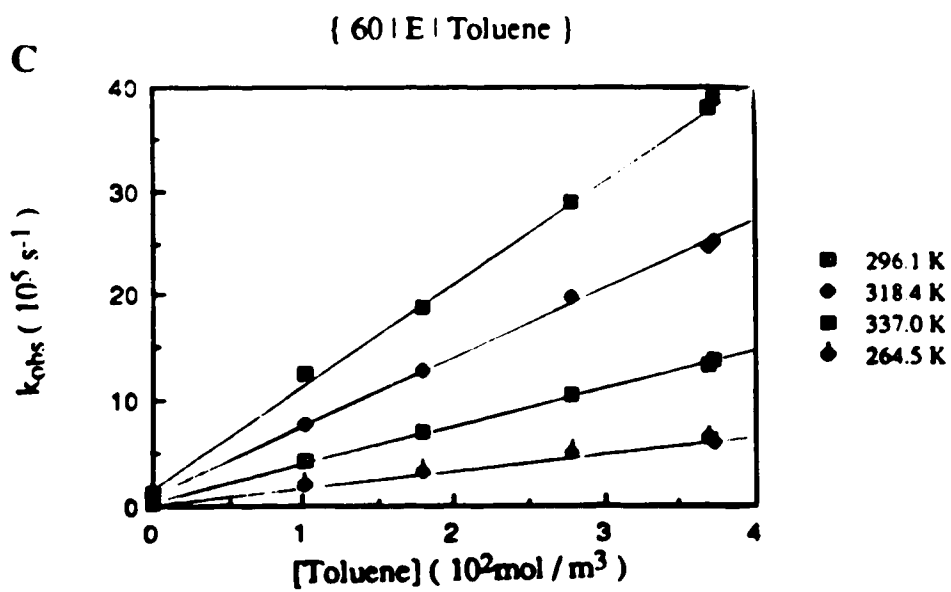
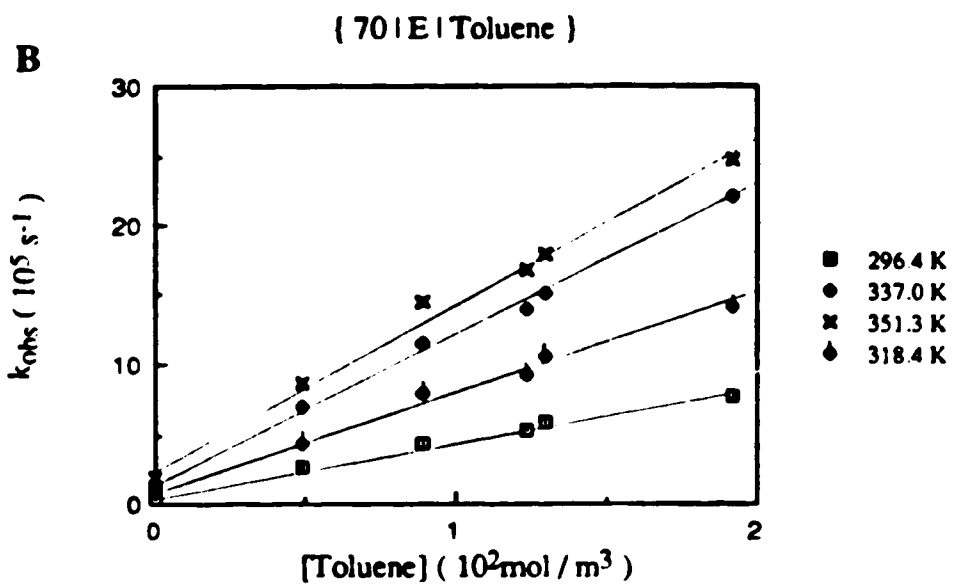
$\chi_w$	$k_{298}$ ( $10^4 \text{ m}^3/\text{mol.s}$ )	$E_a$ (kJ/mol.)	LogA	$\Delta S^\ddagger$ (J/mol.K)
1.00	3.0	18	10.58	-42
0.95	1.6	20	10.80	-38
0.90	1.3	21	10.77	-39
0.80	0.70	22	10.67	-41
0.70	0.64	21	10.54	-43
0.60	0.65	20	10.40	-45
0.45	0.77	19	10.13	-51
0.30	1.1	17	9.96	-54
0.20	1.5	16	10.11	-51
0.10	2.7	16	10.29	-48
0.00	5.9	20	11.35	-27

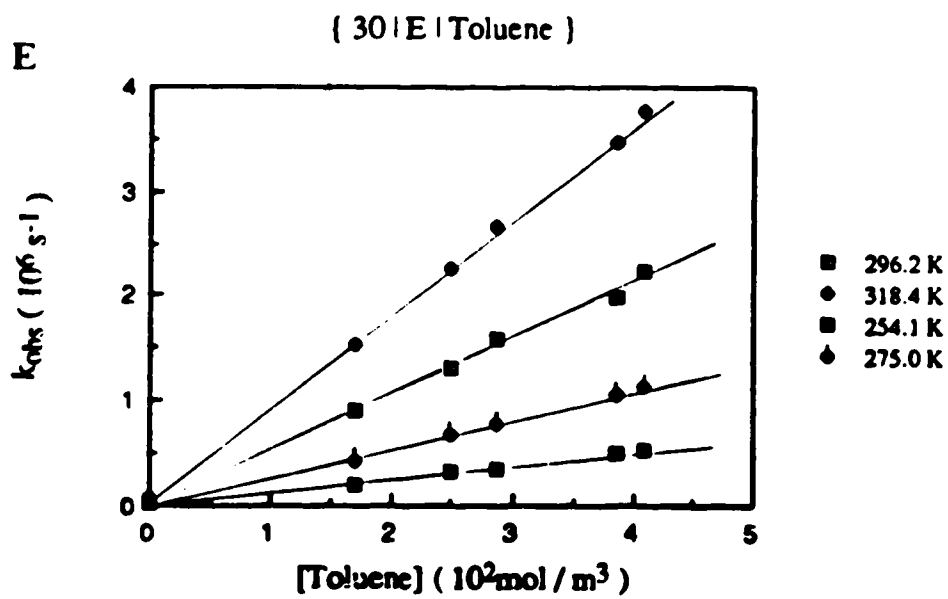
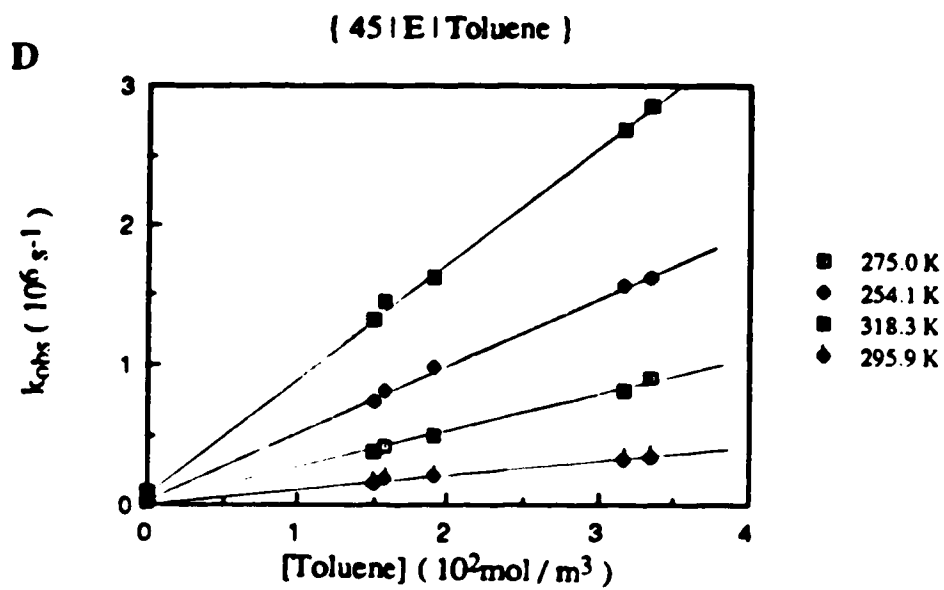
#### D. Reaction of solvated electrons with toluene

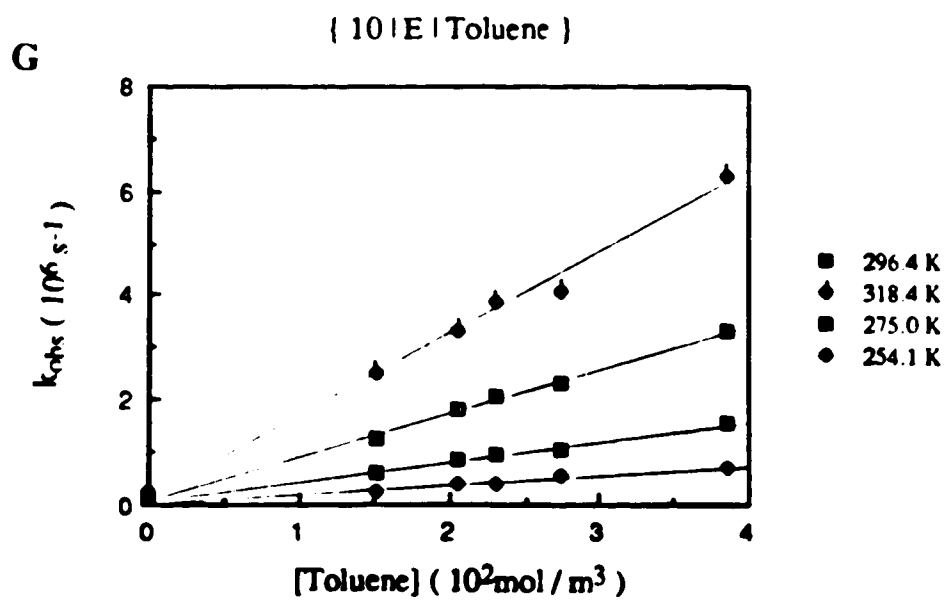
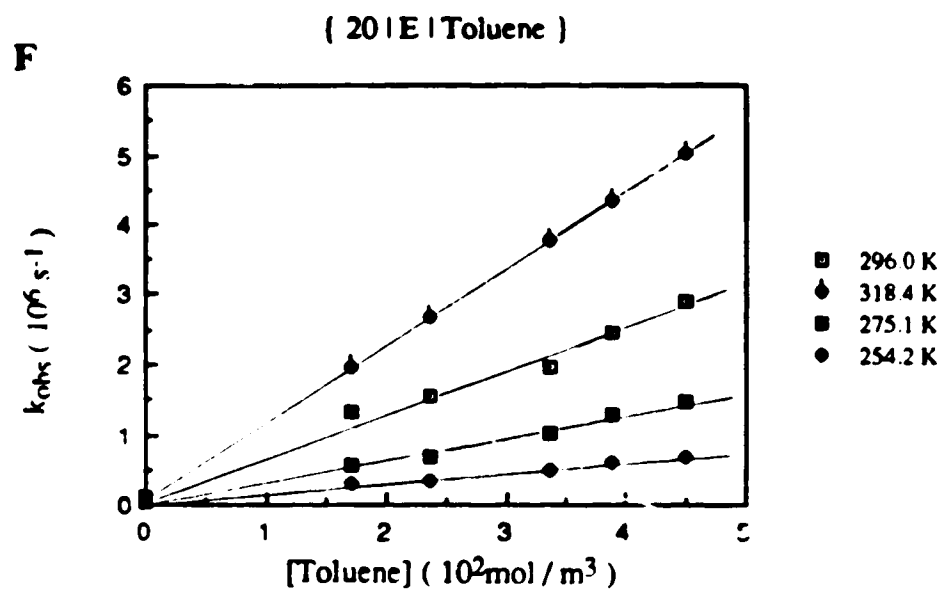
The temperature and concentration dependence of the first-order rate constant for the reaction of solvated electrons with toluene are shown in Figs.3-17(A-H). The concentration range of toluene was 21-450 mol/m<sup>3</sup>. The second-order rate constants at various temperatures are listed in Table 3-15. The rate parameters are obtained from the Arrhenius plots in Fig.3-18. They are summarized in Table 3-16. The rate constant in ethanol at 298K is  $9.2 \times 10^3$  m<sup>3</sup>/mol.s. The literature results are  $5.1 \times 10^3$  m<sup>3</sup>/mol.s (99) and  $6.4 \times 10^3$  m<sup>3</sup>/mol.s (98).

Fig. 3-17  
(A-H) Temperature and concentration dependence of the first-order rate constant for the reaction of solvated electrons with toluene in ethanol / water mixtures











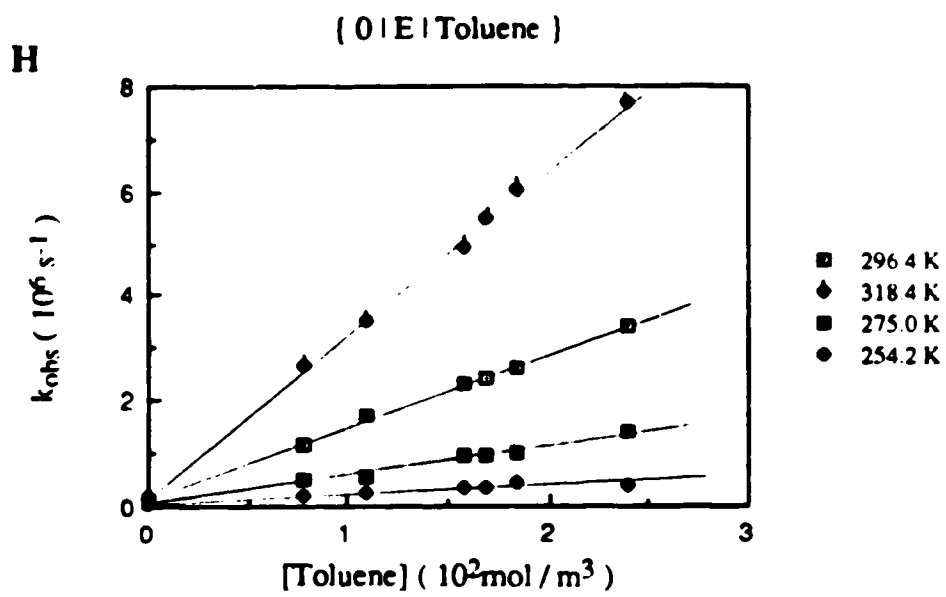
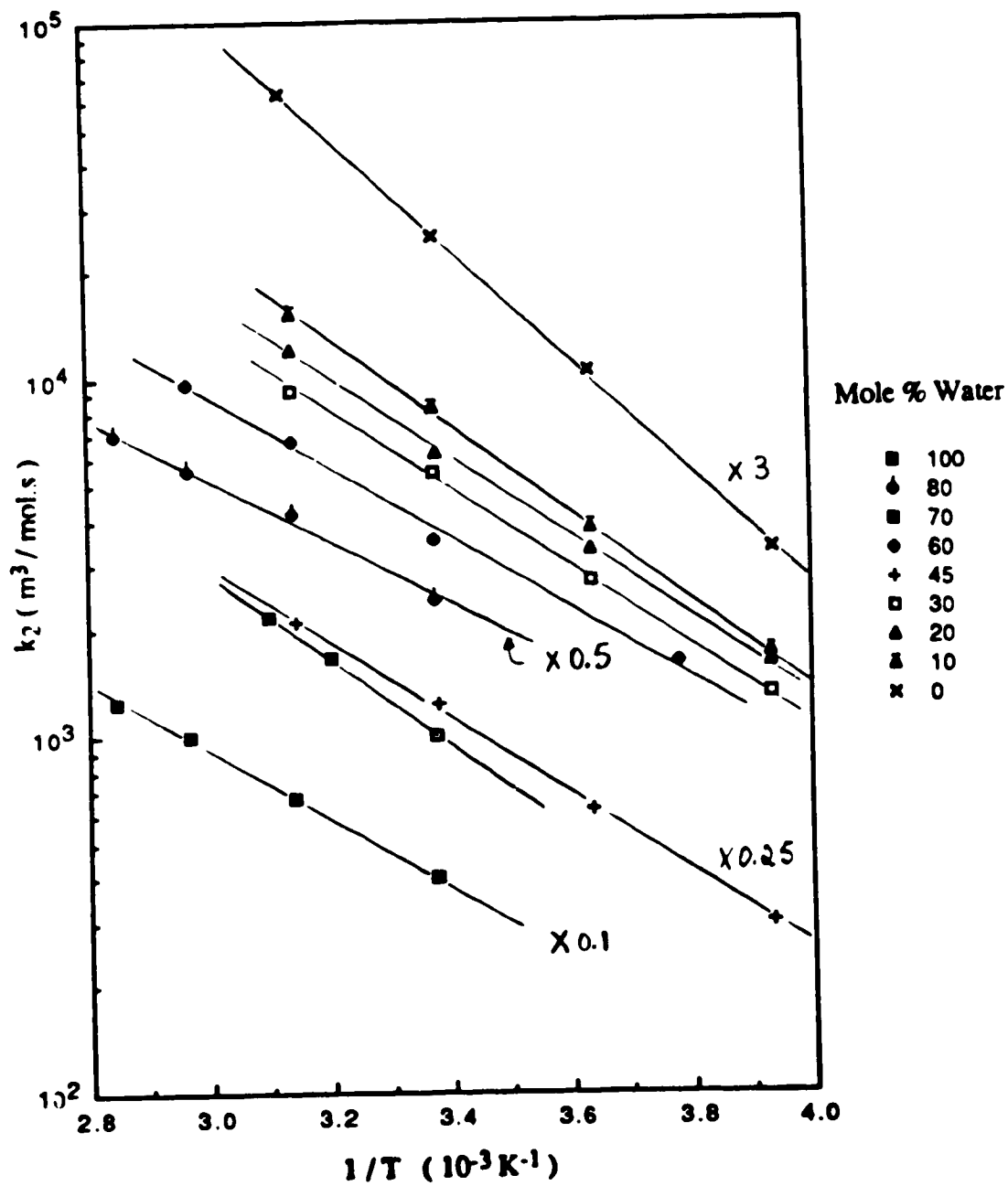


Fig. 3-18 Arrhenius plots for the reaction of solvated electrons with toluene in ethanol / water mixtures



**Table 3-15 Second-order rate constants for the reaction of solvated electrons with toluene in ethanol / water mixtures at various temperatures**

$\chi_w$	Temp.	$k_2$	$\chi_w$	Temp.	$k_2$	$\chi_w$	Temp.	$k_2$
	(K)	( $10^3 \text{ m}^3/\text{mol.s}$ )		(K)	( $10^3 \text{ m}^3/\text{mol.s}$ )		(K)	( $10^3 \text{ m}^3/\text{mol.s}$ )
1.00	296.1	1.0	0.60	264.5	1.6	0.10	254.1	1.7
	312.3	1.7		296.1	3.5		275.0	3.8
	322.6	2.1		318.4	6.6		296.4	8.2
				337.0	9.7		318.4	15
0.80	296.3	4.8	0.45	254.1	1.2	0.20	254.2	1.6
	318.4	8.4		275.0	2.5		275.0	3.3
	337.0	11		295.9	4.9		296.0	6.2
	351.3	14		318.3	8.3		318.4	12
0.70	296.4	4.0	0.30	254.1	1.3	0.00	254.2	1.1
	318.4	6.8		275.0	2.7		275.0	3.4
	337.0	10		296.2	5.4		296.4	8.3
	351.3	12		318.4	9.2		318.4	19

**Table 3-16** Rate parameters for the reaction of solvated electrons with  
toluene in ethanol / water mixtures

$\chi_w$	$k_{298}$ ( $10^3 \text{ m}^3/\text{mol.s}$ )	$E_a$ (kJ/mol.)	LogA	$\Delta S^\ddagger$ (J/mol.K)
1.00	11.3	18	10.14	-51
0.80	4.8	18	9.85	-56
0.70	4.2	18	9.83	-56
0.60	4.0	19	9.83	-56
0.45	5.0	20	10.10	-51
0.30	5.4	20	10.31	-47
0.20	6.6	21	10.53	-43
0.10	8.4	23	10.91	-36
0.00	9.2	30	12.20	-11

## **II Reaction kinetics of solvated electrons with inorganic ions**

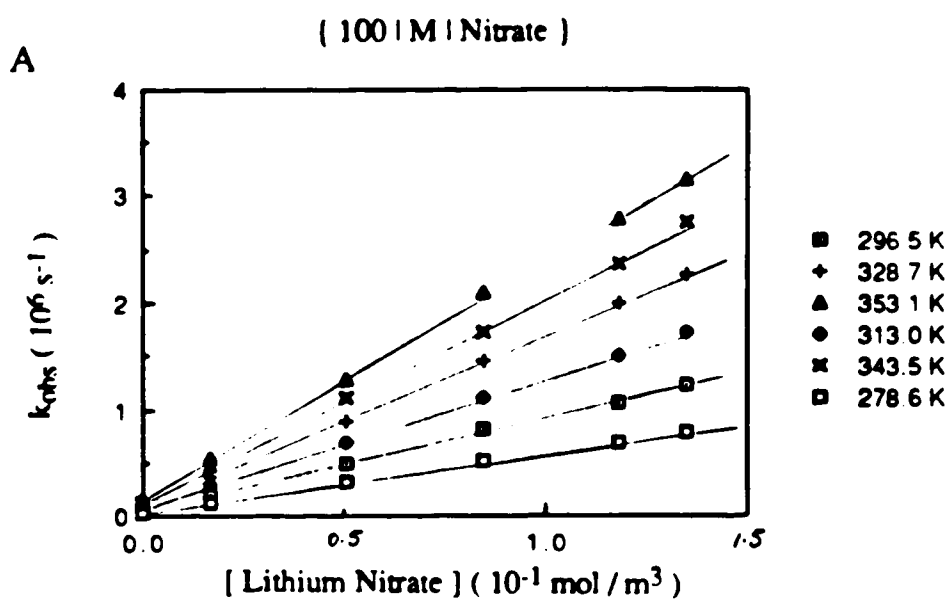
The kinetics of the reaction for solvated electrons with lithium nitrate, silver perchlorate, lithium chromate and copper (II) perchlorate were investigated in the methanol / water and ethanol / water mixed solvents. In aqueous solution, these compounds capture solvated electrons very efficiently so that the rate of reaction is mainly controlled by the rate of diffusion. Since the electron capture rate constant for lithium perchlorate is very low ( $\sim 10^4$  m<sup>3</sup>/mol.s) (134), the nearly diffusion controlled rate constants ( $\sim 10^7$  m<sup>3</sup>/mol.s) obtained here can only be attributed to NO<sub>3</sub><sup>-</sup>, Ag<sup>+</sup>, CrO<sub>4</sub><sup>=</sup> and Cu<sup>2+</sup>, and not their counter ions.

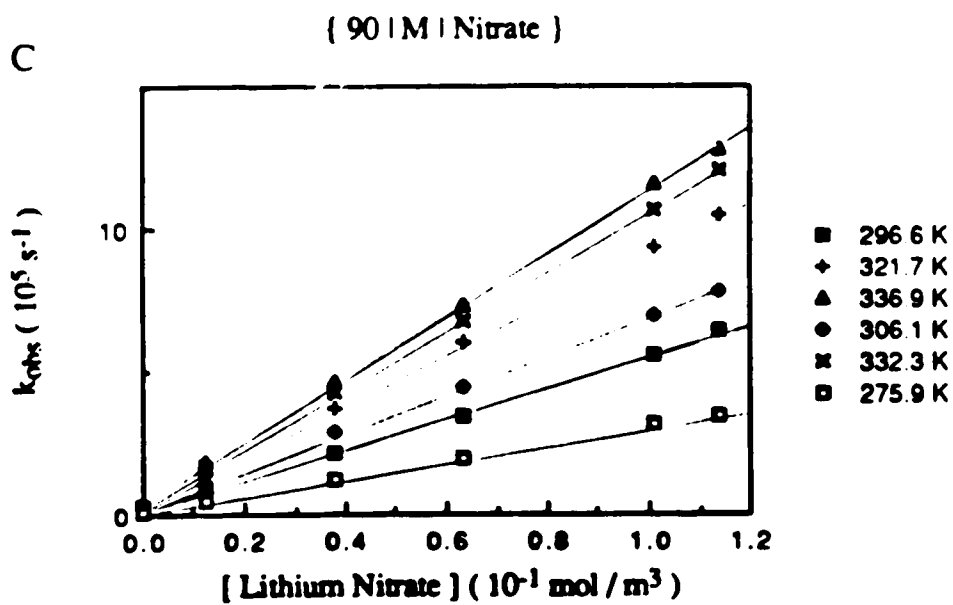
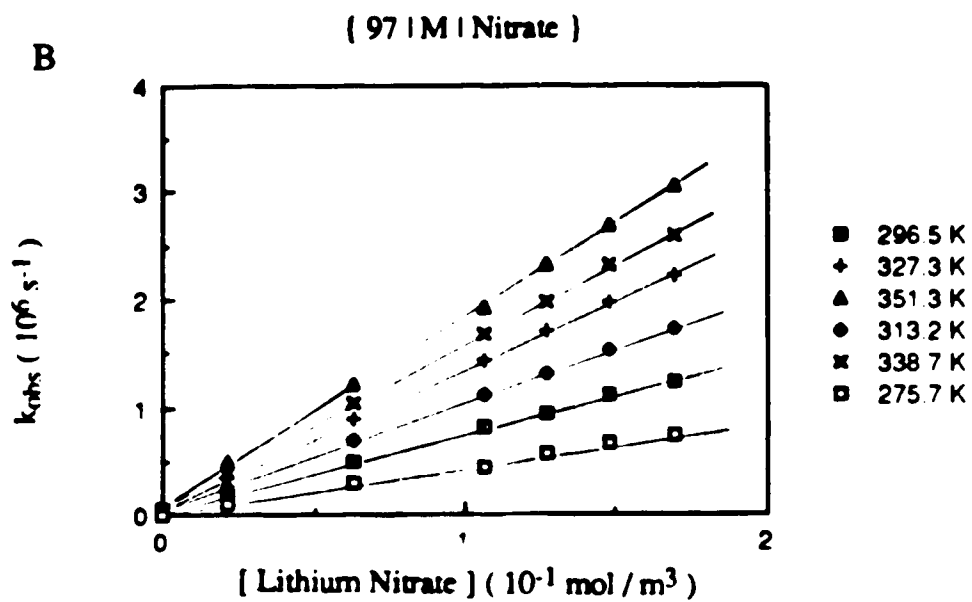
### **1. Reactions of solvated electrons in methanol / water mixed solvents**

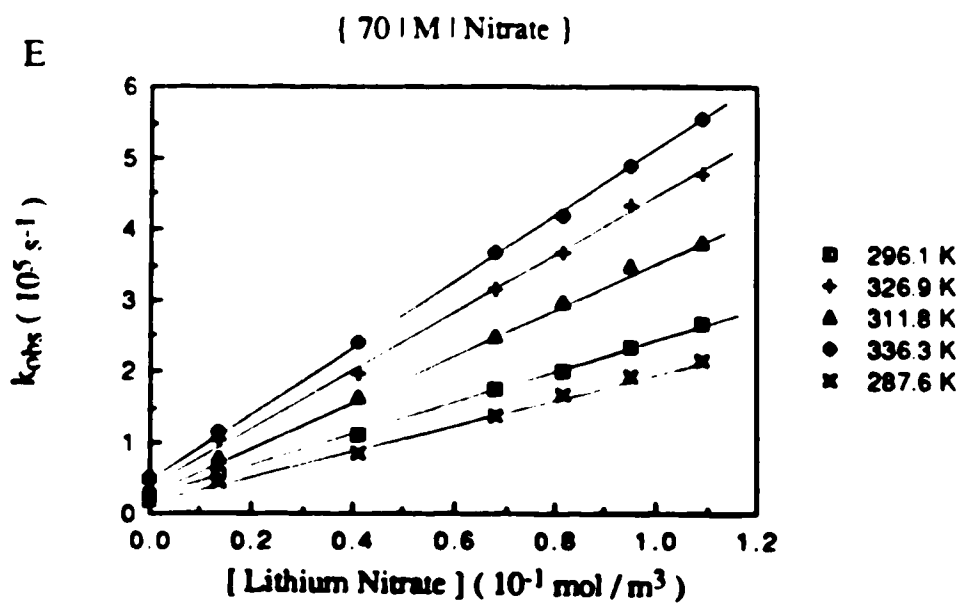
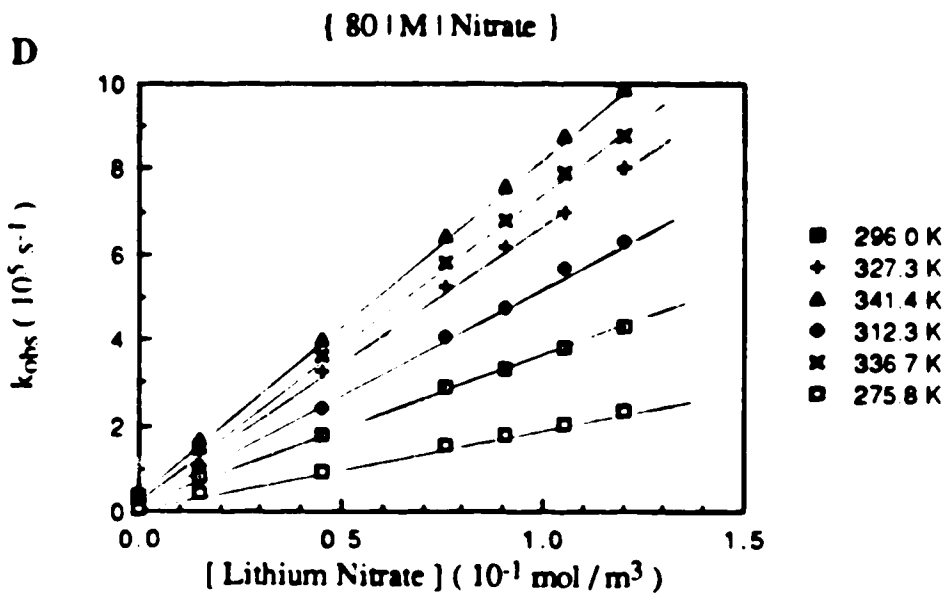
#### **A. Reaction of solvated electrons with nitrate ion**

The temperature and concentration dependence of the first-order rate constant for the reaction of solvated electrons with NO<sub>3</sub><sup>-</sup> are shown in Figs.3-19(A-K). The concentration range of NO<sub>3</sub><sup>-</sup> was 0.02-1.45 mol/m<sup>3</sup>. The second-order rate constants at various temperatures are listed in Table 3-17. The rate constant in water at 298K is  $8.7 \times 10^6$  m<sup>3</sup>/mol.s. The literature results are  $8.5 \times 10^6$  m<sup>3</sup>/mol.s (135) and  $9.4 \times 10^6$  m<sup>3</sup>/mol.s (115). The rate parameters are obtained from the Arrhenius plots in Fig.3-20. They are summarized in Table 3-18. Graphic representation of these results is presented in Discussion (Chapter Four), together with other inorganic electron-scavengers for comparison.

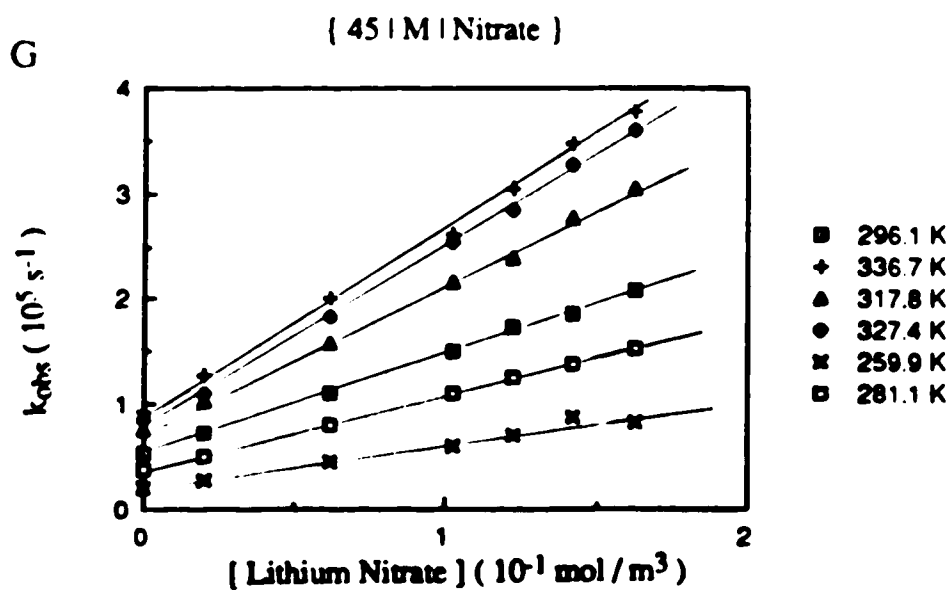
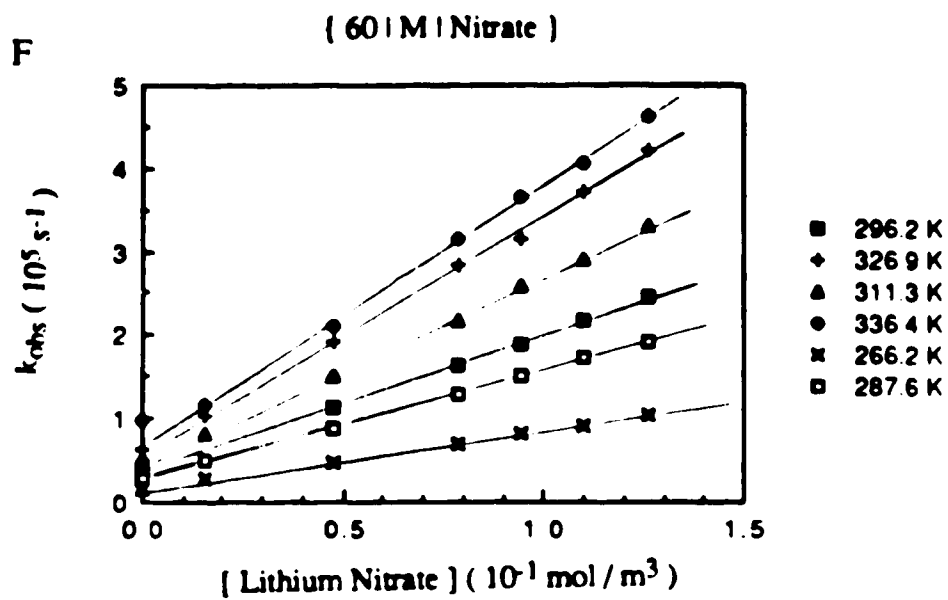
Fig. 3-19 Temperature and concentration dependence of the first-order rate constant for the reaction of solvated electrons with lithium nitrate in methanol / water mixtures (A-K)

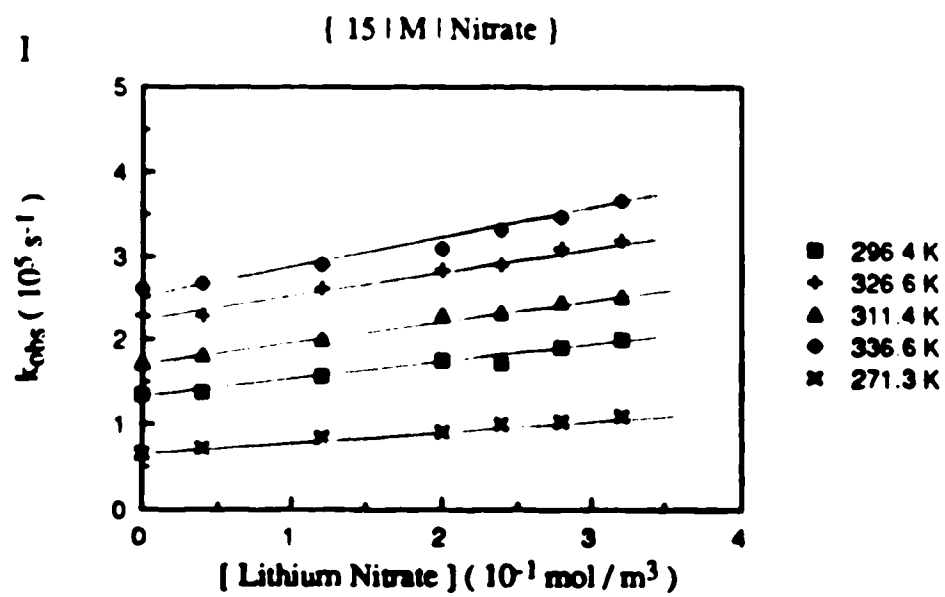
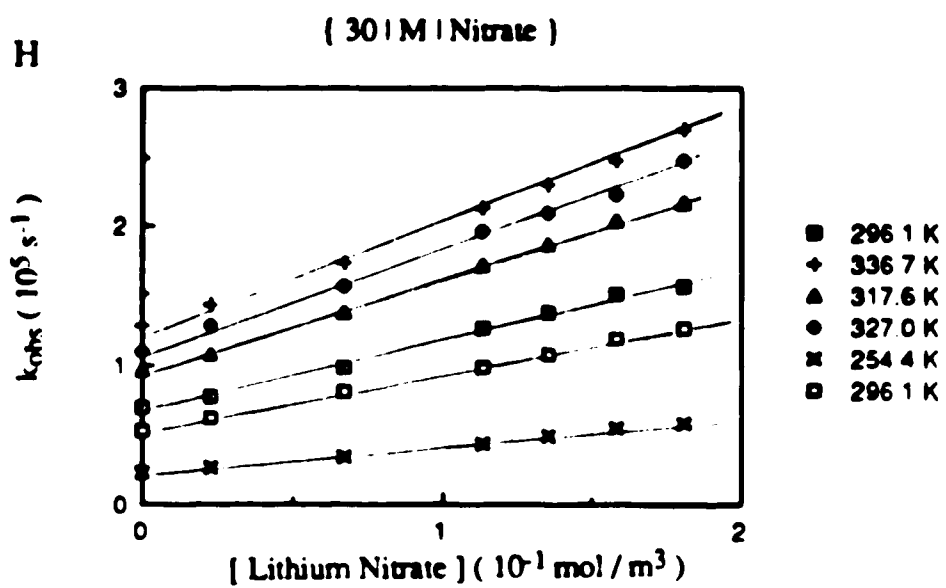












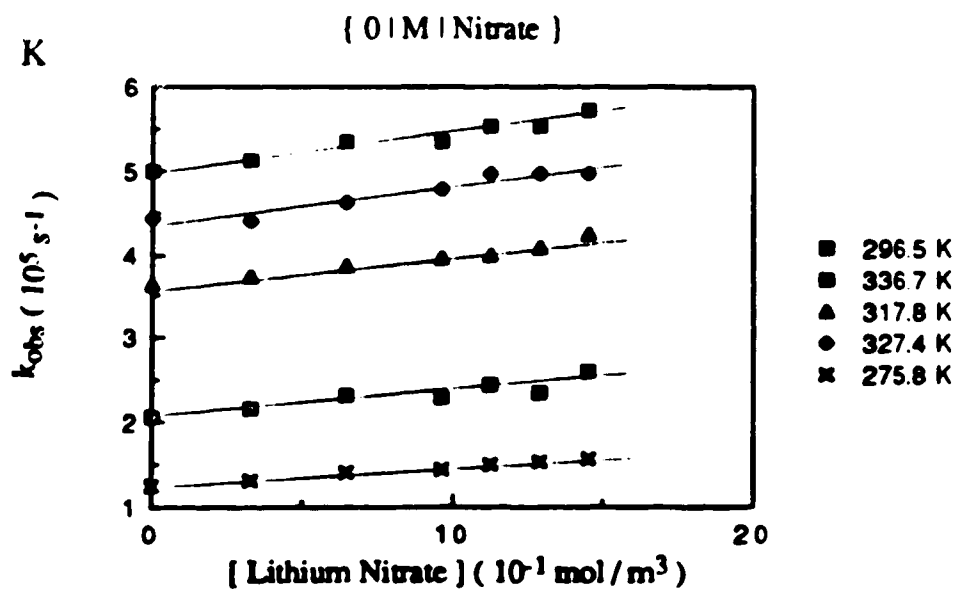
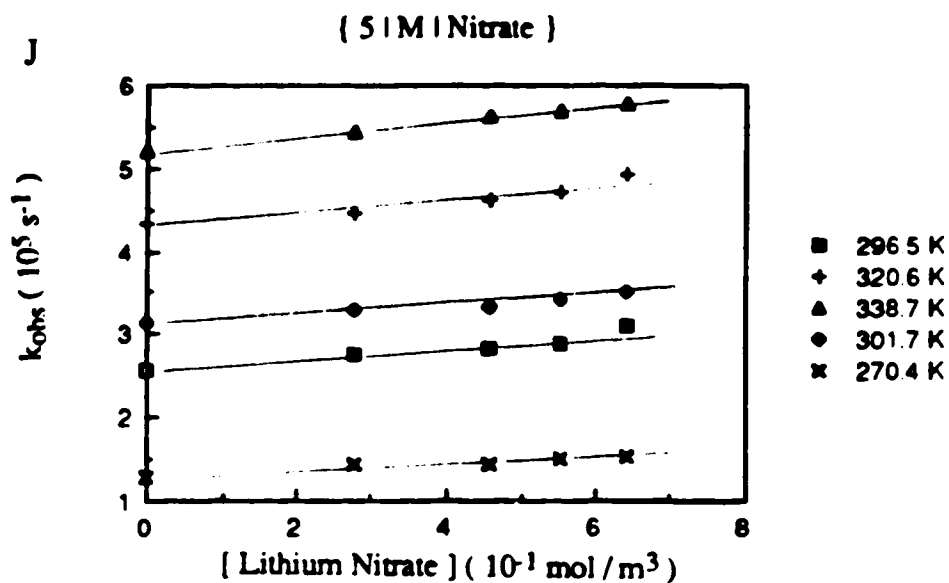
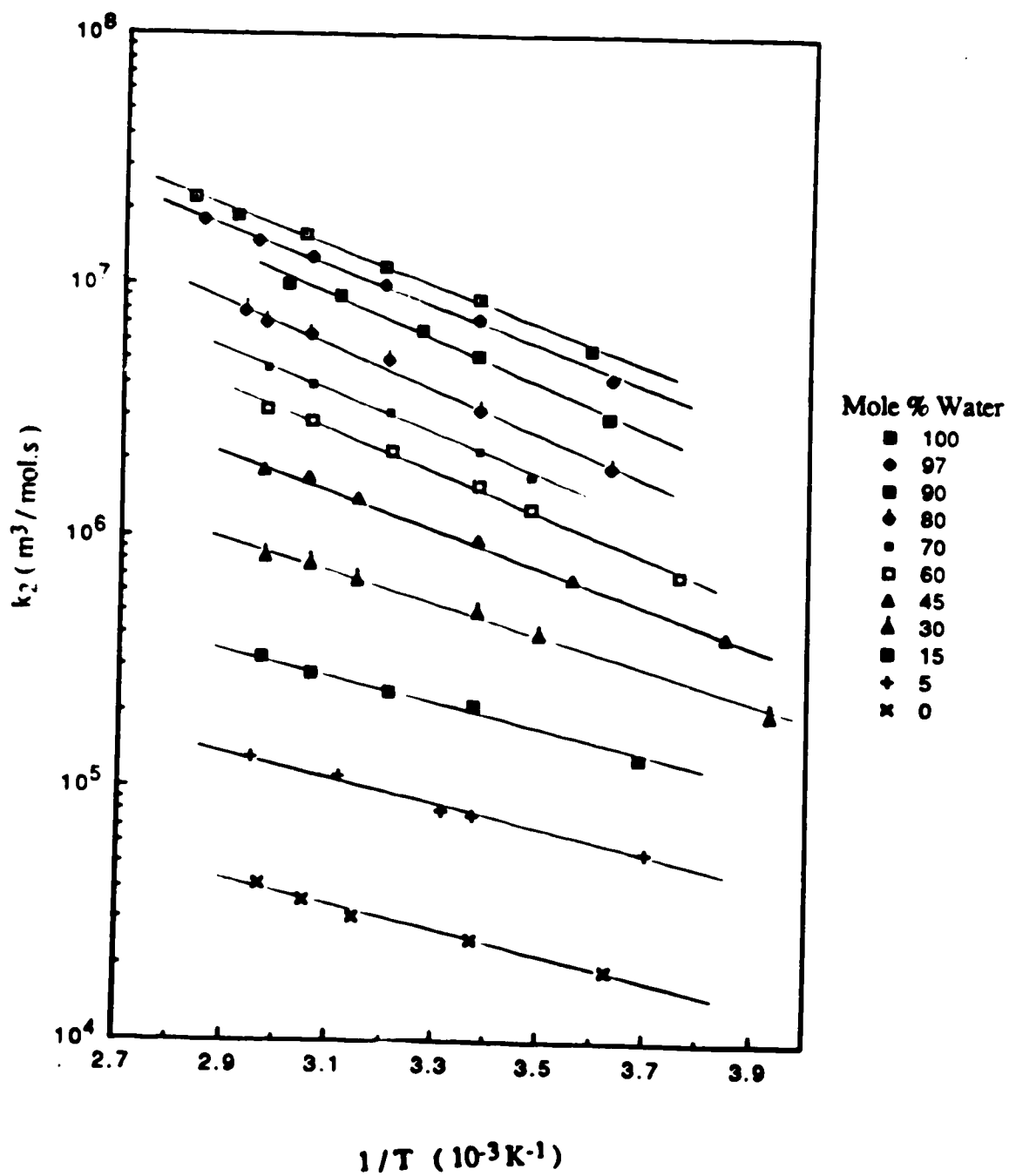


Fig. 3-20 Arrhenius plots for the reaction of solvated electrons with lithium nitrate in methanol / water mixtures



**Table 3-17** Second-order rate constants for the reaction of solvated electrons with lithium nitrate in methanol / water mixtures at various temperatures

$\chi_w$	Temp.	$k_2$	$\chi_w$	Temp.	$k_2$	$\chi_w$	Temp.	$k_2$
	(K)	( $10^6 \text{ m}^3/\text{mol.s}$ )		(K)	( $10^6 \text{ m}^3/\text{mol.s}$ )		(K)	( $10^6 \text{ m}^3/\text{mol.s}$ )
1.00	278.6	5.6	0.70	287.6	1.4	0.30	254.4	0.20
	296.5	8.8		296.1	2.2		286.1	0.40
	313.0	12		311.8	3.1		296.1	0.50
	328.7	16		326.9	4.0		317.6	0.67
	343.5	19		336.3	4.6		327.0	0.77
	353.1	22					336.4	0.82
0.97	275.7	4.3	0.60	266.2	0.71	0.15	271.3	0.13
	296.5	7.3		287.6	1.3		296.4	0.21
	313.2	10		296.2	1.6		311.4	0.24
	327.3	13		311.3	2.2		326.6	0.28
	338.7	15		326.9	2.9		336.6	0.33
	351.3	18		336.4	3.2			
0.90	275.9	3.0	0.45	259.9	0.40	0.05	270.4	0.055
	296.6	5.3		281.1	0.68		296.5	0.077
	306.1	6.6		296.1	0.96		301.7	0.080
	321.7	9.0		317.8	1.4		320.6	0.11
	332.3	10		327.4	1.7		338.7	0.13
				336.7	1.8			
0.80	275.8	1.9	0.00	275.8	0.019			
	296.0	3.2		296.5	0.025			
	312.3	5.0		317.8	0.031			
	327.3	6.3		357.4	0.036			
	336.7	7.1		336.7	0.041			
	341.4	7.9						

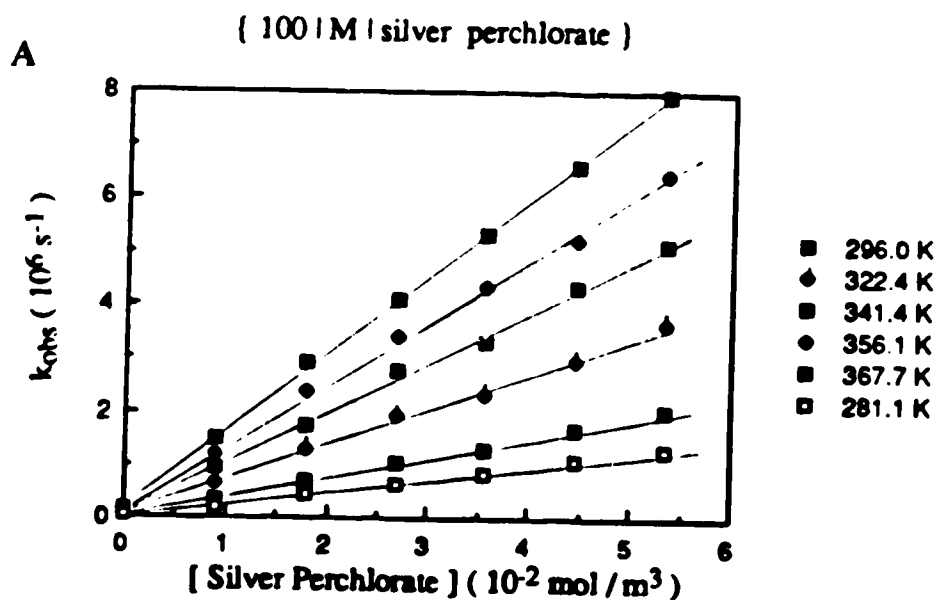
**Table 3-18** Rate parameters for the reaction of solvated electrons with  
lithium nitrate in methanol / water mixtures

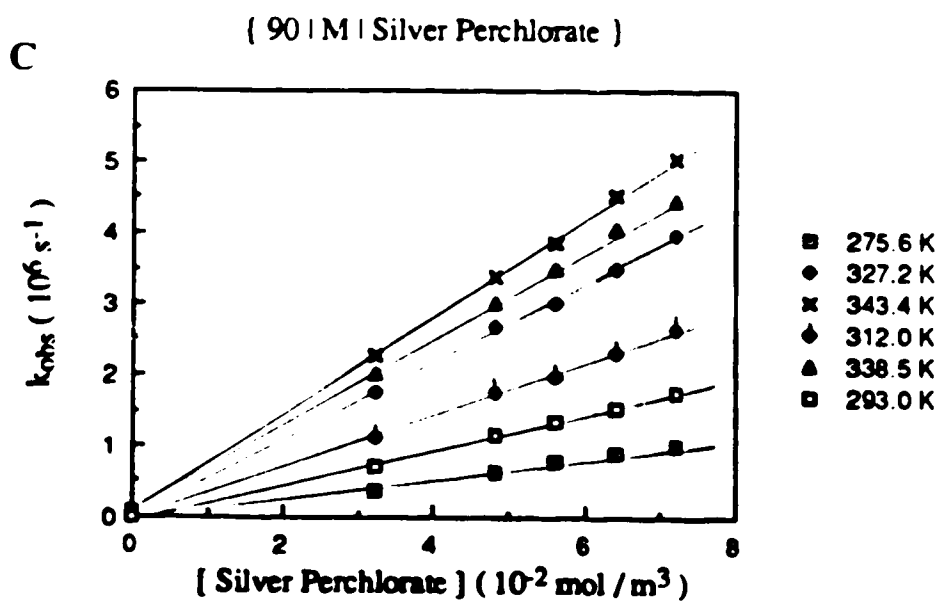
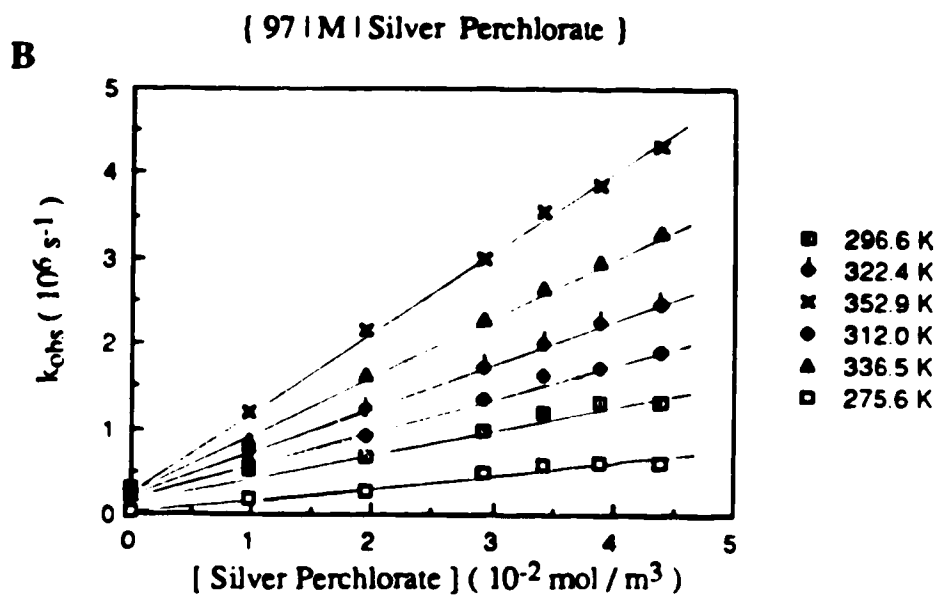
$\chi_w$	$k_{298}$ ( $10^6 \text{ m}^3/\text{mol.s}$ )	$E_a$ (kJ/mol.)	LogA	$\Delta S^\ddagger$ (J/mol.K)
1.00	8.7	16	12.66	-3
0.97	7.3	16	12.60	-4
0.90	5.3	17	12.64	-3
0.80	3.3	17	12.55	-5
0.70	2.3	16	12.31	-9
0.60	1.7	17	12.18	-12
0.45	0.98	15	11.59	-23
0.30	0.49	13	10.84	-37
0.15	0.19	11	10.16	-50
0.05	0.083	10	9.60	-61
0.00	0.026	9	9.01	-72

### B. Reaction of solvated electrons with silver ion

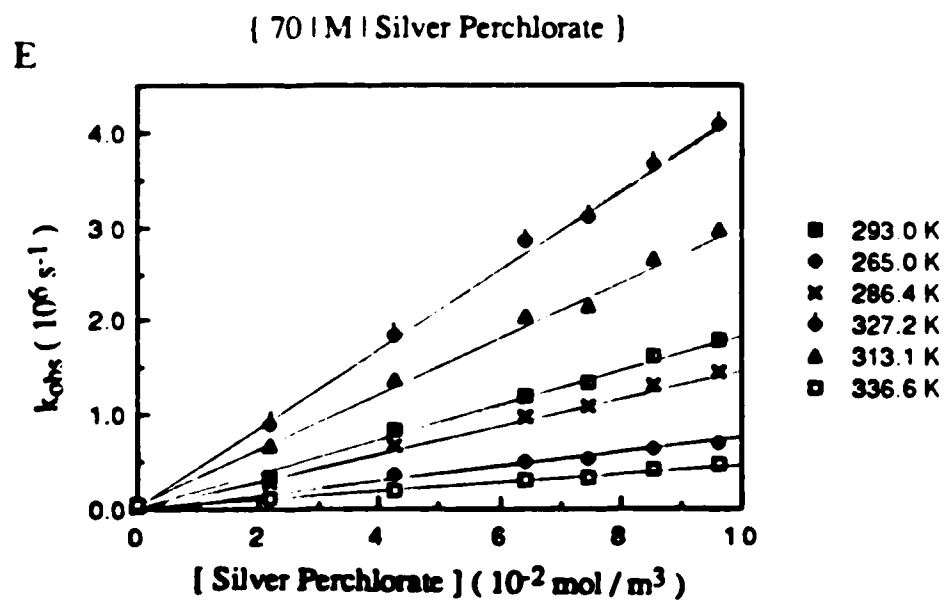
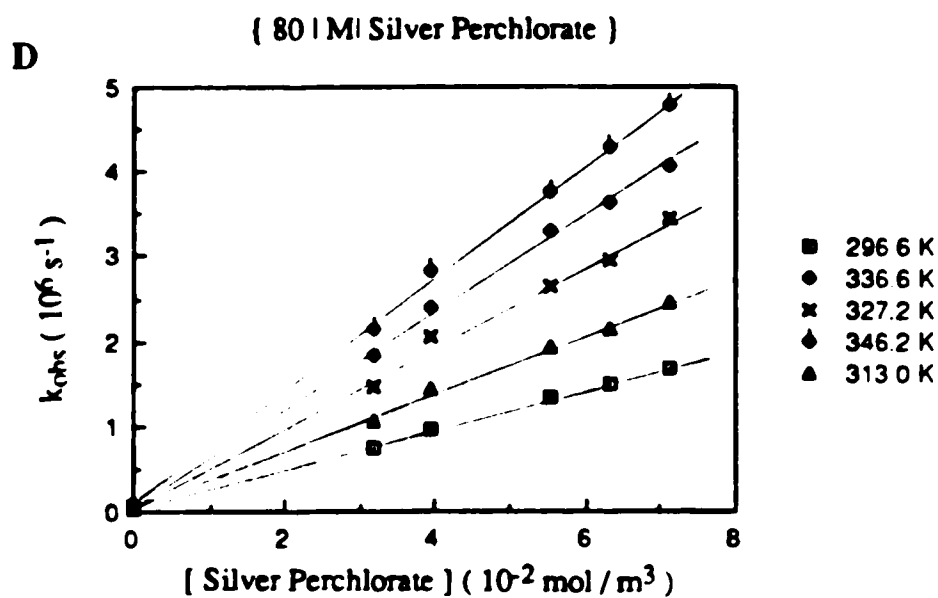
The temperature and concentration dependence of the first-order rate constant for the reaction of solvated electrons with silver ion are shown in Figs.3-21(A-J). The concentration range of  $\text{Ag}^+$  was 10-120 mmol/m<sup>3</sup>. The second-order rate constants at various temperatures are listed in Table 3-19. The rate parameters are obtained from the Arrhenius plots in Fig.3-22. They are summarized in Table 3-20. The rate constant at 298K is  $3.8 \times 10^7$  m<sup>3</sup>/mol.s in water and  $2.5 \times 10^7$  m<sup>3</sup>/mol.s in methanol. The literature results are  $3.6 \times 10^7$  m<sup>3</sup>/mol.s (136) and  $4.2 \times 10^7$  m<sup>3</sup>/mol.s (115) in water, and  $2.4 \times 10^7$  m<sup>3</sup>/mol.s (102) in methanol.

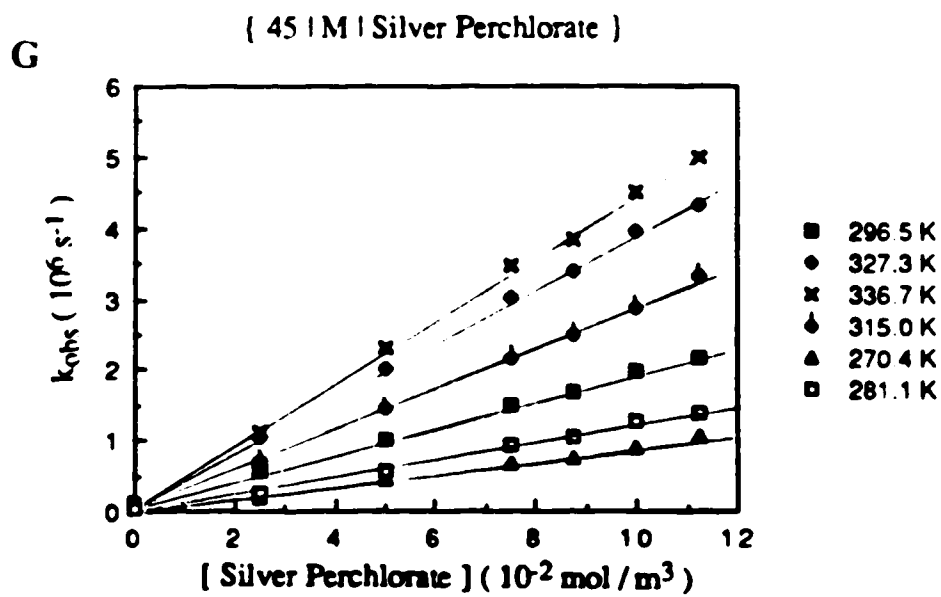
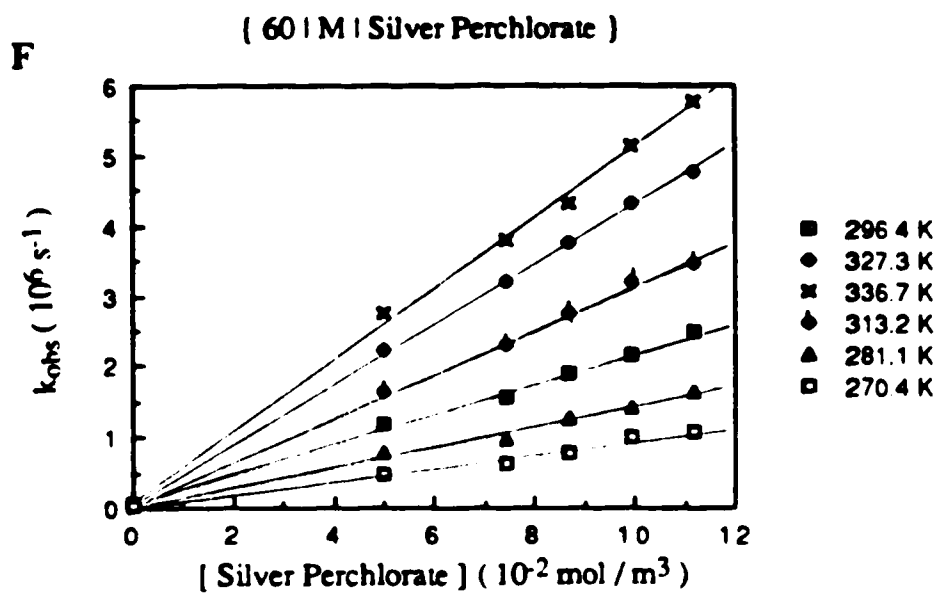
Fig. 3-21 (A-J) Temperature and concentration dependence of the first-order rate constant for the reaction of solvated electrons with silver perchlorate in methanol / water mixtures

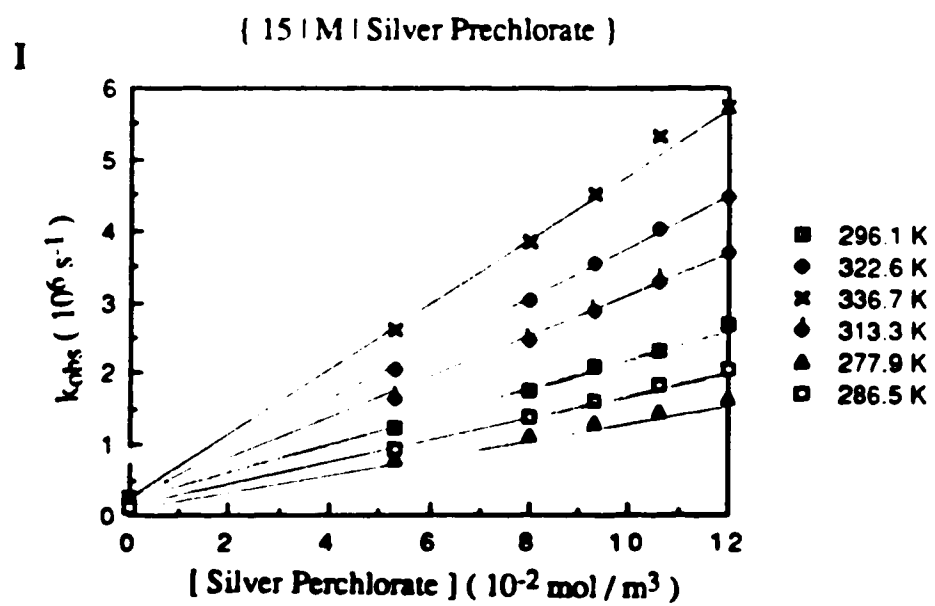
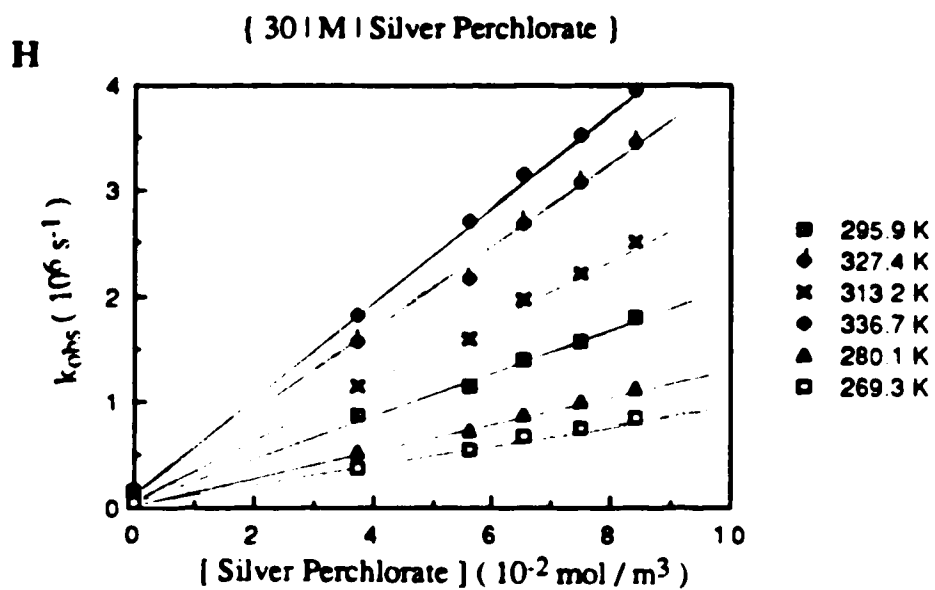












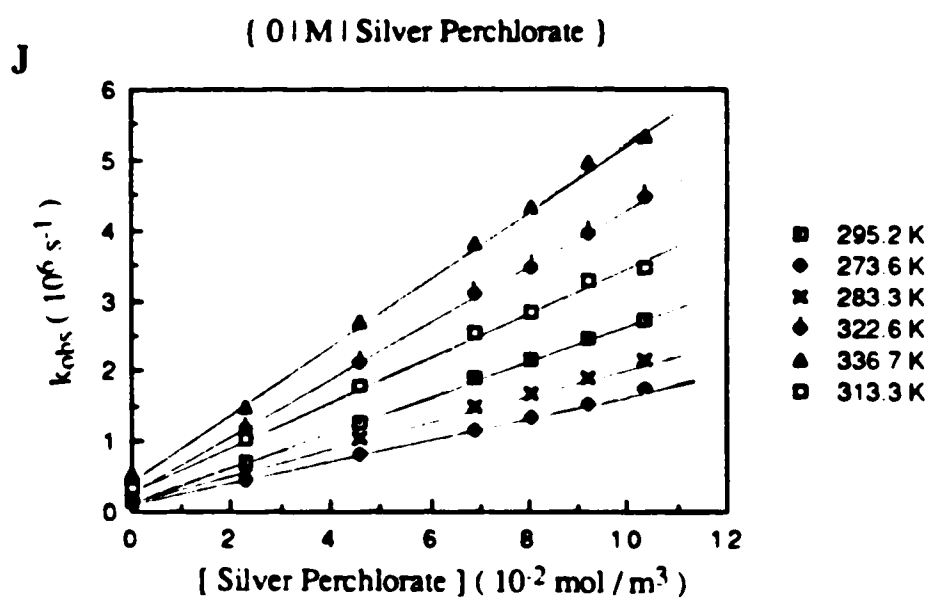
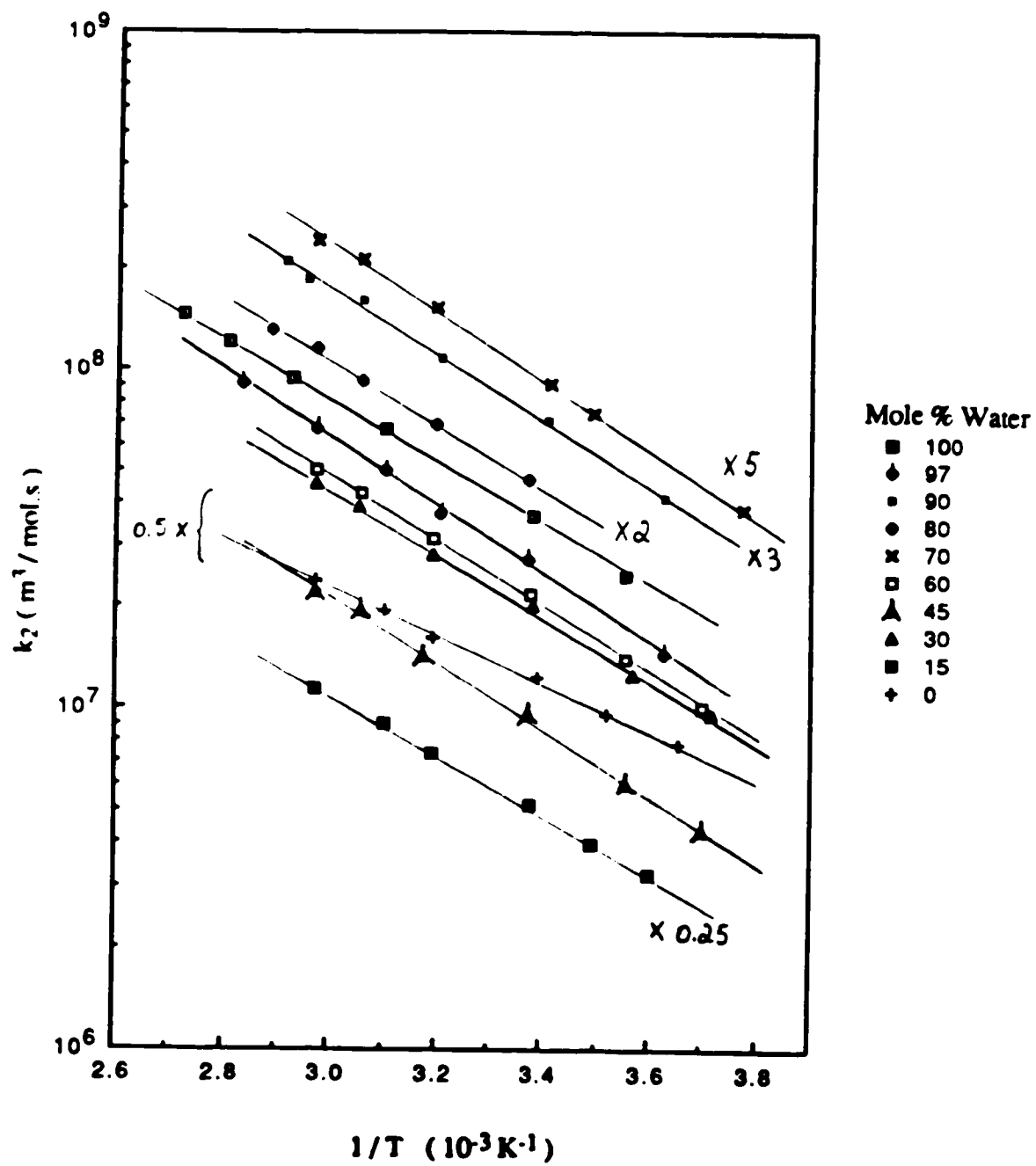


Fig. 3-22 Arrhenius plots for the reaction of solvated electrons with silver perchlorate in methanol / water mixtures



**Table 3-19 Second-order rate constants for the reaction of solvated electrons with silver perchlorate in methanol / water mixtures at various temperatures**

$\chi_w$	Temp.	$k_2$	$\chi_w$	Temp.	$k_2$	$\chi_w$	Temp.	$k_2$
	(K)	( $10^7 \text{ m}^3/\text{mol.s}$ )		(K)	( $10^7 \text{ m}^3/\text{mol.s}$ )		(K)	( $10^7 \text{ m}^3/\text{mol.s}$ )
1.00	281.1	2.5	0.70	265.0	0.77	0.30	280.1	0.95
	296.0	3.7		286.4	1.5		296.3	1.3
	322.4	6.7		293.0	1.8		295.9	2.0
	341.4	9.4		313.1	3.0		313.2	2.8
	356.1	12		327.2	4.2		327.4	3.9
	367.7	15		336.6	4.8		336.7	4.5
0.97	275.6	1.4	0.60	270.4	0.10	0.15	277.9	1.3
	296.6	2.7		281.1	1.4		186.5	1.6
	312.0	3.7		296.4	2.1		296.1	2.1
	322.4	5.0		313.2	3.1		313.3	2.9
	336.5	6.7		327.3	4.3		322.6	3.6
	352.9	9.2		336.7	5.0		336.7	4.6
0.90	275.6	1.4	0.45	270.4	0.87	0.00	273.6	1.6
	293.6	2.4		281.1	1.2		284.3	1.9
	312.0	3.6		296.5	1.9		295.2	2.5
	327.2	5.3		315.0	2.8		313.3	3.2
	338.5	6.1		327.3	3.9		322.6	3.9
	343.4	7.0		336.7	4.4		336.7	4.8
0.80	296.6	2.4						
	313.0	3.4						
	327.0	4.6						
	336.2	5.8						
	346.2	6.6						

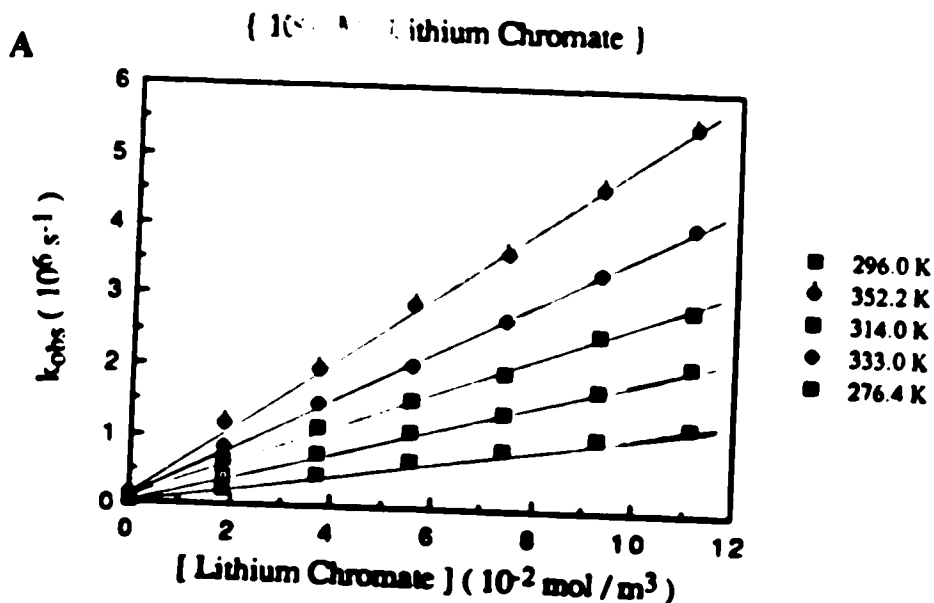
**Table 3-20** Rate parameters for the reaction of solvated electrons with silver perchlorate in methanol / water mixtures

$\chi_w$	$k_{298}$ ( $10^7 \text{ m}^3/\text{mol}\cdot\text{s}$ )	$E_a$ (kJ/mol.)	LogA	$\Delta S^\ddagger$ (J/mol.K)
1.00	3.8	18	13.70	17
0.97	2.9	18	13.60	15
0.90	2.6	18	13.64	16
0.80	2.5	18	13.60	15
0.70	2.1	19	13.60	15
0.60	2.2	18	13.54	14
0.45	1.9	18	13.50	13
0.30	2.1	17	13.35	11
0.15	2.1	16	13.17	7
0.00	2.5	14	12.76	-1

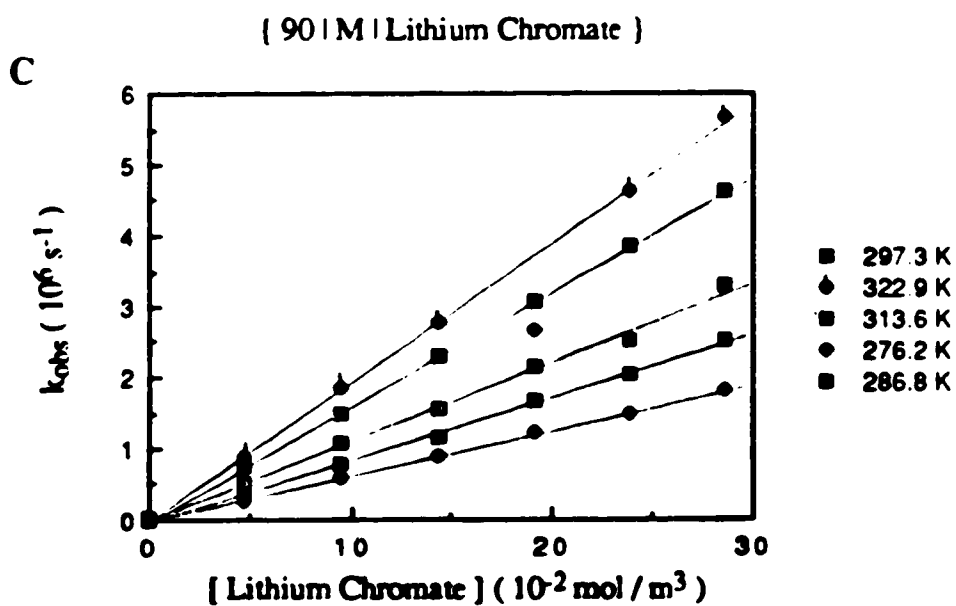
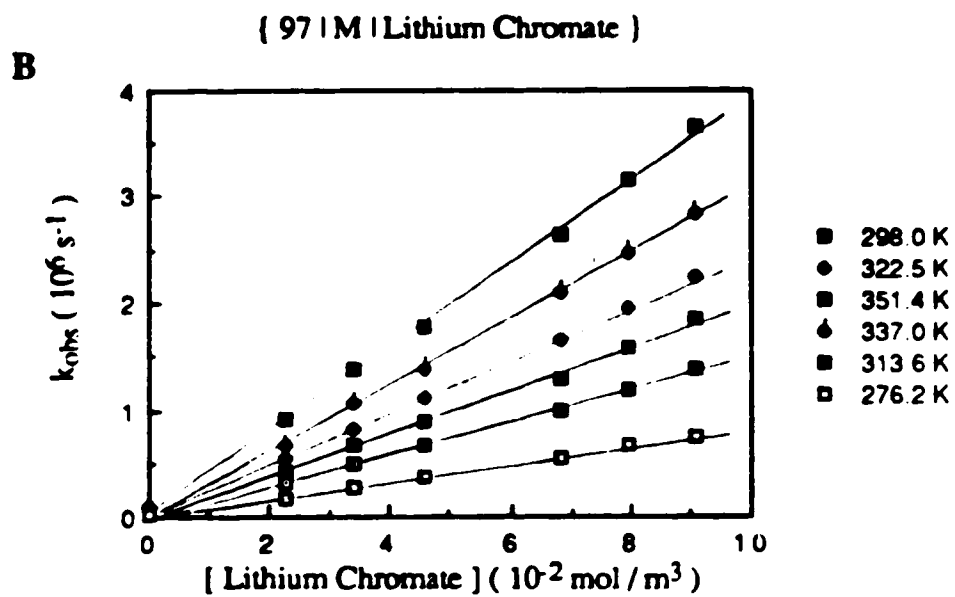
### C. Reaction of solvated electrons with chromate ion

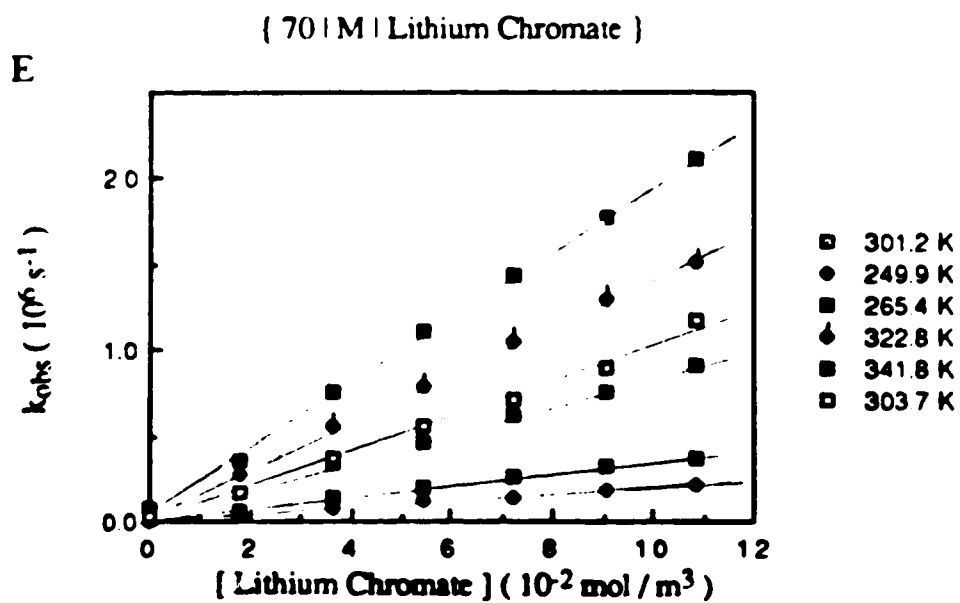
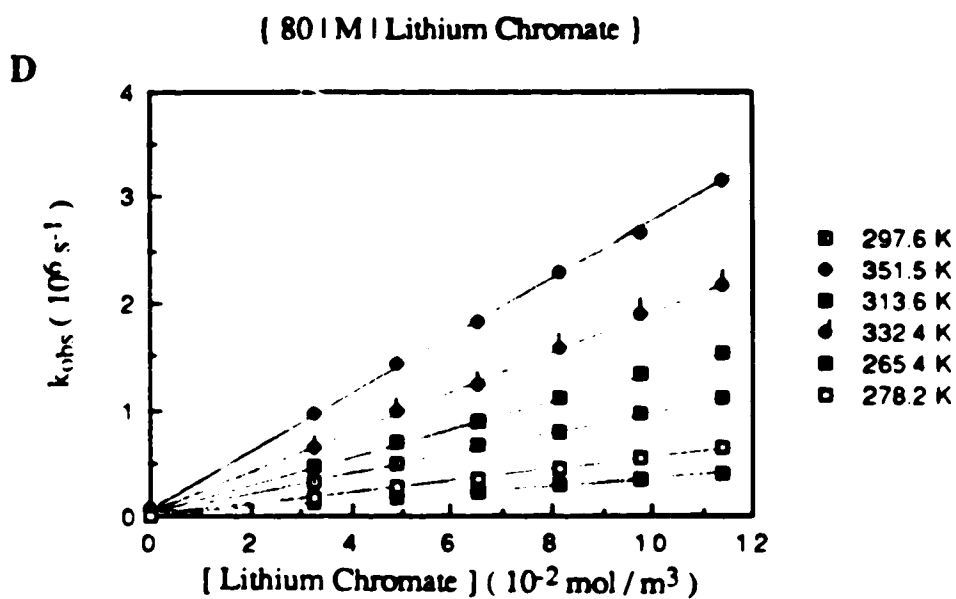
The temperature and concentration dependence of the first-order rate constant for the reaction of solvated electrons with chromate ion are shown in Figs.3-23(A-K). The concentration range of  $\text{CrO}_4^{2-}$  was 20-430  $\text{mmol/m}^3$ . The second-order rate constants at various temperatures are listed in Table 3-21. The rate parameters are obtained from the Arrhenius plots in Fig.3-24. They are summarized in Table 3-22. The rate constant in water at 298K is  $1.7 \times 10^6 \text{ m}^3/\text{mol.s}$ . The literature results are  $1.7 \times 10^6 \text{ m}^3/\text{mol.s}$  (115) and  $1.8 \times 10^6 \text{ m}^3/\text{mol.s}$  (136).

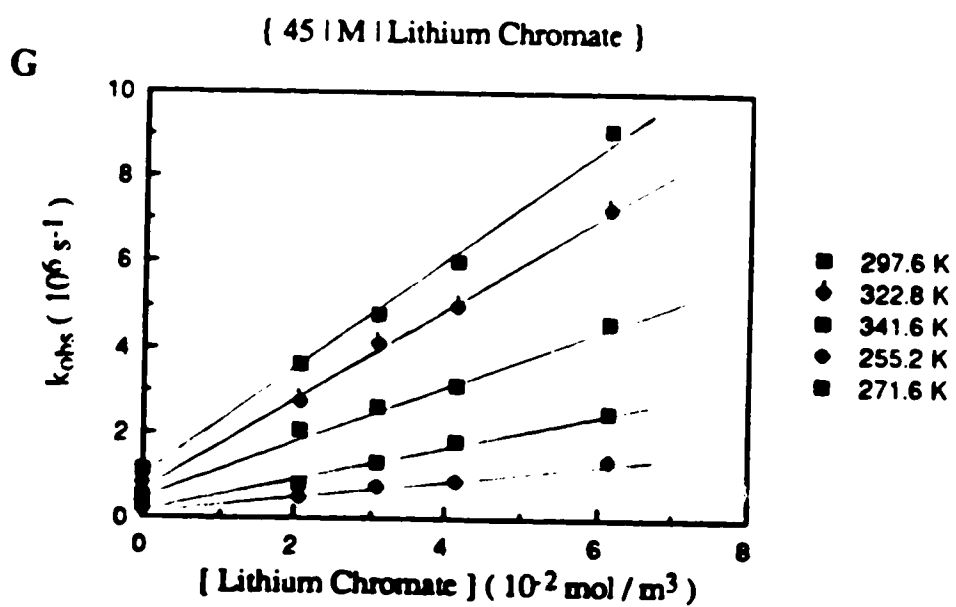
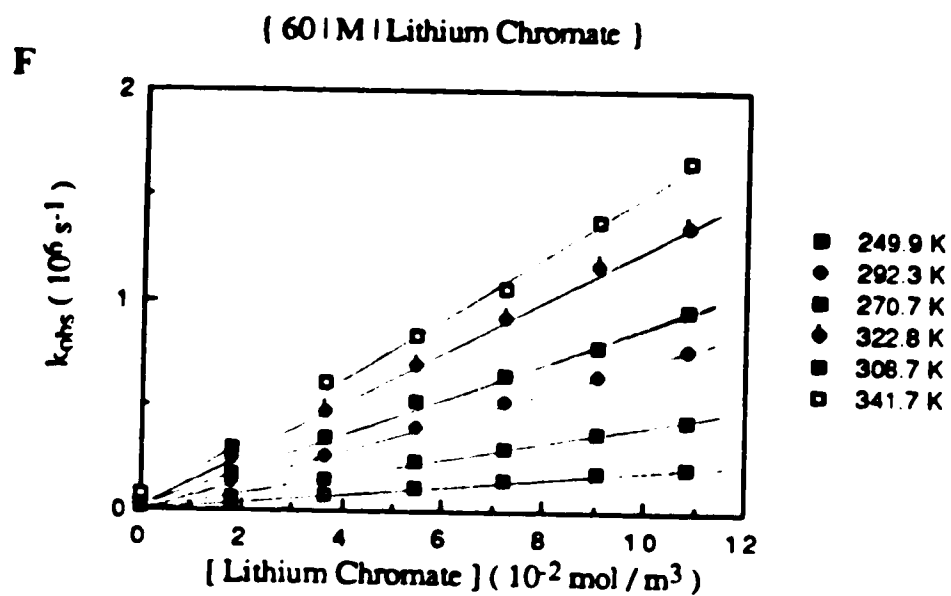
Fig. 3-23  
(A-K) Temperature and concentration dependence of the first-order rate constant for the reaction of solvated electrons with lithium chromate in methanol / water mixtures

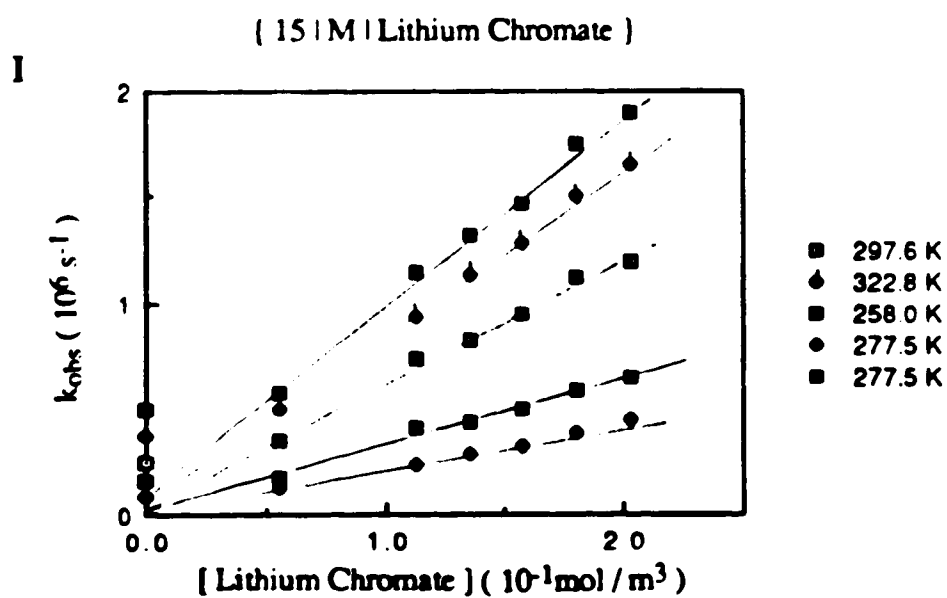
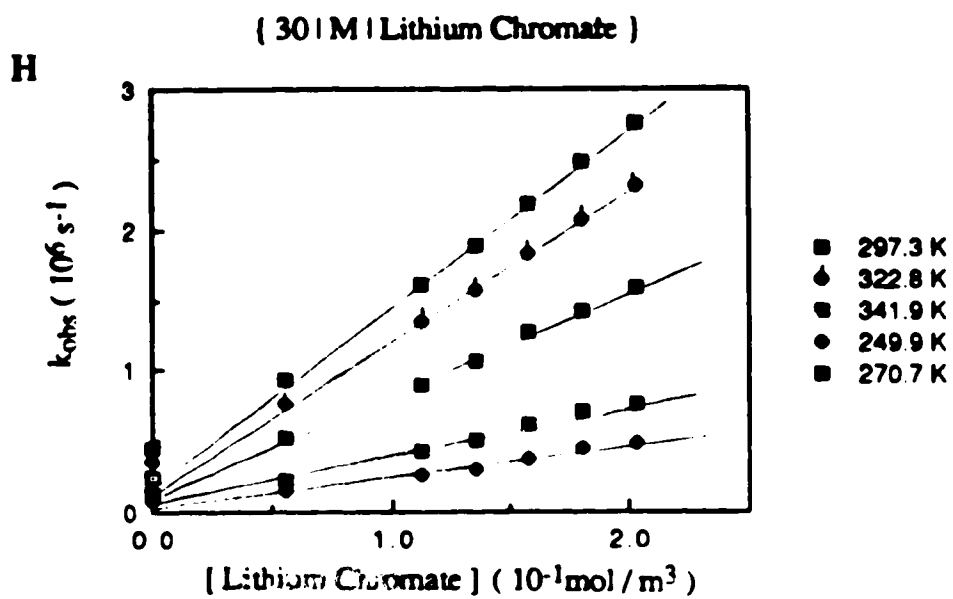












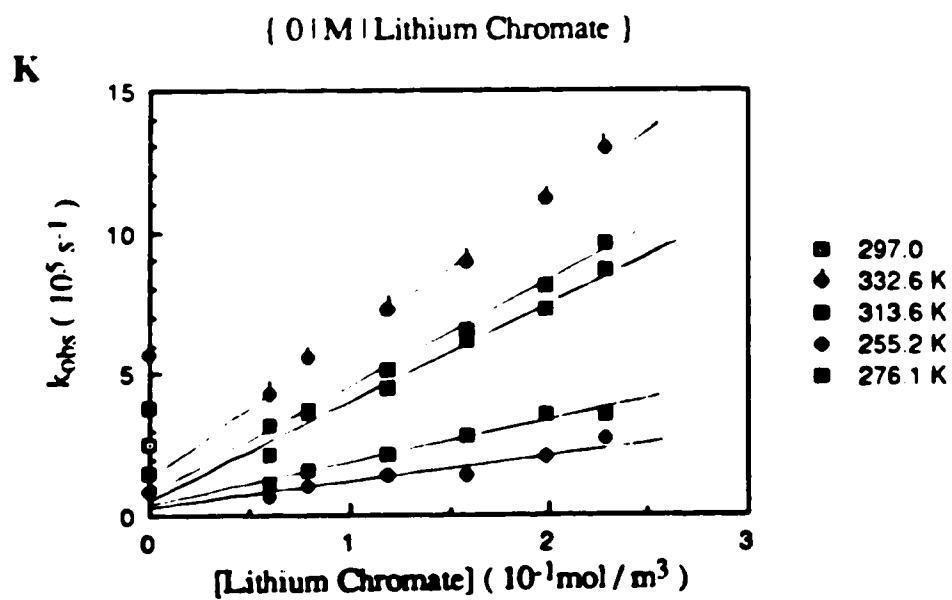
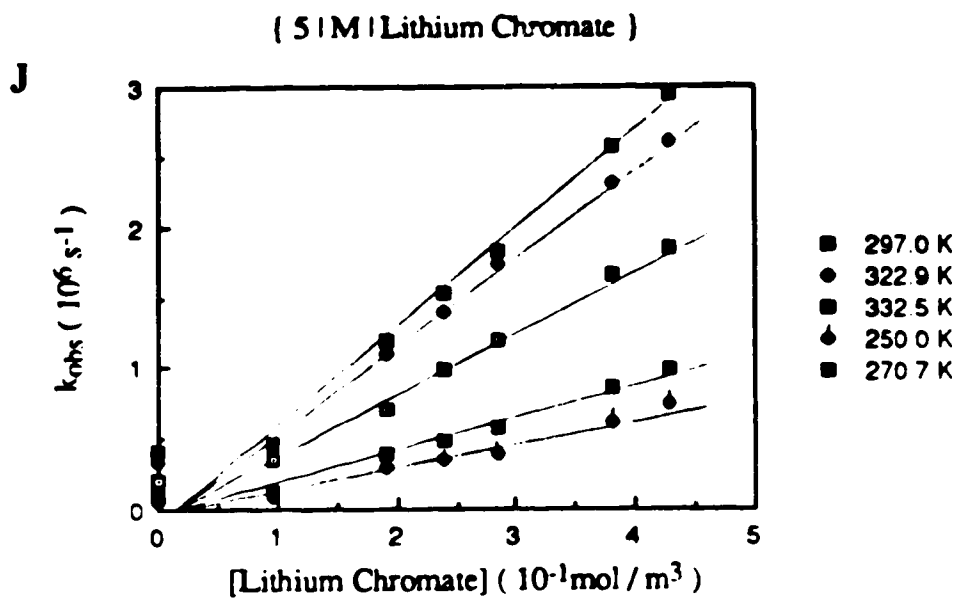
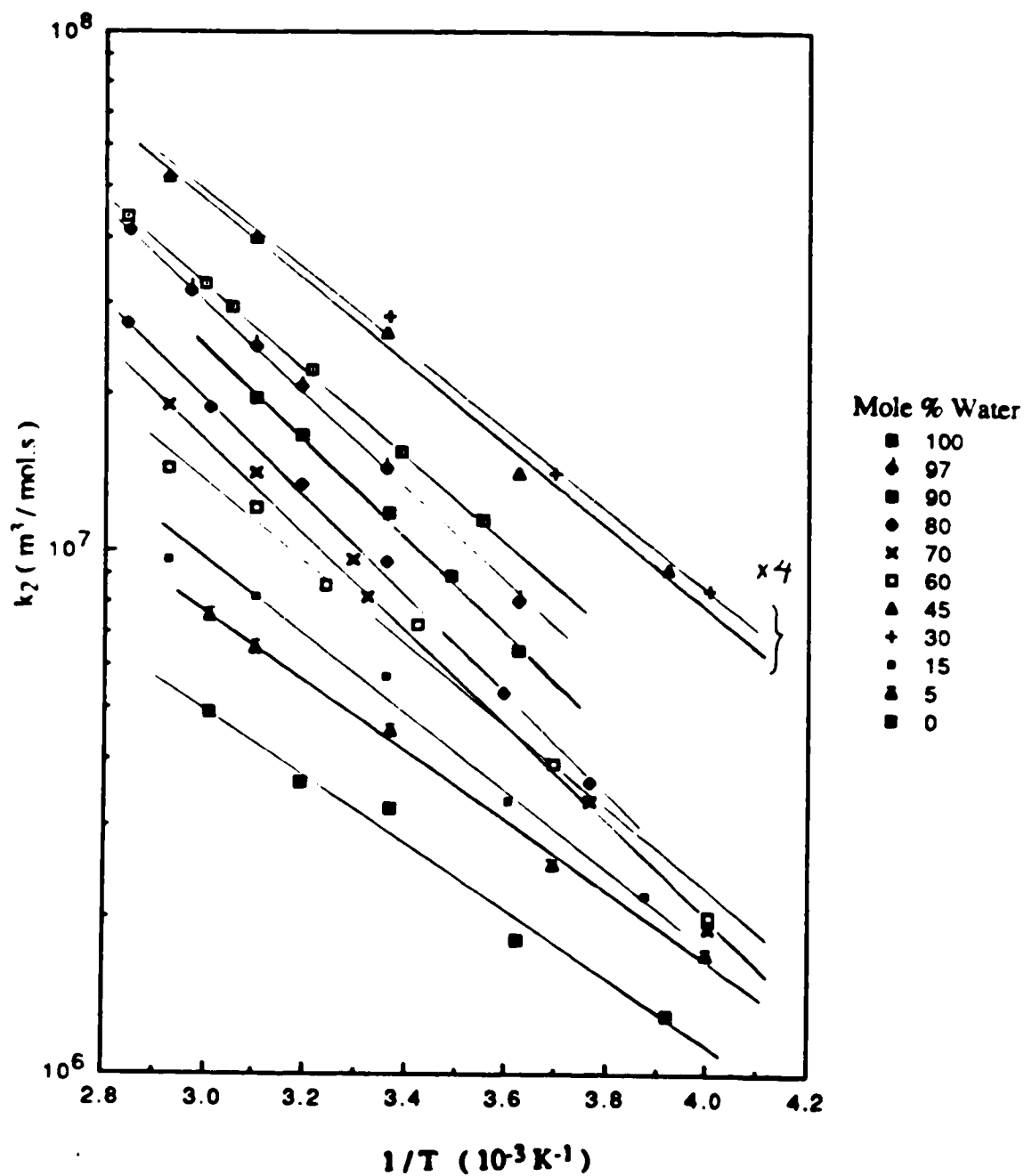


Fig. 3-24 Arrhenius plots for the reaction of solvated electrons with lithium chromate in methanol / water mixtures



**Table 3-21 Second-order rate constants for the reaction of solvated electrons with lithium chromate in methanol / water mixtures at various temperatures**

$\chi_w$	Temp. (K)	$k_2$ ( $10^7 \text{ m}^3/\text{mol.s}$ )	$\chi_w$	Temp. (K)	$k_2$ ( $10^7 \text{ m}^3/\text{mol.s}$ )	$\chi_w$	Temp. (K)	$k_2$ ( $10^7 \text{ m}^3/\text{mol.s}$ )
1.00	281.5	1.1	0.80	265.4	0.36	0.30	249.9	0.21
	295.4	1.6		278.2	0.53		270.7	0.35
	311.7	2.2		297.6	0.95		297.3	0.70
	327.8	2.9		313.6	1.3		322.8	1.0
	333.4	3.3		332.4	1.9		341.9	1.3
	351.6	4.4		351.5	2.7			
0.97	276.2	0.80	0.70	249.9	0.19	0.15	258.0	0.22
	298.0	1.4		265.4	0.33		277.5	0.33
	313.6	2.1		301.2	0.81		297.6	0.57
	322.8	2.5		303.7	0.96		322.8	0.81
	337.0	3.2		322.8	1.4		341.8	0.96
	351.4	4.1		341.8	1.9			
0.90	276.2	0.64	0.60	249.9	0.20	0.05	250.0	0.17
	286.8	0.89		270.7	0.39		270.7	0.25
	297.3	1.2		292.3	0.72		297.0	0.45
	313.6	1.7		308.7	0.86		322.9	0.68
	322.9	2.0		322.8	1.2		332.5	0.75
				341.7	1.4			
0.45	255.2	0.23	0.00	255.2	0.13			
	276.1	0.35		276.1	0.18			
	297.6	0.65		297.0	0.32			
	322.8	1.0		313.6	0.36			
	341.6	1.3		332.6	0.49			

**Table 3-22** Rate parameters for the reaction of solvated electrons with  
lithium chromate in methanol / water mixtures

$\chi_w$	$k_{298}$ ( $10^7 \text{ m}^3/\text{mol.s}$ )	$E_a$ (kJ/mol.)	LogA	$\Delta S^\ddagger$ (J/mol.K)
1.00	1.7	16	13.00	4
0.97	1.5	17	13.05	5
0.90	1.2	18	13.23	8
0.80	0.91	18	13.14	7
0.70	0.76	18	12.95	3
0.60	0.73	17	12.81	0
0.45	0.62	16	12.53	-5
0.30	0.64	14	12.27	-10
0.15	0.52	13	12.00	-15
0.05	0.45	11	11.68	-21
0.00	0.29	11	11.35	-27

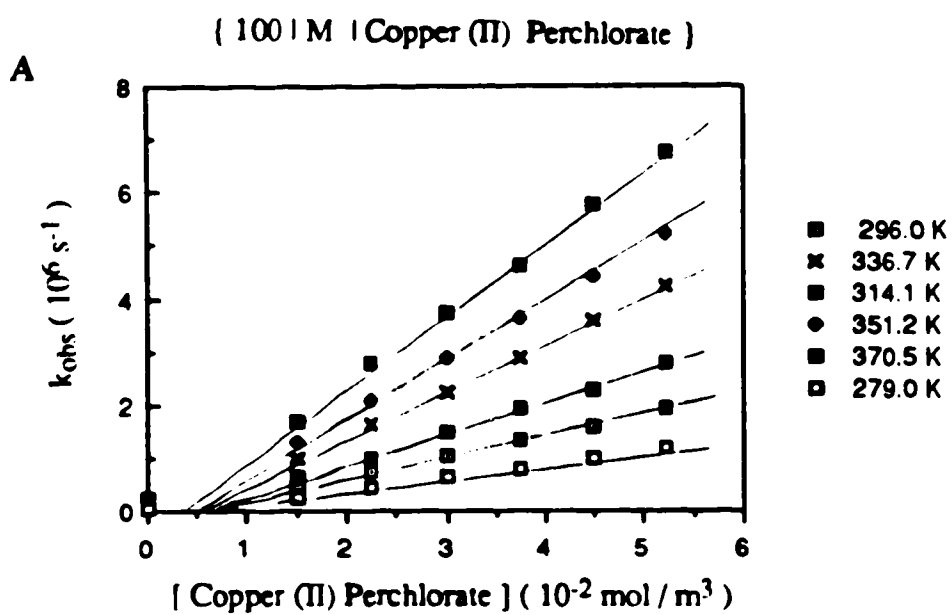


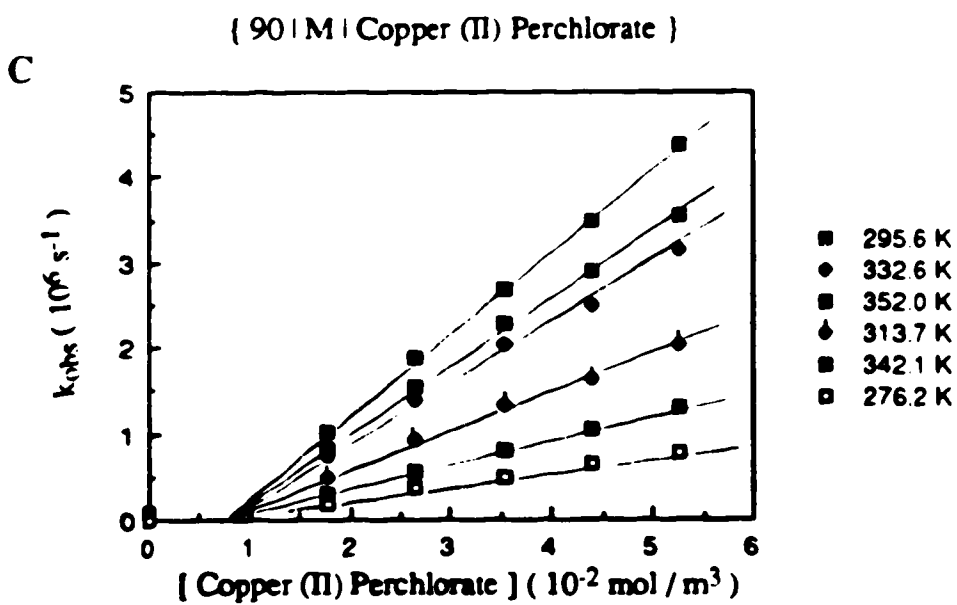
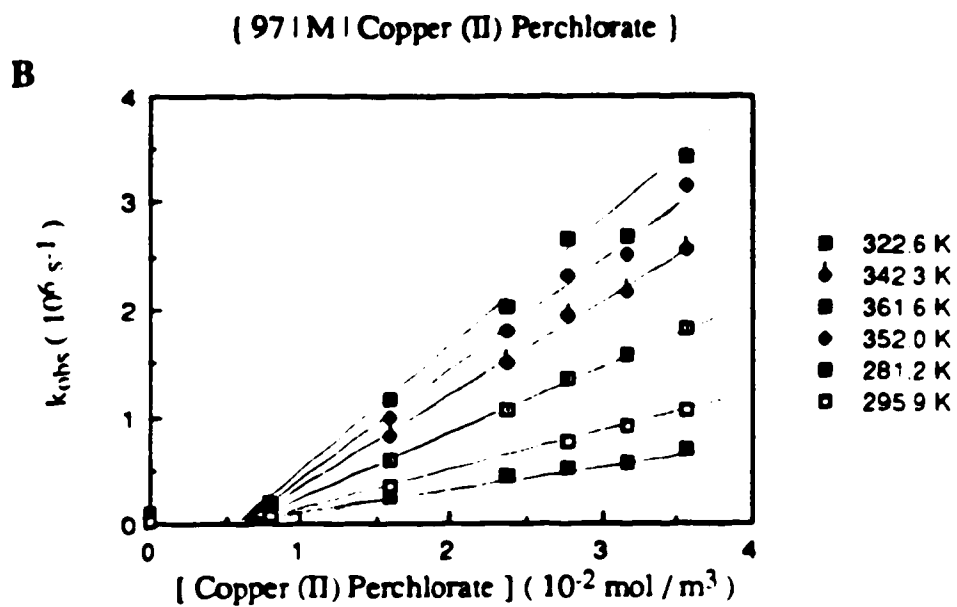
#### D. Reaction of solvated electrons with copper (II) ion

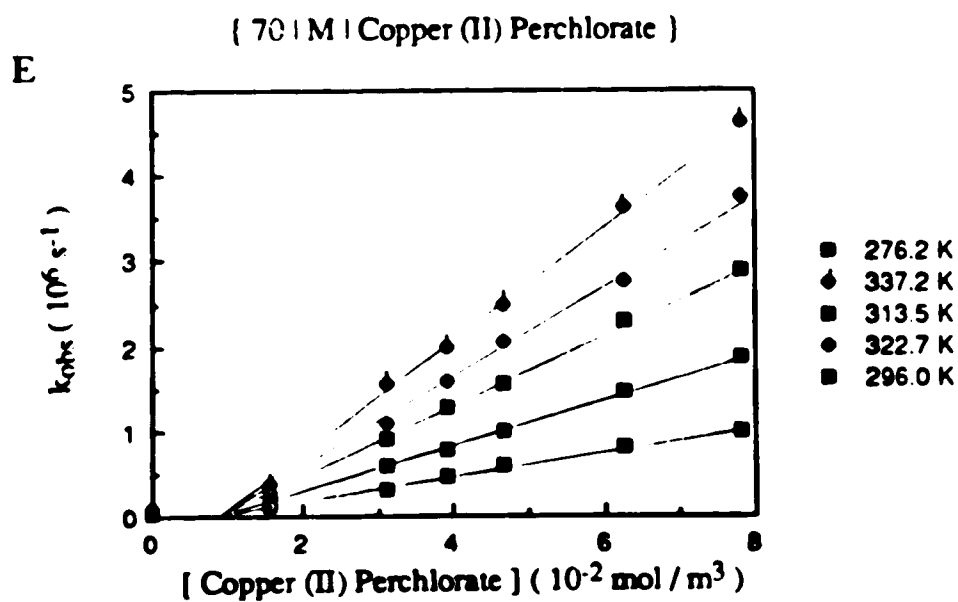
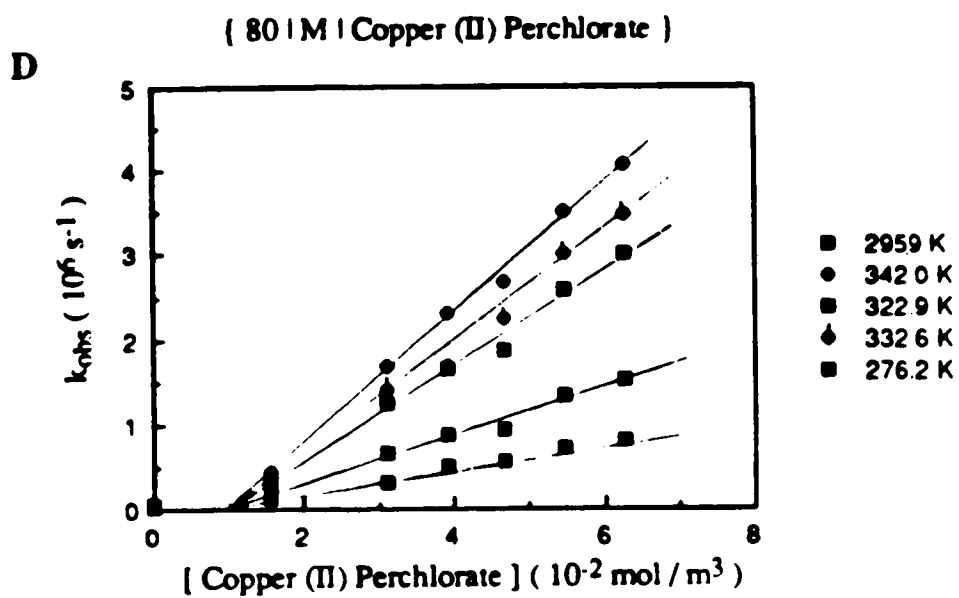
The temperature and concentration dependence of the first-order rate constant for the reaction of solvated electrons with copper (II) ion are shown in Figs.3-25(A-J). The concentration range of  $\text{Cu}^{2+}$  was 7-78 mmol/m<sup>3</sup>. It is observed that in all the  $k_{\text{obs}}$  versus  $[\text{Cu}^{2+}]$  plots, the best fit lines are always below the points corresponding to the solvent sample. This has also been observed in the water / *t*-butyl alcohol (137), water / 1-propanol and water / 2-propanol (138) mixed solvent systems. It has been explained (137) in terms of the presence of a small level of (~10 mmol/m<sup>3</sup>) of chelating or precipitating agent in the solvent. Since the dependence of  $k_{\text{obs}}$  on copper concentration is not affected, there is no effect on the second-order rate constants.

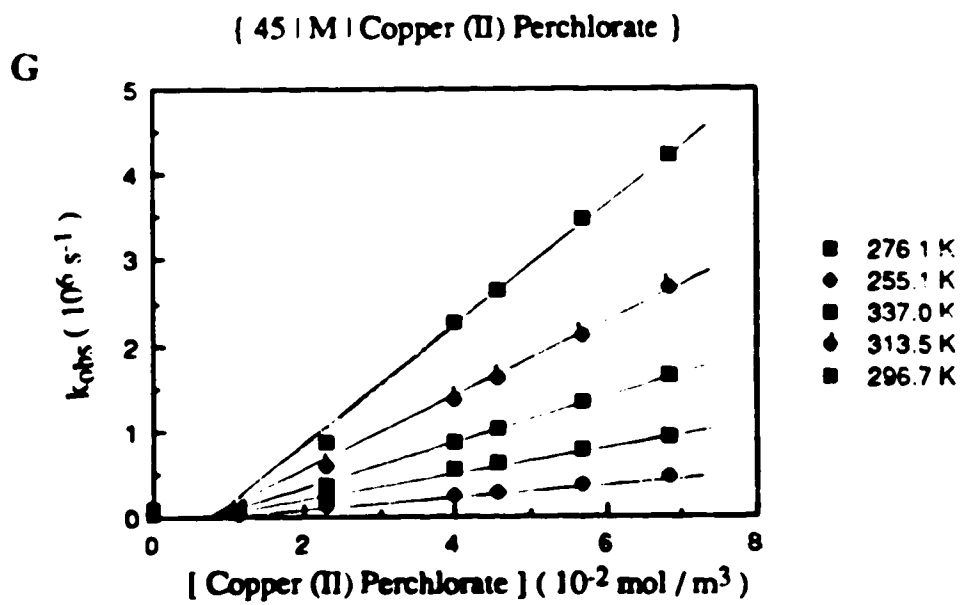
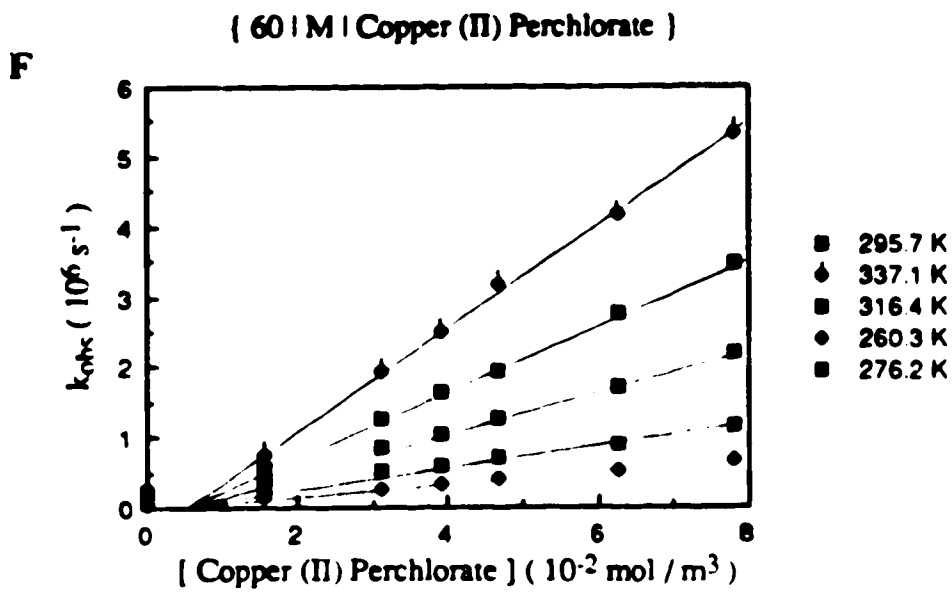
The second-order rate constants at various temperatures are listed in Table 3-23. The rate parameters are obtained from the Arrhenius plots in Fig.3-26. They are summarized in Table 3-24. The rate constant in water at 298K is  $3.8 \times 10^7 \text{ m}^3/\text{mol.s}$ . The literature results are  $3.8 \times 10^7 \text{ m}^3/\text{mol.s}$  (115) and  $4.0 \times 10^7 \text{ m}^3/\text{mol.s}$  (97).

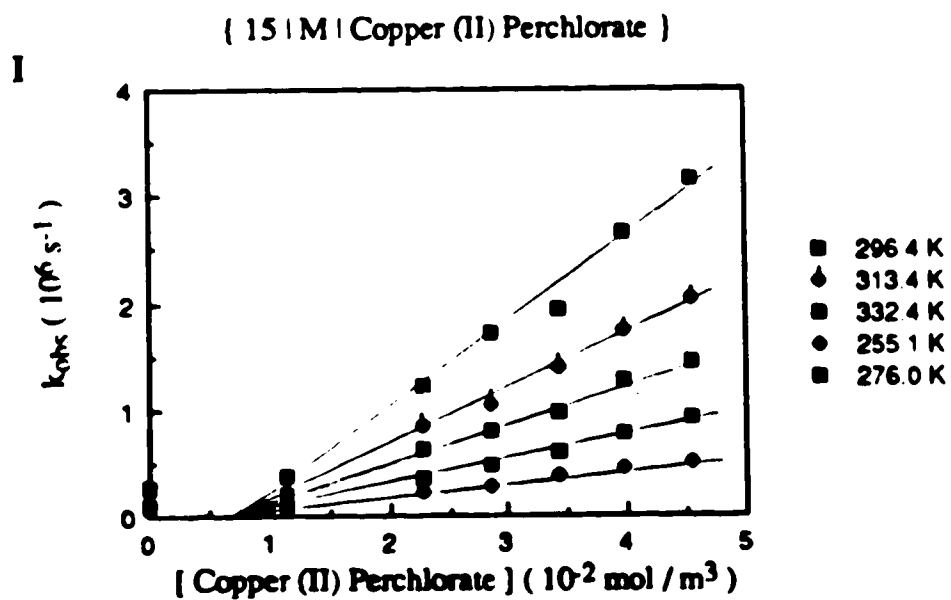
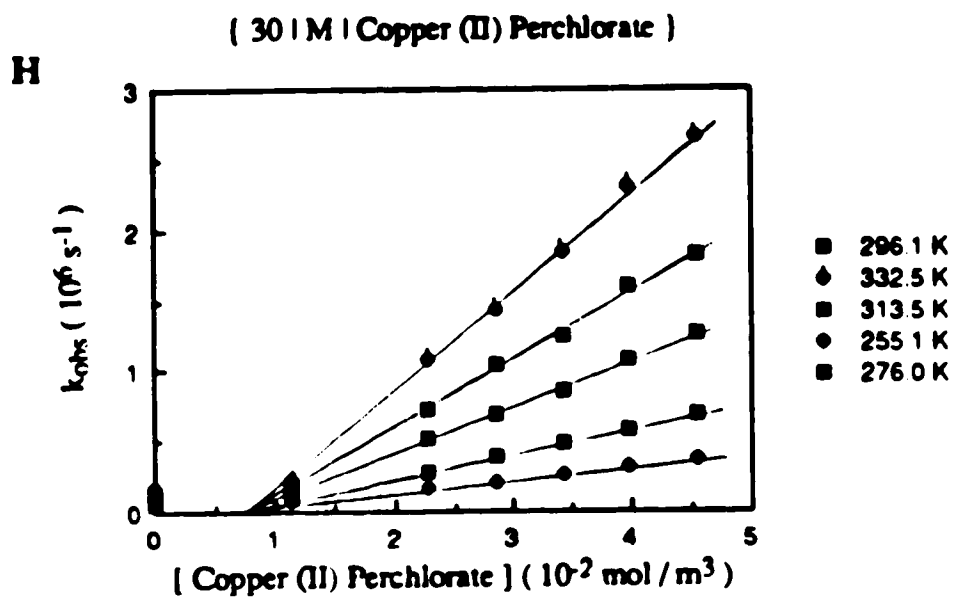
Fig. 3-25  
(A-J) Temperature and concentration dependence of the first-order rate constant for the reaction of solvated electrons with copper (II) perchlorate in methanol / water mixtures











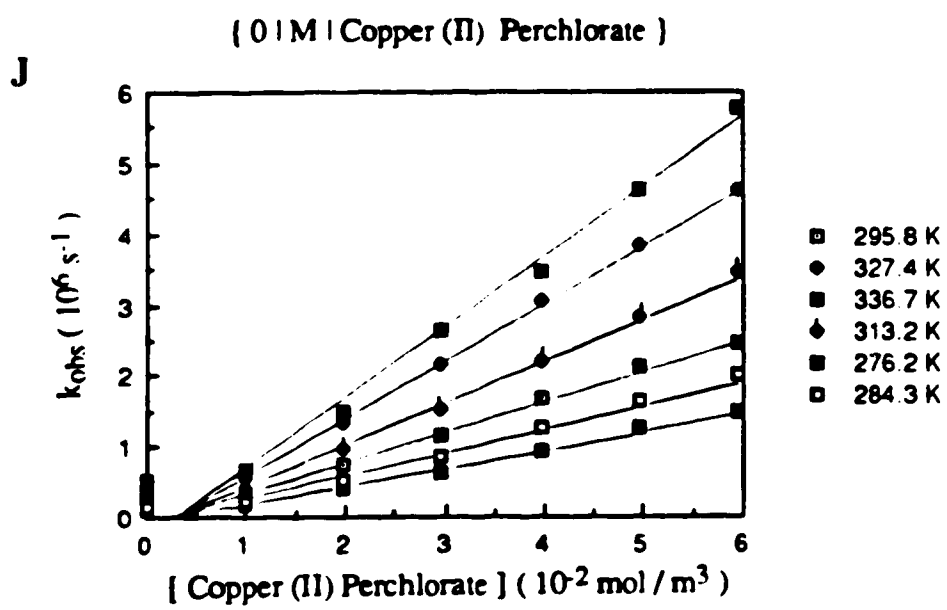


Fig. 3-26 Arrhenius plots for the reaction of solvated electrons with copper (II) perchlorate in methanol / water mixtures

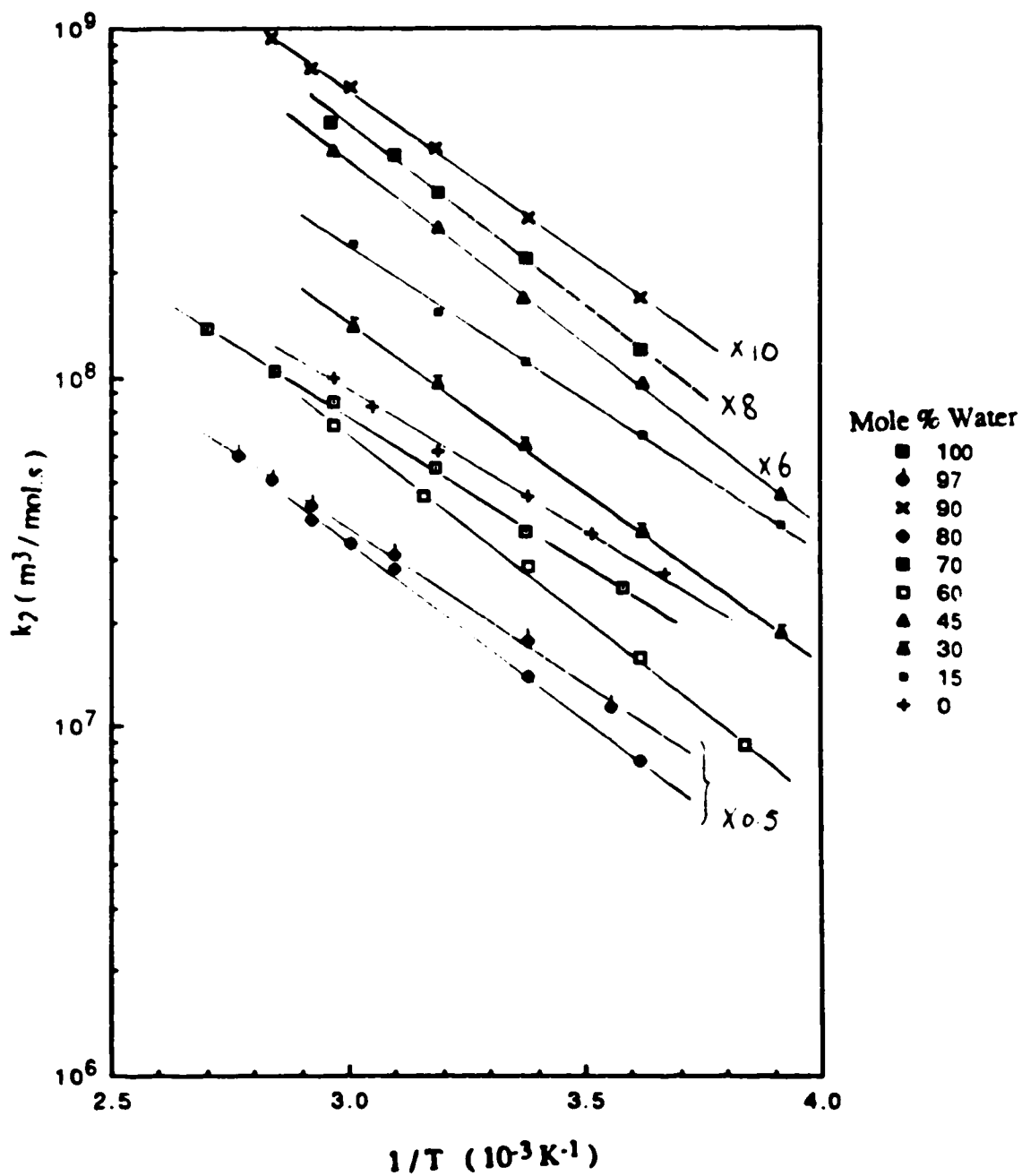




Table 3-23 Second-order rate constants for the reaction of solvated electrons with copper (II) perchlorate in methanol / water mixtures at various temperatures

$\chi_w$	Temp. (K)	$k_2$ ( $10^7 \text{ m}^3/\text{mol.s}$ )	$\chi_w$	Temp. (K)	$k_2$ ( $10^7 \text{ m}^3/\text{mol.s}$ )	$\chi_w$	Temp. (K)	$k_2$ ( $10^7 \text{ m}^3/\text{mol.s}$ )	
1.00	279.0	2.5	0.80	276.2	1.6	0.30	255.1	0.93	
	296.0	3.7		295.9	2.8		276.0	1.8	
	314.1	5.5		322.9	5.7		296.1	3.2	
	336.7	8.6		332.6	6.8		313.5	4.8	
	351.2	11		342.0	7.8		332.5	7.0	
	370.5	14							
0.97	281.2	2.3	0.70	276.2	1.5	0.15	255.1	1.3	
	295.9	3.5		296.0	2.7		276.0	2.3	
	322.6	6.3		313.5	4.2		296.4	3.7	
	342.3	8.6		322.7	5.4		313.4	5.1	
	352.0	10		337.2	6.7		332.4	8.1	
	361.6	12							
0.90	276.2	1.7	0.60	260.3	0.89	0.00	272.6	2.7	
	295.6	2.9		276.2	1.6		284.3	3.6	
	313.7	4.5		295.7	2.9		295.8	4.6	
	332.6	6.8		316.4	4.6		313.2	6.2	
	342.1	7.7		337.1	7.3		327.4	8.3	
	352.0	9.5					336.7	10	
				0.45	255.1		0.78		
					276.1		1.6		
					296.7		2.8		
					313.5		4.5		
		337.0	7.4						

**Table 3-24** Rate parameters for the reaction of solvated electrons with  
copper (II) perchlorate in methanol / water mixtures

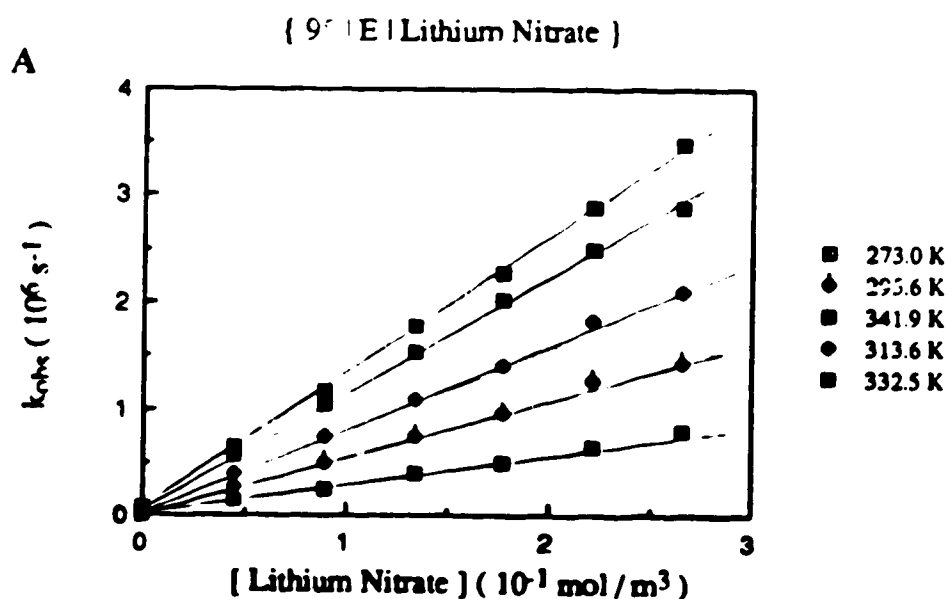
$\chi_w$	$k_{298}$ ( $10^7 \text{ m}^3/\text{mol}\cdot\text{s}$ )	$E_a$ (kJ/mol.)	LogA	$\Delta S^\ddagger$ (J/mol.K)
1.00	3.8	16	13.46	13
0.79	3.6	17	13.52	14
0.90	3.0	18	13.67	17
0.80	3.0	19	13.87	20
0.70	2.9	20	13.93	22
0.60	2.9	20	13.94	22
0.45	3.0	20	13.91	21
0.30	3.4	19	13.82	19
0.15	4.0	17	13.56	14
0.00	4.8	15	13.31	10

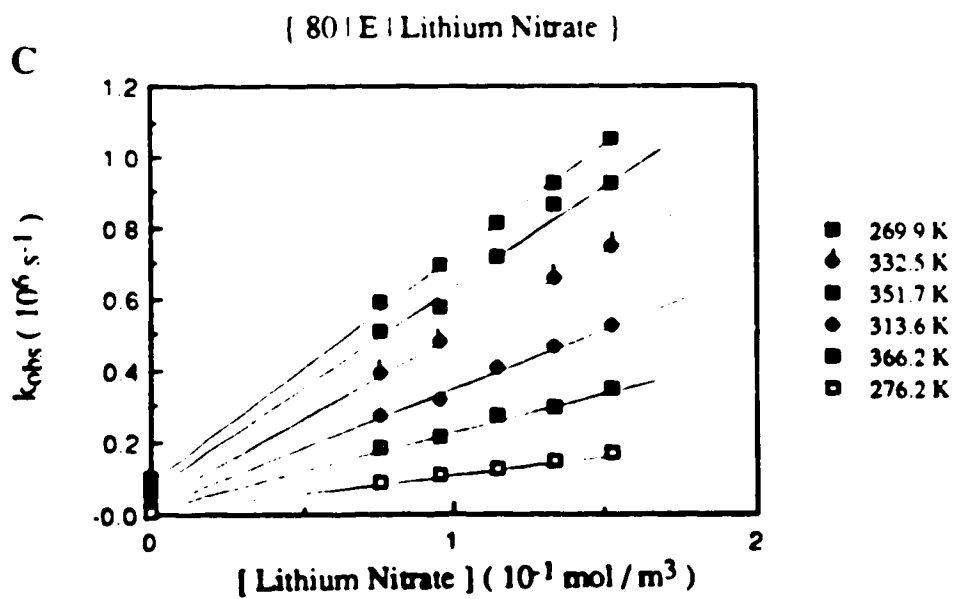
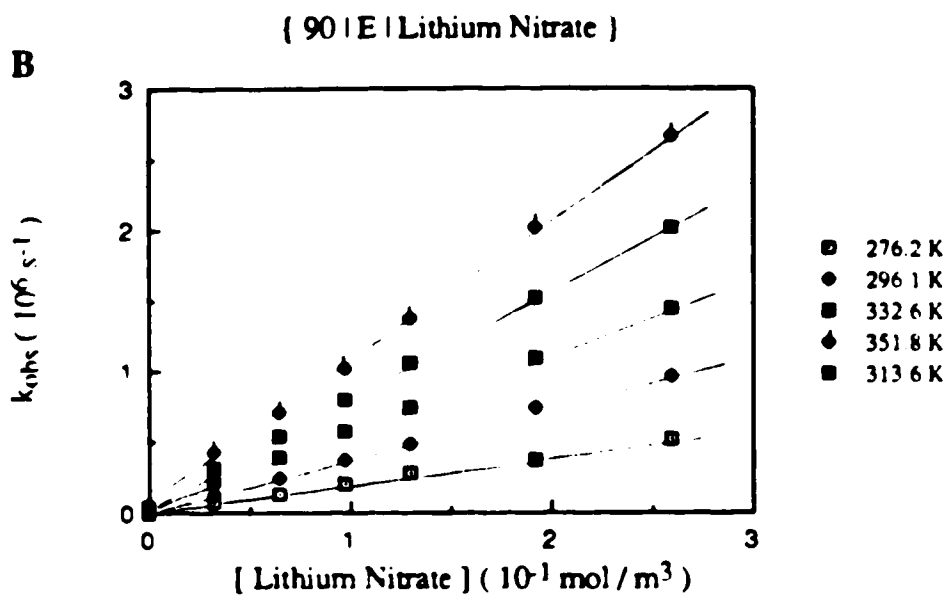
## 2. Reactions of solvated electrons in ethanol / water mixed solvents

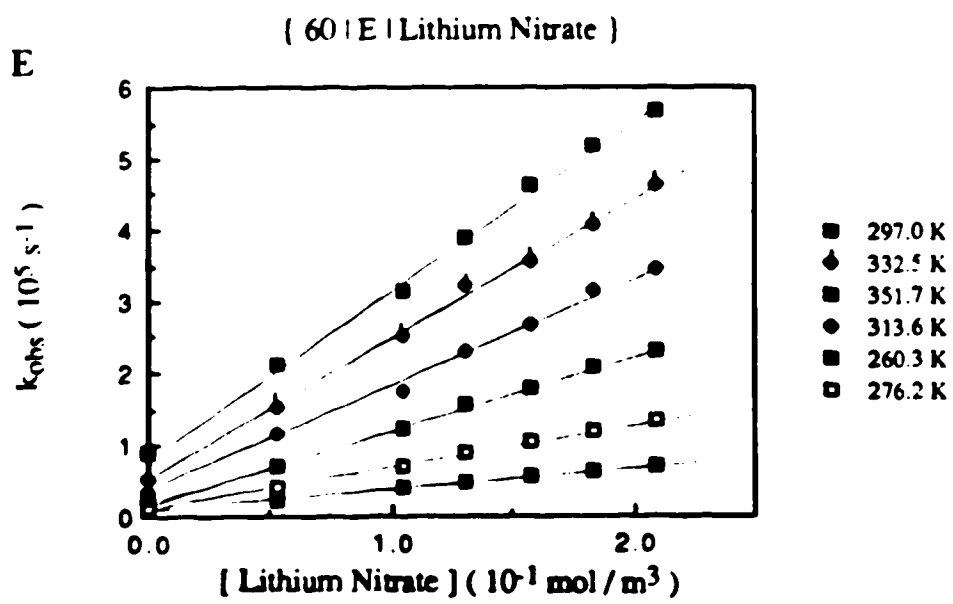
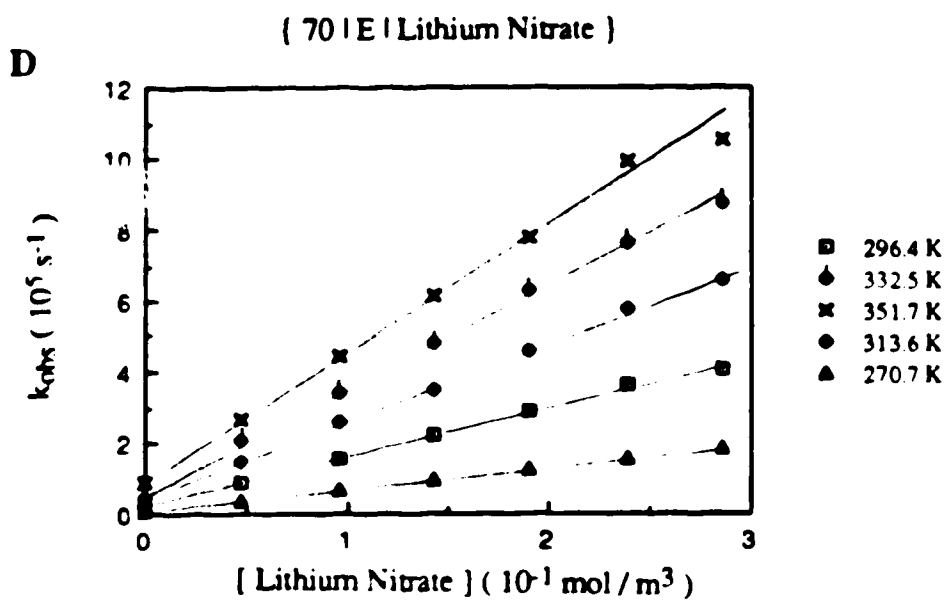
### A. Reaction of solvated electrons with nitrate ion

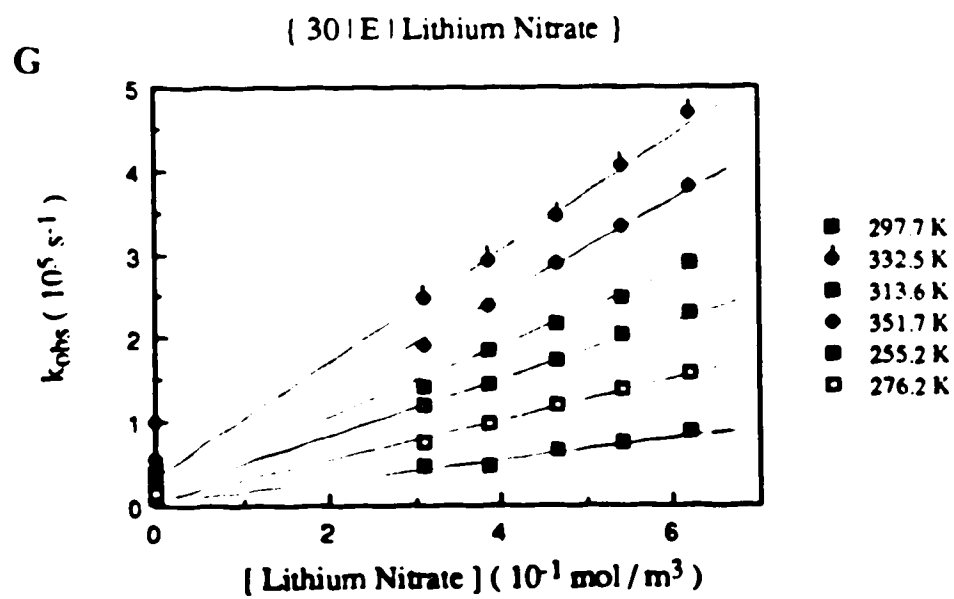
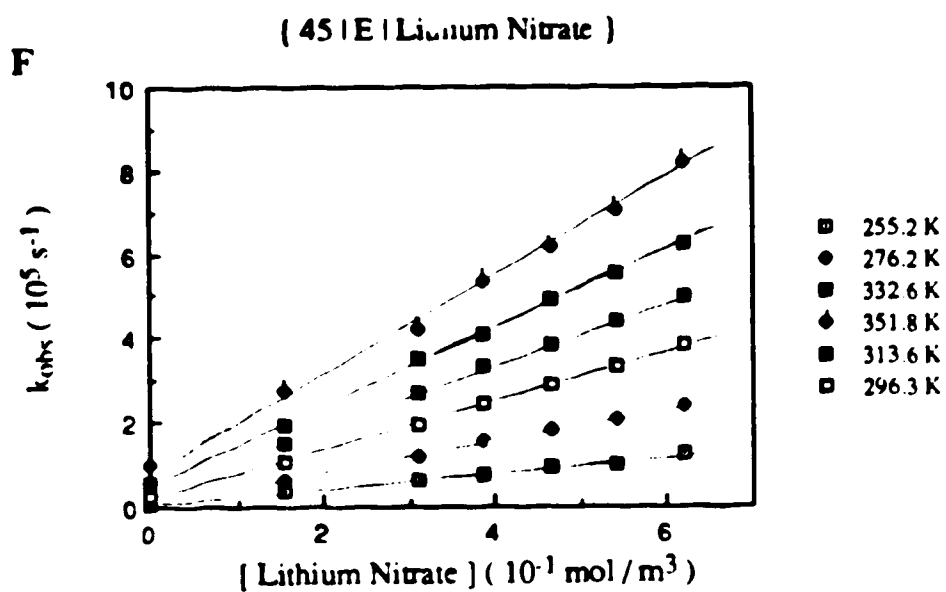
The temperature and concentration dependence of the first-order rate constant for the reaction of solvated electrons with  $\text{NO}_3^-$  are shown in Figs.3-27(A-L). The concentration range of  $\text{NO}_3^-$  was 0.05-2.8 mol/m<sup>3</sup>. The second-order rate constants at various temperatures are listed in Table 3-25. The rate parameters are obtained from the Arrhenius plots in Fig.3-28. They are summarized in Table 3-26. The rate constants in methanol / water mixtures at 298K are compared with those in the literature (109) in Fig.3-29.

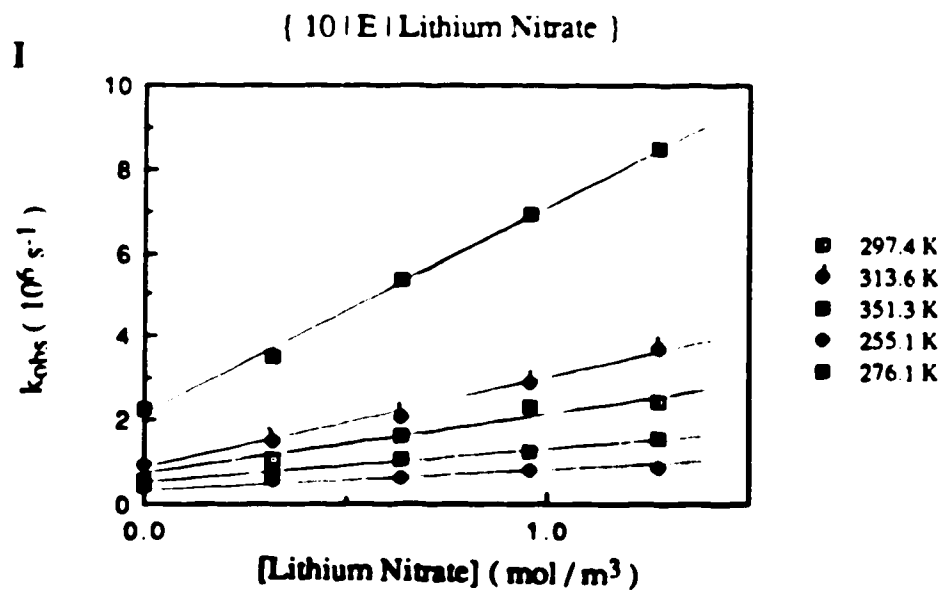
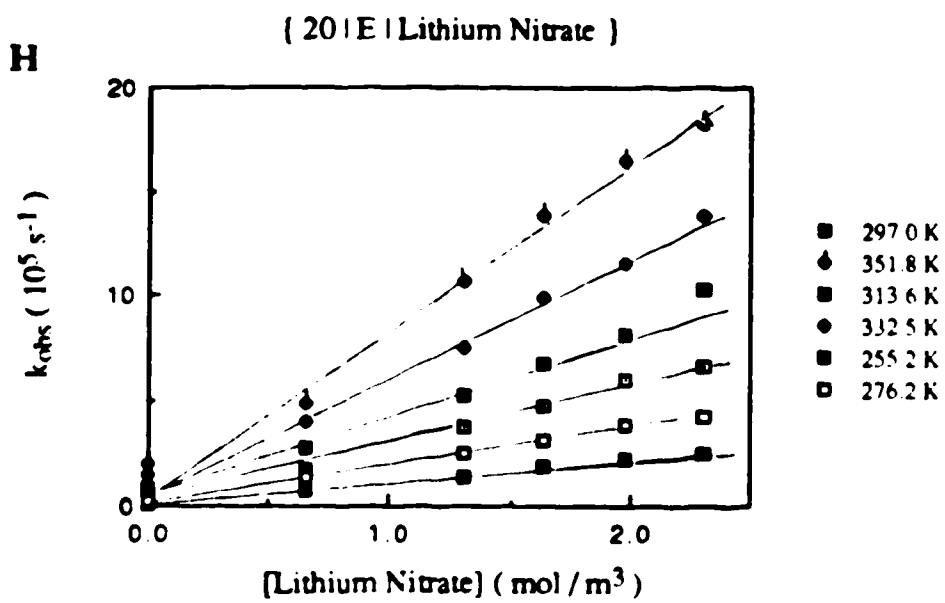
Fig. 3-27 (A-L) Temperature and concentration dependence of the first-order rate constant for the reaction of solvated electrons with lithium nitrate in ethanol / water mixtures

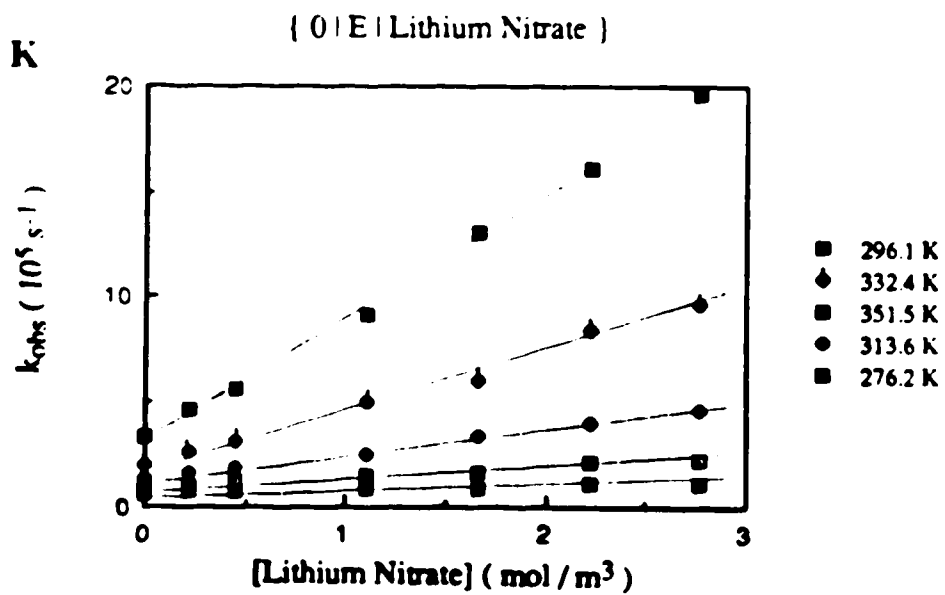
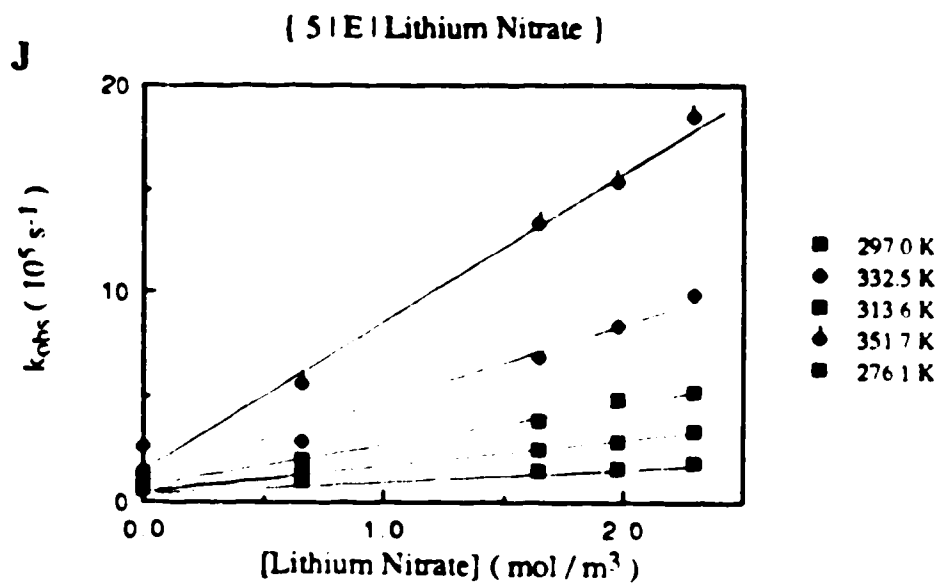














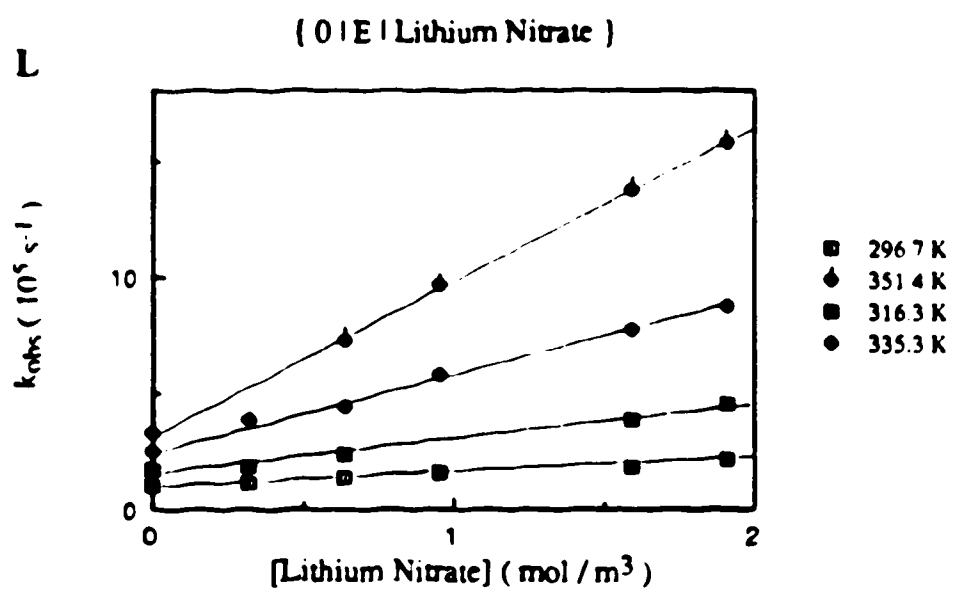


Fig. 3-28 Arrhenius plots for the reaction of solvated electrons with lithium nitrate in ethanol / water mixtures

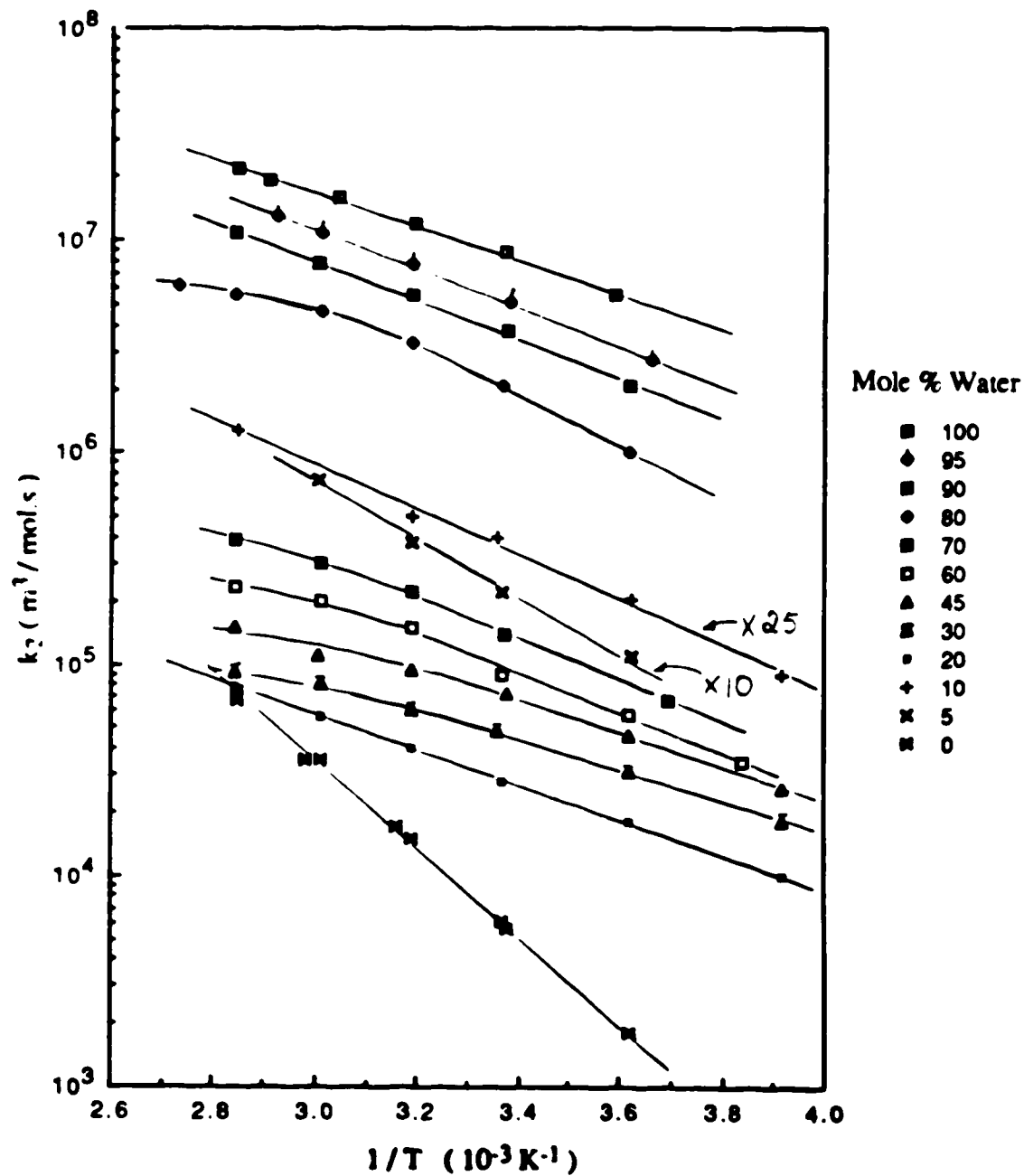


Fig. 3-29 Composition dependence of  $k_{298}$  for the reaction of solvated electrons with lithium nitrate in ethanol / water mixtures

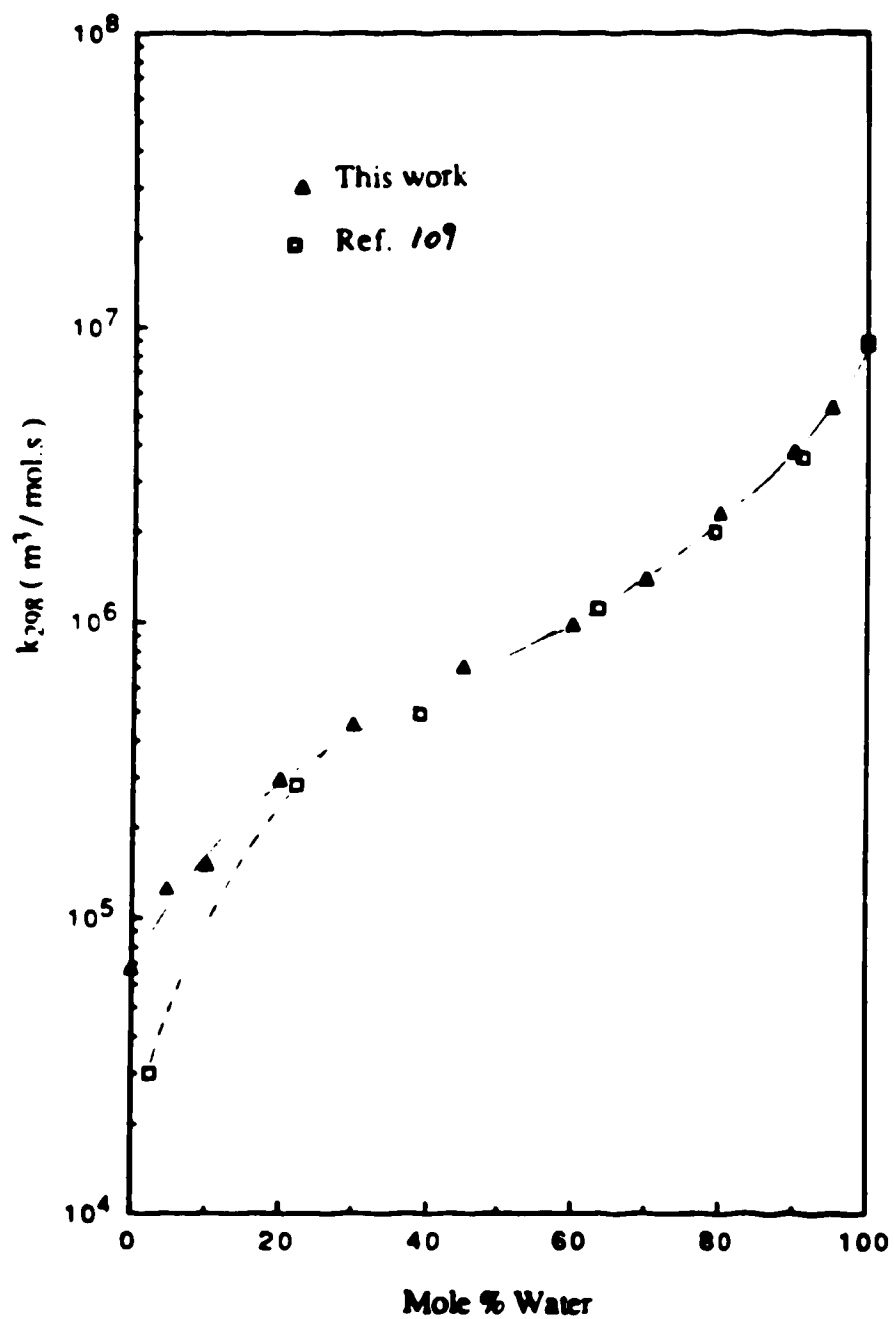


Table 3-25 Second-order rate constants for the reaction of solvated electrons with lithium nitrate in ethanol / water mixtures at various temperatures

$\chi_w$	Temp. (K)	$k_2$ ( $10^6 \text{ m}^3/\text{mol.s}$ )	$\chi_w$	Temp. (K)	$k_2$ ( $10^6 \text{ m}^3/\text{mol.s}$ )	$\chi_w$	Temp. (K)	$k_2$ ( $10^6 \text{ m}^3/\text{mol.s}$ )
1.00	278.6	5.6	0.70	270.7	0.067	0.20	255.2	0.010
	296.5	8.8		296.4	0.14		276.2	0.018
	313.0	12		313.6	0.22		297.0	0.028
	328.7	16		332.5	0.30		313.6	0.040
	343.5	19		351.7	0.39		332.5	0.056
	351.1	22					351.8	0.079
0.95	273.0	2.8	0.60	260.3	0.034	0.10	255.1	0.0036
	295.6	5.2		276.2	0.058		276.1	0.081
	313.6	7.8		297.0	0.090		297.9	0.016
	332.5	11		313.6	0.15		313.6	0.020
	341.9	13		332.5	0.20		351.3	0.051
				351.7	0.22			
0.90	276.2	2.1	0.45	255.2	0.025	0.05	276.1	0.0052
	296.1	3.8		276.2	0.046		297.0	0.011
	313.6	5.5		296.3	0.073		313.6	0.022
	332.6	7.8		313.6	0.094		332.5	0.038
	351.8	11		332.6	0.11		351.7	0.074
				351.8	0.15			
0.80	276.2	1.0	0.30	255.2	0.018	0.00	276.2	0.0018
	296.9	2.1		276.2	0.031		296.1	0.0057
	313.6	3.3		297.7	0.048		313.6	0.015
	332.5	4.6		313.6	0.060		332.4	0.035
	351.5	5.6		332.5	0.080		351.5	0.075
	366.2	6.2		351.7	0.092			
						0.00	296.7	0.0061
							316.3	0.0168
							335.3	0.035
							351.4	0.067

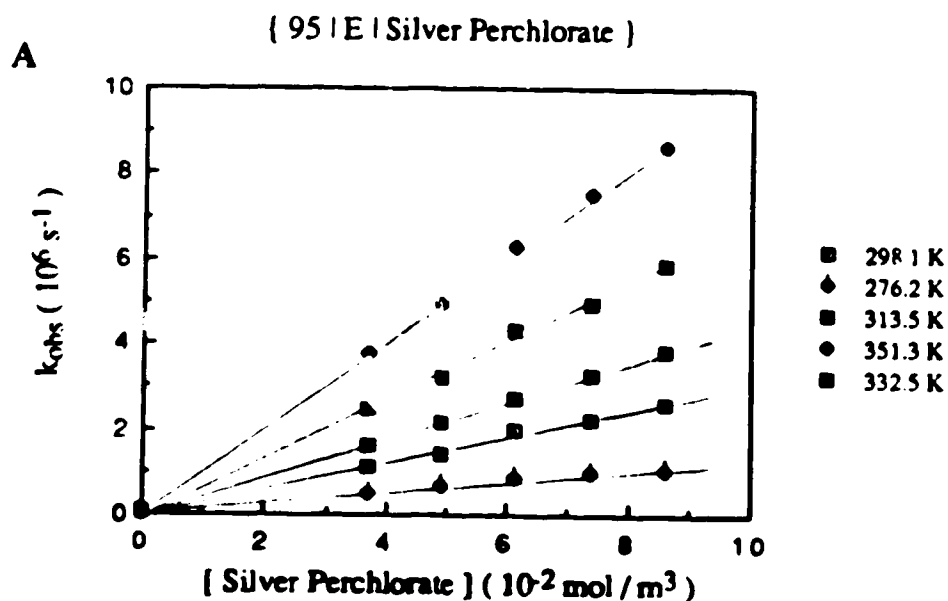
**Table 3-26** Rate parameters for the reaction of solvated electrons with  
lithium nitrate in ethanol / water mixtures

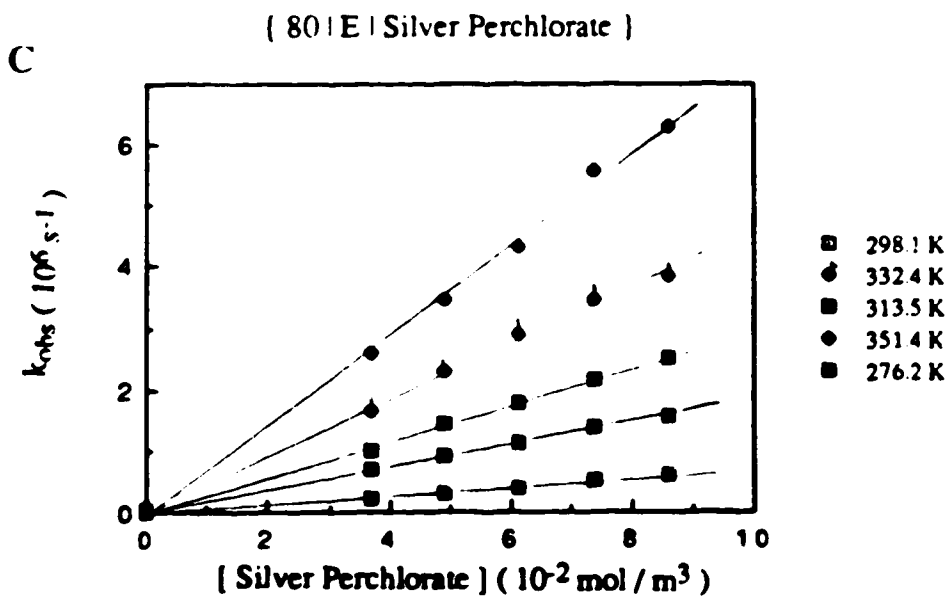
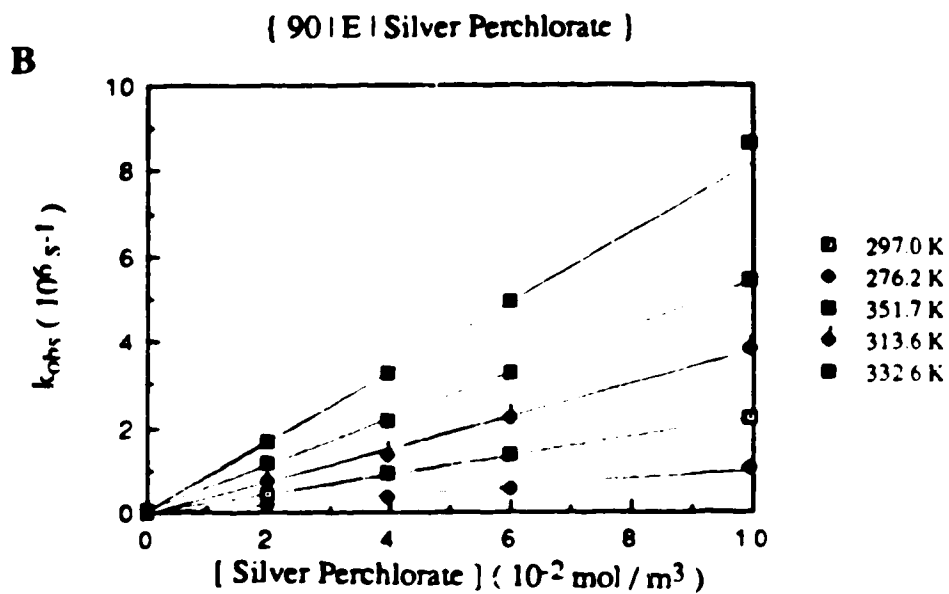
$\chi_w$	$k_{298}$ ( $10^6 \text{ m}^3/\text{mol}\cdot\text{s}$ )	$E_a$ (kJ/mol.)	LogA	$\Delta S^\ddagger$ (J/mol.K)
1.00	8.7	16	12.66	-3
0.95	5.3	18	12.81	0
0.90	3.8	18	12.73	-1
0.80	2.3	19	12.69	-2
0.70	1.4	18	12.33	-9
0.60	0.98	16	11.84	-18
0.45	0.70	13	11.08	-33
0.30	0.45	13	10.92	-36
0.20	0.29	16	11.22	-30
0.10	0.15	20	11.73	-20
0.05	0.13	29	13.14	6
0.00	0.068	40	14.90	40

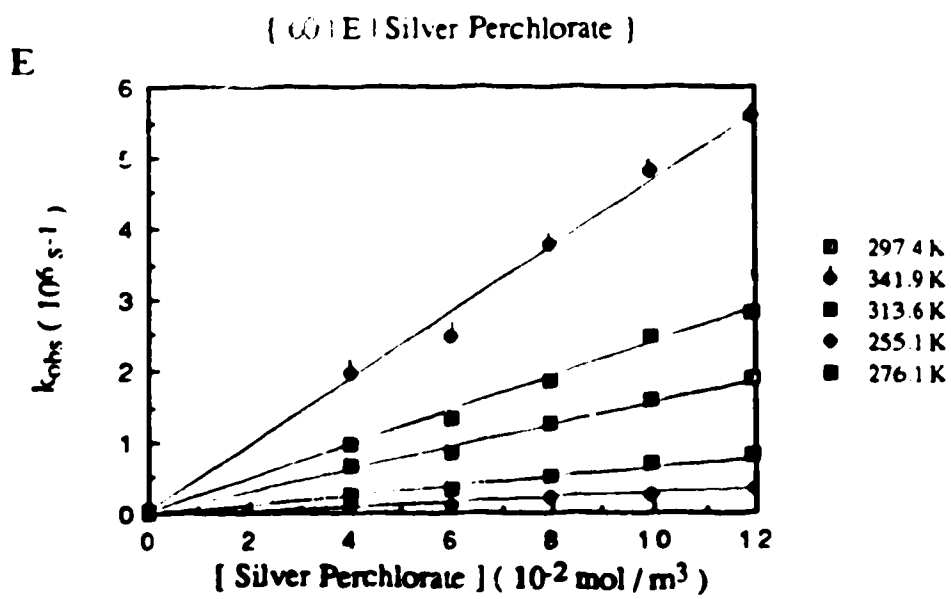
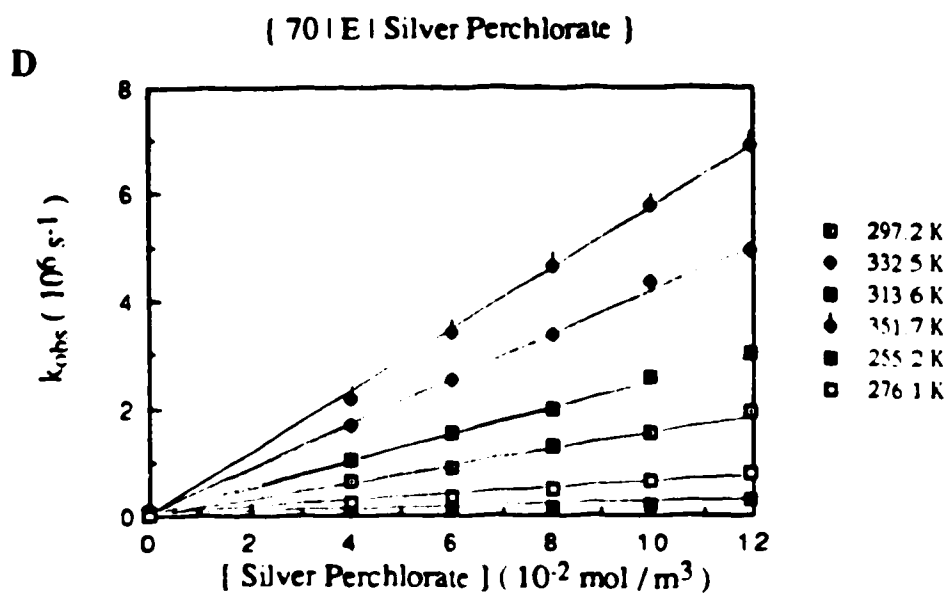
### B. Reaction of solvated electrons with silver ion

The temperature and concentration dependence of the first-order rate constant for the reaction of solvated electrons with silver ion are shown in Figs.3-30(A-K). The concentration range of  $\text{Ag}^+$  was 20-130  $\text{mmol}/\text{m}^3$ . The second-order rate constants at various temperatures are listed in Table 3-27. The rate parameters are obtained from the Arrhenius plots in Fig.3-31. They are summarized in Table 3-28. The rate constant at 298K is  $1.5 \times 10^7 \text{ m}^3/\text{mol}\cdot\text{s}$  in ethanol. The literature value is  $1.2 \times 10^7 \text{ m}^3/\text{mol}\cdot\text{s}$  (102).

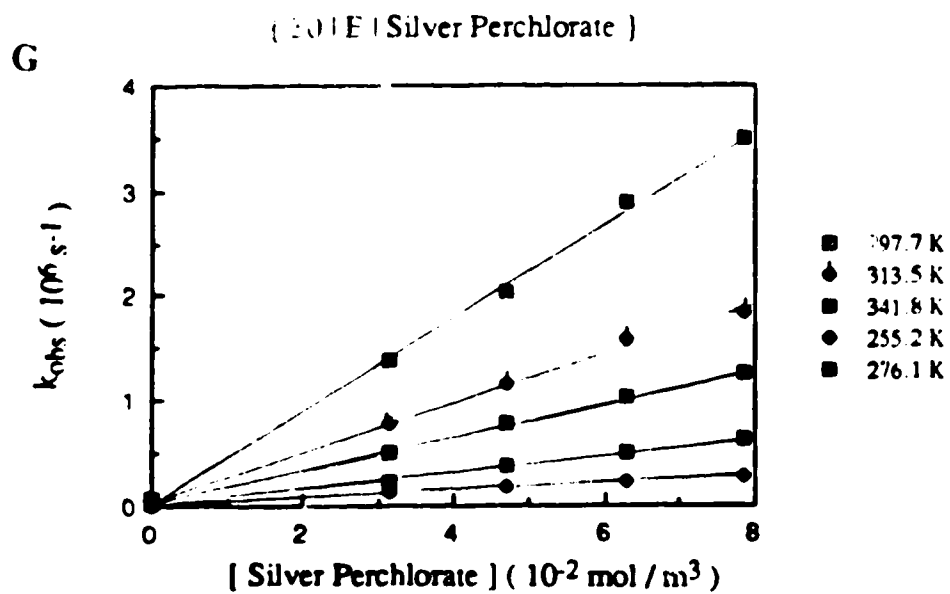
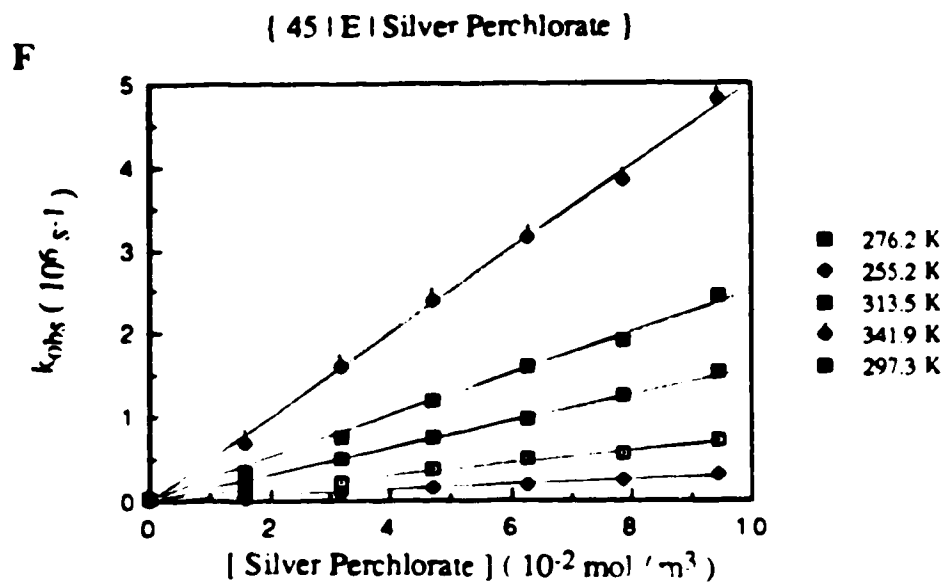
Fig. 3-30 Temperature and concentration dependence of the first-order rate constant for the reaction of solvated electrons with silver perchlorate in ethanol / water mixtures

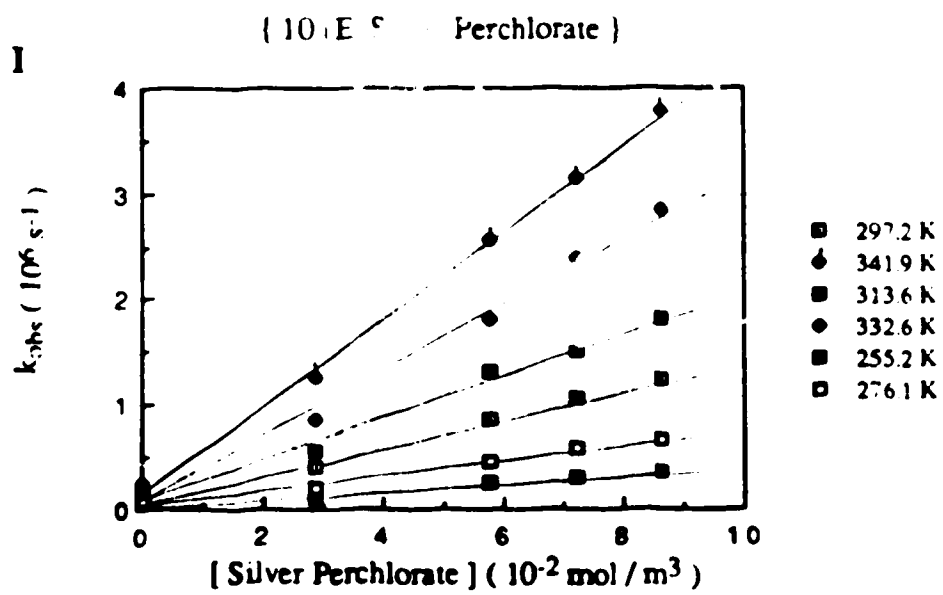
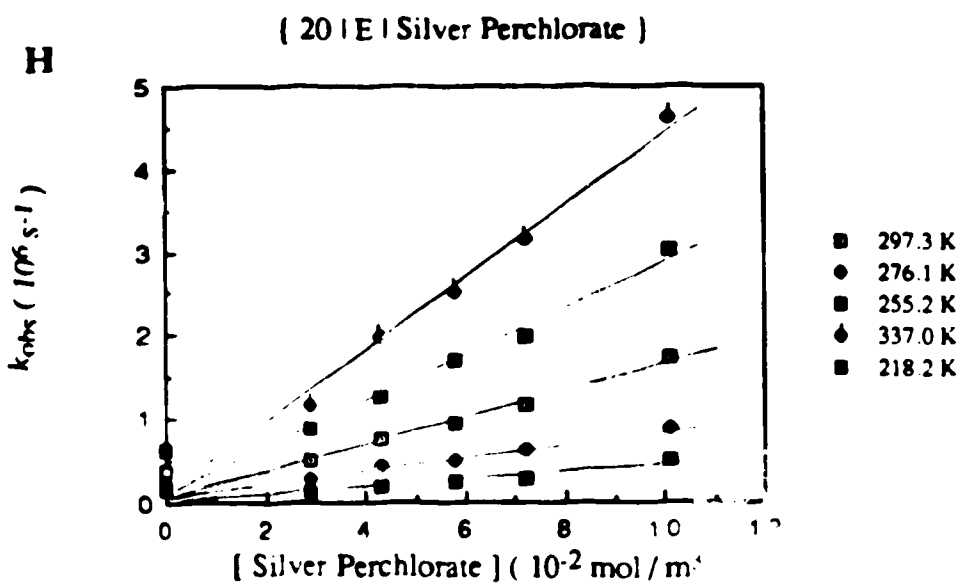












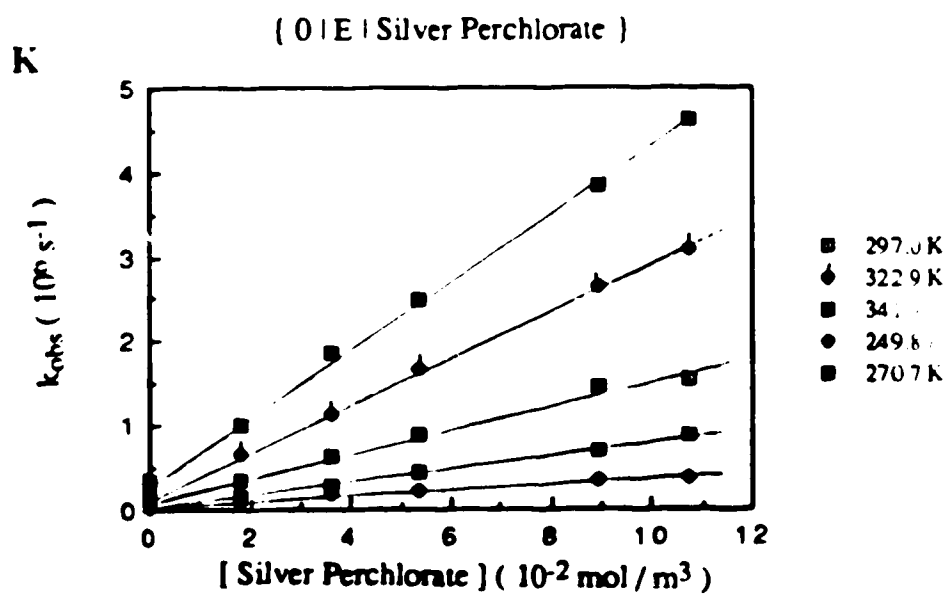
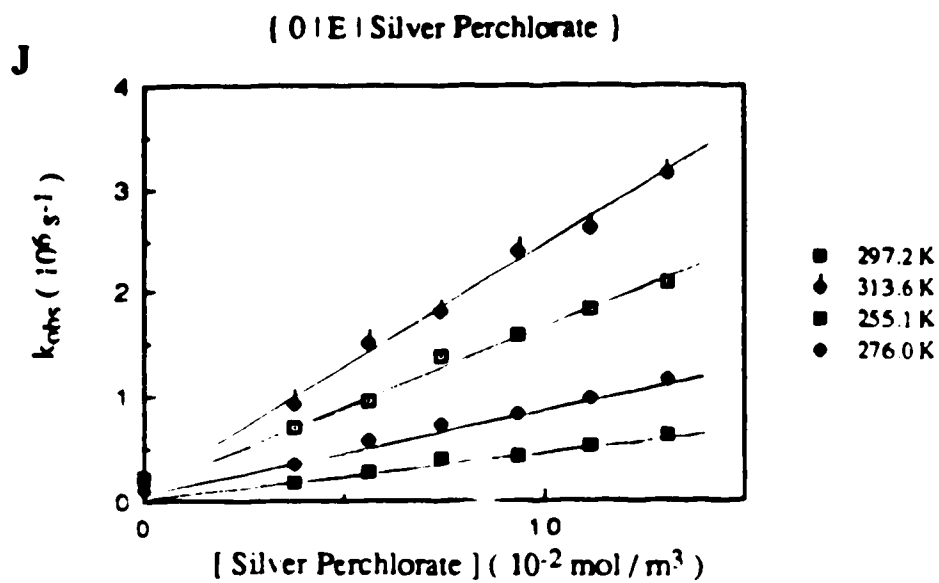
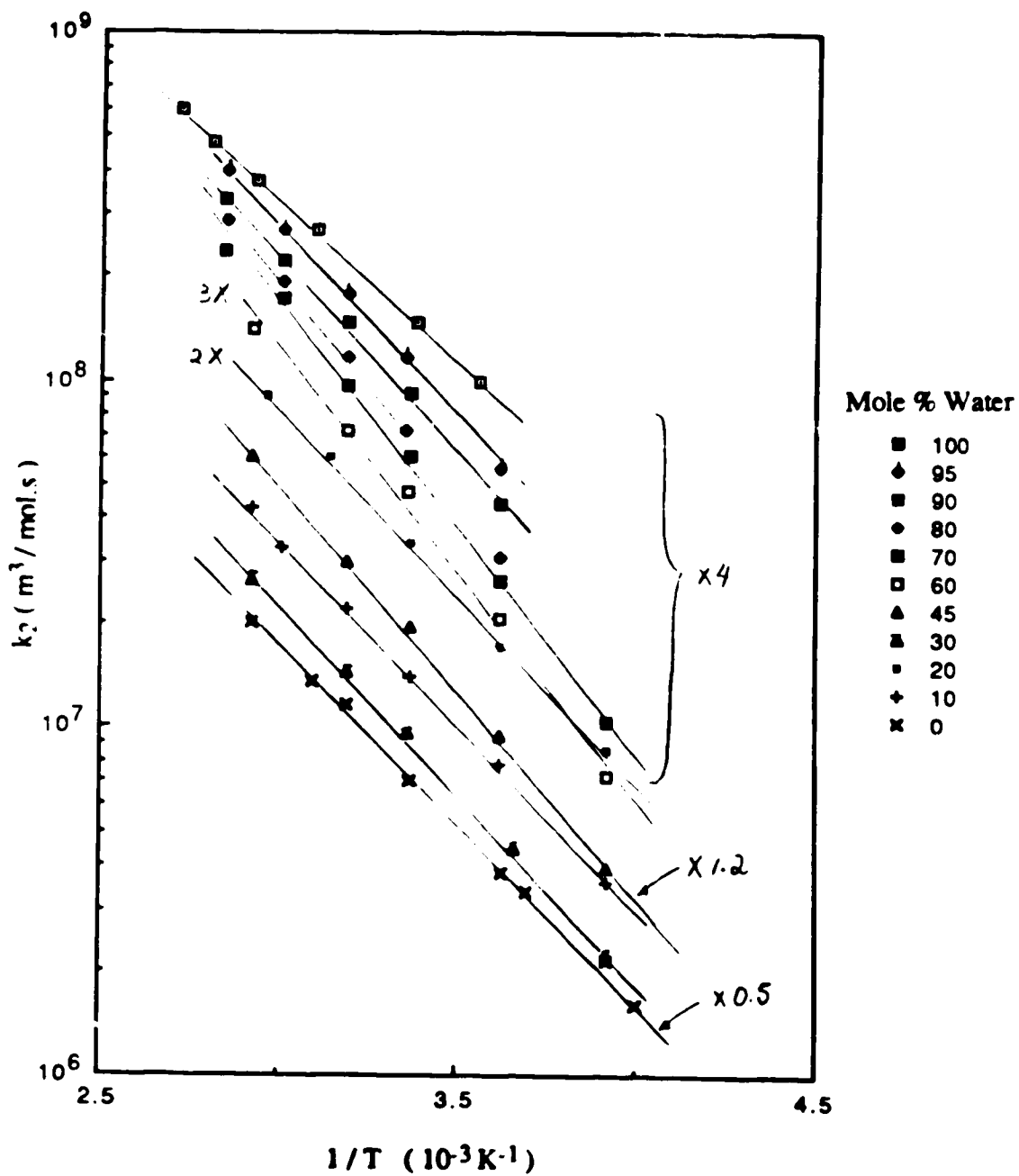


Fig. 3-31 Arrhenius plots for the reaction of solvated electrons with silver perchlorate in ethanol / water mixtures



**Table 3-27 Second-order rate constants for the reaction of solvated electrons with silver perchlorate in ethanol / water mixtures at various temperatures**

$\chi_w$	Temp.	$k_2$	$\chi_w$	Temp.	$k_2$	$\chi_w$	Temp.	$k_2$
	(K)	( $10^7 \text{ m}^3/\text{mol}\cdot\text{s}$ )		(K)	( $10^7 \text{ m}^3/\text{mol}\cdot\text{s}$ )		(K)	( $10^7 \text{ m}^3/\text{mol}\cdot\text{s}$ )
1.00	281.1	2.5	0.70	255.2	0.26	0.20	255.2	0.43
	296.0	3.7		276.1	0.66		276.1	0.86
	322.4	6.7		297.2	1.5		297.3	1.7
	341.4	9.4		313.6	2.4		318.2	3.0
	356.1	12		332.5	4.3		337.0	4.5
	357.7	15		351.7	5.9			
0.95	276.5	1.4	0.60	255.1	0.24	0.10	255.2	0.36
	298.1	2.9		276.1	0.69		276.1	0.78
	313.5	4.4		297.4	1.6		297.2	1.4
	332.5	6.7		313.6	2.4		313.6	2.2
	351.3	10		341.9	4.7		332.6	3.3
						341.9	4.3	
0.90	276.2	1.1	0.45	255.2	0.33	0.00	255.1	0.43
	297.0	2.3		276.2	0.79		276.0	0.77
	313.6	3.7		297.3	1.6		297.2	1.4
	332.6	5.5		313.5	2.5		313.6	2.3
	351.7	8.3		341.9	5.0			
0.85	276.2	0.77	0.30	255.2	0.37	0.00	249.8	0.32
	298.1	1.8		276.1	0.74		270.7	0.68
	313.5	2.9		297.7	1.6		297.0	1.4
	332.4	4.8		313.5	2.4		322.9	2.7
	351.4	7.2		341.8	4.4		341.9	4.0

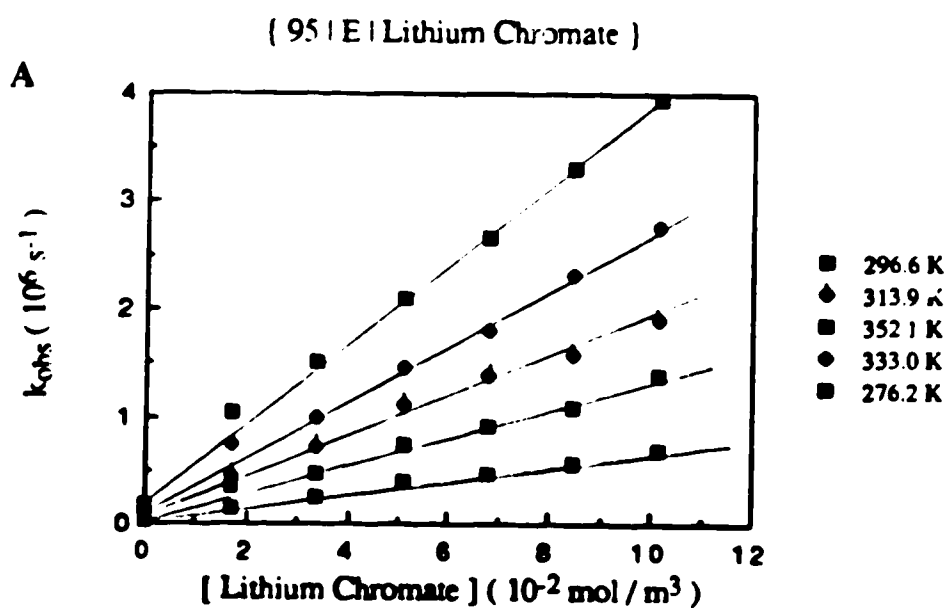
**Table 3-28 Rate parameters for the reaction of solvated electrons with silver perchlorate in ethanol / water mixtures**

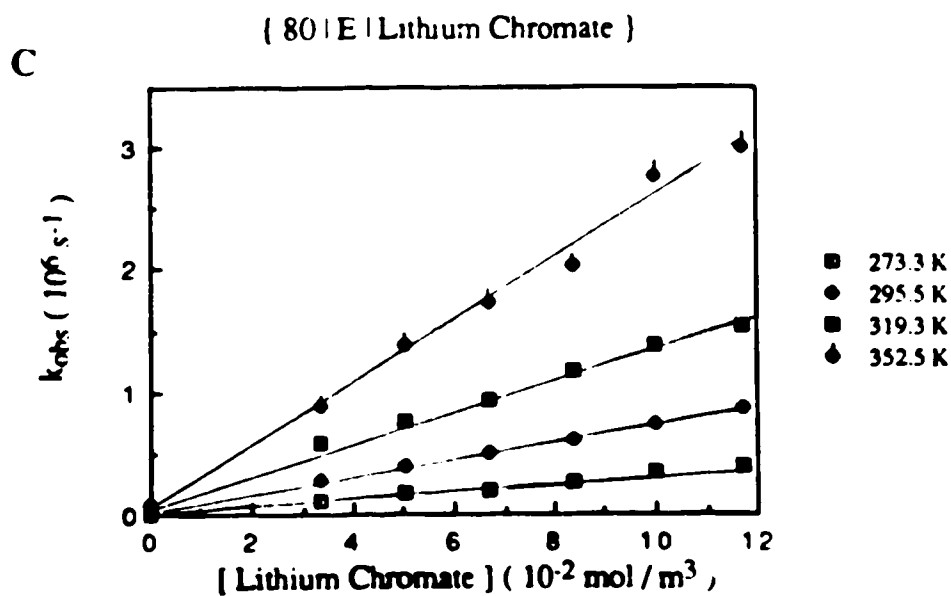
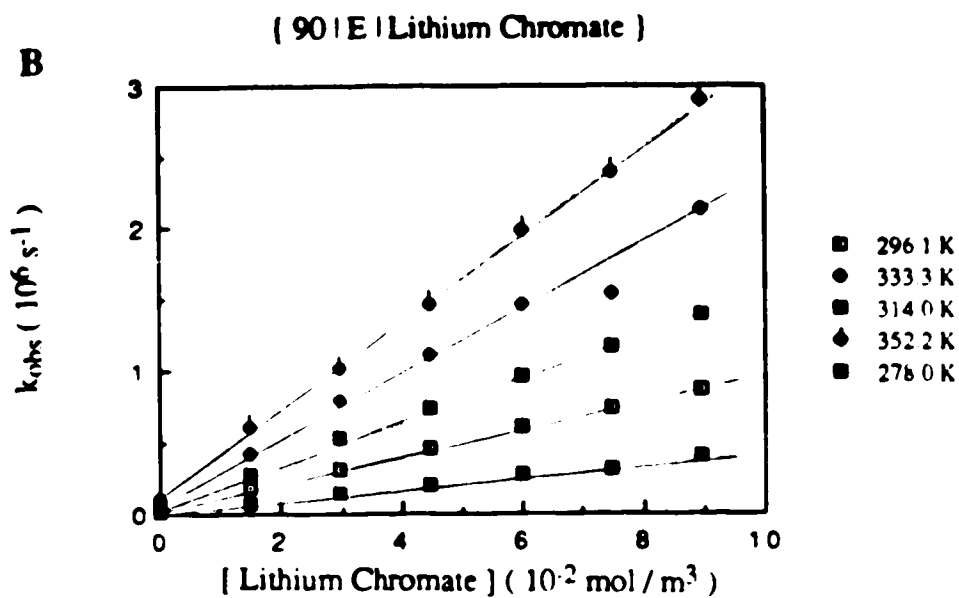
$\chi_w$	$k_{298}$ ( $10^7 \text{ m}^3/\text{mol}\cdot\text{s}$ )	$E_a$ (kJ/mol.)	LogA	$\Delta S^\ddagger$ (J/mol.K)
1.00	3.8	18	13.70	17
0.95	2.8	21	14.00	23
0.90	2.3	22	14.20	28
0.80	1.7	25	14.57	34
0.70	1.5	24	14.40	34
0.60	1.5	26	14.63	35
0.45	1.6	23	14.15	26
0.30	1.6	21	13.89	21
0.20	1.7	20	13.80	19
0.10	1.5	20	13.74	18
0.00	1.5	19	13.53	14

### C. Reaction of solvated electrons with chromate ion

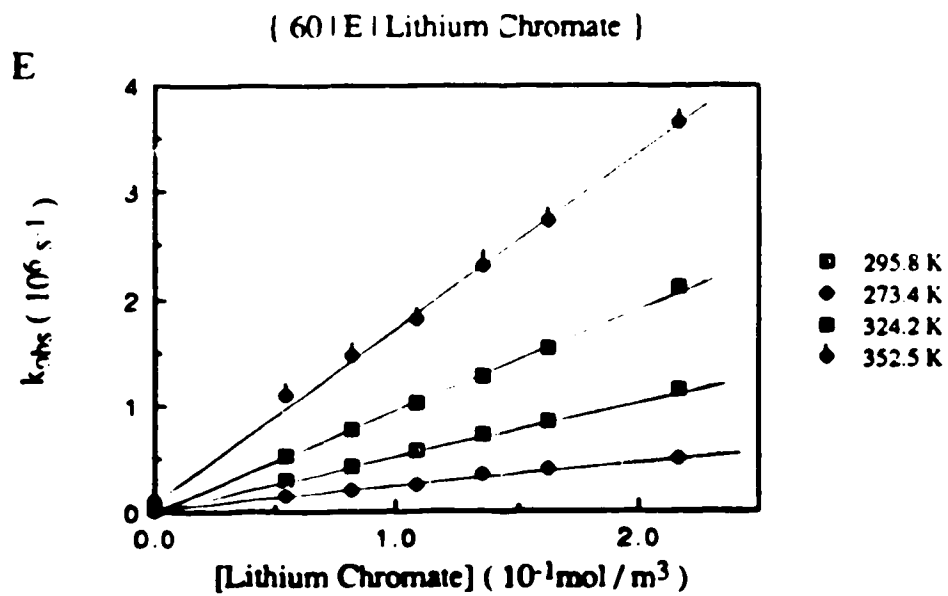
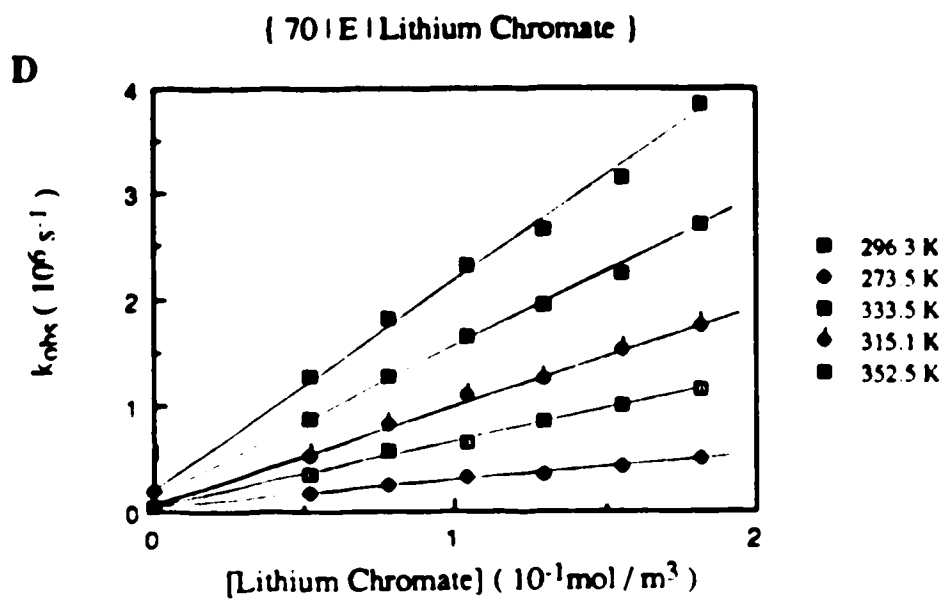
The temperature and concentration dependence of the first-order rate constant for the reaction of solvated electrons with chromate ion are shown in Figs.3-32(A-I). The concentration range of  $\text{CrO}_4^{2-}$  was 17-520  $\text{mmol/m}^3$ . It was found that a minimum of 10 mole% of water in ethanol was needed in order to prepare soluble lithium chromate solutions for the kinetic studies. The second-order rate constants at various temperatures are listed in Table 3-29. The rate parameters are obtained from the Arrhenius plots in Fig.3-33. They are summarized in Table 3-30.

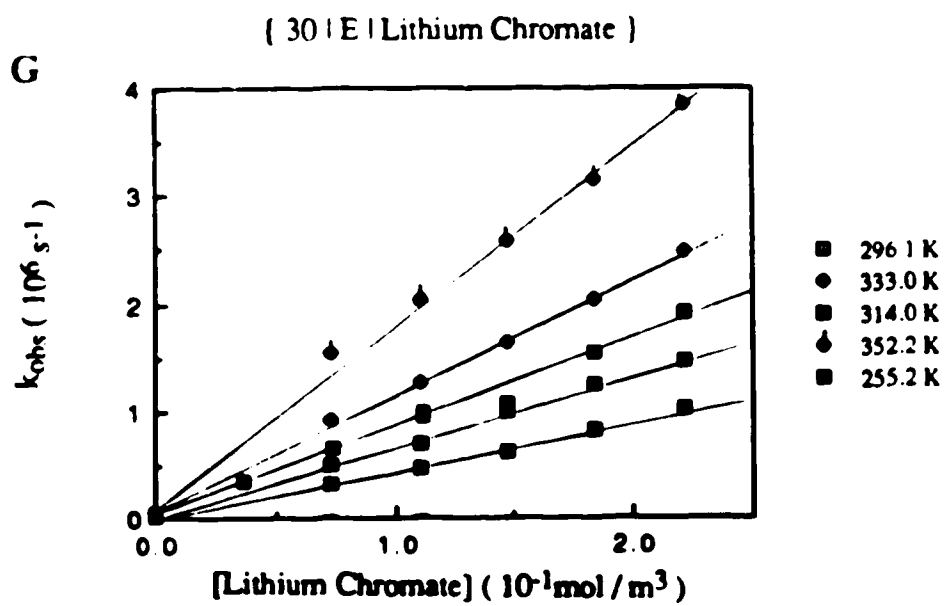
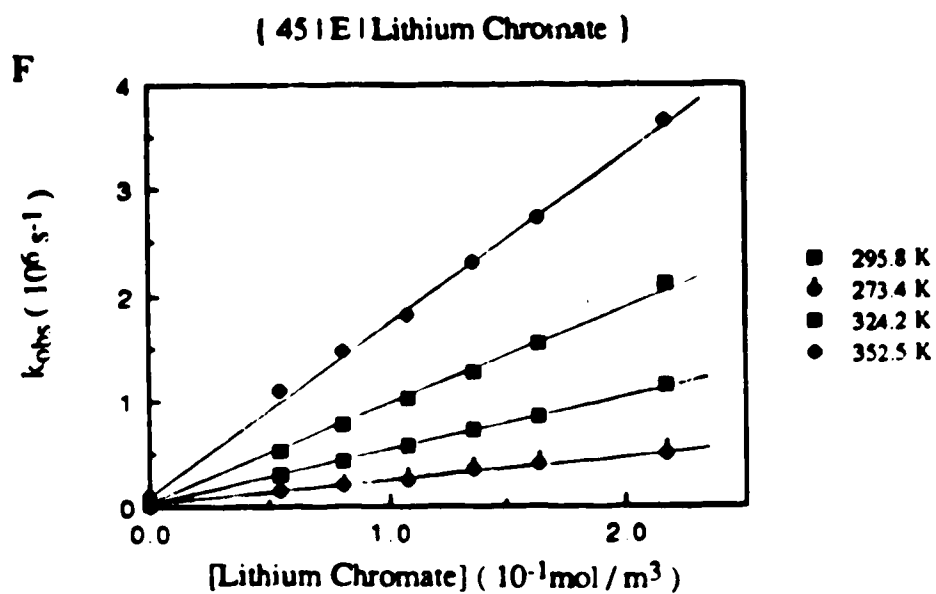
Fig. 3-32 Temperature and concentration dependence of the first-order rate constant for the reaction of solvated electrons with lithium chromate in ethanol / water mixtures











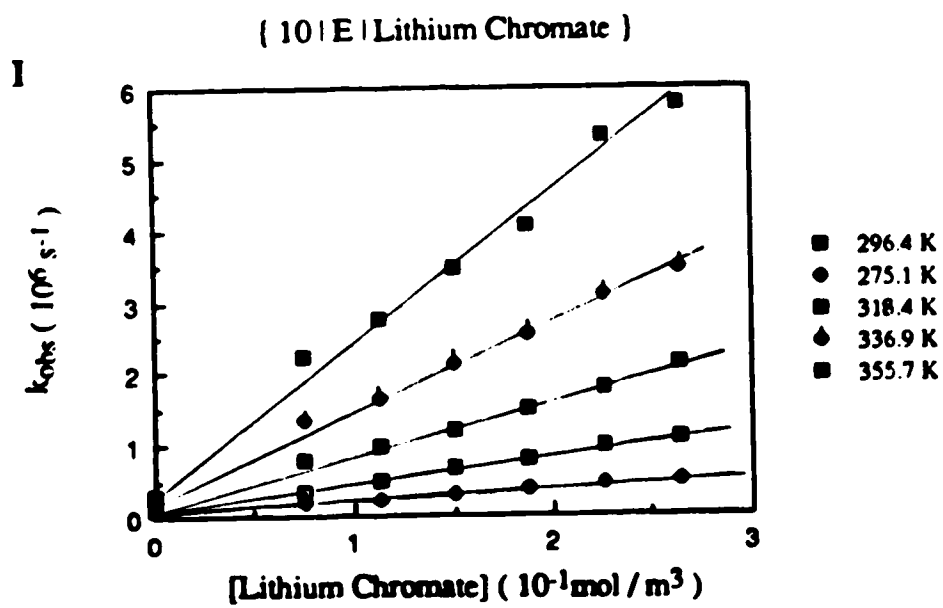
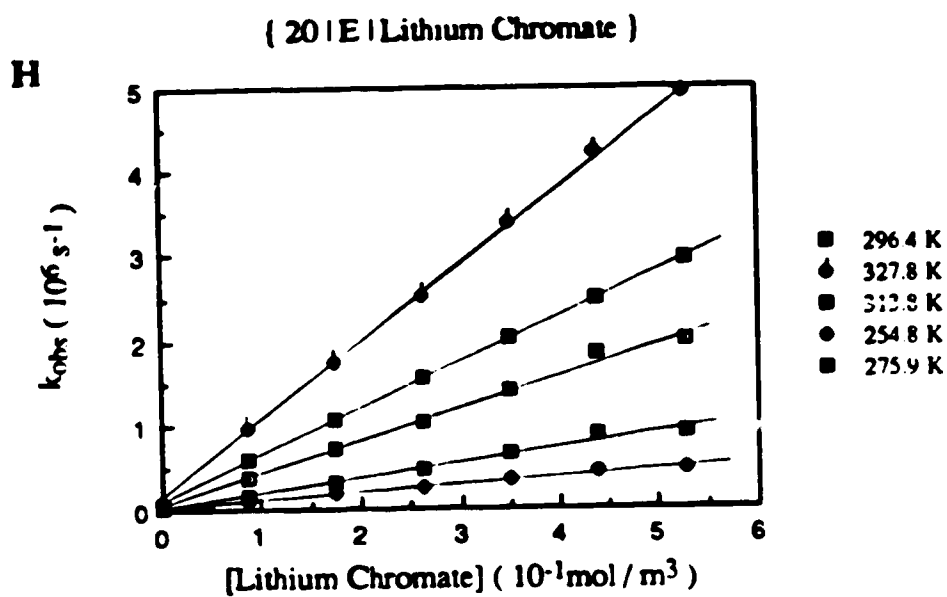
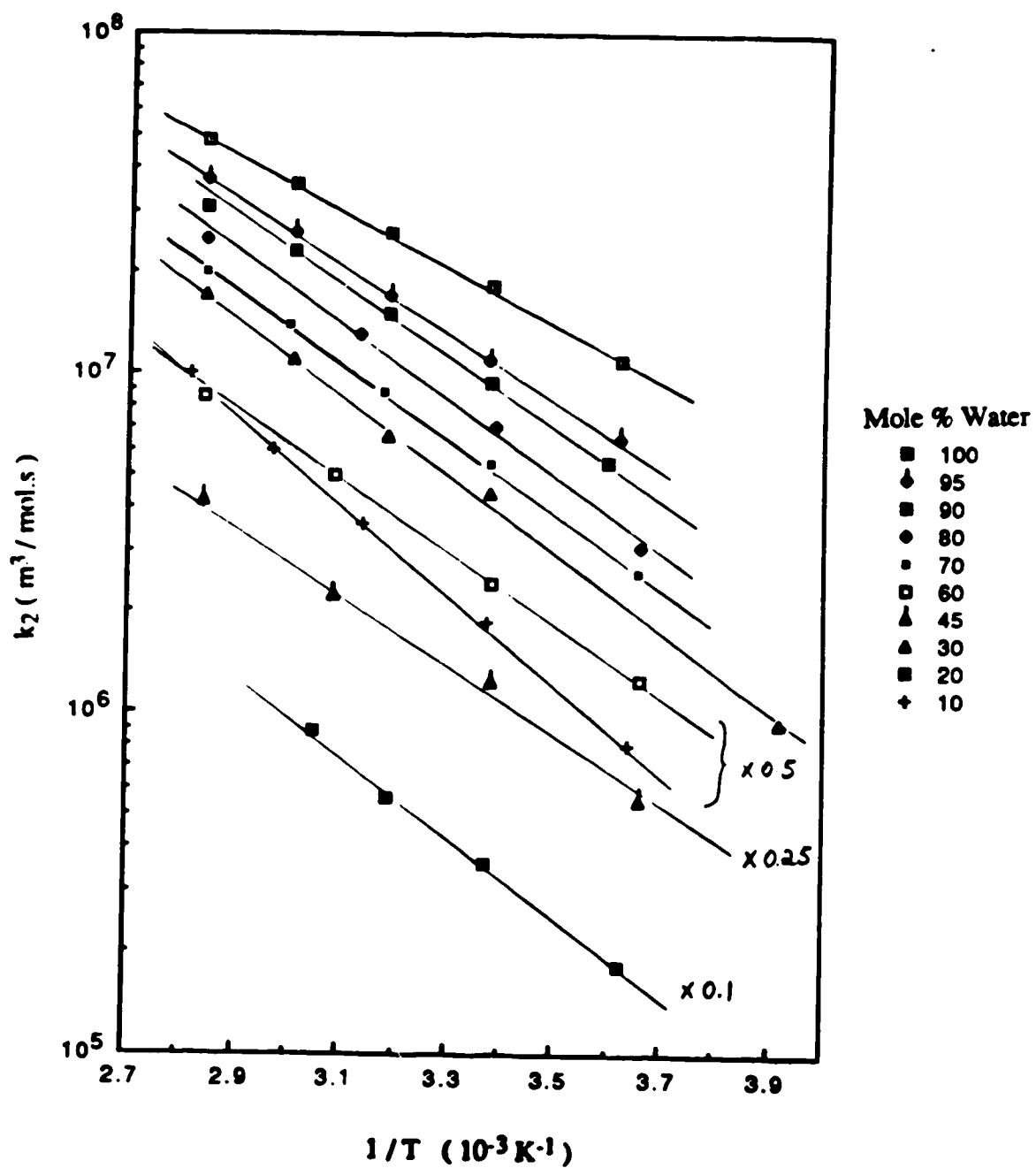


Fig. 3-33 Arrhenius plots for the reaction of solvated electrons with lithium chromate in ethanol / water mixtures



**Table 3-29** Second-order rate constants for the reaction of solvated electrons with lithium chromate in ethanol / water mixtures at various temperatures

$\chi_w$	Temp. (K)	$k_2$ ( $10^7$ m <sup>3</sup> /mol.s)	$\chi_w$	Temp. (K)	$k_2$ ( $10^7$ m <sup>3</sup> /mol.s)	$\chi_w$	Temp. (K)	$k_2$ ( $10^7$ m <sup>3</sup> /mol.s)
1.00	276.4	1.1	0.70	273.5	0.26	0.30	255.2	0.094
	296.0	1.8		296.3	0.54		296.1	0.44
	314.0	2.6		315.1	0.88		314.0	0.66
	333.0	3.6		333.5	1.4		333.0	1.1
	352.2	4.9		352.5	2.0		352.2	1.7
0.95	276.2	0.65	0.60	273.3	0.25	0.20	257.8	0.082
	296.6	1.1		295.7	0.48		275.9	0.18
	313.9	1.7		324.2	1.0		296.4	0.36
	333.0	2.6		352.5	1.7		313.8	0.56
	352.1	3.7					327.8	0.88
0.90	278.0	0.55	0.45	273.4	0.22	0.10	275.1	0.16
	296.1	0.94		295.8	0.49		296.4	0.37
	314.0	1.5		324.2	0.89		318.4	0.72
	333.0	2.3		352.5	1.7		336.9	1.2
	352.2	3.1					355.7	2.0
0.80	273.3	0.32						
	295.5	0.70						
	319.3	1.3						
	352.5	2.5						

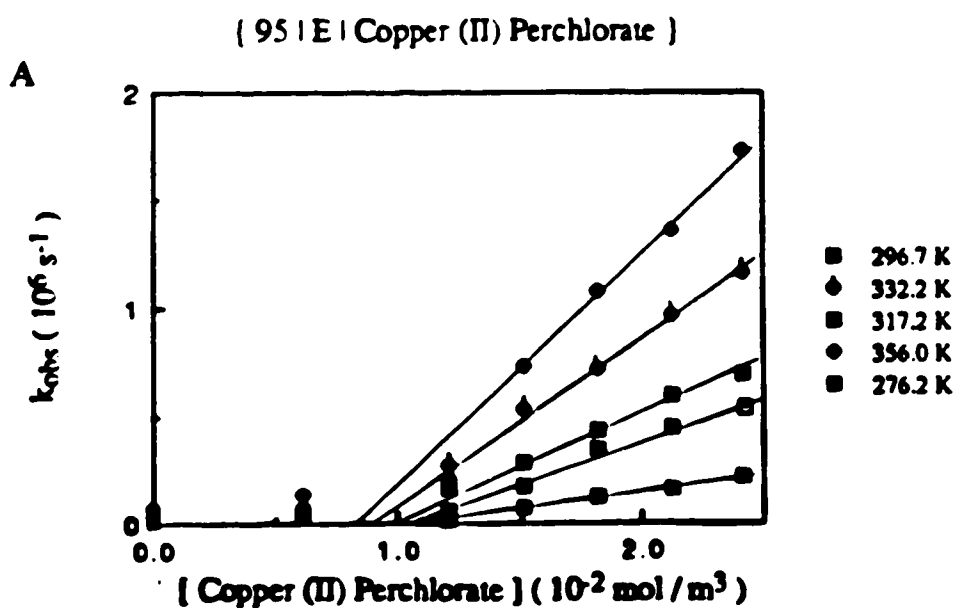
**Table 3-30** Rate parameters for the reaction of solvated electrons with  
lithium chromate in ethanol / water mixtures

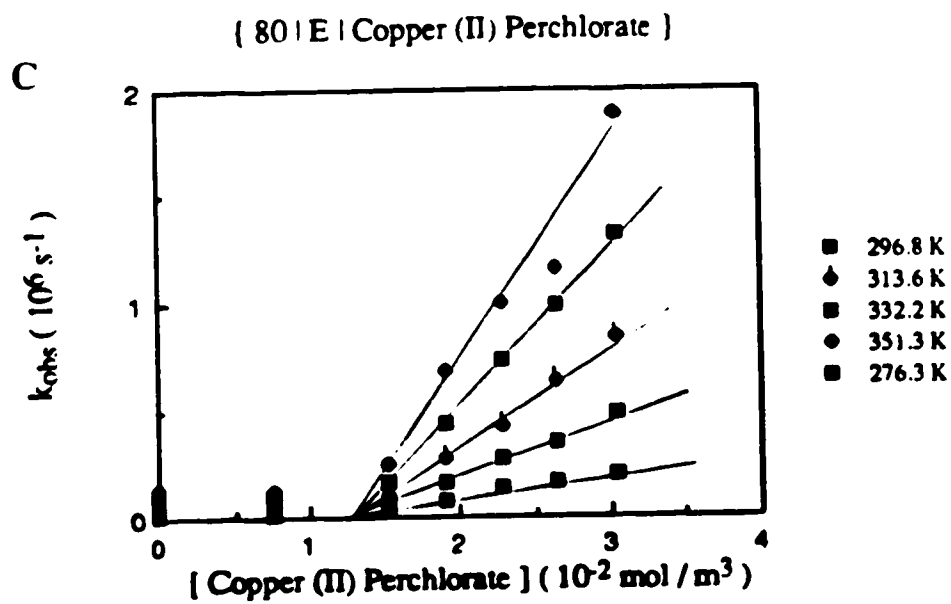
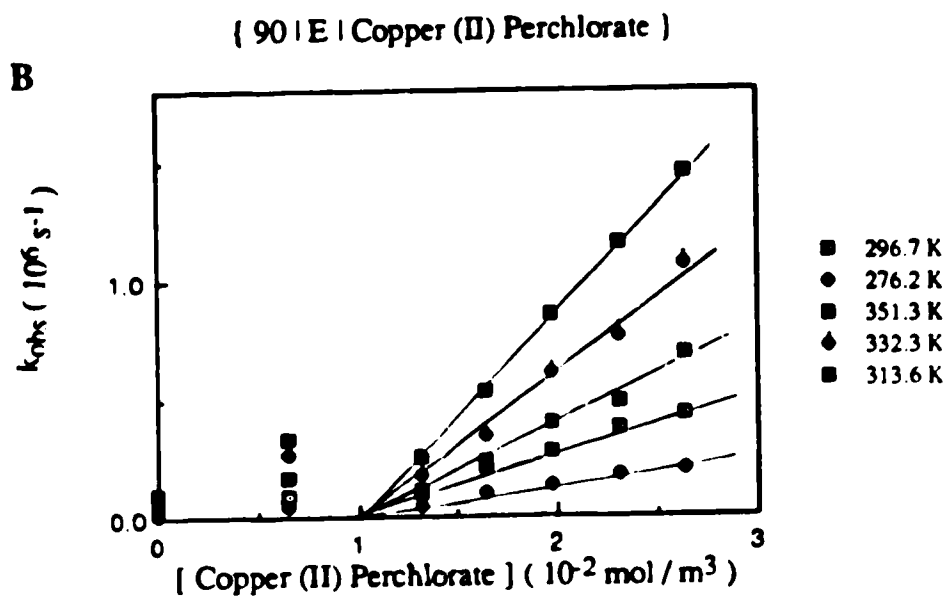
$\chi_w$	$k_{298}$ ( $10^7$ m <sup>3</sup> /mol.s)	$E_a$ (kJ/mol.)	LogA	$\Delta S^\ddagger$ (J/mol.K)
1.00	1.67	16	13.00	4
0.95	1.2	18	13.27	9
0.90	0.99	19	13.34	10
0.80	0.76	19	13.27	9
0.70	0.57	20	13.25	9
0.60	0.50	20	13.15	7
0.45	0.46	20	13.19	8
0.30	0.42	22	13.42	12
0.20	0.39	23	13.61	15
0.10	0.38	25	13.92	21

#### D. Reaction of solvated electrons with copper (II) ion

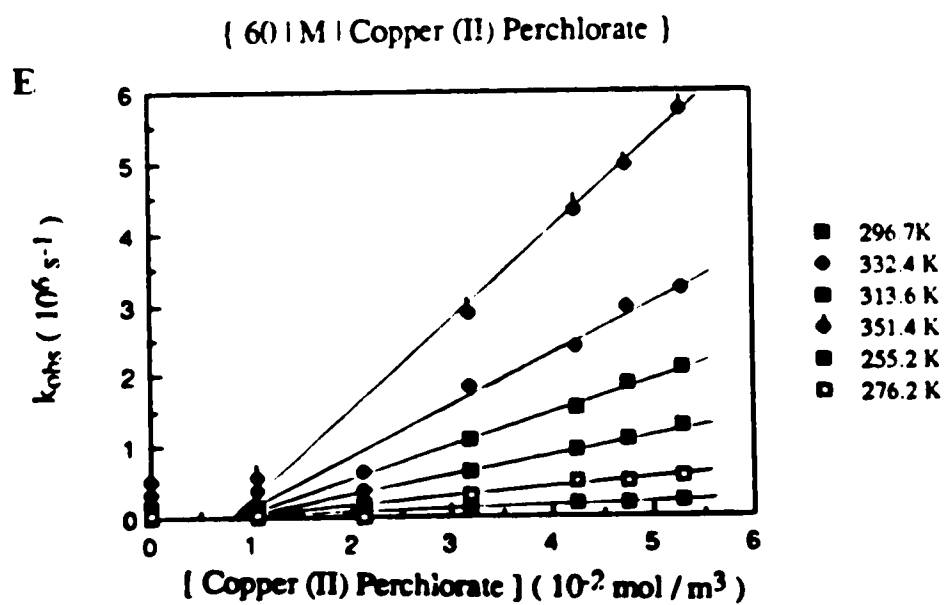
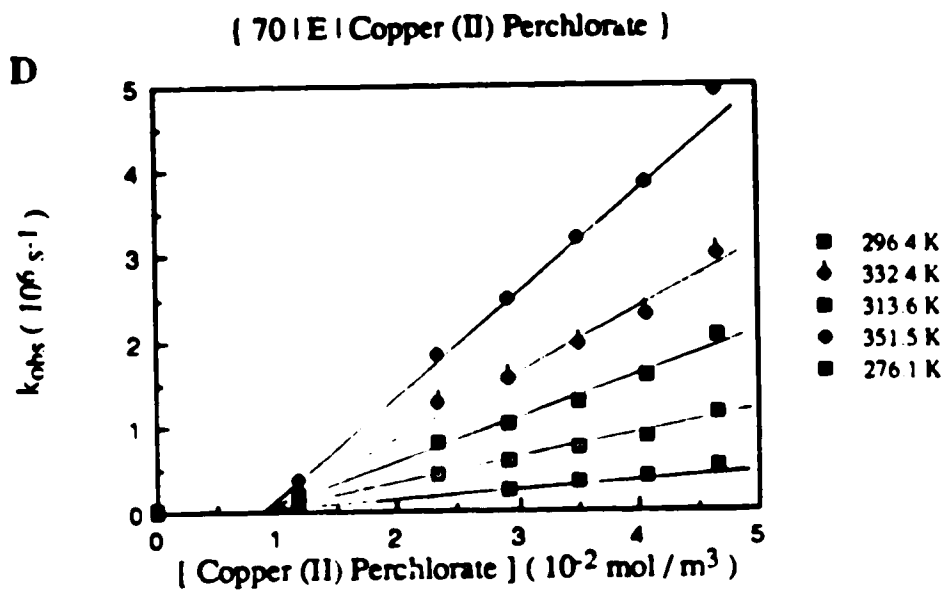
The temperature and concentration dependence of the first-order rate constant for the reaction of solvated electrons with copper (II) ion are shown in Figs.3-34(A-J). Negative y-intercepts, which are similar to those observed in the methanol / water systems earlier, are also observed in the ethanol / water mixed solvent systems. Since they do not affect the dependence of  $k_{\text{obs}}$  on copper concentration, there is no effect on the second-order rate constants. The concentration range of  $\text{Cu}^{2+}$  was 6-530 mmol/m<sup>3</sup>. The second-order rate constants at various temperatures are listed in Table 3-31. The rate parameters are obtained from the Arrhenius plots in Fig.3-35. They are summarized in Table 3-32.

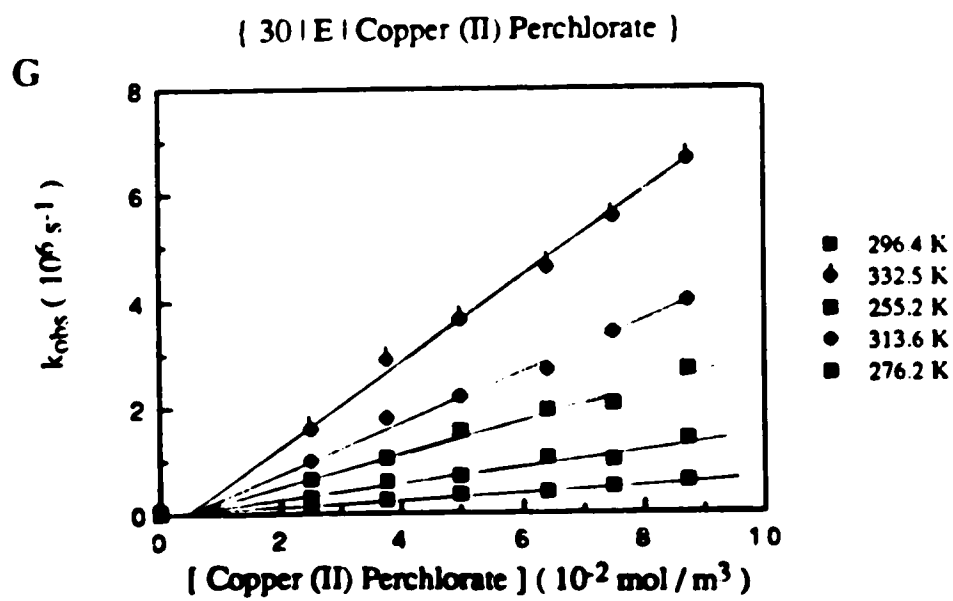
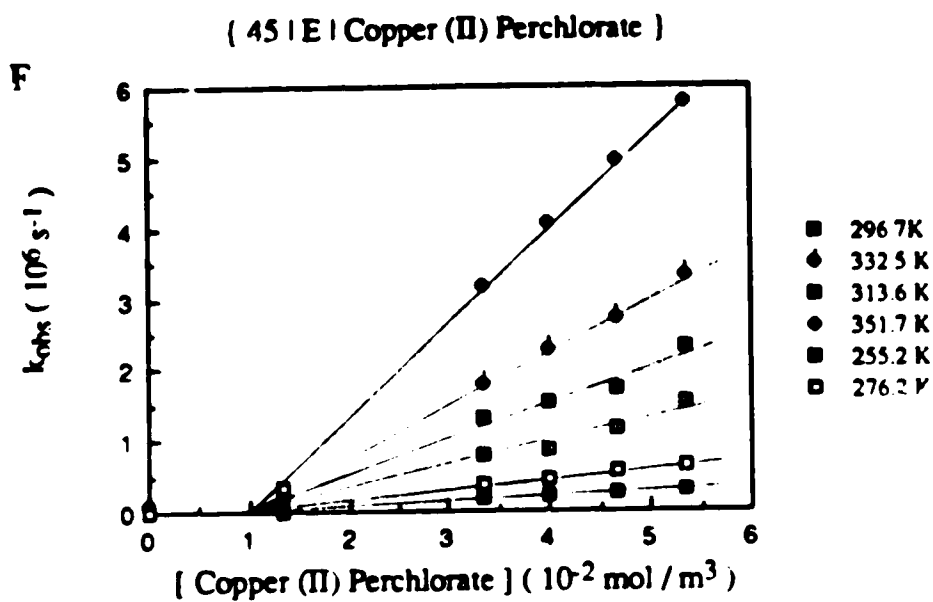
Fig. 3-34  
(A-J) Temperature and concentration dependence of the first-order rate constant for the reaction of solvated electrons with copper (II) perchlorate in ethanol / water mixtures

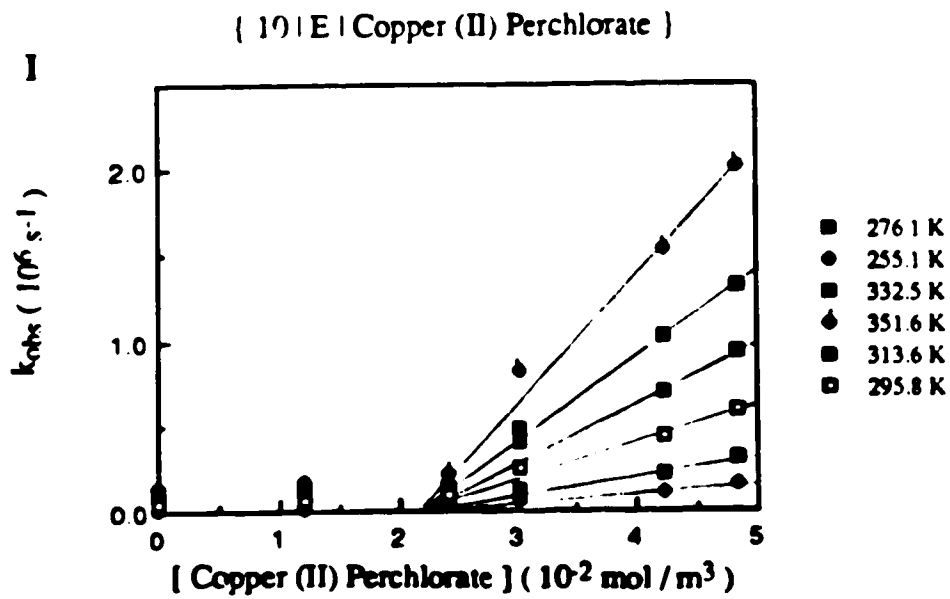
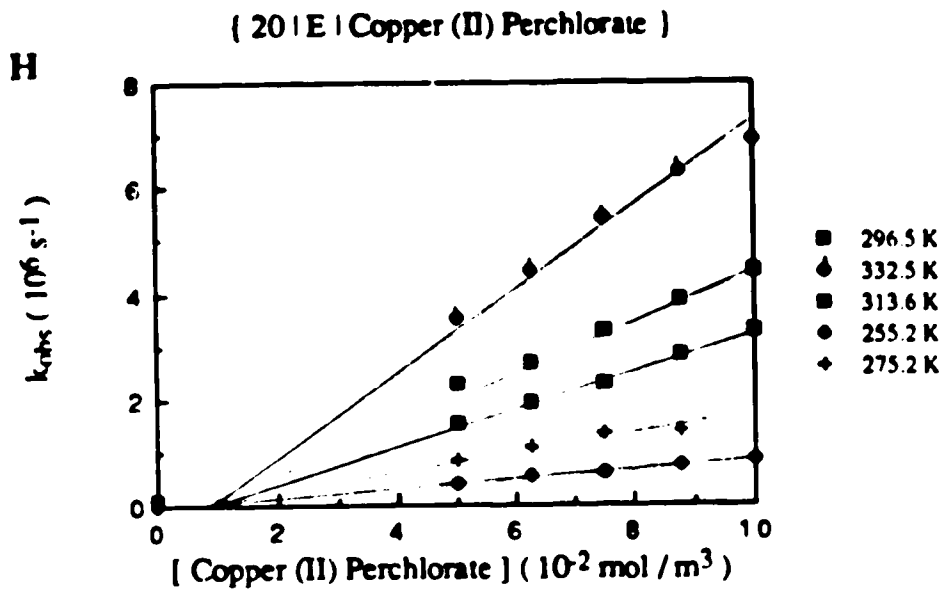












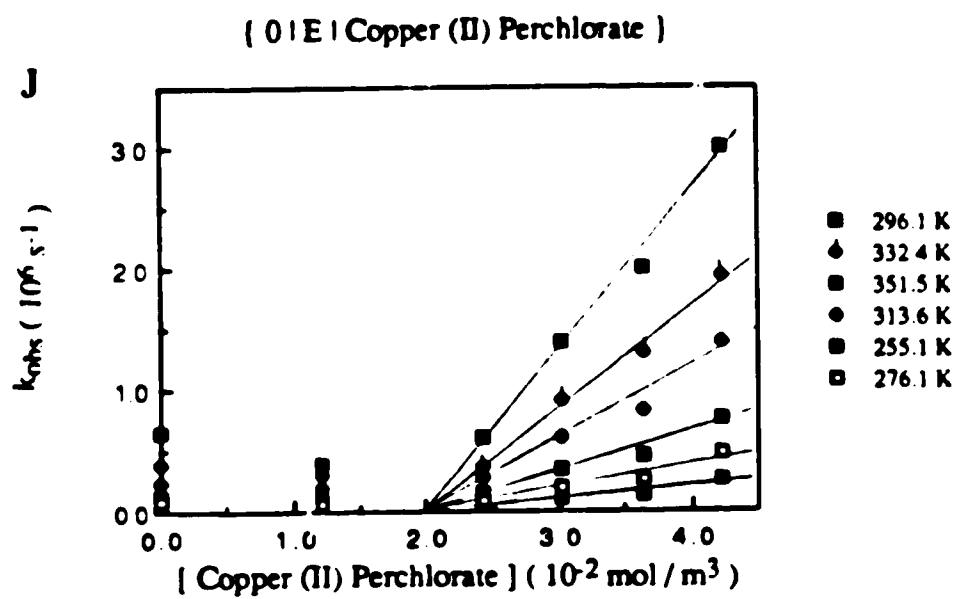
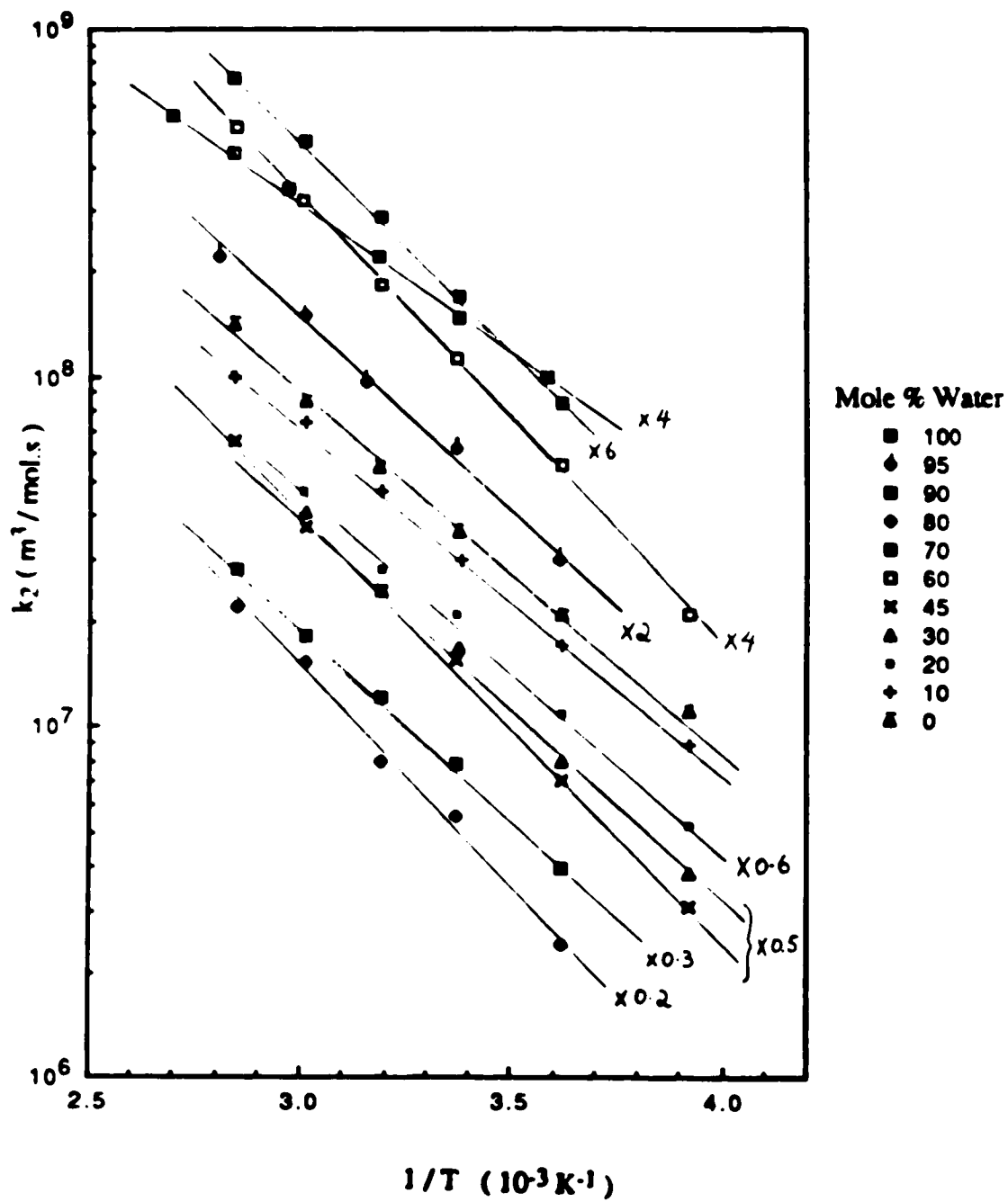


Fig 3-35 Arrhenius plots for the reaction of solvated electrons with copper (II) perchlorate in ethanol / water mixtures



**Table 3-31 Second-order rate constants for the reaction of solvated electrons with copper (II) perchlorate in ethanol / water mixtures at various temperatures**

$\chi_w$	Temp.	$k_2$	$\chi_w$	Temp.	$k_2$	$\chi_w$	Temp.	$k_2$
	(K)	( $10^7 \text{ m}^3/\text{mol}\cdot\text{s}$ )		(K)	( $10^7 \text{ m}^3/\text{mol}\cdot\text{s}$ )		(K)	( $10^7 \text{ m}^3/\text{mol}\cdot\text{s}$ )
1.00	279.0	2.5	0.70	276.1	1.4	0.20	255.2	0.87
	296.0	3.7		296.4	2.8		276.2	1.8
	314.1	5.5		313.6	4.8		296.5	3.5
	336.7	8.6		332.4	7.9		313.6	4.7
	351.2	11		351.5	12		332.6	7.8
370.5	14							
0.95	276.2	1.5	0.60	255.2	0.52	0.10	255.1	0.89
	296.7	3.1		276.2	1.4		276.1	1.7
	317.2	4.8		296.7	2.8		295.8	3.0
	332.2	7.2		313.6	4.6		313.6	4.7
	356.0	11		332.6	8.0		332.5	7.4
			351.4	13	351.6	10		
0.90	276.2	1.4	0.45	255.2	0.61	0.00	255.0	1.1
	296.7	2.8		276.2	1.4		276.1	2.1
	313.6	4.3		296.7	3.1		296.1	3.6
	332.3	6.5		313.6	4.9		313.8	5.5
	351.3	10		332.5	7.4		332.4	8.5
			351.7	13	351.5	14		
0.80	276.3	1.2	0.30	276.2	0.77			
	296.8	2.8		255.2	1.6			
	313.6	4.0		296.4	3.4			
	332.2	7.7		313.6	4.9			
	351.3	11		332.5	8.2			

**Table 3-32** Rate parameters for the reaction of solvated electrons with copper (II) perchlorate in ethanol / water mixtures

$\chi_w$	$k_{298}$ ( $10^7 \text{ m}^3/\text{mol.s}$ )	$E_a$ (kJ/mol.)	LogA	$\Delta S^\ddagger$ (J/mol.K)
1.00	3.8	16	13.46	13
0.95	3.0	20	13.94	22
0.90	2.8	21	14.09	25
0.80	2.8	24	14.63	35
0.70	3.0	24	14.73	37
0.60	2.9	24	14.74	37
0.45	3.0	24	14.56	33
0.30	3.3	22	14.34	29
0.20	3.3	20	14.07	24
0.10	3.3	20	13.93	22
0.00	3.9	19	13.90	21

### III Conductivities of inorganic electrolytes in alcohol / water mixtures

The conductivities of lithium nitrate, silver perchlorate, lithium chromate and copper (II) perchlorate in two series of alcohol / water mixed solvents were measured at various temperatures. The concentrations of the electrolytes are in the same range as those used for the kinetic studies.

#### 1. Methanol / water mixtures

The molar conductances ( $\Lambda$ ) of the electrolytes were obtained from the specific conductance ( $\kappa$ ) versus electrolytes concentration plots :  $\text{LiNO}_3$ , Fig.3-36(A-F);  $\text{AgClO}_4$ , Fig.3-37(A-K);  $\text{Li}_2\text{CrO}_4$ , Fig.3-38(A-F);  $\text{Cu}(\text{ClO}_4)_2$ , Fig.3-39(A-F). The molar conductance values were plotted against  $1/\text{Temp.}$  to obtain the activation energy ( $E_A$ ) for the ion migration process. The Arrhenius plots of the molar conductance are shown in Fig.3-40 for  $\text{LiNO}_3$ , Fig.3-41 for  $\text{AgClO}_4$ , Fig.3-42 for  $\text{Li}_2\text{CrO}_4$ , and Fig.3-43 for  $\text{Cu}(\text{ClO}_4)_2$ . The results are summarized in Fig.3-44 and Table 3-33.

#### 2. Ethanol / water mixtures

The specific conductance ( $\kappa$ ) versus electrolytes concentration plots are shown in Fig.3-45(A-G) for  $\text{LiNO}_3$ , Fig.3-46(A-G) for  $\text{AgClO}_4$ , Fig.3-47(A-F) for  $\text{Li}_2\text{CrO}_4$ , and Fig.3-48(A-G) for  $\text{Cu}(\text{ClO}_4)_2$ . The Arrhenius plots of the molar conductance are shown in Fig.3-49 for  $\text{LiNO}_3$ , Fig.3-50 for  $\text{AgClO}_4$ , Fig.3-51 for  $\text{Li}_2\text{CrO}_4$ , and Fig.3-52 for  $\text{Cu}(\text{ClO}_4)_2$ . The results are summarized in Figs.3-53,54 and Table 3-34.



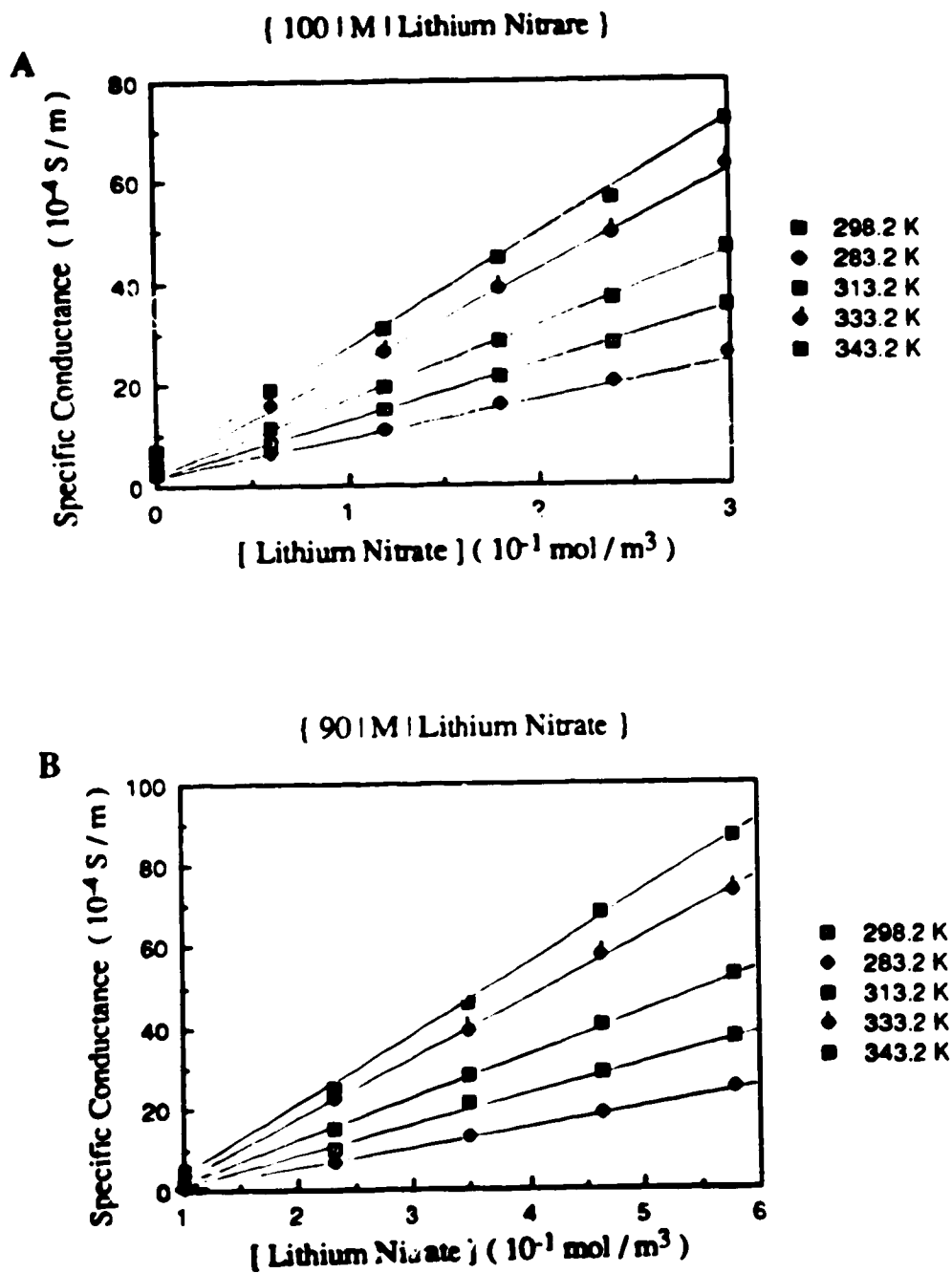
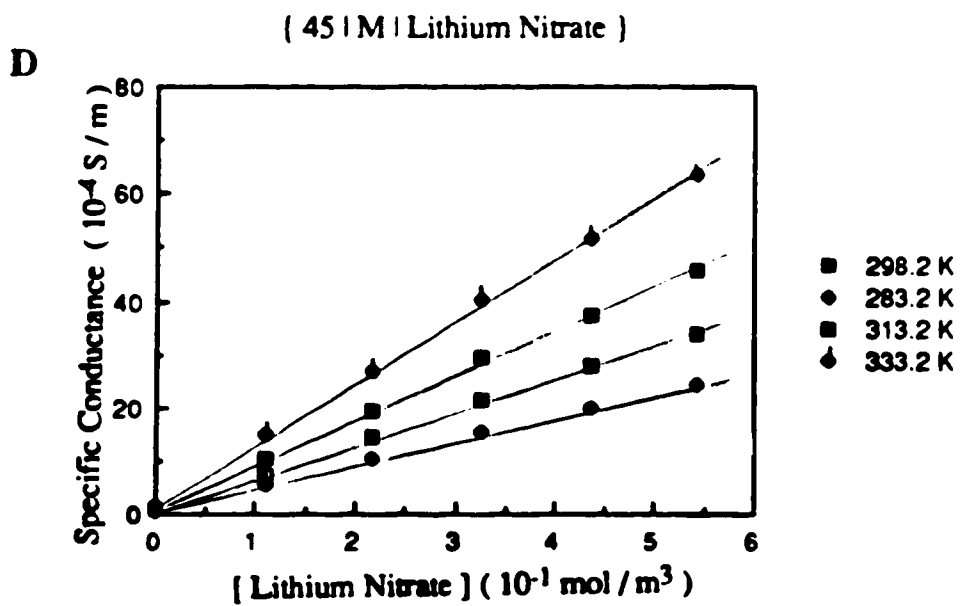
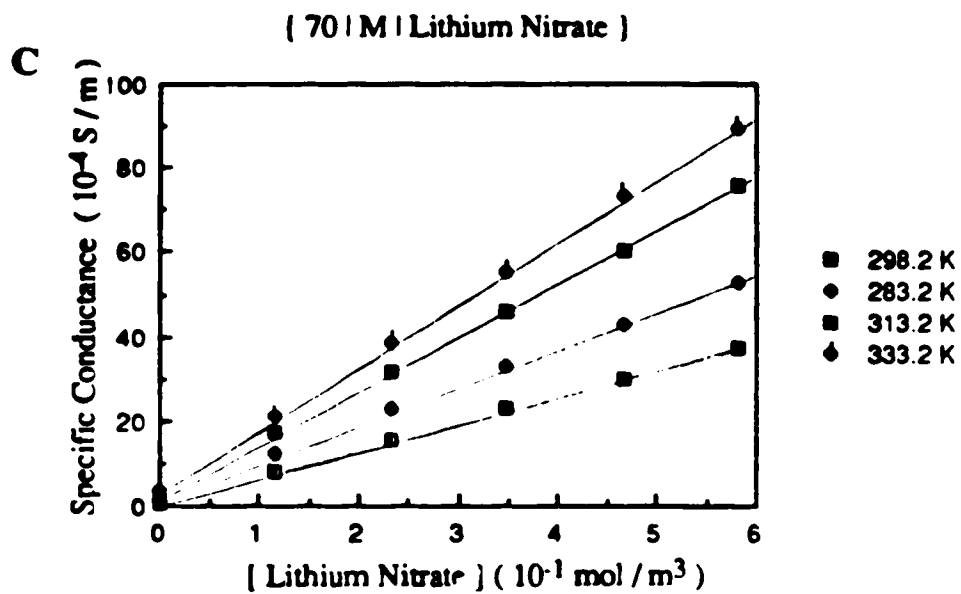
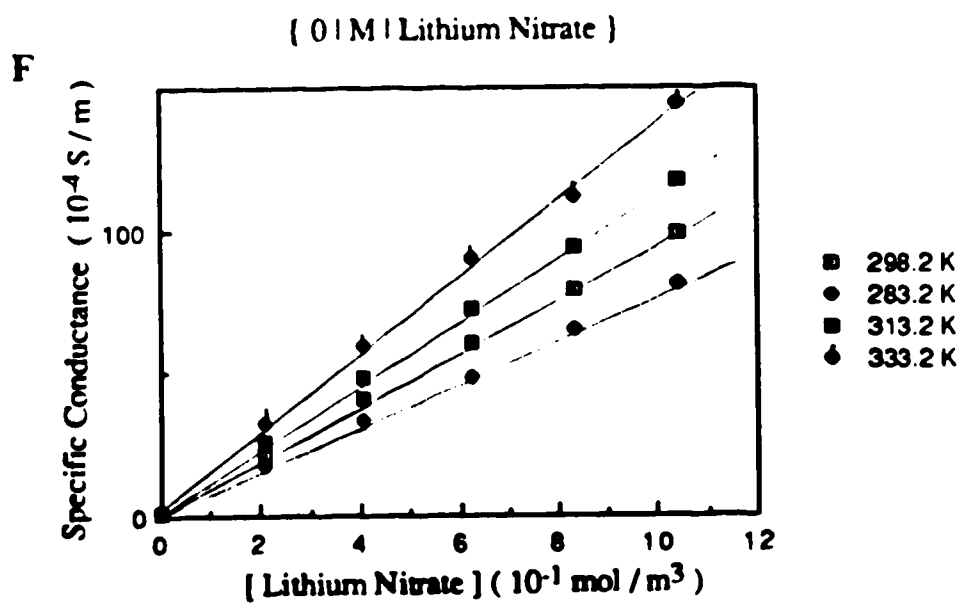
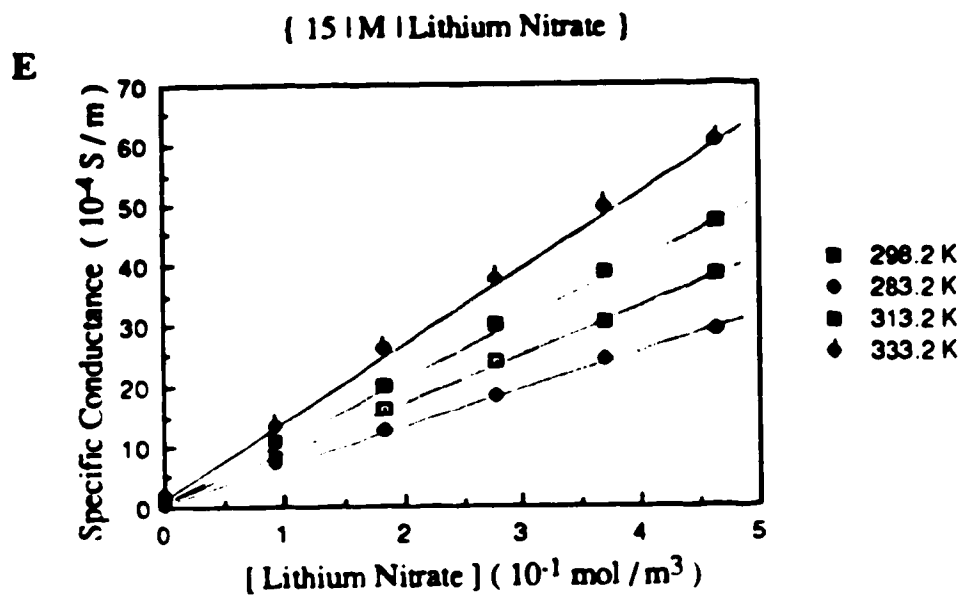
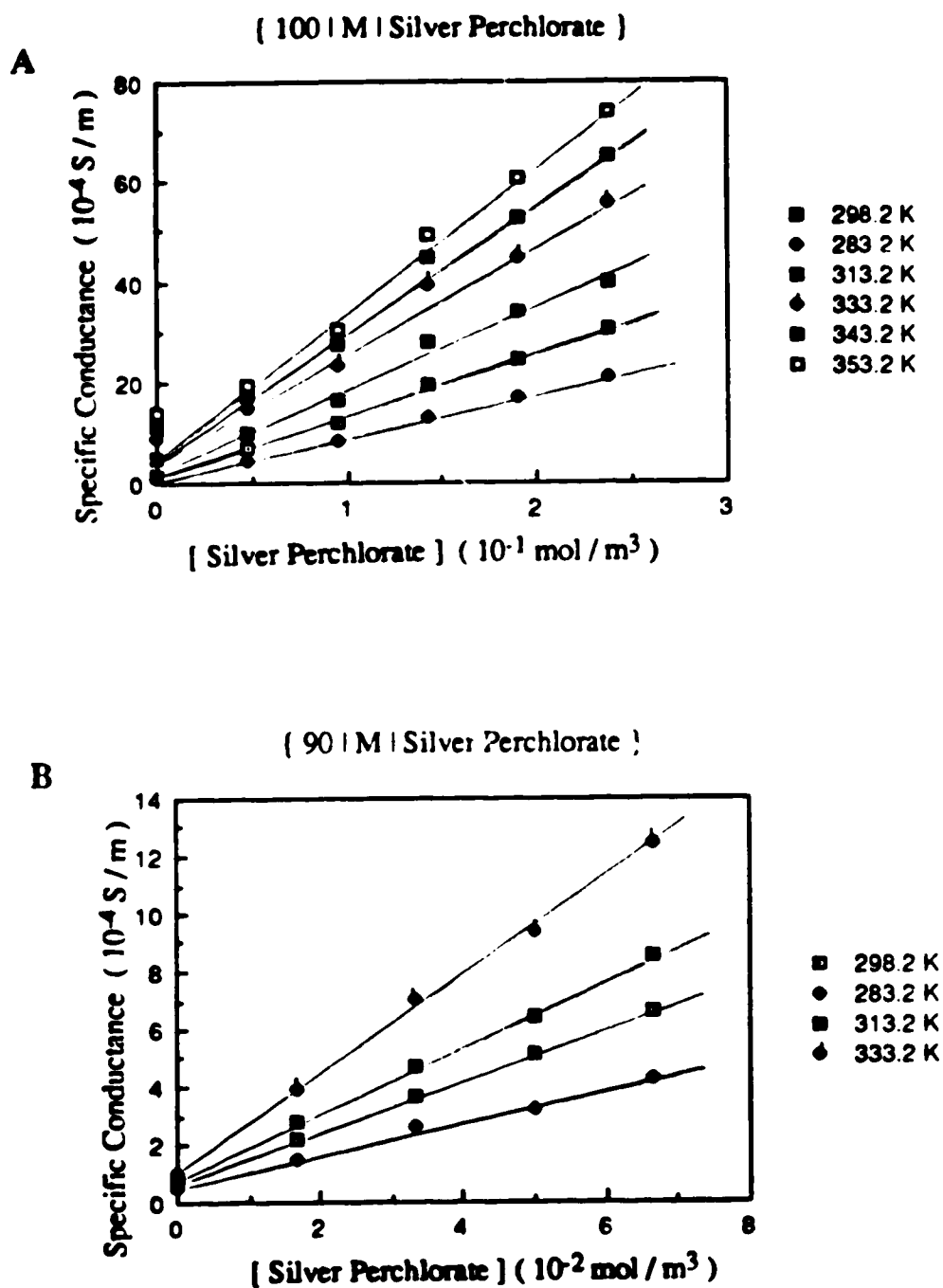


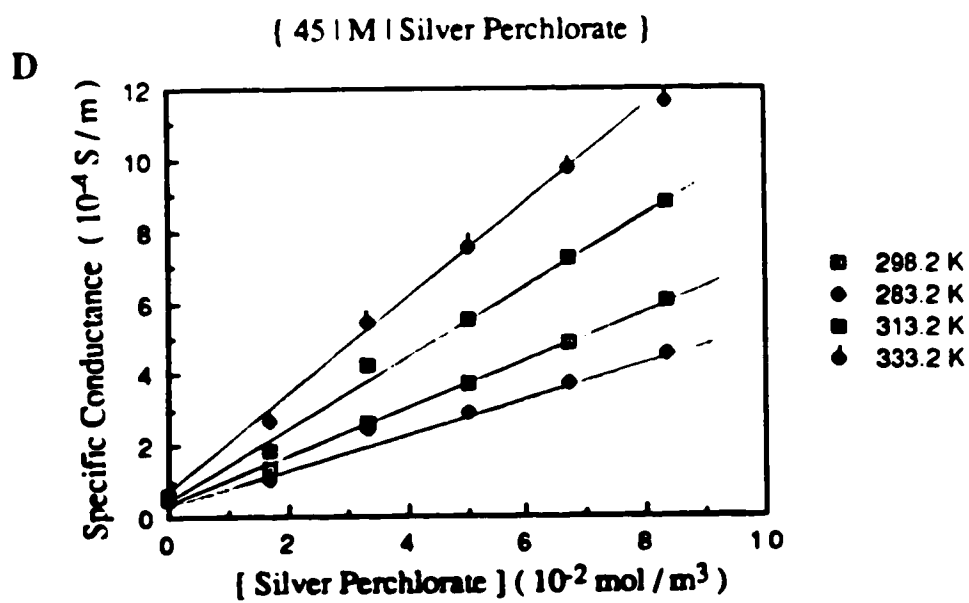
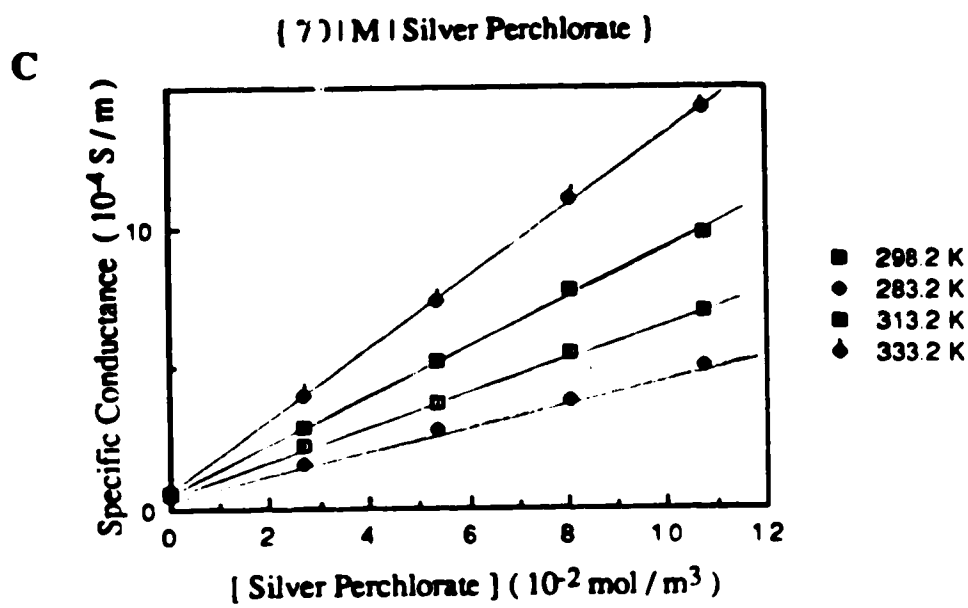
Fig. 3-36 Temperature and concentration dependence of the conductance of lithium nitrate in methanol / water mixtures (A-F)

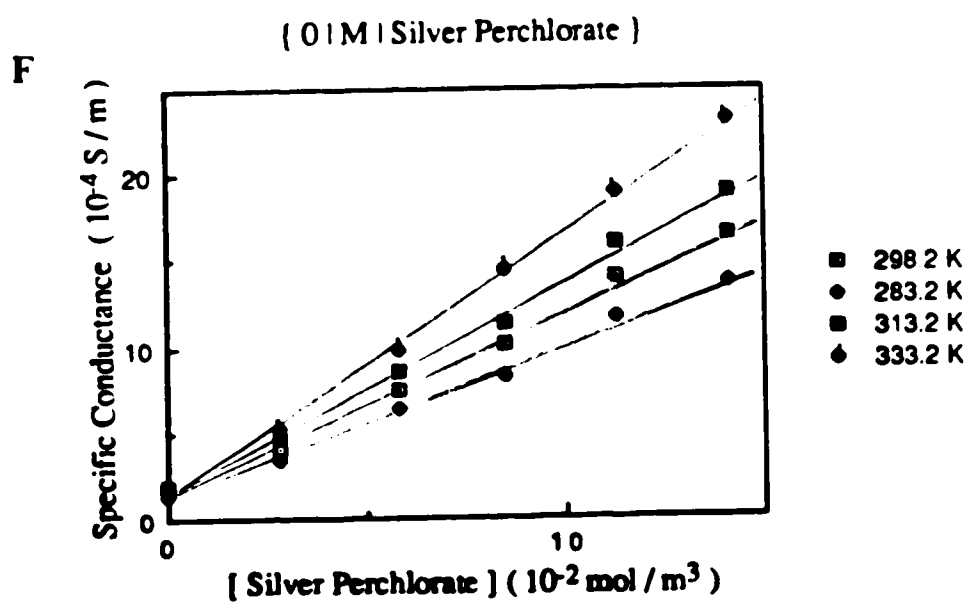
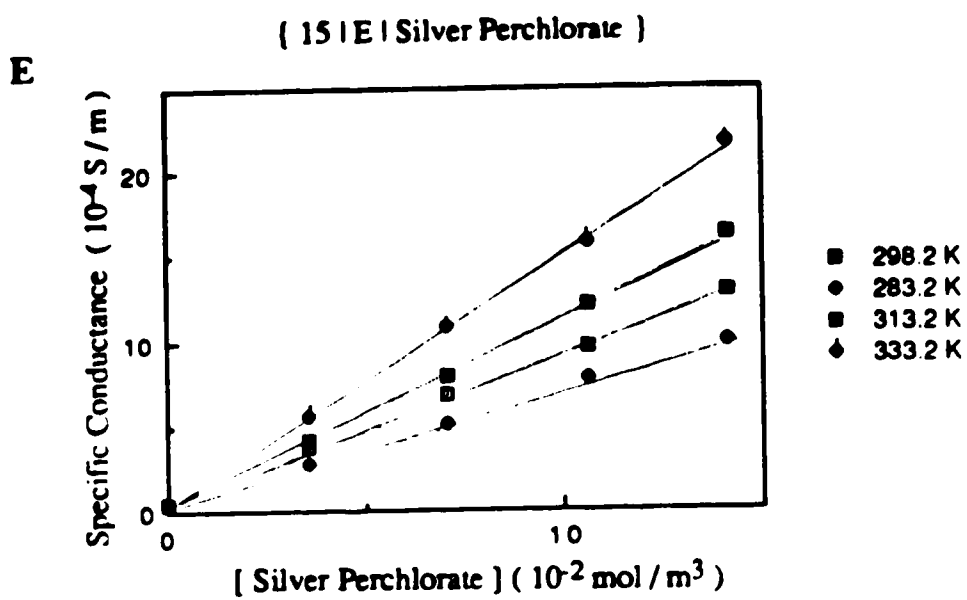


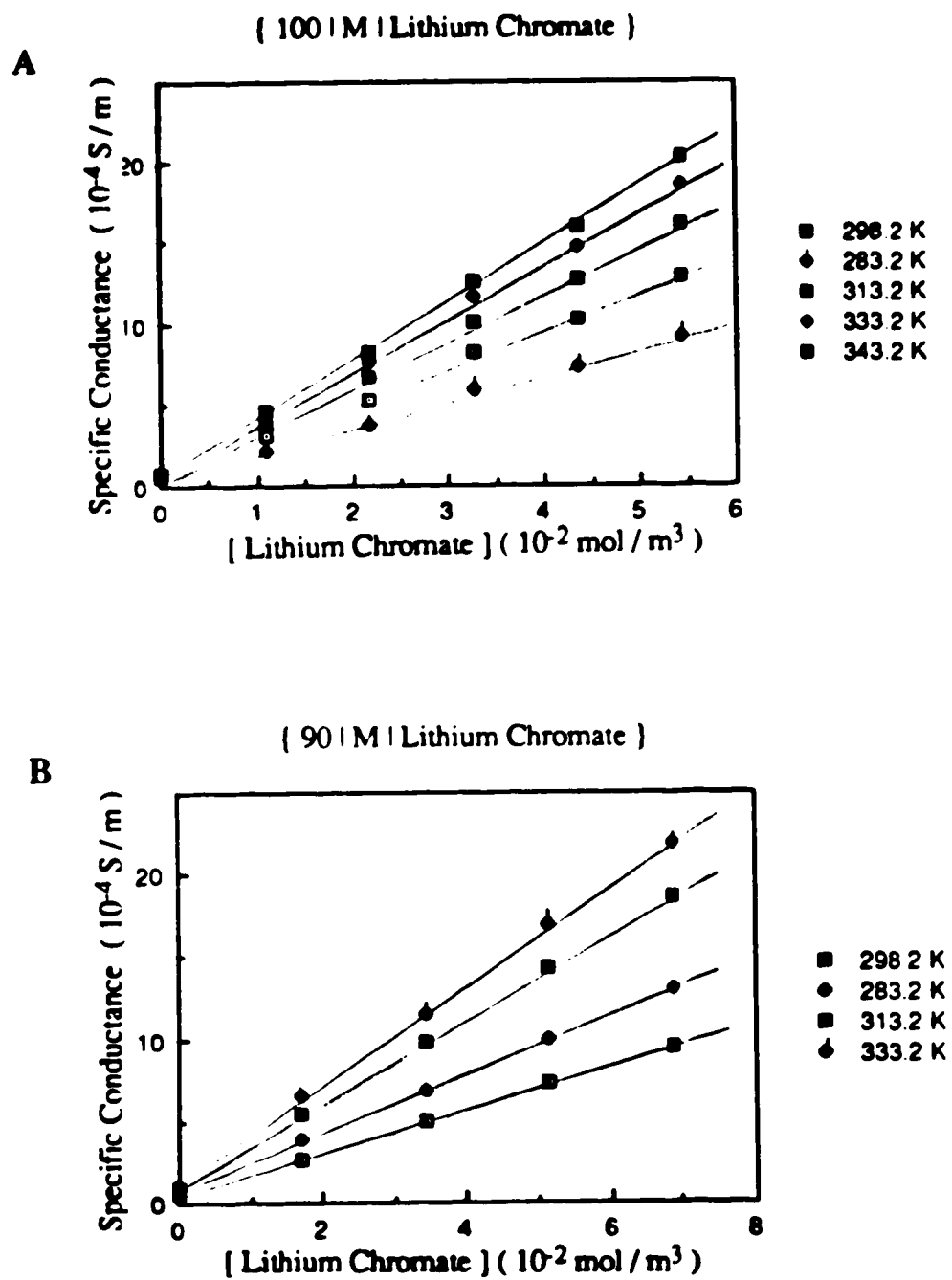




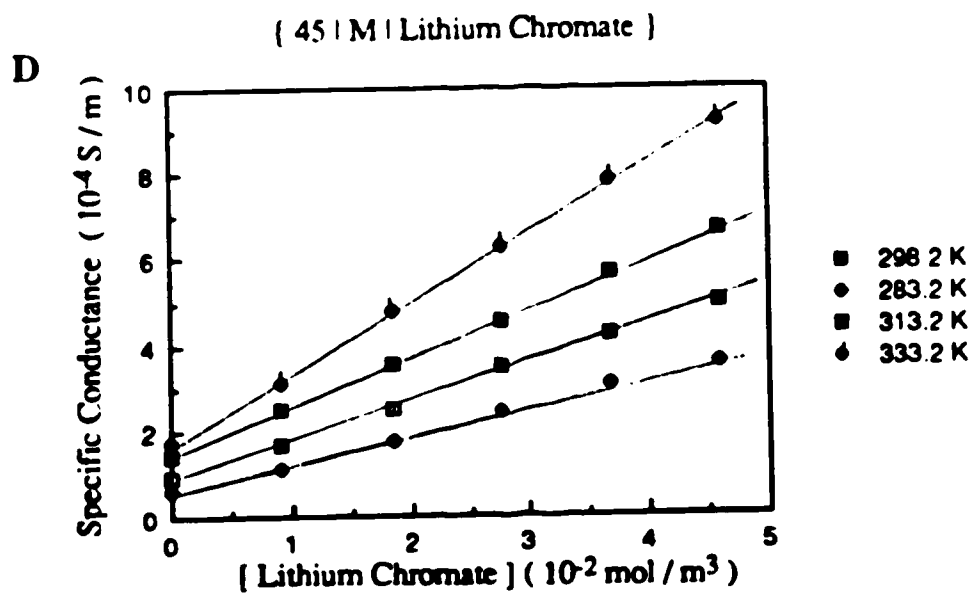
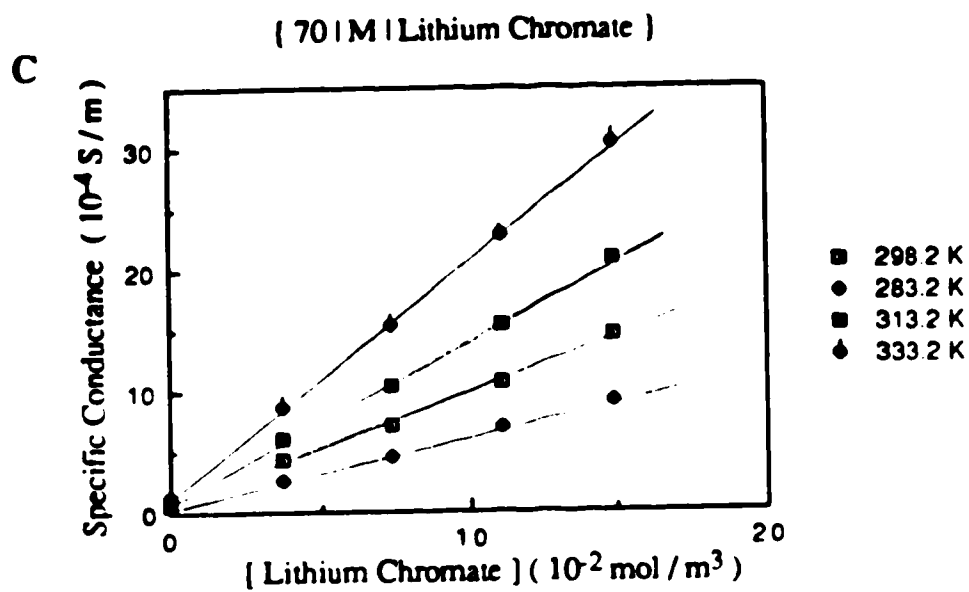
**Fig. 3-27** Temperature and concentration dependence of the conductance of silver perchlorate in methanol / water mixtures (A-F)



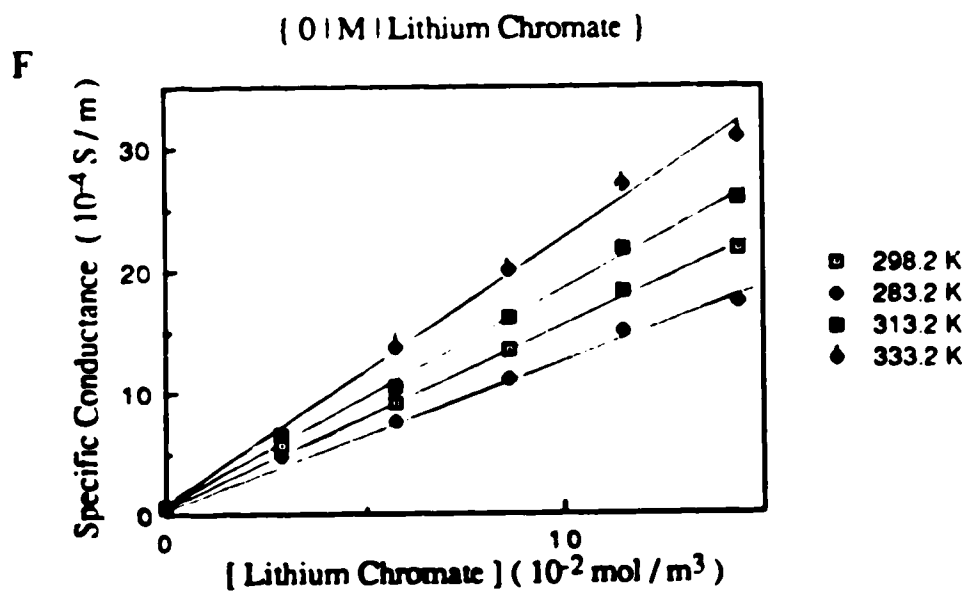
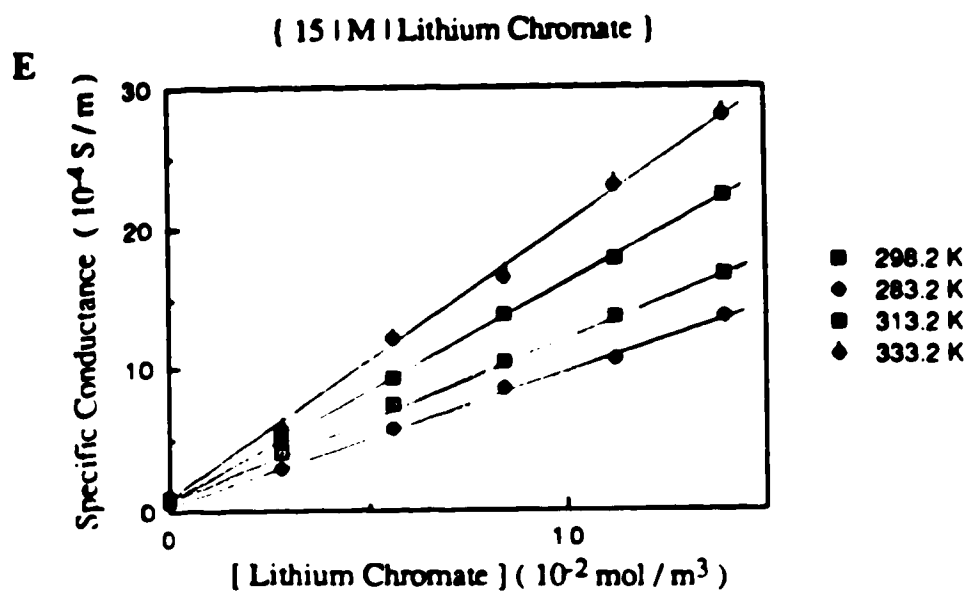




**Fig. 3-38** Temperature and concentration dependence of the conductance of lithium chromate in methanol / water mixtures (A-F)







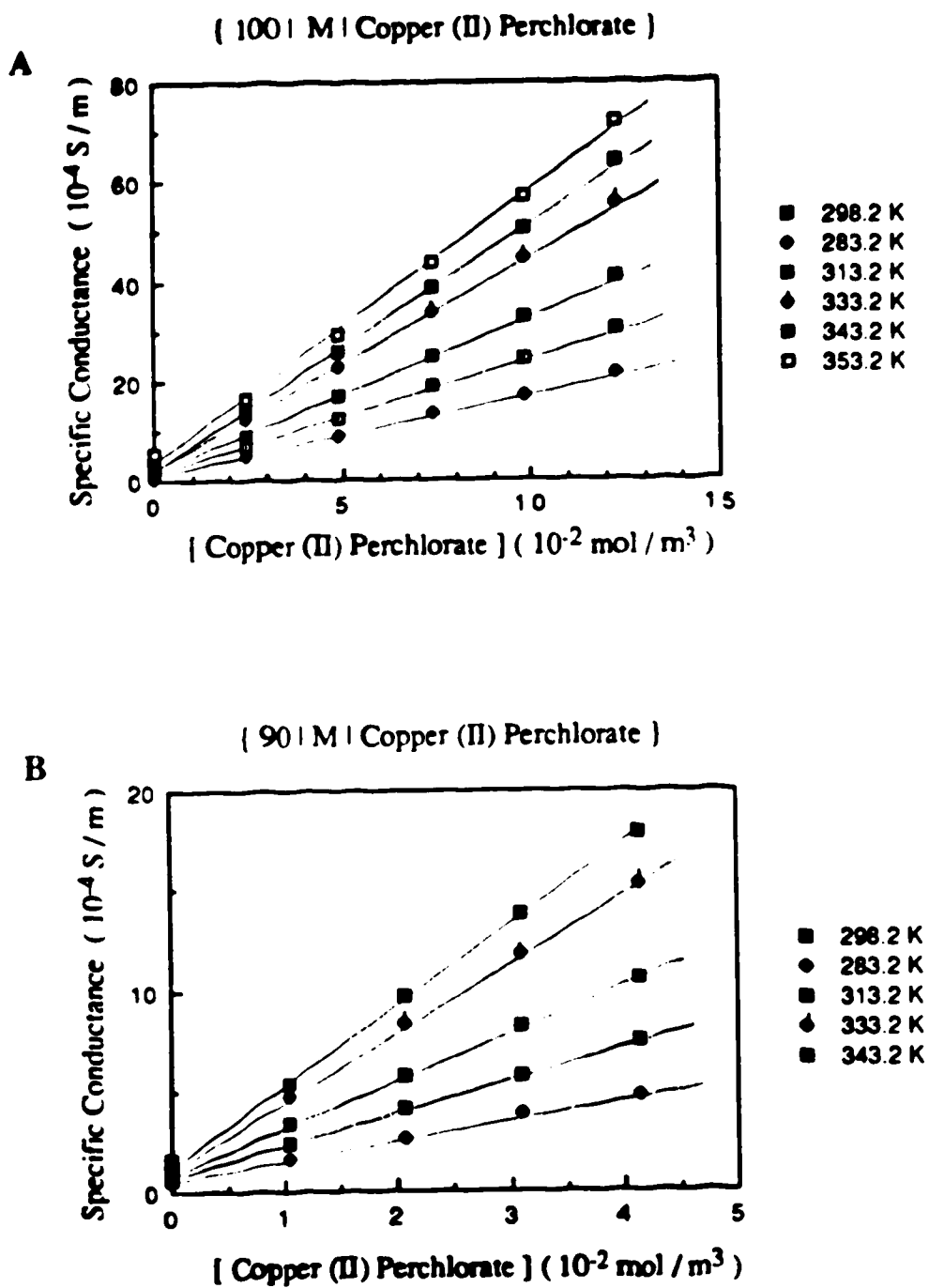
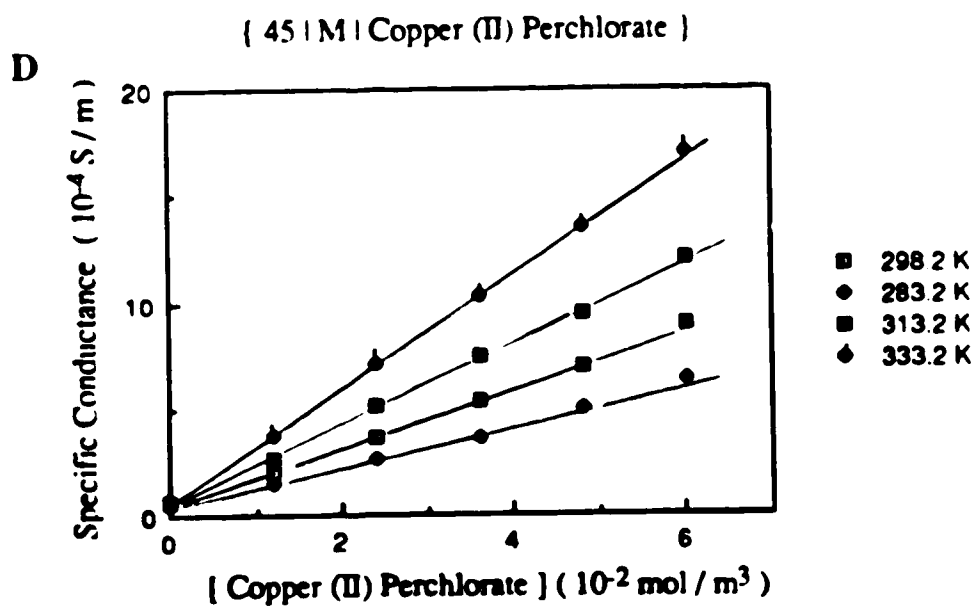
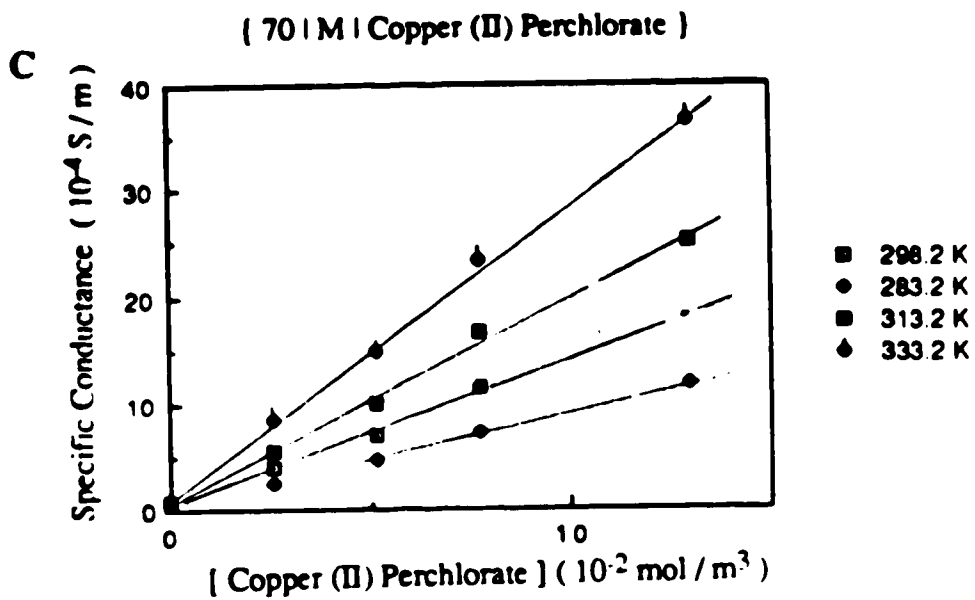
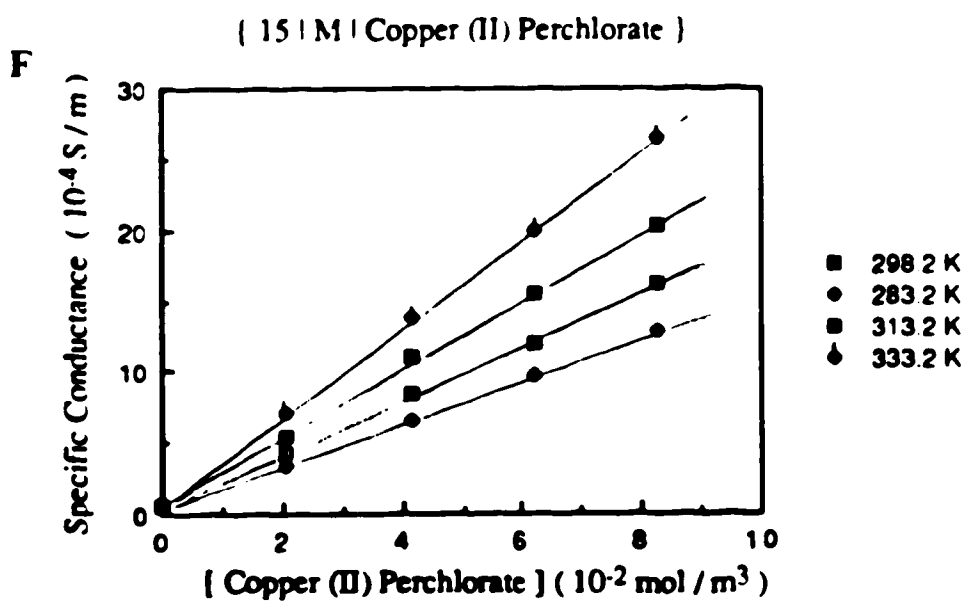
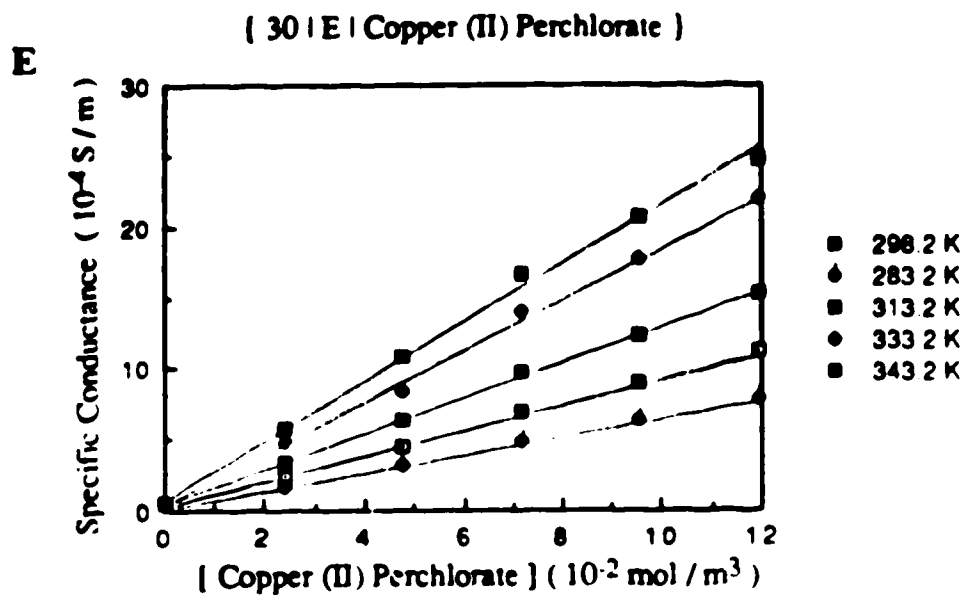
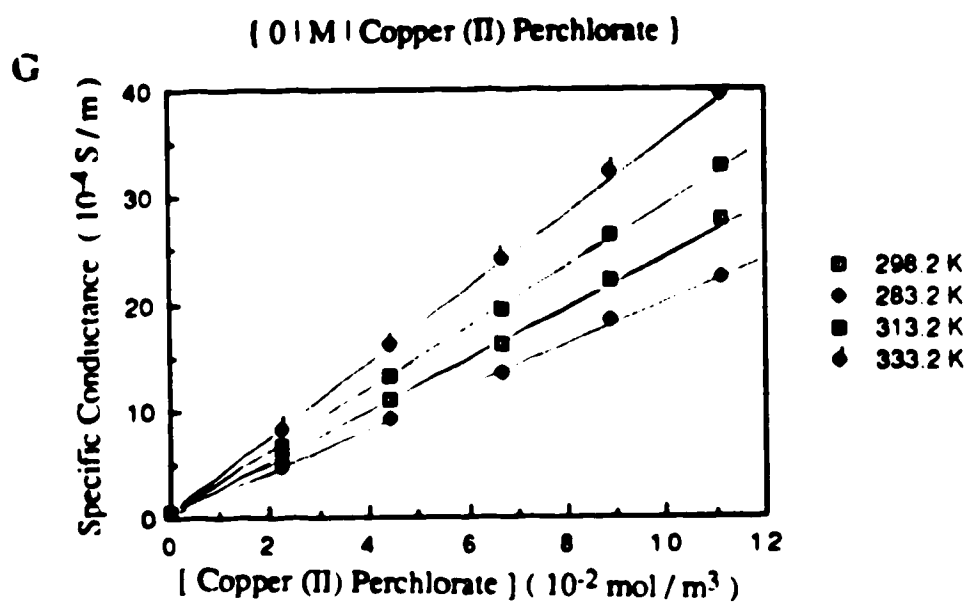


Fig. 3-39 Temperature and concentration dependence of the conductance of copper (II) perchlorate in methanol / water mixtures ( A-F )







## Lithium Nitrate : Methanol/Water

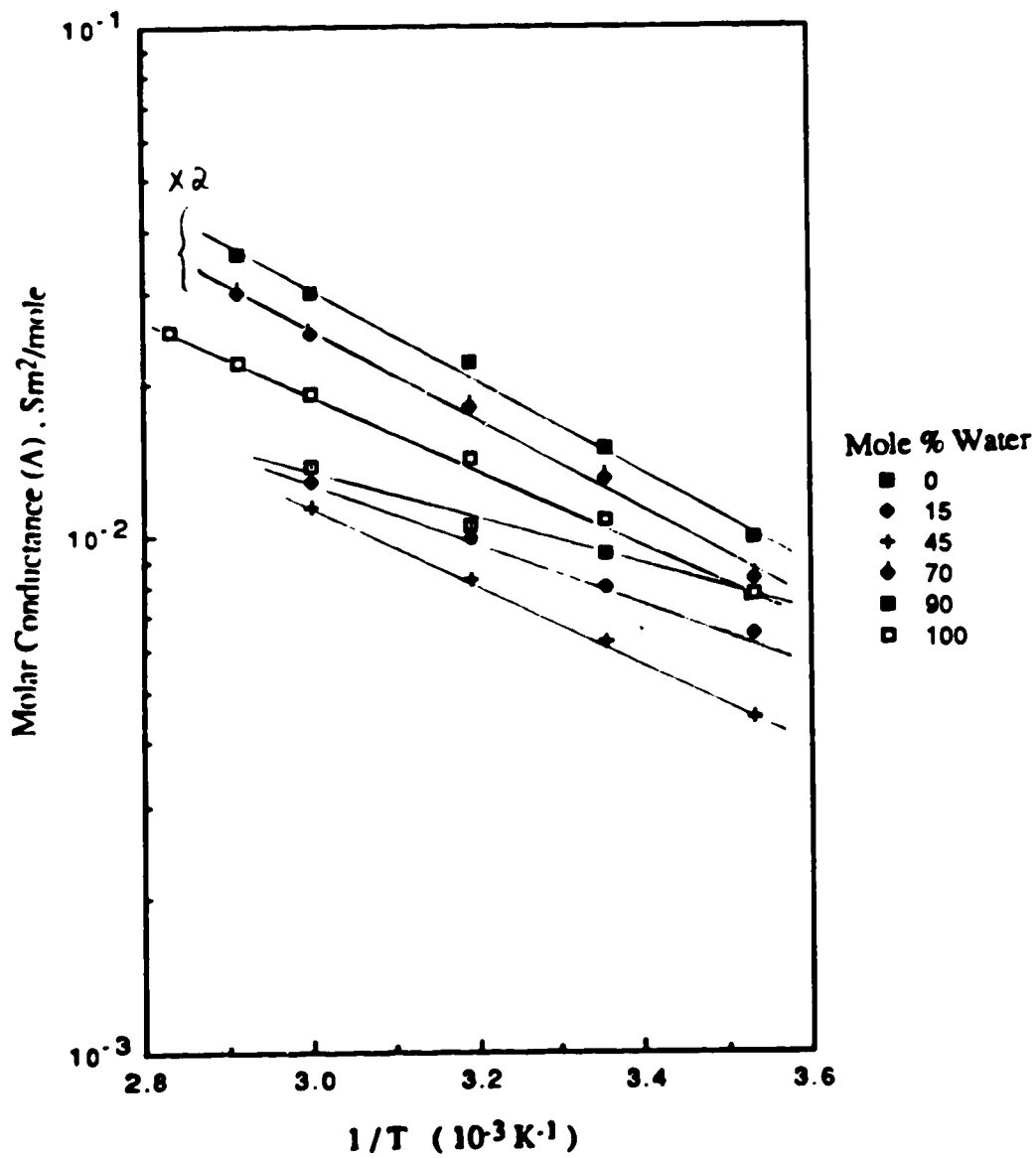


Fig. 3-40 Arrhenius plots of molar conductance of lithium nitrate in methanol / water mixtures

## Silver Perchlorate : Methanol/Water

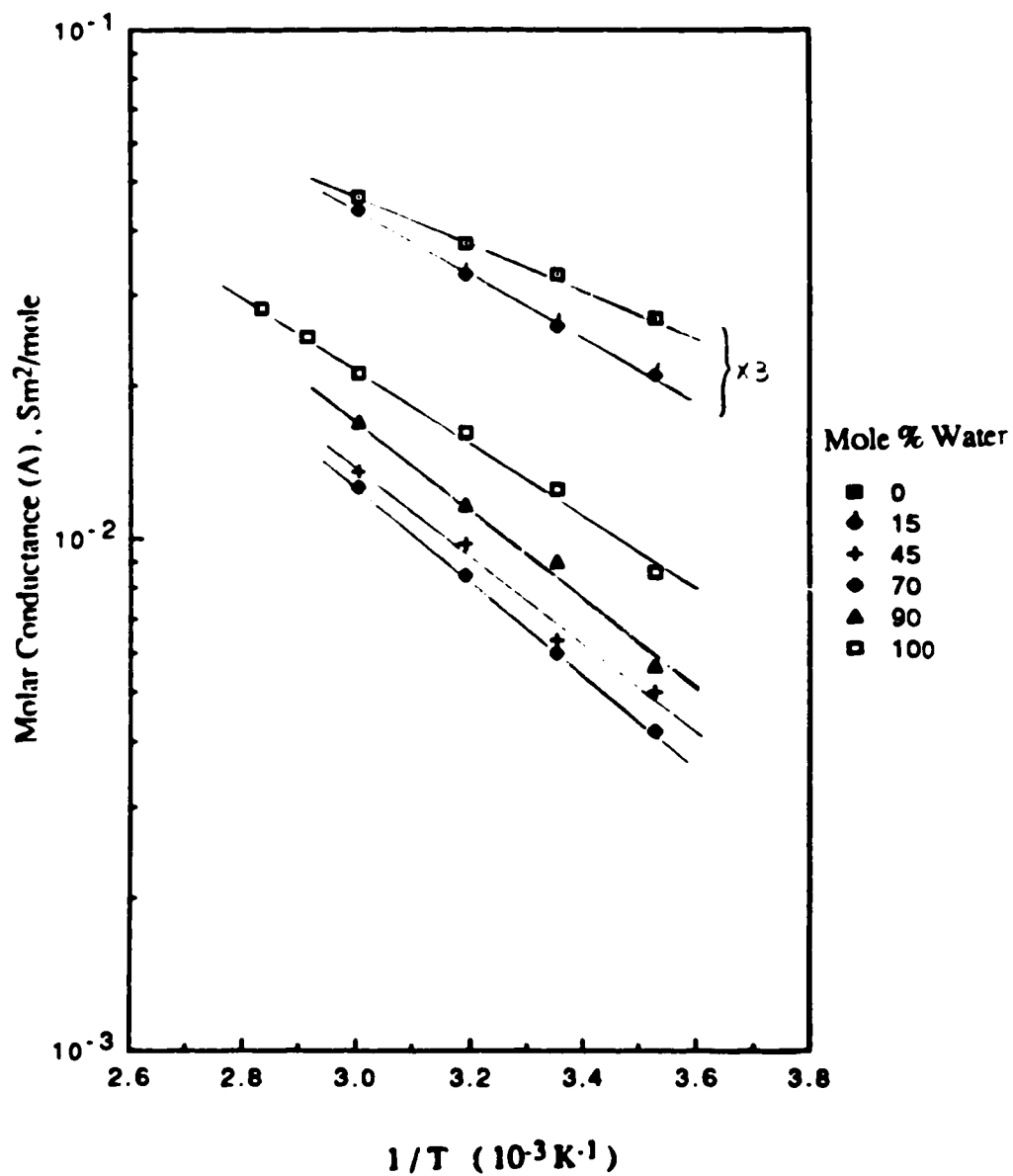


Fig 3-41 Arrhenius plots of molar conductance of silver perchlorate in methanol / water mixtures

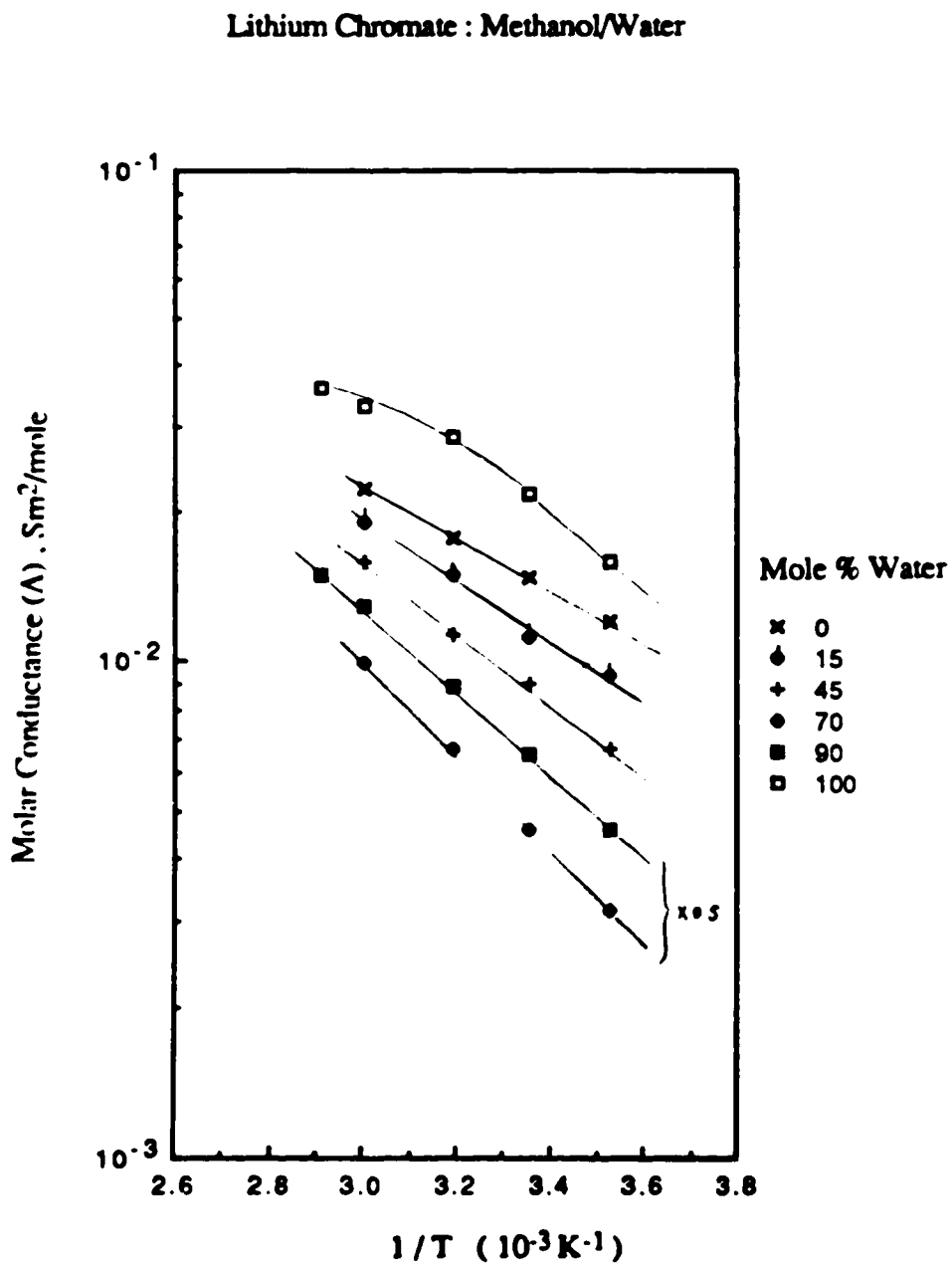


Fig. 3-42 Arrhenius plots of molar conductance of lithium chromate in methanol / water mixtures



## Copper (II) Perchlorate : Methanol/Water

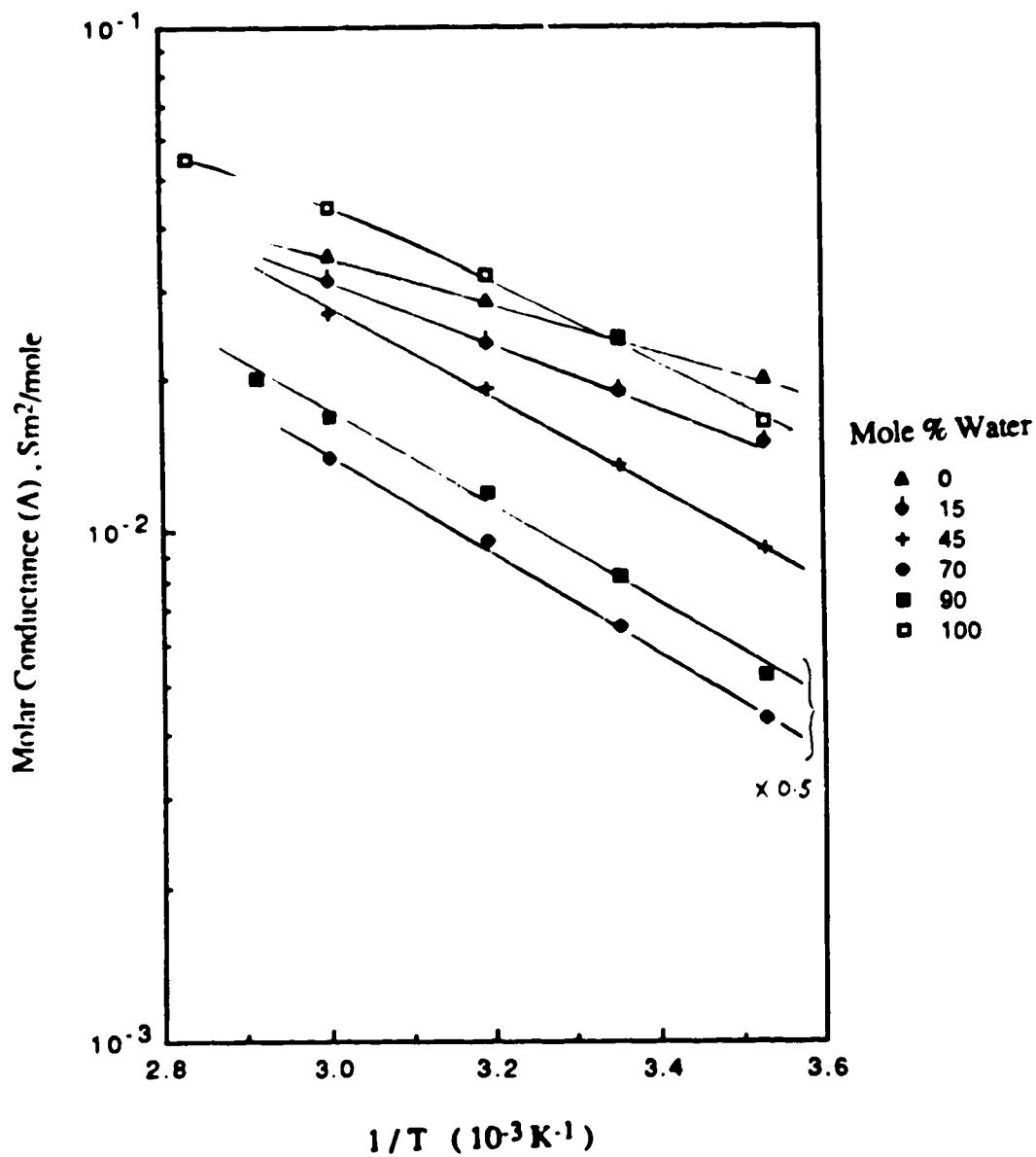


Fig. 3-43 Arrhenius plots of molar conductance of copper (II) perchlorate in methanol / water mixtures

Fig. 3-44 Composition dependence of the activation energy of conductance of some inorganic electrolytes in methanol / water mixtures

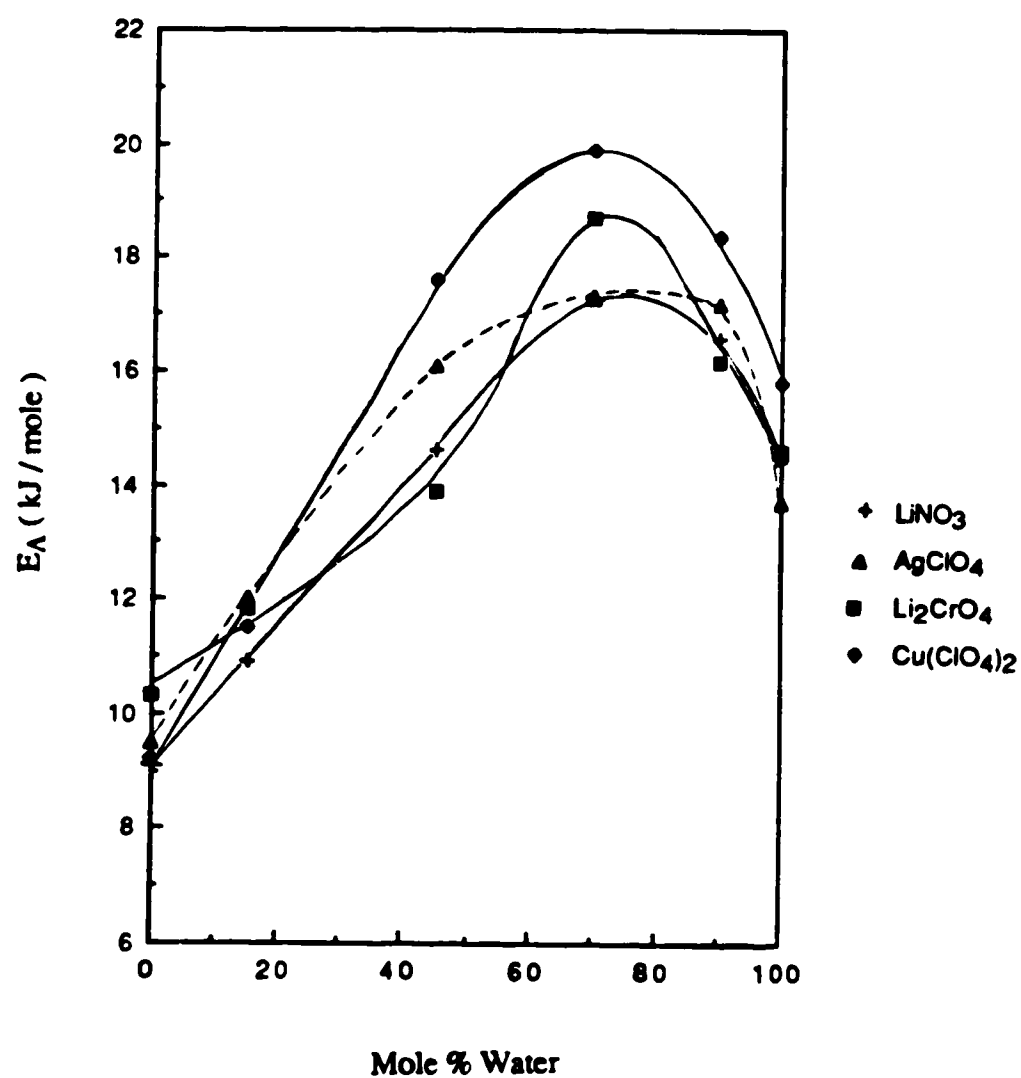


Table 3-33 Temperature and composition dependence of molar conductances  $\kappa$  ( $\Lambda$ )  
inorganic electrolytes in methanol / water mixtures

$\chi_w$	0.00	0.15	0.45	0.70	0.90	1.00
<u>Lithium Nitrate</u>						
Temp. (K)						
283.2	7.65	6.43	4.44	4.14	5.05	7.69
298.2	9.30	8.00	6.25	6.25	7.69	10.8
313.2	10.6	10.0	8.23	8.82	10.8	14.3
333.2	13.7	12.9	11.5	12.5	15.2	19.2
343.2				14.8	17.9	21.9
353.2						25.4
$E_A$ , kJ / mole	9.4	10.9	14.6	17.3	16.6	14.5
<u>Silver Perchlorate</u>						
Temp. (K)						
283.2	9.13	6.84	5.00	4.21	5.62	8.57
298.2	11.1	8.75	6.36	6.00	9.00	12.5
313.2	12.7	10.9	9.76	8.53	11.6	16.1
333.2	15.7	14.8	13.6	12.6	17.0	21.1
343.2						25.0
353.2						28.3
$E_A$ , kJ / mole	9.5	12.02	16.1	17.3	17.2	13.7
<u>Lithium Chromate</u>						
Temp. (K)						
283.2	12.0	9.33	6.66	6.27	9.09	16.0
298.2	14.8	11.2	9.05	9.16	13.0	22.8
313.2	17.9	15.0	11.3	13.3	17.8	28.6
333.2	22.3	19.2	16.0	19.8	25.9	33.1
343.2					30.0	36.0
$E_A$ , kJ / mole	10.3	11.8	13.9	18.7	16.2	14.6
<u>Copper (II) Perchlorate</u>						
Temp. (K)						
283.2	20.0	15.0	9.28	8.57	10.4	16.6
298.2	24.2	18.9	13.6	13.0	16.3	24.3
313.2	28.8	23.7	19.2	19.1	23.1	32.3
333.2	35.3	31.4	27.0	27.5	34.0	44.1
343.2					40.0	50.0
353.2						55.0
$E_A$ , kJ / mole	9.2	11.5	17.6	19.9	18.4	15.8

<sup>a</sup> molar conductance in  $10^{-3}\text{Sm}^2/\text{mole}$

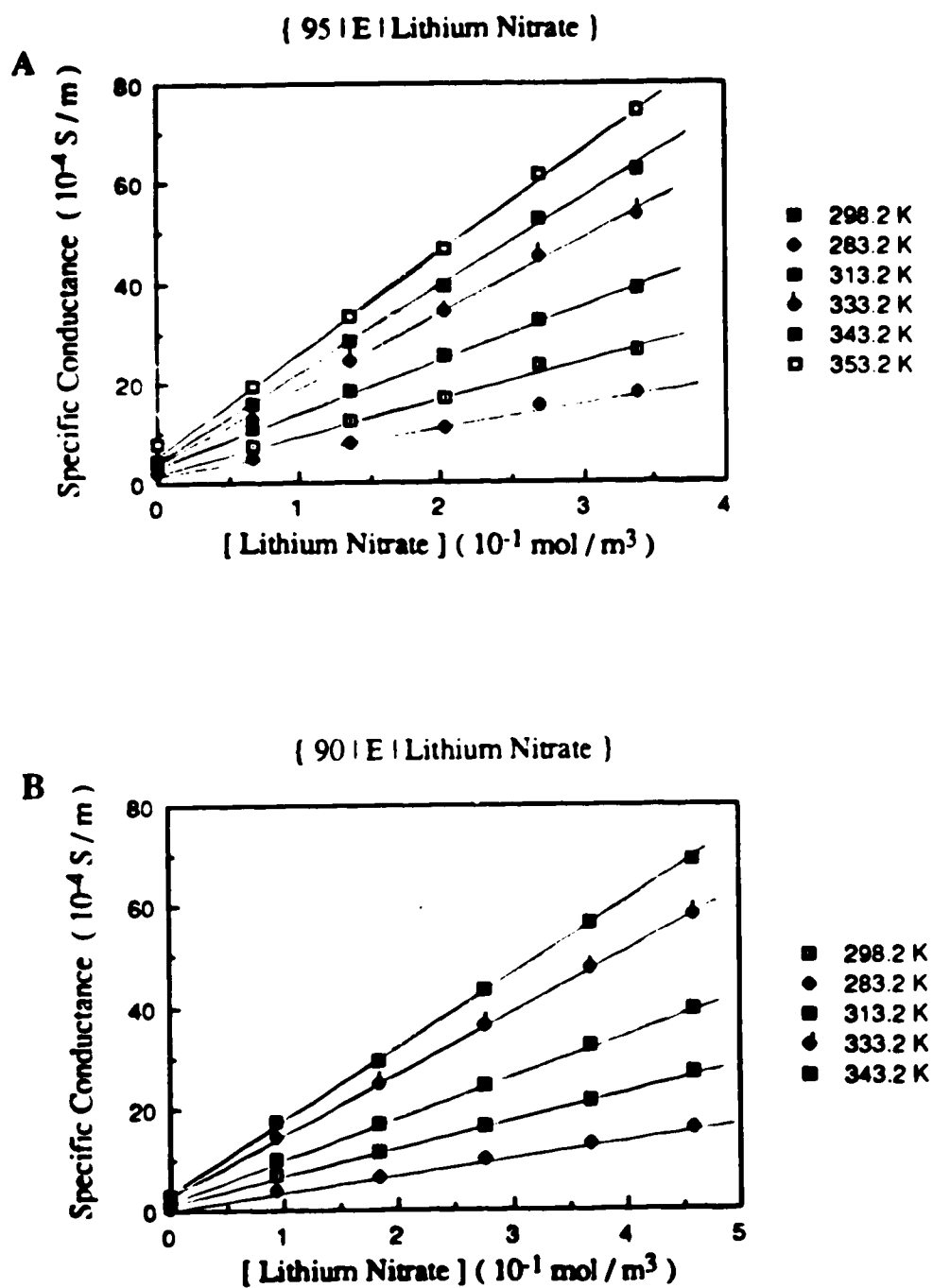
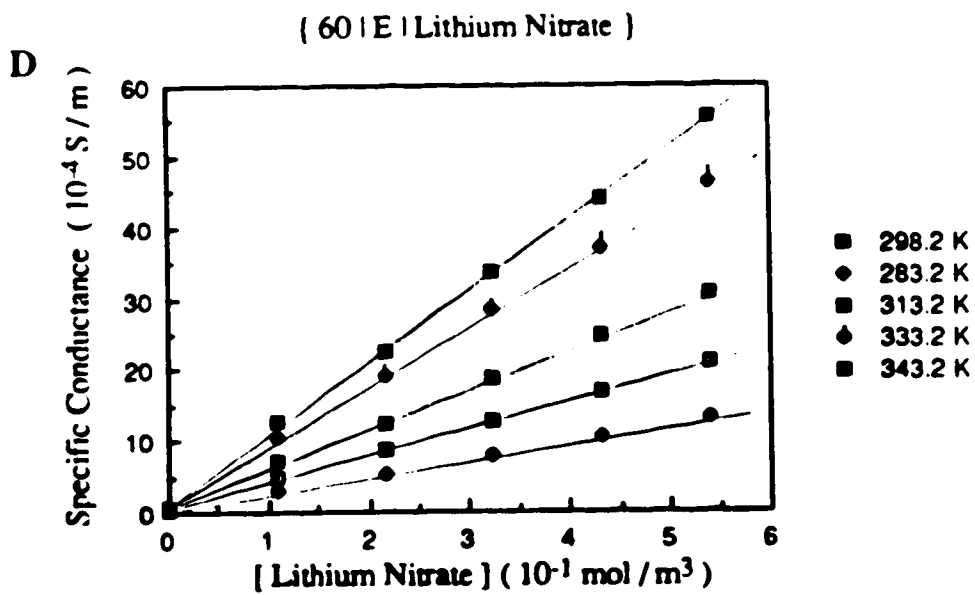
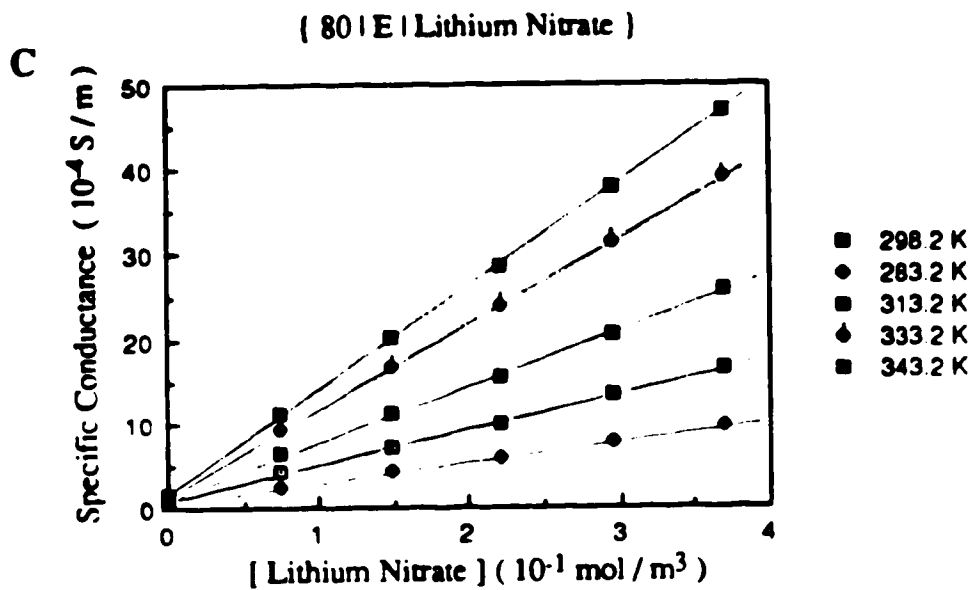
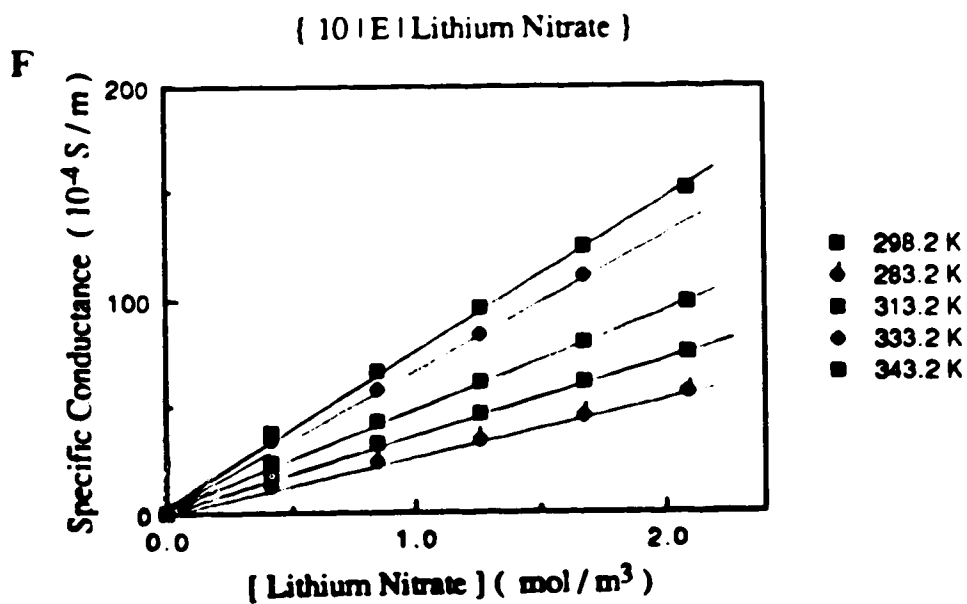
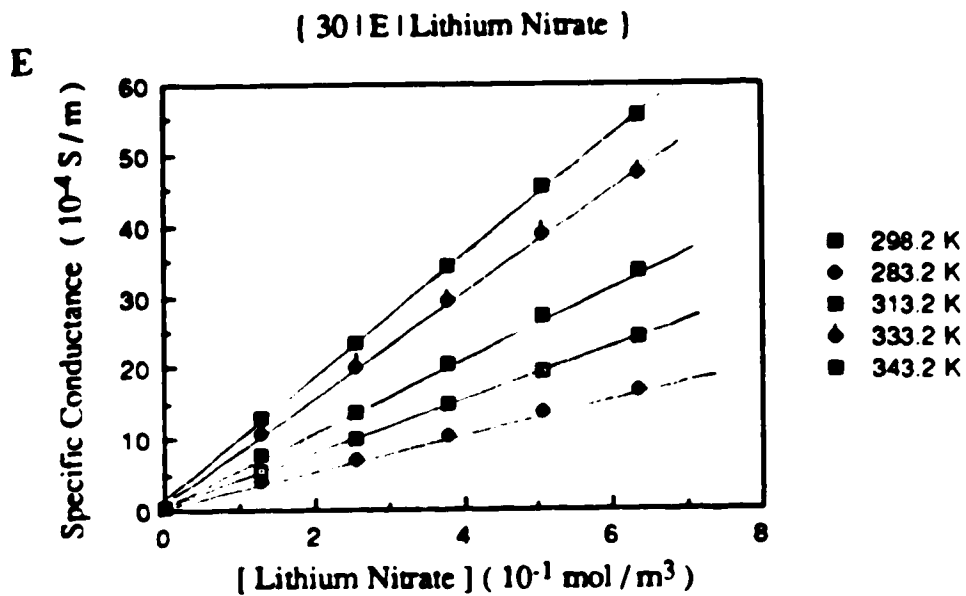
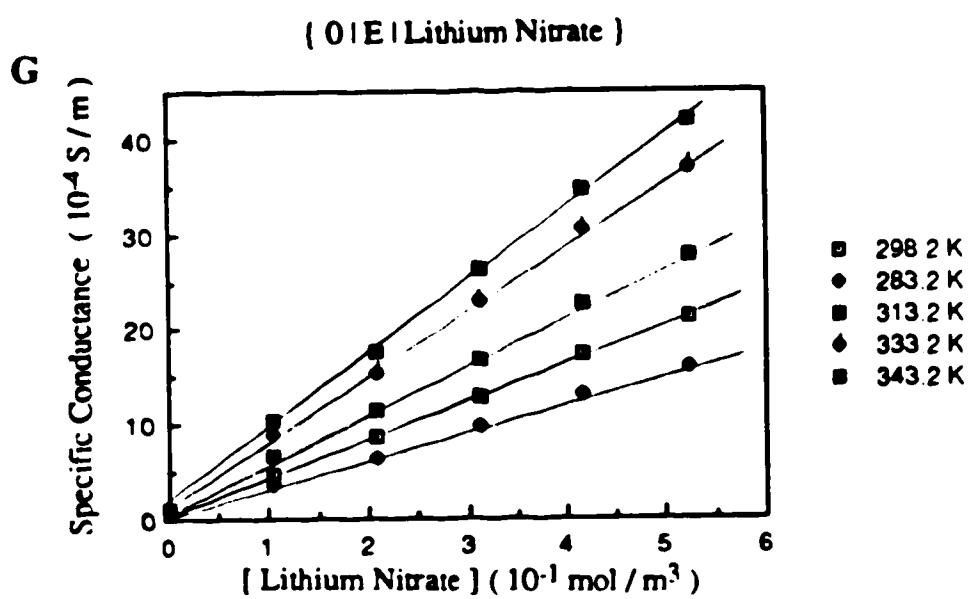
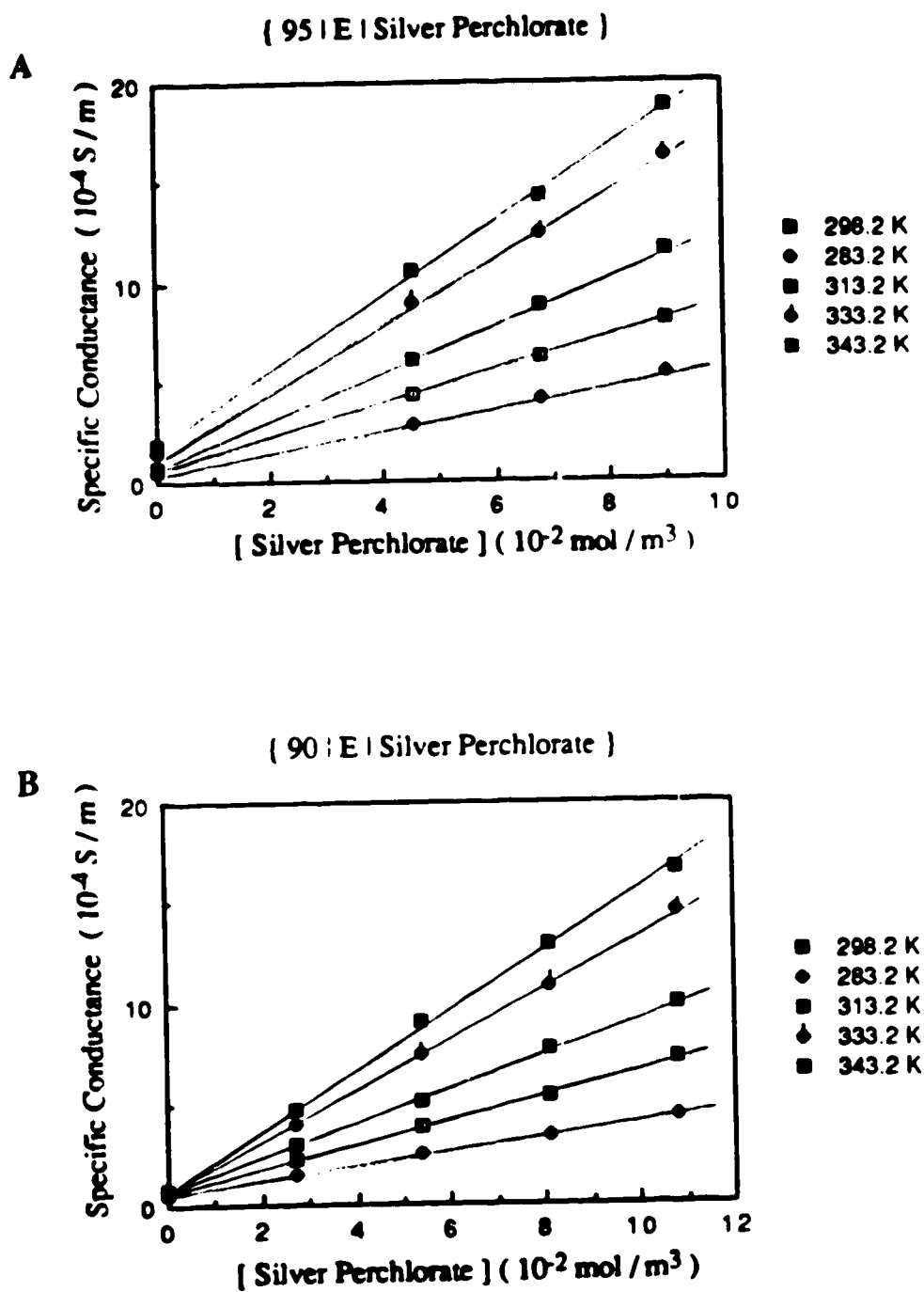


Fig.3-45. Temperature and concentration dependence of the conductance of lithium nitrate in ethanol / water mixtures (A-G)



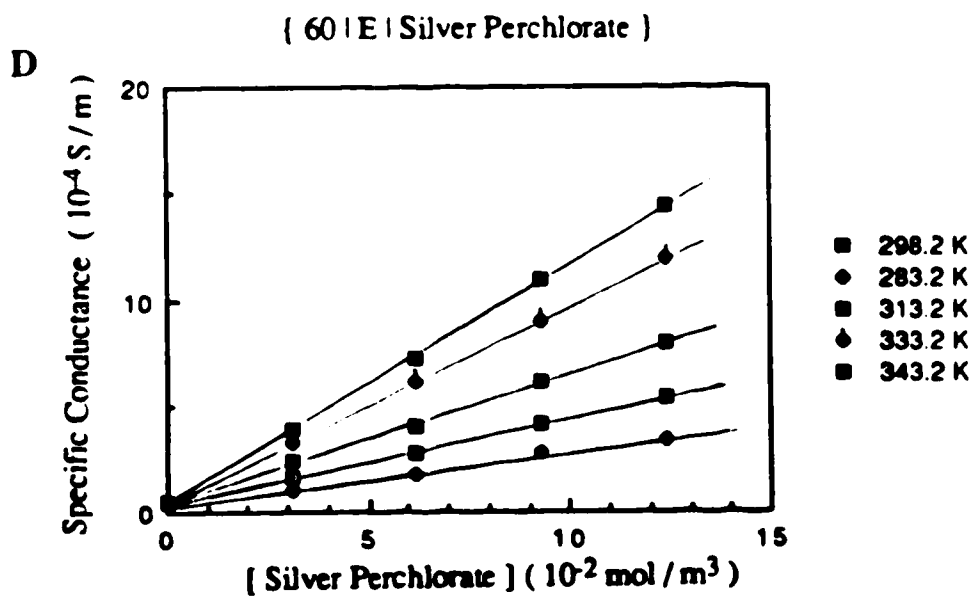
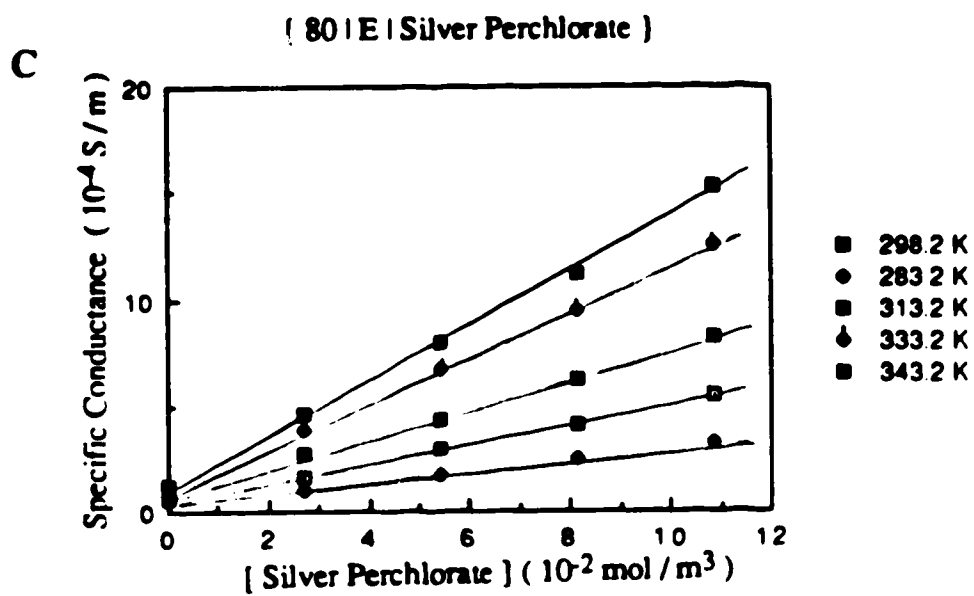


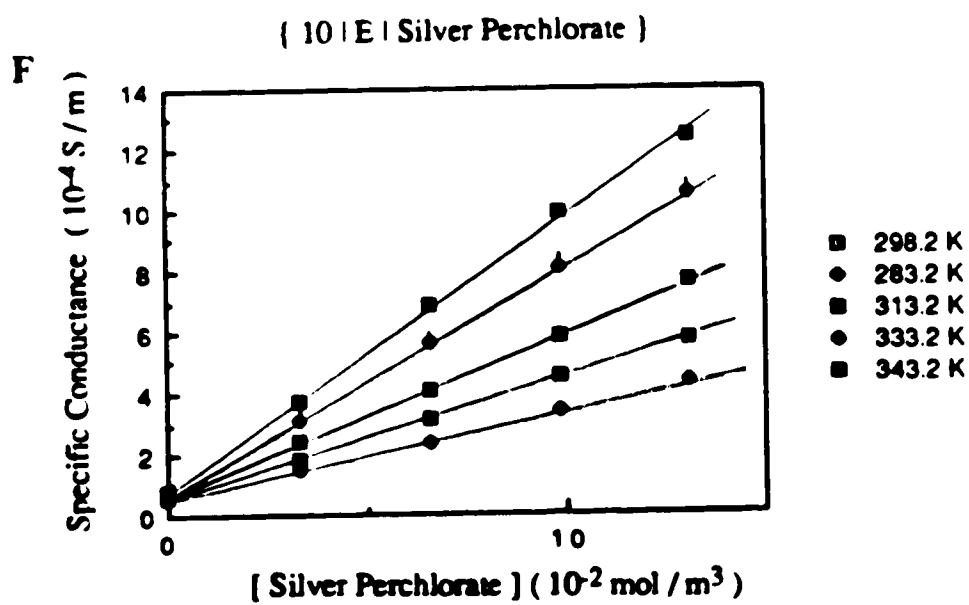
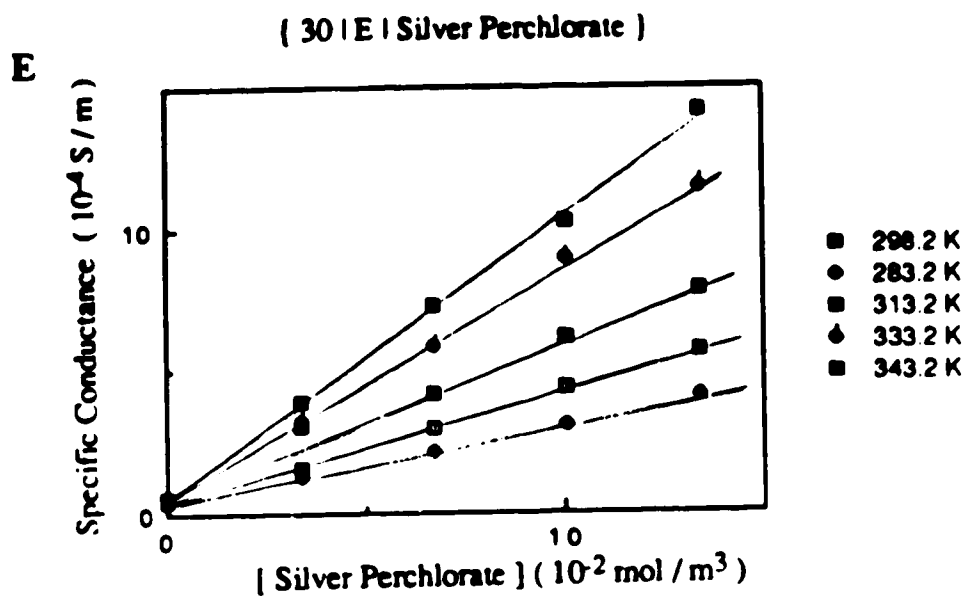


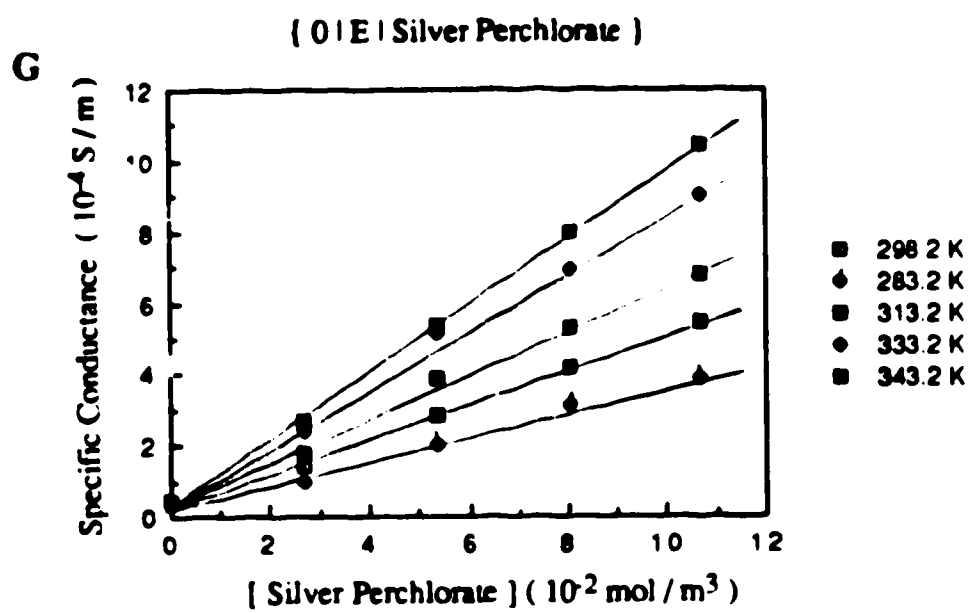


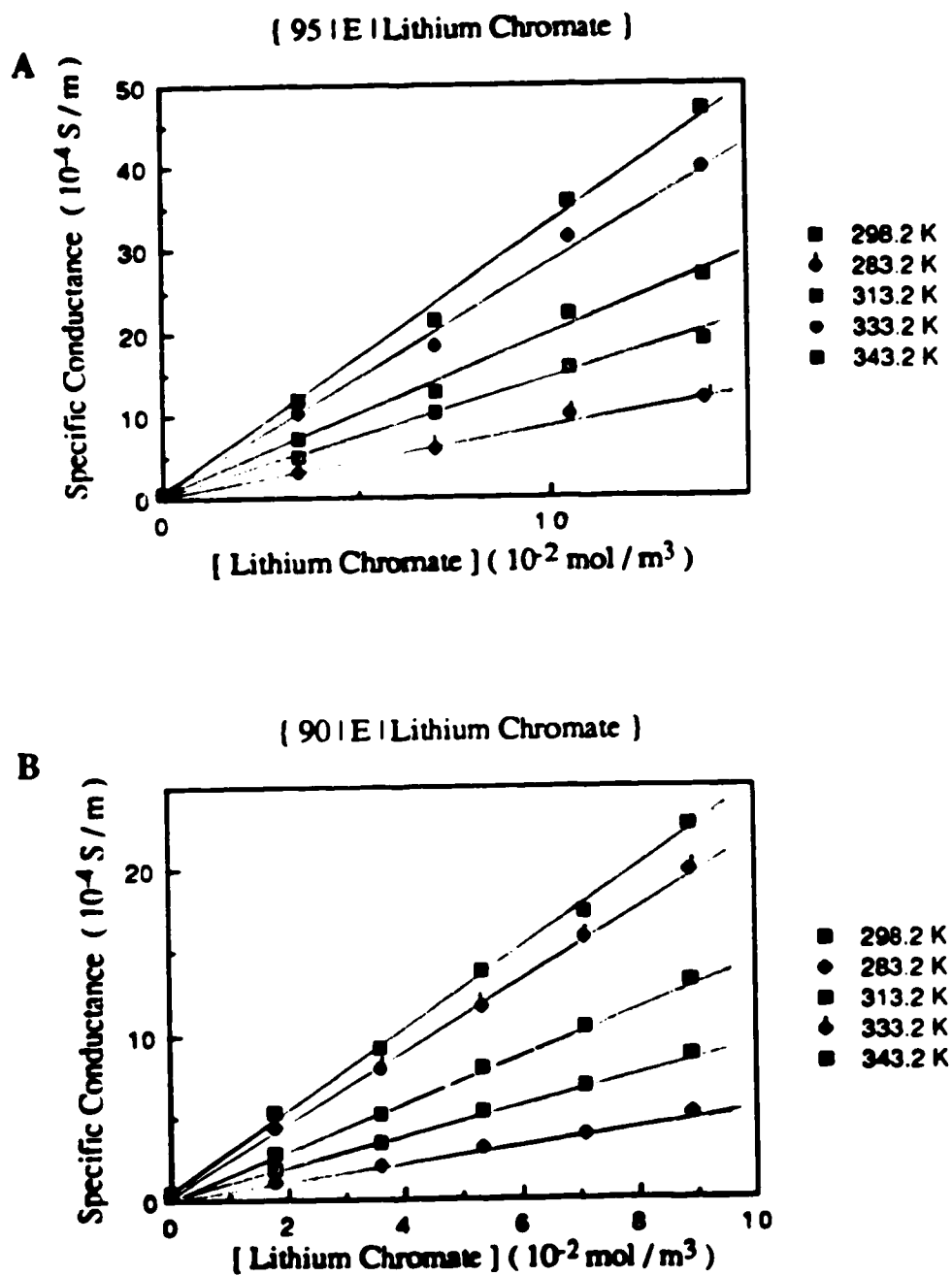
**Fig.3-46** Temperature and concentration dependence of the conductance of silver perchlorate in ethanol / water mixtures (A-G)



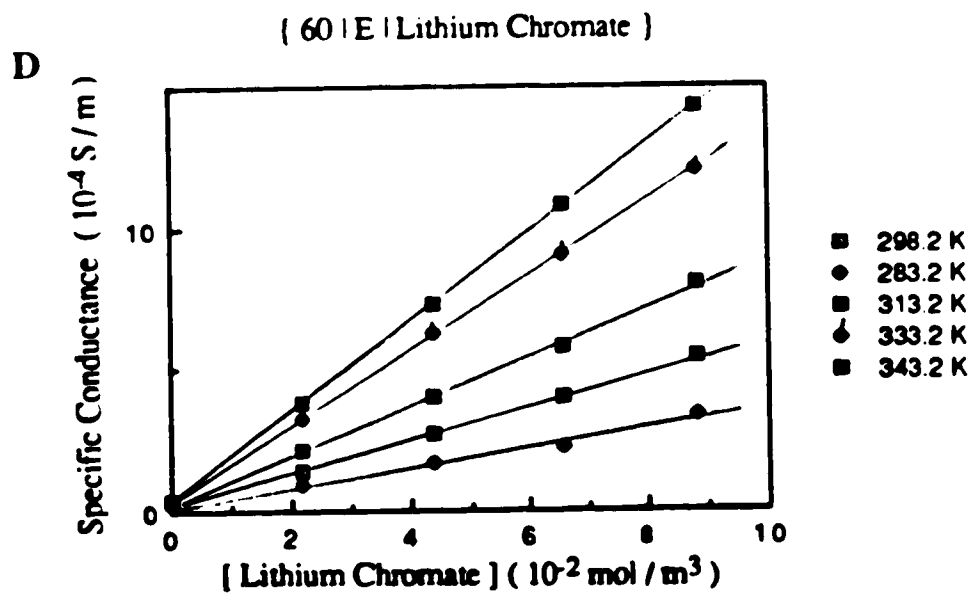
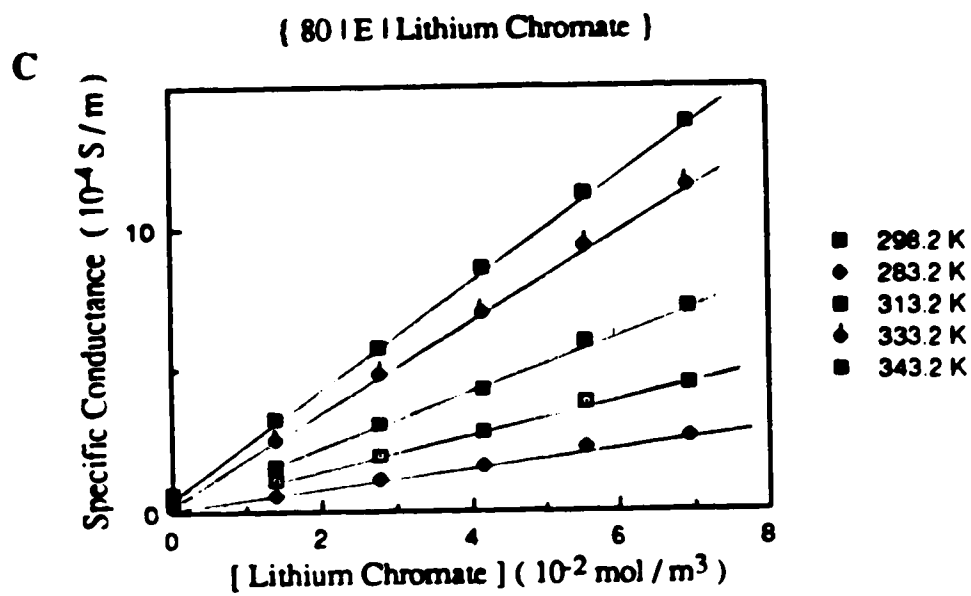


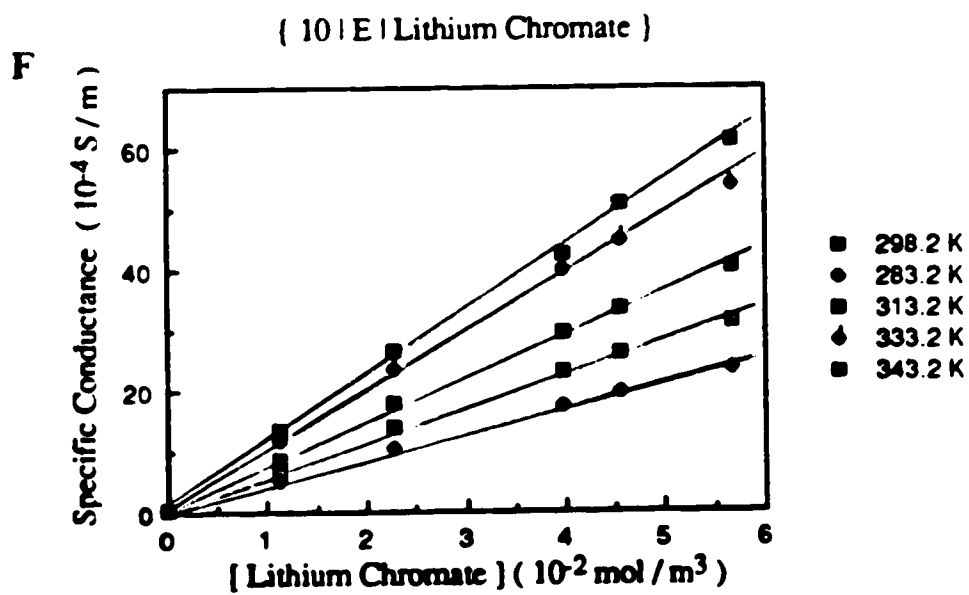
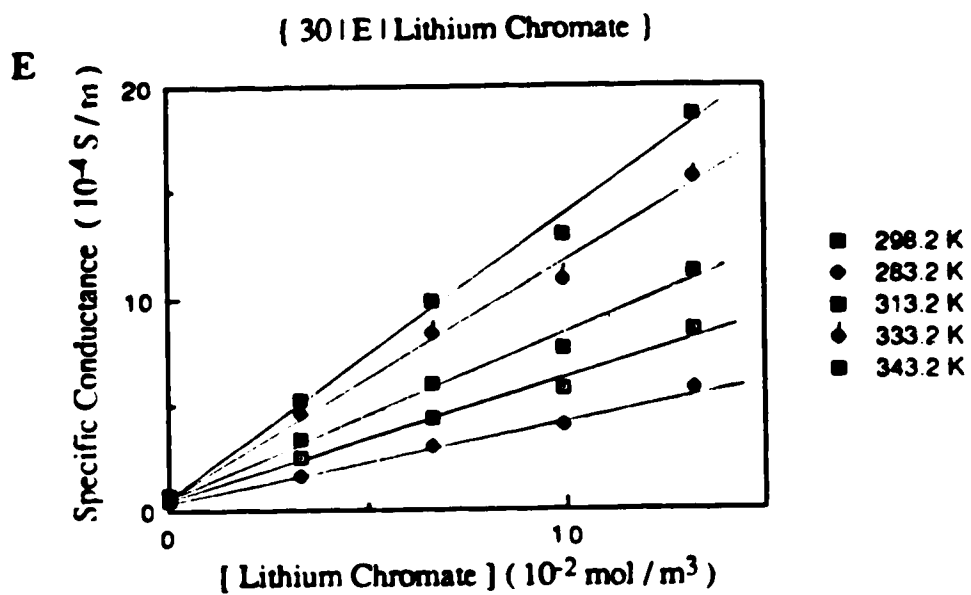






**Fig.3-47** Temperature and concentration dependence of the conductance of lithium chromate in ethanol / water mixtures (A-G)





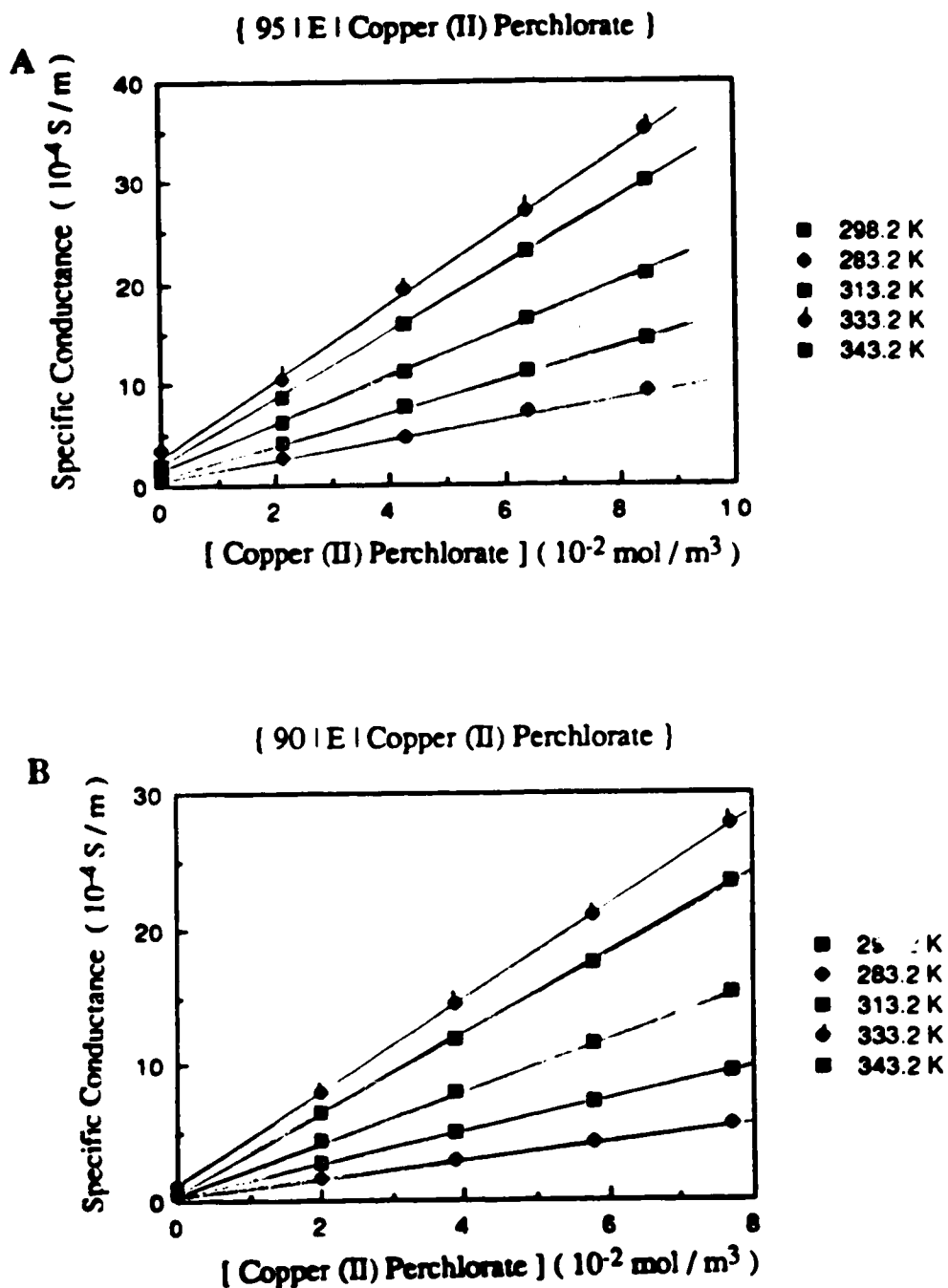
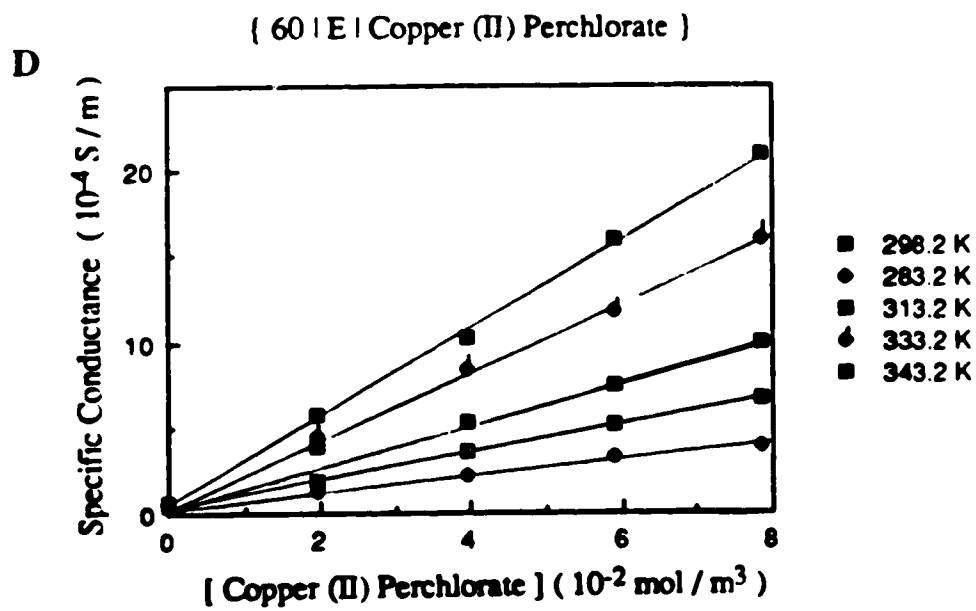
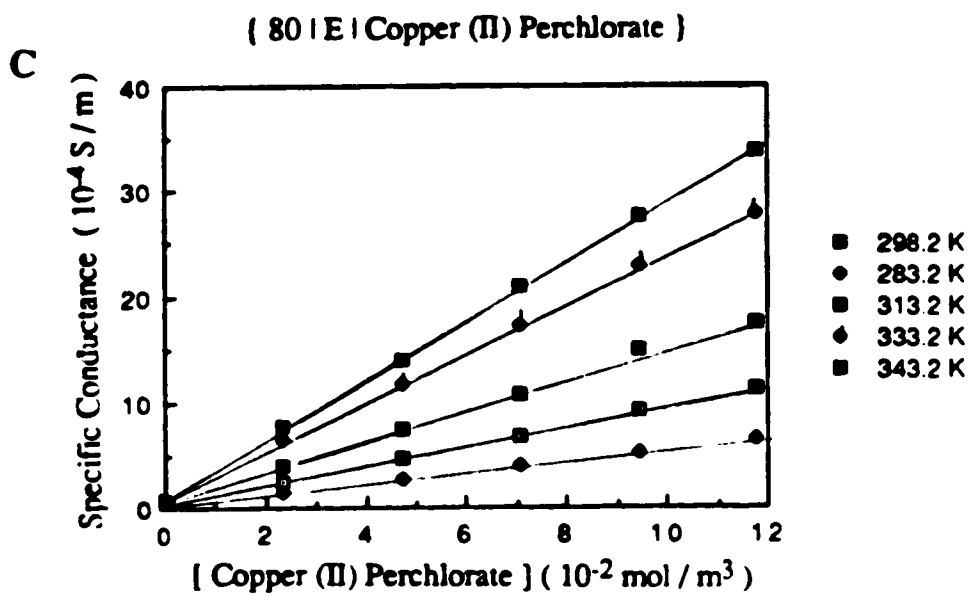
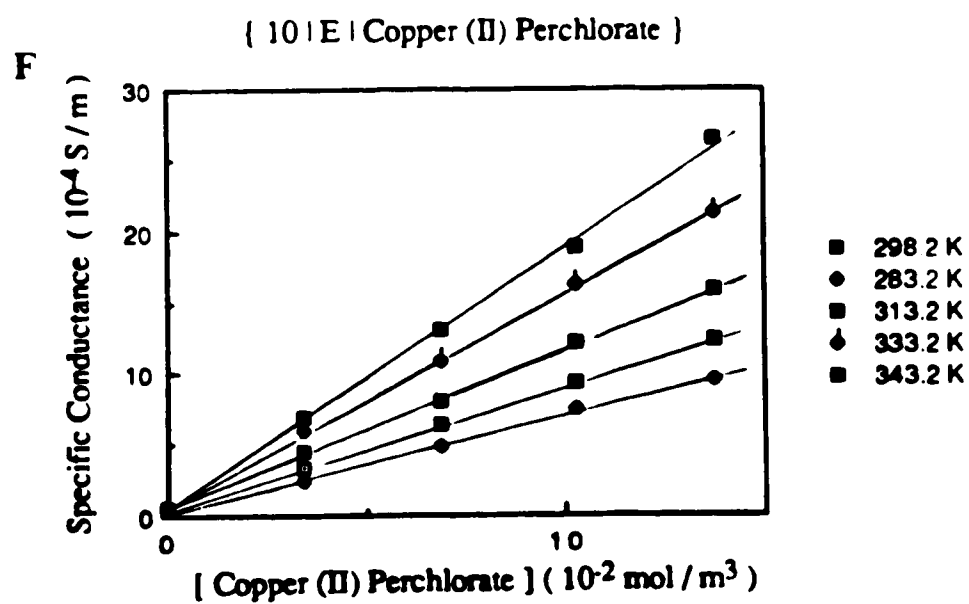
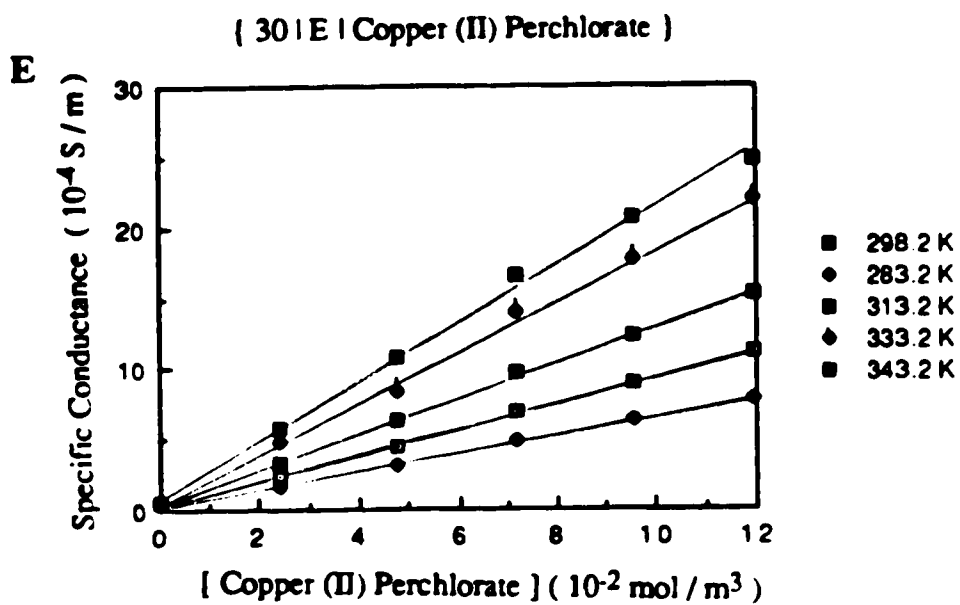
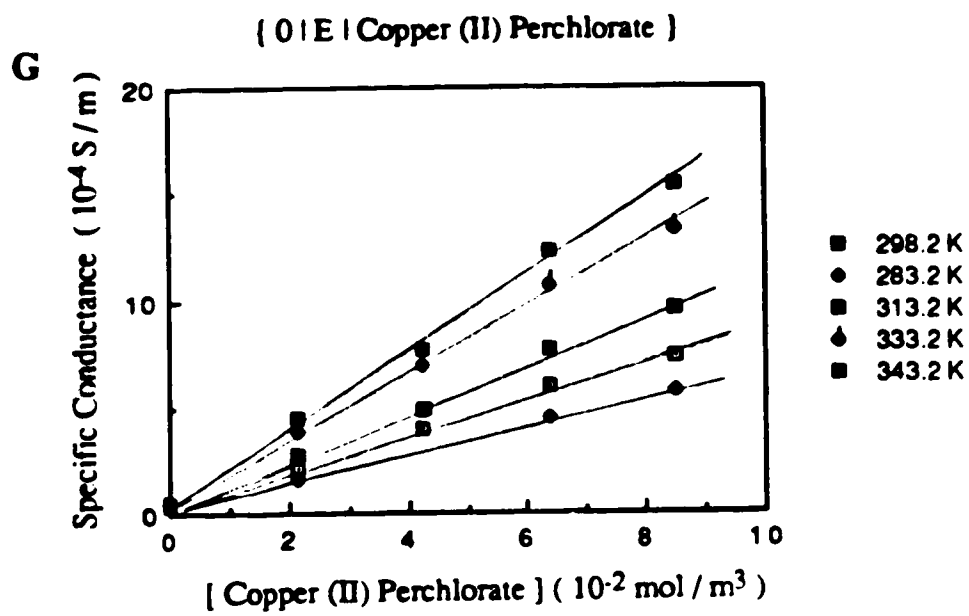


Fig. 3-48 Temperature and concentration dependence of the conductance of copper (II) perchlorate in ethanol / water mixtures (A-G)









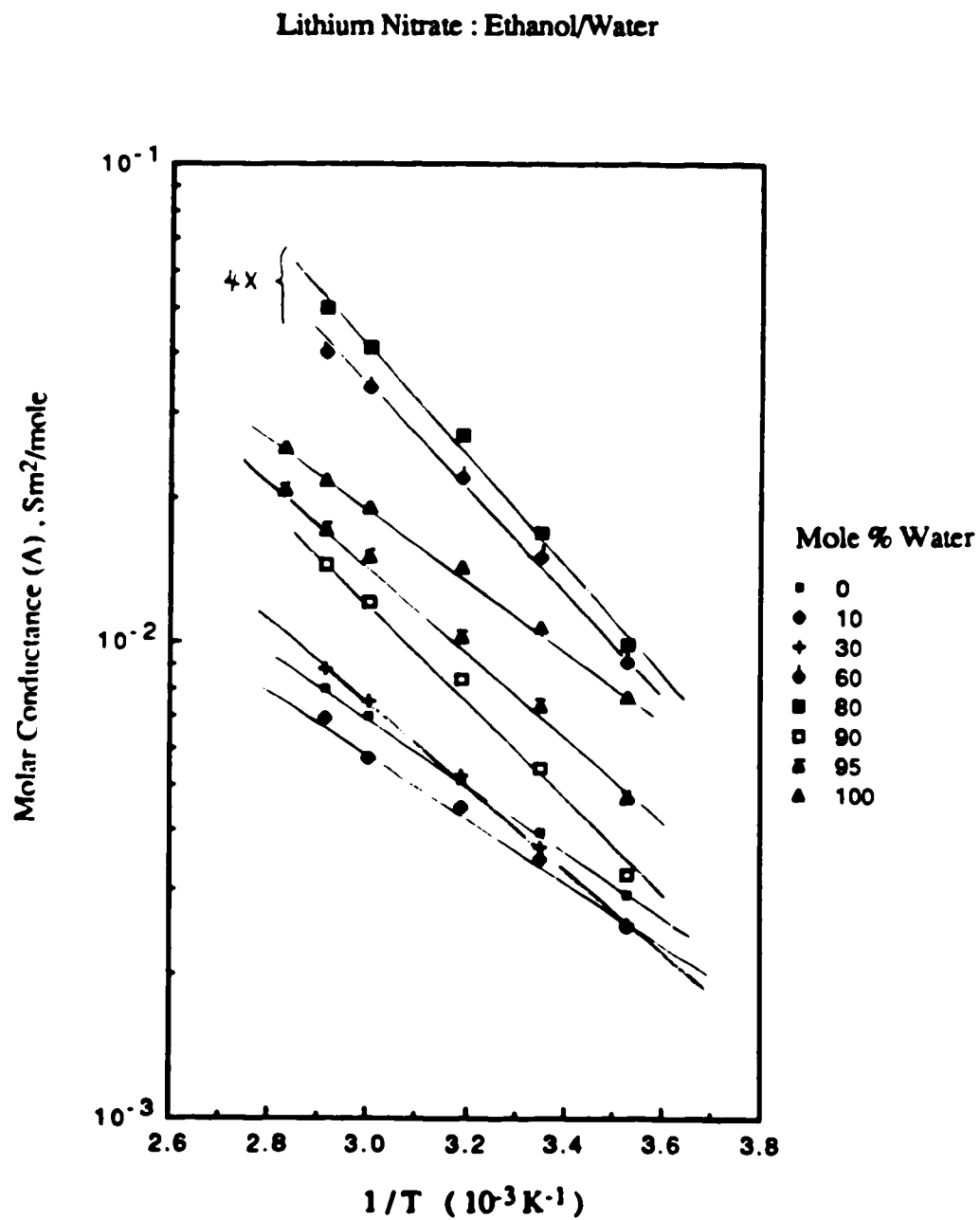


**Fig. 3-49** Arrhenius plots of molar conductance of lithium nitrate in ethanol / water mixtures

## Silver Perchlorate : Ethanol/Water

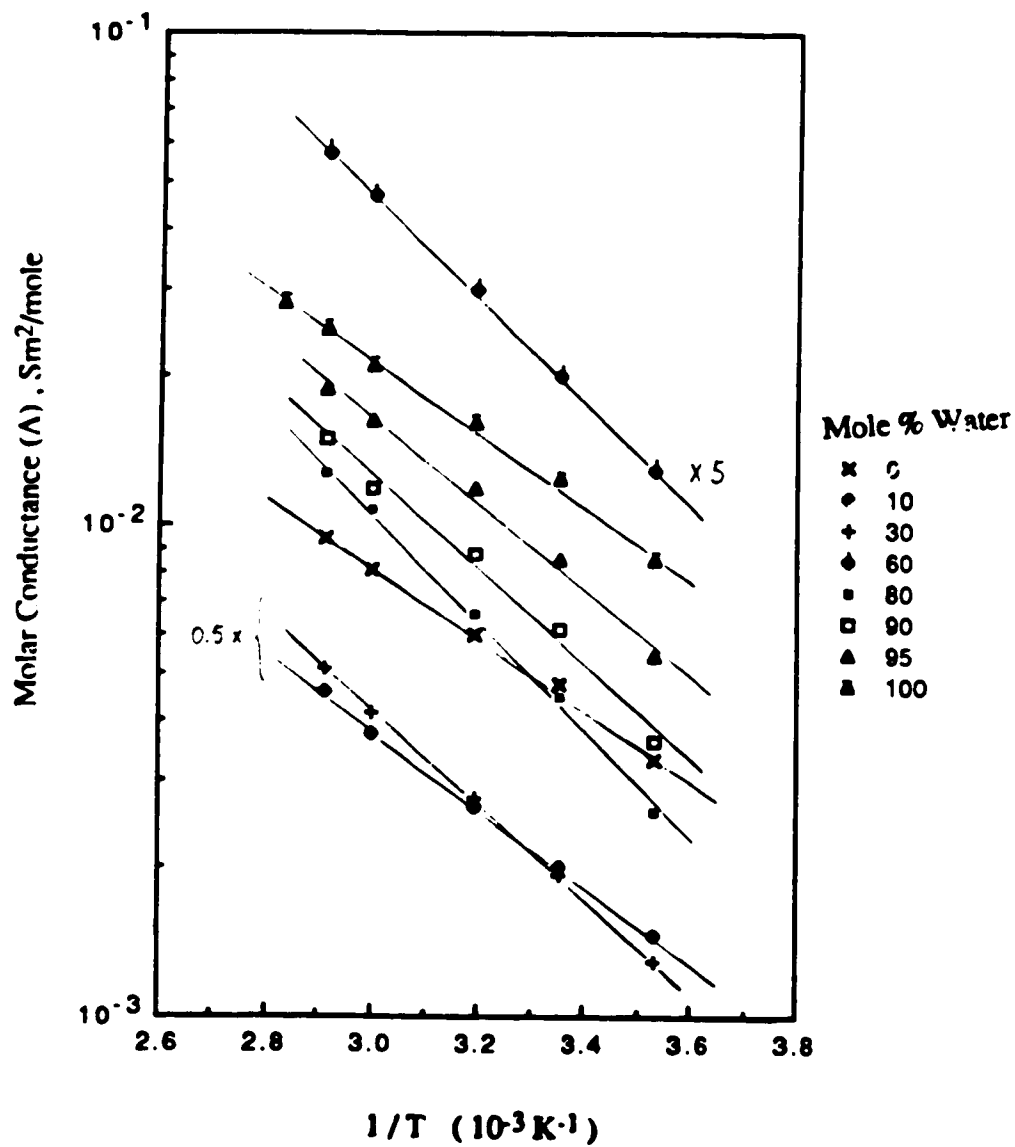


Fig. 3-50 Arrhenius plots of molar conductance of silver perchlorate in ethanol / water mixtures

## Lithium Chromate : Ethanol/Water

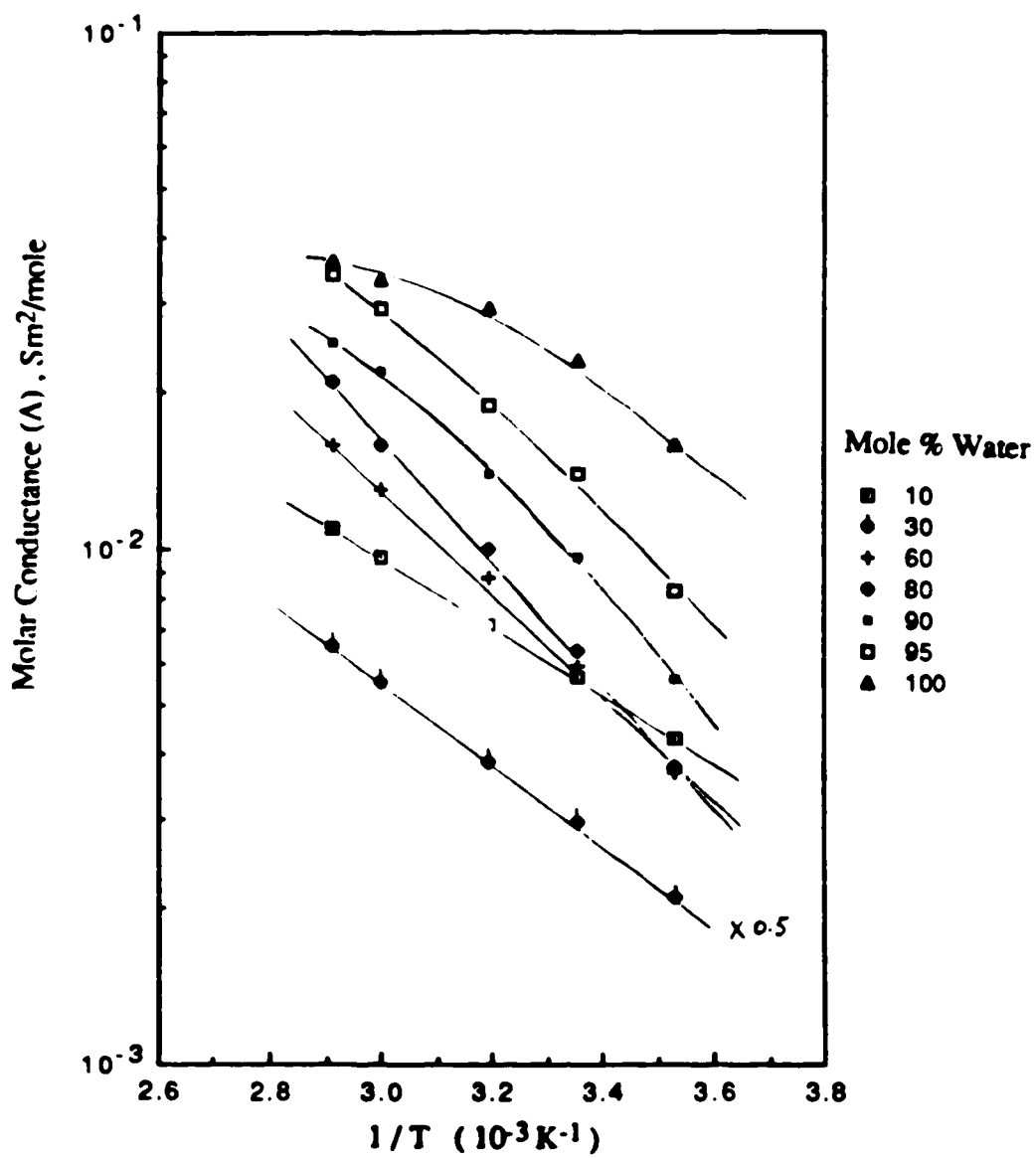


Fig. 3-51 Arrhenius plots of molar conductance of lithium chromate in ethanol / water mixtures

## Copper (II) Perchlorate : Ethanol/Water

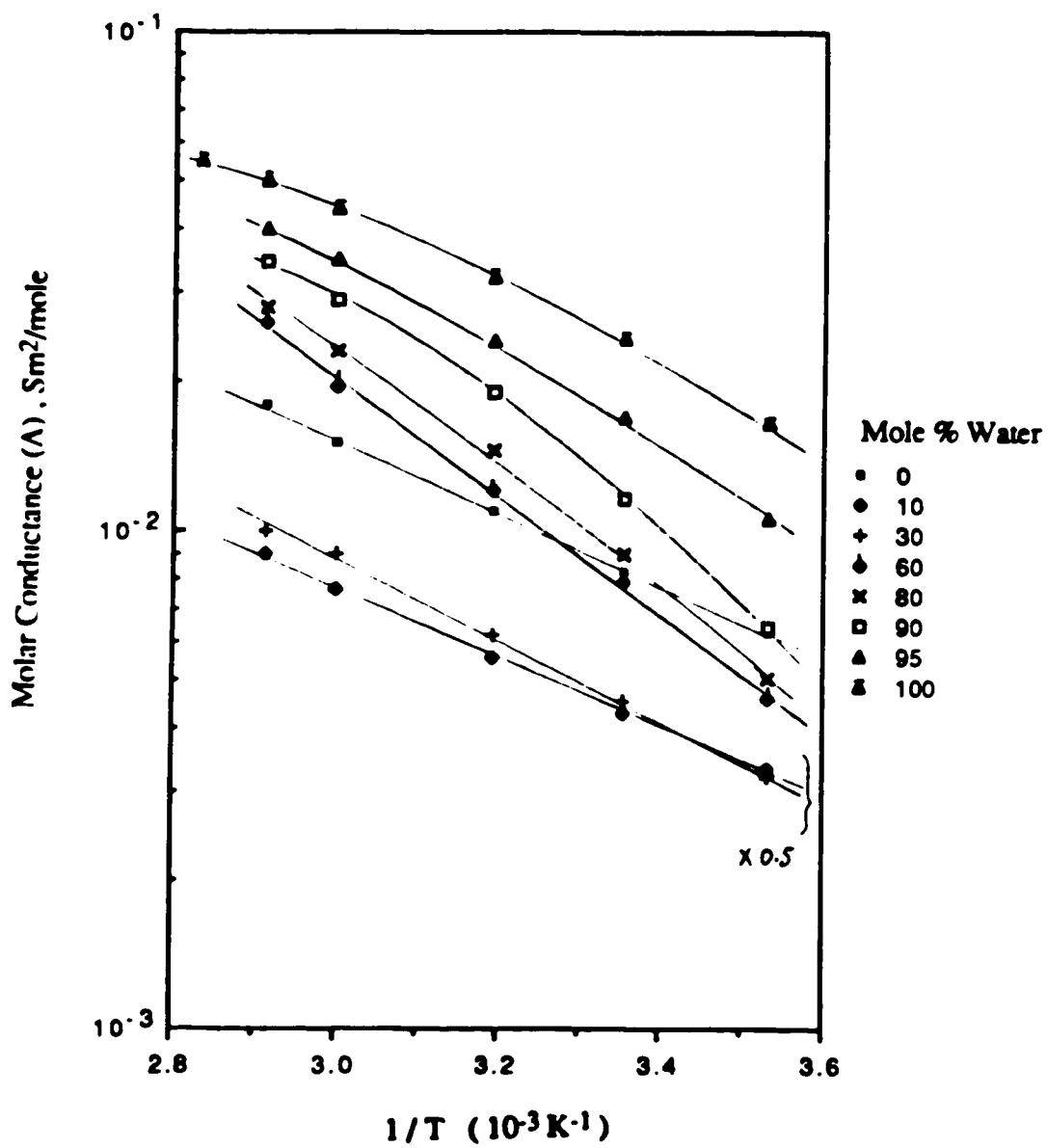


Fig. 3-52 Arrhenius plots of molar conductance of copper (II) perchlorate in ethanol / water mixtures

Fig. 3-53 Composition dependence of the activation energy of conductance of some inorganic electrolytes in ethanol / water mixtures

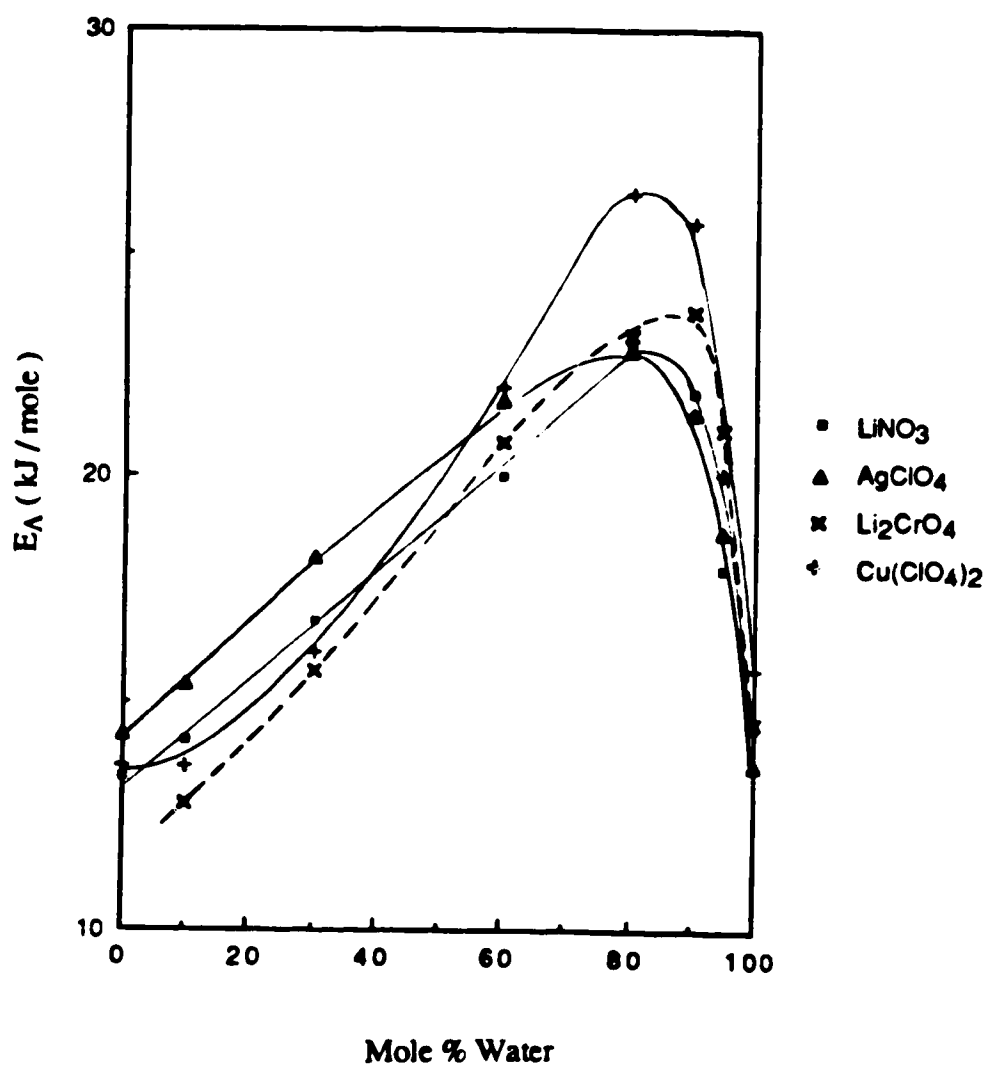


Fig. 3-54 Composition dependence of the molar conductance of some inorganic electrolytes in methanol / water and ethanol / water mixtures

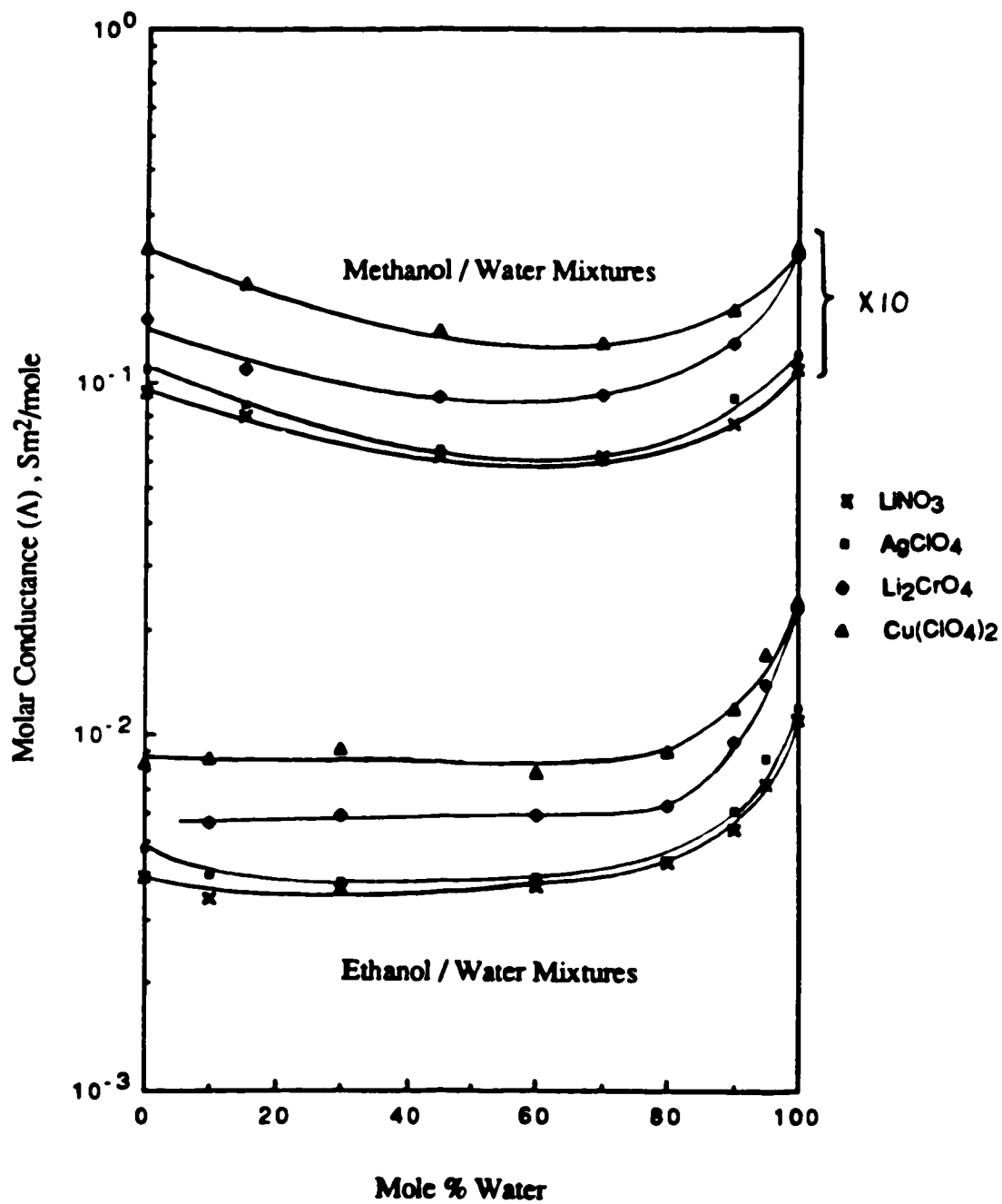




Table 3-34 Temperature and composition dependence of molar conductances <sup>a</sup> ( $\Lambda$ )  
inorganic electrolytes in ethanol / water mixtures

$\chi_w$	0.00	0.10	0.30	0.60	0.80	0.90	0.95	1.00
<u>Lithium Nitrate</u>								
Temp. (K)								
283.2	2.95	2.53	2.56	2.28	2.46	3.23	4.69	7.69
298.2	3.95	3.46	3.69	3.75	4.37	5.44	7.29	10.8
313.2	5.11	4.47	5.26	5.50	6.63	8.33	10.2	14.3
333.2	6.97	5.71	7.50	8.44	10.2	12.1	15.0	19.2
343.2	7.95	6.88	8.80	10.0	12.4	14.5	17.1	21.9
353.2							20.7	25.4
$E_A$ , kJ/mole	13.4	14.2	16.8	20.0	23.0	21.9	18.0	14.5
<u>Silver Perchlorate</u>								
Temp. (K)								
283.2	3.33	2.91	2.59	2.50	2.60	3.60	5.41	8.57
298.2	4.76	4.00	3.87	3.95	4.44	6.15	8.57	12.5
313.2	6.00	5.36	5.55	6.00	6.60	8.69	11.9	16.1
333.2	8.09	7.50	8.30	9.33	10.7	11.8	16.3	21.1
343.2	9.37	9.10	10.2	11.3	12.8	15.0	19.0	25.0
353.2								28.3
$E_A$ , kJ/mole	14.3	15.4	18.2	21.7	22.8	21.4	18.8	13.7
<u>Lithium Chloride</u>								
Temp. (K)								
283.2		4.28	4.23	2.68	2.75	5.60	8.33	16.0
298.2		5.63	5.91	5.92	6.36	9.61	13.6	22.8
313.2		7.14	7.73	8.82	10.0	14.2	19.4	28.6
333.2		9.63	11.0	13.5	16.0	21.9	28.6	33.1
343.2		10.8	13.5	15.9	21.3	24.8	34.0	36.0
$E_A$ , kJ/mole		12.8	15.7	20.8	23.2	23.7	21.1	14.6
<u>Copper (II) Perchlorate</u>								
Temp. (K)								
283.2	6.26	6.66	6.46	4.61	5.10	6.45	10.6	16.6
298.2	8.33	8.63	9.09	7.90	9.00	11.6	16.9	24.3
313.2	10.8	11.2	12.4	12.0	14.5	19.1	24.0	32.3
333.2	15.3	15.2	17.9	19.5	23.0	29.1	35.0	44.1
343.2	17.7	18.0	20.9	26.0	28.0	34.6	40.0	50.0
353.2								55.0
$E_A$ , kJ/mole	13.6	13.6	16.1	22.0	26.3	25.7	20.1	15.8

<sup>a</sup> molar conductance in  $10^{-3} \text{ Sm}^2/\text{mole}$

## CHAPTER FOUR

### DISCUSSION

The solvent effects on the reactivity of solvated electrons with a number of organic and inorganic solutes were studied as a function of temperature in methanol/water and ethanol/water mixtures.

The second order rate constants,  $k_2$ , for solvated electron reaction with nitrobenzene, acetone, phenol and toluene in methanol/water and ethanol/water mixtures at 298 K are shown in Fig.4-1 and Fig.4-2, respectively. Nitrobenzene is an excellent electron scavenger. It captures electrons so efficiently ( $k_2 \geq 10^7 \text{m}^3/\text{mol.s}$ ) that the rate of reaction is nearly controlled by the rate of diffusive encounter of the reactants. As the rate constants for acetone are about three times smaller than those of the nitrobenzene, acetone is a less efficient electron scavenger. Phenol and toluene are inefficient electron scavengers. They are about three orders of magnitude less reactive than nitrobenzene.

#### I Reactions with Organic Electron Scavengers

##### 1. Efficient Organic Electron Scavengers

##### A. Solvent Viscosity Effects

The relationship between the solvent viscosity  $\eta$  and the rate constants ( $k_d$ ) of diffusion controlled reactions of species x with y is illustrated by inserting the Stokes-Einstein relation for diffusion coefficients D (equation [4-1] ) (139a) into the Smoluchowski equation [4-2] (130),

$$D_x = k_B T / 6\pi\eta r_x \quad [4-1]$$

$$k_d = 4\pi N_A (D_x + D_y) (R_x + R_y) \quad [4-2]$$

where  $k_B$  is Boltzmann's constant,  $r_x$  is the effective radius of x for diffusion,  $N_A$  is Avogadro's constant, and  $R_x$  and  $R_y$  are the reaction radii. The Stokes relation holds

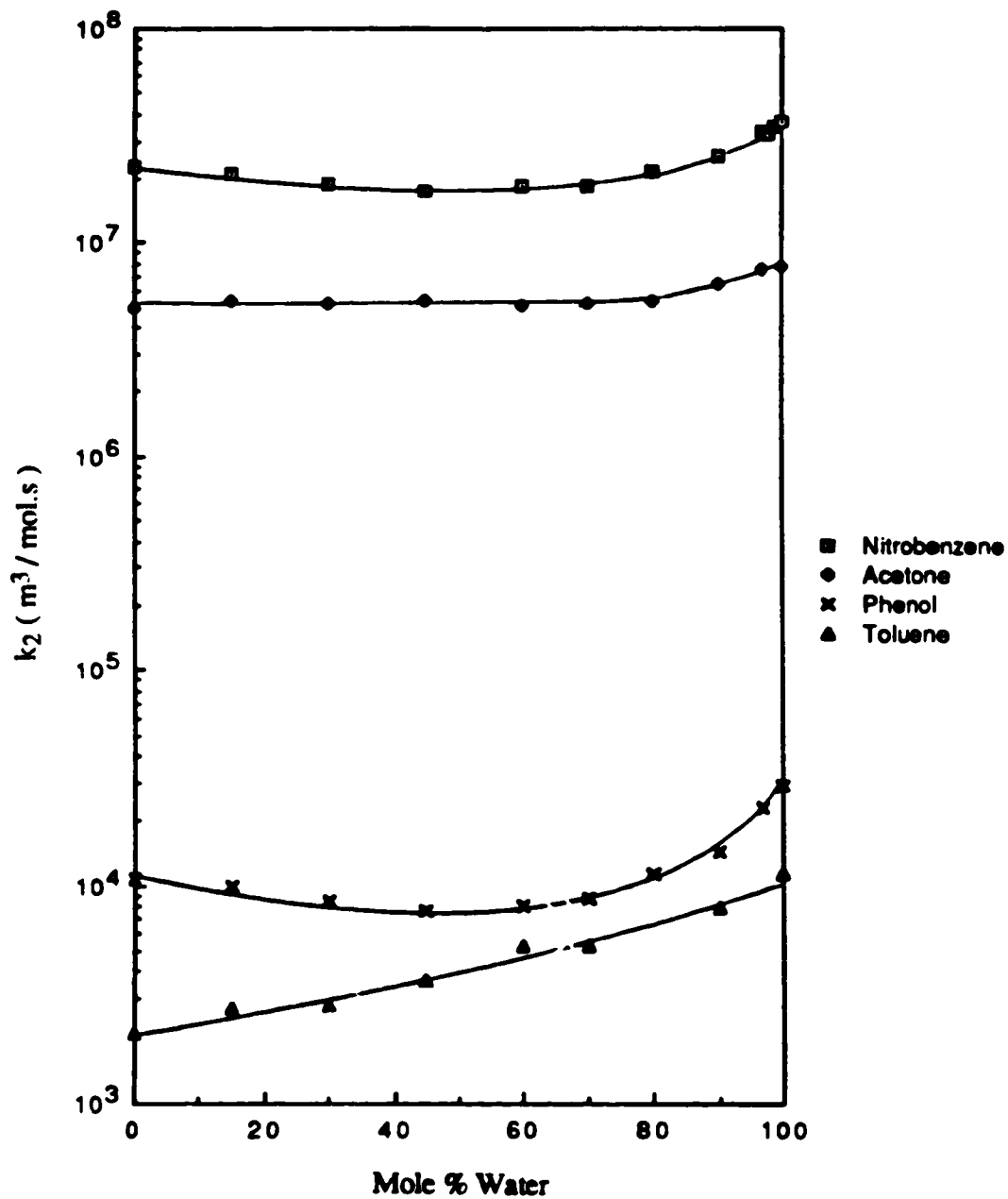


**Fig.4-1** The composition dependence of the second-order rate constants for the reaction of solvated electrons with organic electron-scavengers in methanol/water mixtures at 298 K

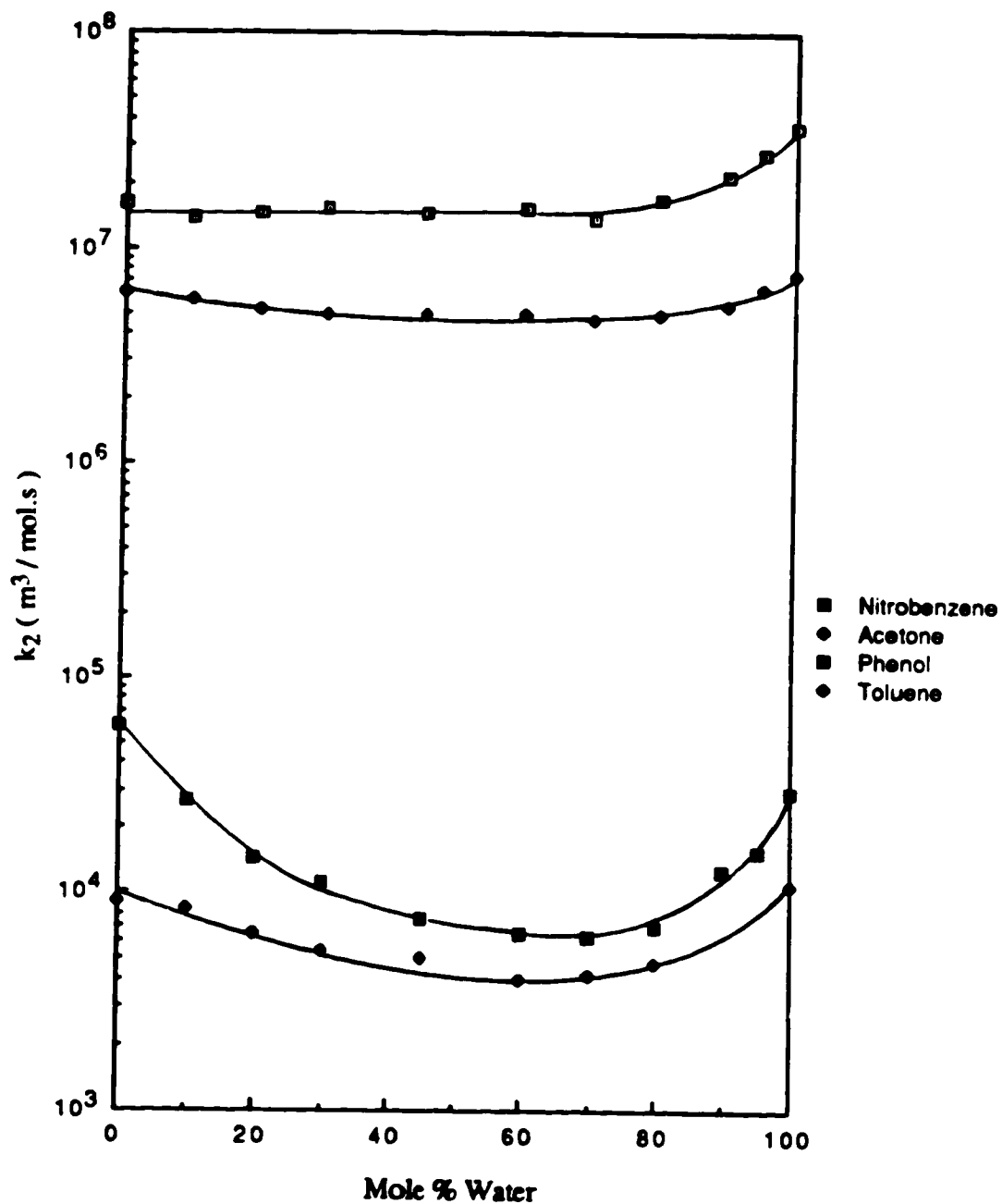


**Fig.4-2** The composition dependence of the second-order rate constants for the reaction of solvated electrons with organic electron-scavengers in ethanol/water mixtures at 298 K

relatively well if the diffusing molecule is as large or larger than those of the solvent (139b). However if the diffusing molecule is much smaller than those of the solvent,  $D \propto \eta^{-x}$ , where  $x < 1.0$ . For example,  $\text{CO}_2$  diffusing in a series of organic liquids displays  $D \propto \eta^{-0.5}$  (139b).

The Stokes-Smoluchowski equation for the reaction between solvated electron ( $e$ ) and scavenger ( $S$ ) is

$$k_d = \frac{N_A k_B T}{1.5 \eta} \left( \frac{1}{r_e} + \frac{1}{r_s} \right) (R_e + R_s) \quad [4-3]$$

The reaction radius and diffusion radius are not necessarily the same as the molecular radius. The deformable solvated electrons can diffuse more flexibly through the fluid than the rigid molecules. The effective radius of diffusion for the solvated electron is therefore smaller than a molecular radius. For example, in water, using values of  $D_e = 4.9 \times 10^{-9} \text{ m}^2/\text{s}$  (107),  $D_{\text{H}_2\text{O}} = 2.3 \times 10^{-9} \text{ m}^2/\text{s}$  (140) and  $\eta = 8.95 \times 10^{-4} \text{ Pa}\cdot\text{s}$  (141) at 298K in equation [4-1], the diffusion radii for electron and water are calculated to be 0.05 nm and 0.10 nm, respectively. Although  $e_s^-$  can spread over a diffuse space that covers several water molecules, it diffuses more easily than a water molecule and has a correspondingly smaller effective radius for diffusion. The values of  $D_e$  in alcohols can also be calculated from the mobility  $\mu_e$  (20,144-146) using

$$D_e = \mu_e k_B T / q \quad [4-4]$$

where  $q$  is the charge of the electron. Then at  $296 \pm 3\text{K}$ , using the liquid viscosities (142,143), equation [4-1] gives the following values of  $r_e$  (nm): methanol, 0.28; ethanol, 0.28; *i*-propanol, 0.09; *n*-butanol, 0.04; 3-methyl-1-butanol, 0.02 (115). In water/alcohol mixtures, one expects the diffusion radii of the reactants to vary with solvent composition. The Stokes-Smoluchowski equation is used as a framework to correlate the reactivity and the ease of diffusion of the solvated electrons in this study.

If the variation of the factor  $(1/r_e + 1/r_s) (R_e + R_s)$  with solvent composition is small, the Stokes-Smoluchowski formulation predicts that the plot of  $\log k_2$  against  $\log \eta$  would be linear with slope of negative one, that is

$$k_2 = \text{constant} / \eta \quad [4-5]$$

The composition dependence of viscosity in methanol/water (147) and ethanol/water (148) systems is shown in Fig.4-3. The values of  $\log k_2$  for nitrobenzene are plotted against  $\log \eta$  for the reactions in methanol/water mixtures at 298 K (Fig.4-4). Equation [4-5] is obeyed in only the water rich solvents ( $0.70 \leq \chi_w \leq 1.0$ ). For reactions which take place in solvents with water content of less than 70 mole %, the  $k_2$  values only increase slightly with the decrease of solvent viscosities. In ethanol/water mixtures, the  $k_2 \propto \eta^{-1}$  behavior occurs in the  $0.80 \leq \chi_w \leq 0.95$  region (Fig.4-5). These regions correspond to  $\chi_w > \chi_{\eta \max}$  (Fig.4-3). The viscosity dependence of rate constant is lower ( $k_2 \propto \eta^{-0.6}$ ) near the pure water region ( $0.95 \leq \chi_w \leq 1.0$ ), similar to those reported for the 1-propanol/water (112) and *t*-butyl alcohol/water (115) solvent systems. In the region where equation [4-5] is followed, the value of  $\eta k_2$  at 298 K for methanol/water is  $3.4 \times 10^7 \text{ m}^3 \cdot \text{mPa} / \text{mol}$ , lower than that for ethanol/water ( $4.0 \times 10^3 \text{ m}^3 \cdot \text{mPa} / \text{mol}$ ) and *t*-butanol/water ( $4.7 \times 10^3 \text{ m}^3 \cdot \text{mPa} / \text{mol}$ ) (115). The factor  $(1/r_e + 1/r_s) (R_e + R_s)$  in methanol/water is therefore 0.85 and 0.72 times smaller than that of the ethanol/water and *t*-butanol/water mixtures, respectively. The smaller factor is due to either a smaller reaction radius and/or the larger effective diffusion radii in the water-rich methanol solvents.

The reaction between nitrobenzene and solvated electrons is not completely diffusion controlled (98,115). The mean physical radius of nitrobenzene is 0.28 nm (149). Assuming  $r_e = 0.05$  nm for the water rich region, one obtains the effective reaction radii  $(R_e + R_s)$  of 0.087 nm for methanol/water mixtures, 0.10 nm for ethanol/water mixtures and 0.12 nm for *t*-butanol/water mixtures. These are smaller than the physical radius of the nitrobenzene molecule, which indicates that the reaction between solvated electrons and

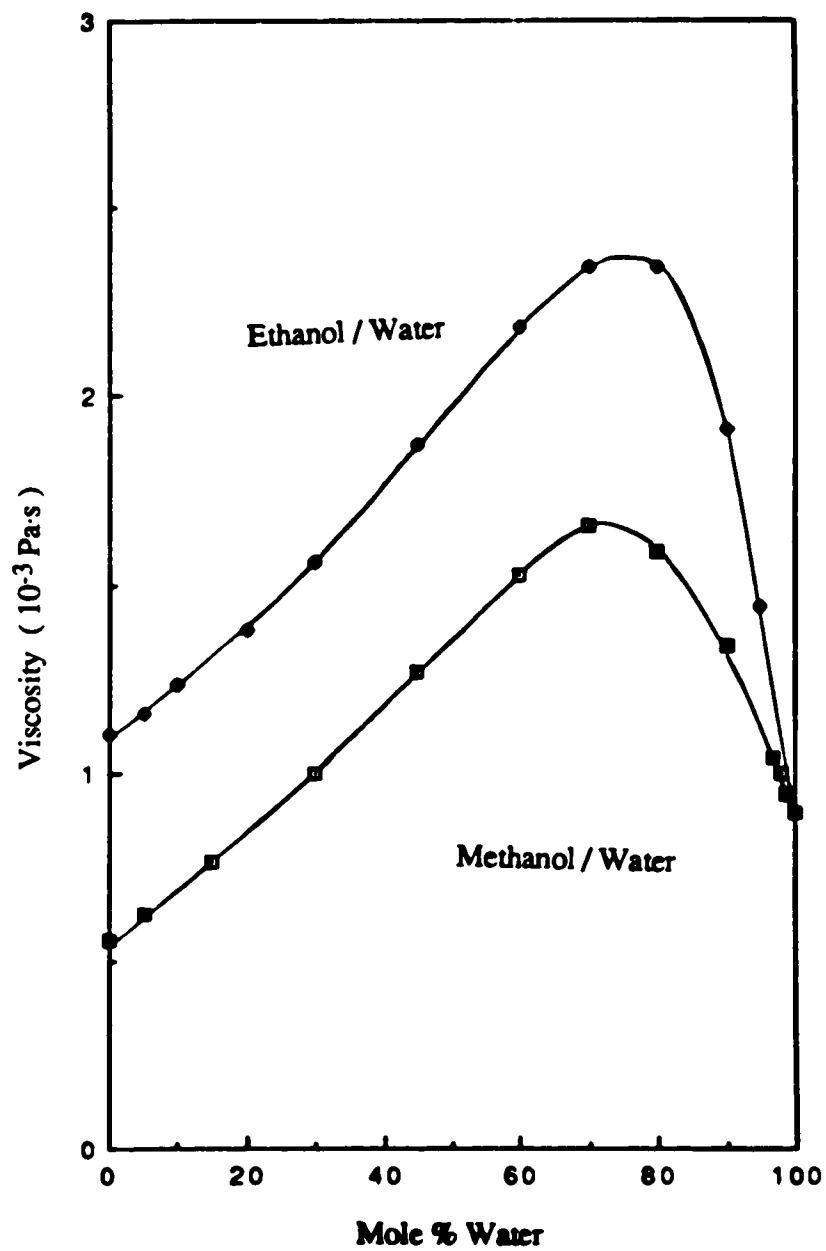
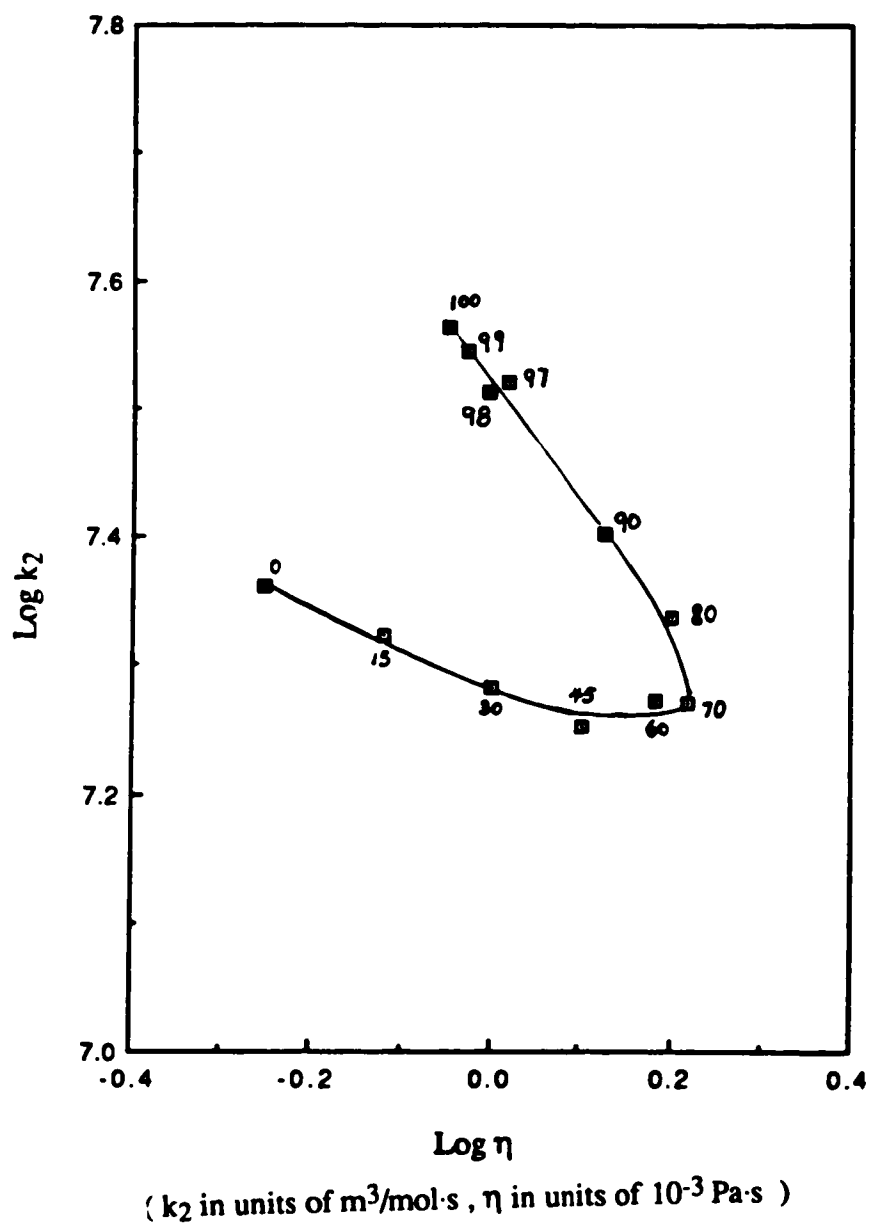
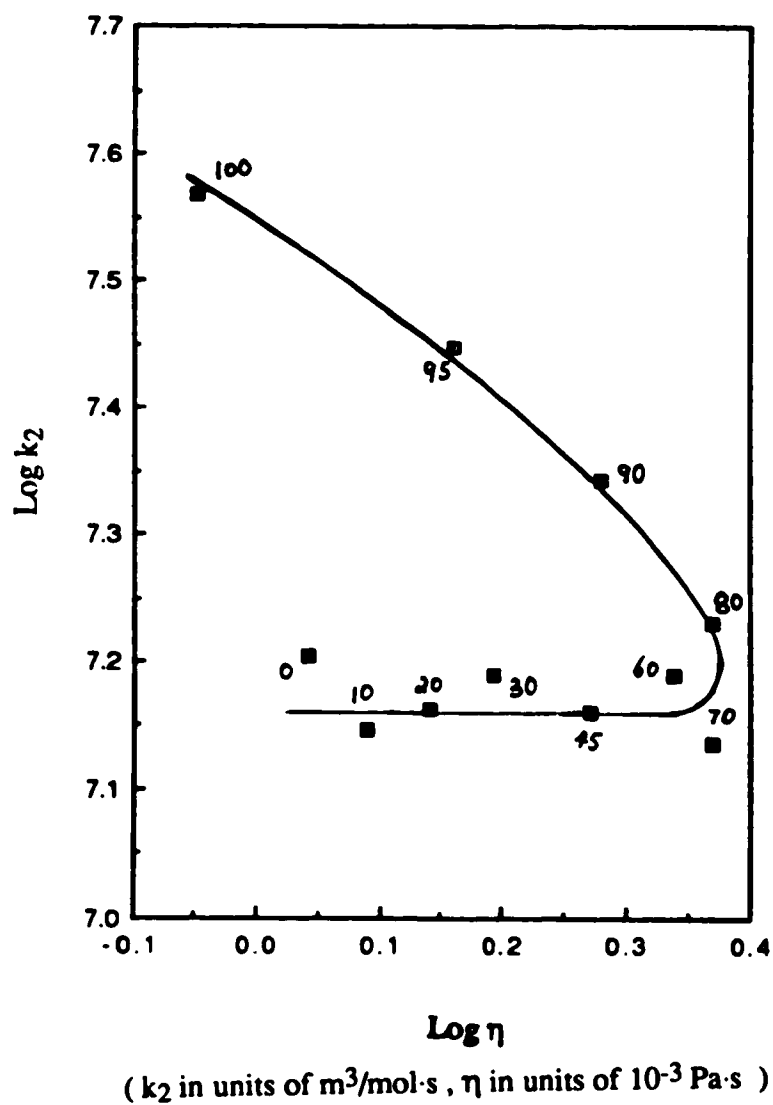


Fig.4-3 The composition dependence of solvent viscosity in methanol/water and ethanol/water mixtures at 298 K ( $\rho$  .fs.147,148)



**Fig.4-4** The viscosity dependence of the second-order rate constants for the reaction of solvated electrons with nitrobenzene in methanol/water mixtures at 298 K





**Fig.4-5** The viscosity dependence of the second-order rate constants for the reaction of solvated electrons with nitrobenzene in ethanol/water mixtures at 298 K

nitrobenzene does not occur at every diffusive encounter. This suggests that an extensive charge-transfer has taken place prior to the transition state. The activation complex therefore resembles the nitrobenzene anion radical. Transition states of this sort probably occur with all the nearly diffusion controlled reactions, the solvent effects on the stabilization of the activation complex therefore are important. The influence of solvent dielectric effects on the solvation of the reactants and the transition state will be discussed in the next section.

Because of the extensive charge-transfer in the water-rich region, the possibility of a large variation of reaction radii in this region will be small. The effective diffusion radii therefore must be unchanged to keep the factor  $(1/r_e + 1/r_s) (R_e + R_s)$  constant. Since the diffusion radii of the reactants depends on the dielectric properties of the solvent, the invariable diffusion radius in the water-rich region can only be rationalized if the solutes are solvated in similar environments. This perhaps can be interpreted according to the clathrate model of the alcohol/water solvent structure (89,90,150,151).

When a small amount of alcohol is added to water, the water molecules organize around the alcohol and form oligomers similar to those of the clathrate compounds. The alcohol molecules thus strengthening the water structure. In the water-rich medium, it may be that the reactants are solvated in these clathrate-like solvent structures (microphases), and it is the diffusion of these microphases that follows the inverse viscosity relationship. In ethanol/water mixtures, the maximum water structure strengthening effect is attained when the bulk solvent contains about 95 mole % of water. The maximum structure enhancement of liquid water results when the hydrophobic alkyl groups of the alcohols fill the cavities of the water structure (152-154).

In the water-rich solvents, if the reaction radii are similar, the decreasing order of the  $\eta k_2$  values in the alcohol/water mixtures ( t-butyl alcohol > ethanol > methanol ) is due to the increase of the effective diffusion radii, which means that the water structure strengthening effects are greater with the smaller alcohols. The small methanol molecules

are more compatible with the water molecules and therefore able to form a more rigid solvent network.

With increasing alcohol content, the rupture of these clathrate-like solvent structures occur, and a random mixture of alcohol/water complexes, water and alcohol aggregates (clusters) are formed (87,150-151). The deviation of the Stokes-Smoluchowski formulation in the  $\chi_{\eta\max} \geq \chi_w \geq 0.0$  region is partly due to the decrease in the diffusion coefficient of the reactants in the alcohol direction.

The composition dependences of  $D_e$  in the methanol/water and ethanol/water mixtures have been measured (107,144,155). The diffusion coefficients of nitrobenzene ( $D_s$ ) in methanol/water mixtures have also been estimated (106). Fig.4-6 shows that in going from water to alcohol, the diffusion coefficients for the solvated electrons decrease rapidly. The sums of the diffusion coefficients ( $D_e + D_s$ ) were used to calculate the reaction radii ( $R = R_x + R_y$ ) for the reaction between solvated electrons and nitrobenzene in methanol/water mixtures at 298 K, using the Smoluchowski equation [4-2]. Fig.4-7 shows that the reaction radii are large (0.85-1.25nm), and are increasing towards the alcohol direction. Large reaction radii for solvated electron reactions with benzoquinone, carbon tetrachloride and iodine in methanol/water and ethanol/water mixtures have also been reported in the literature (106), and are interpreted in terms of the electron tunneling mechanism (106,110). If one visualizes the electron-tunneling process in these reactions as the wave function overlap between the solvated electron and the nitrobenzene molecule from a far distance, one would expect the probability of this occurrence to be higher when the solvated electron is more deformable and/or with a larger size of charge distribution. As discussed earlier, the deformability of the electron is related to its diffusion coefficient, and the size of charge distribution can be linked to the binding energy of the electron in its potential well and the optical absorption maximum energy ( $E_{A\max}$ ) of  $e_s^-$  (52,156). The increase of  $E_{A\max}$  and the rapid decrease of diffusion coefficients of the solvated electrons

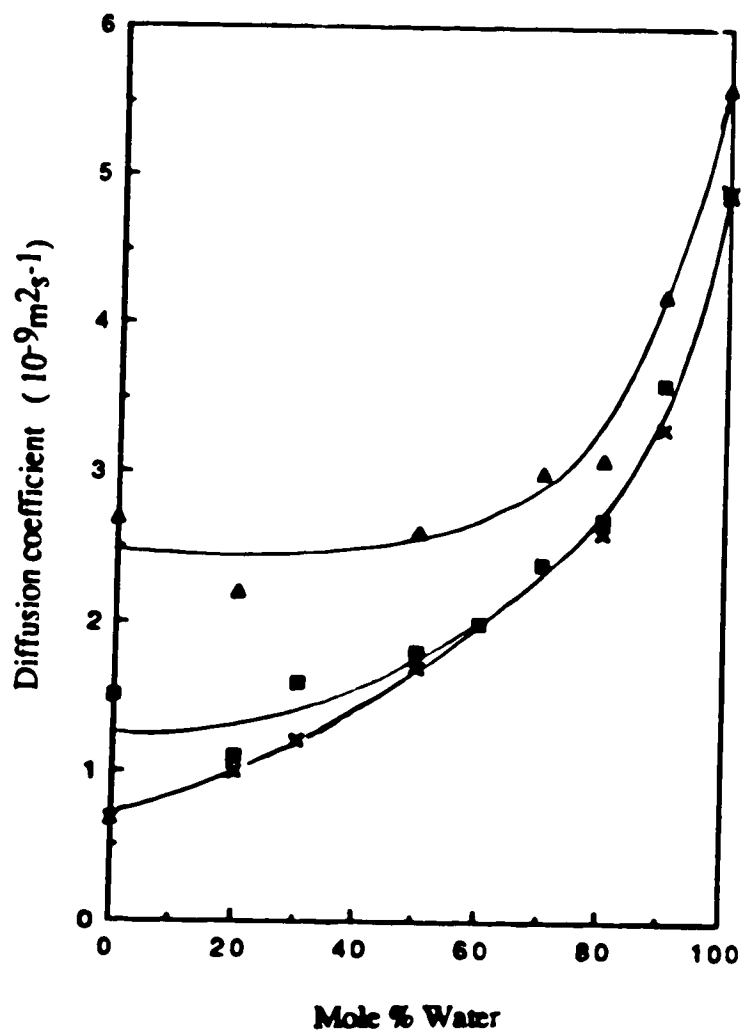
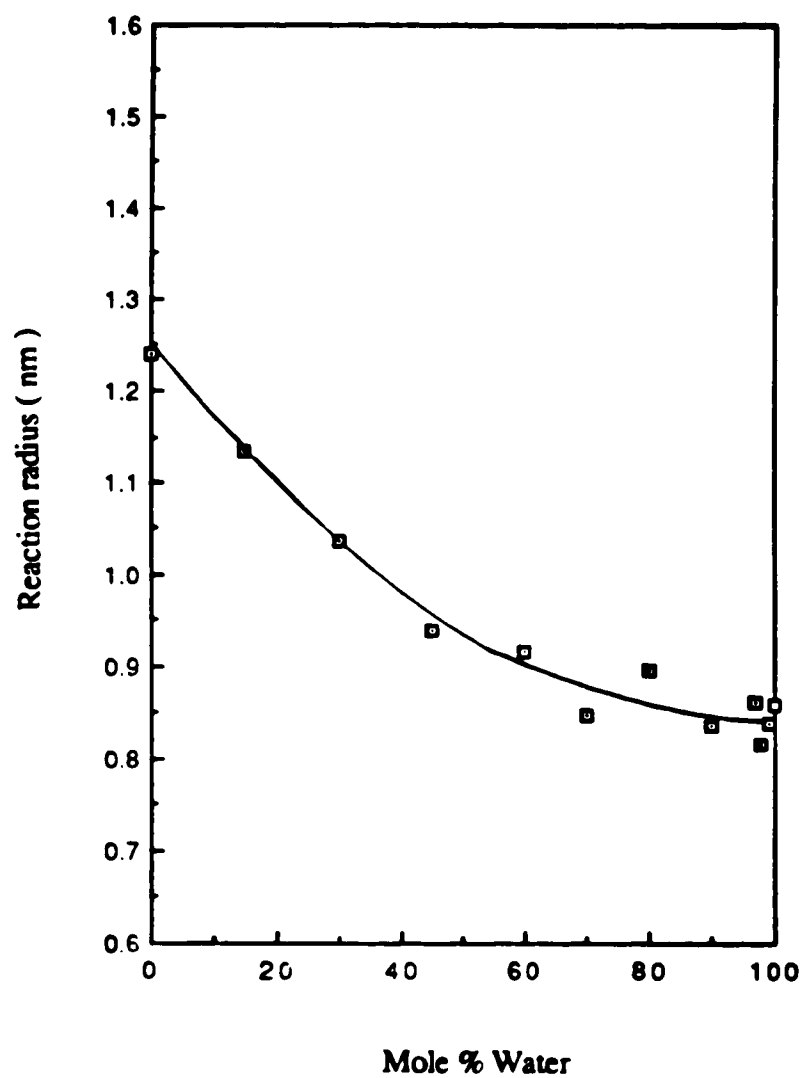


Fig.4-6 The composition dependence of the diffusion coefficients of solvated electrons and nitrobenzene in methanol/water and ethanol/water mixtures at 298 K (Ref. 107)

●,  $D_e(\text{MeOH}/\text{H}_2\text{O})$ ; x,  $D_e(\text{EtOH}/\text{H}_2\text{O})$ ; ▲,  $D_e + D_s(\text{MeOH}/\text{H}_2\text{O})$



**Fig.4-7** The composition dependence of the reaction radii for the reaction of solvated electrons with nitrobenzene in methanol/water mixtures at 298 K

on going from water to methanol therefore do not support the electron tunneling mechanism.

## B. Solvent Dielectric Effects

### (a) The Debye Model

The transport properties, solute-solute and solute-solvent interactions in polar solvent are influenced by the dielectric properties of the solvent. Debye (131) modified the Smoluchowski relation to consider the interaction energy between the reacting species. In the Smoluchowski-Debye model,

$$k_d = 4\pi N_A (D_x + D_y) (R_x + R_y) f \quad [4-6]$$

$$\text{or} \quad k_d = \frac{N_A k_B T}{1.5 \eta} \left( \frac{1}{r_x} + \frac{1}{r_y} \right) (R_x + R_y) f \quad [4-7]$$

$$\text{where} \quad f = (U(R) / k_B T) [ \exp ( U(R) / k_B T ) - 1 ]^{-1} \quad [4-8]$$

and  $U(R)$  is the interaction potential energy between the reactants at distance  $R=R_x+R_y$ . The factor  $f$  reflects the probability of the reactants attaining the approach distance  $R$  at which reaction can occur. The coulombic electron-dipole interaction energy (157) is :

$$U(R) = -Mq \cos\theta / 4\pi\epsilon_0\epsilon R^2 \quad [4-9a]$$

where  $M$  is the dipole moment of the scavenger,  $q$  is the electronic charge,  $\theta$  is the angle of approach of the electron to the line of the dipole,  $\epsilon_0$  is the permittivity of vacuum, and  $\epsilon$  is the relative permittivity (dielectric constant) of the solvent. For reaction between an electron and nitrobenzene, the positive end of the nitrobenzene dipole is probably more electrophilic (reactive), and maximum rate enhancement can be achieved when the electron-dipole interaction is a head-on one ( $\theta = 0^\circ$ ), in which case, equation [4-9a] becomes

$$U(R) = -Mq/4\pi\epsilon_0\epsilon R^2 \quad [4-9b]$$

The dipole alignment increases as the electron and dipole diffuse closer together, which favors [4-9b]. For reaction between an electron and a charged scavenger, the coulombic ion-ion interaction energy is (157):

$$U(R) = -Zq^2/4\pi\epsilon_0\epsilon R \quad [4-10]$$

where Z is the number of charges on the scavenger.

According to the Smoluchowski-Debye model, solvent effects are not only due to viscosity (diffusion), but also due to dielectric constant of the medium (coulombic interaction between reactants). If the diffusive factors for two diffusion controlled reactions are similar, the one with a greater attractive (or less repulsive) interaction will have a higher rate constant.

For the nearly diffusion controlled reactions, the rate constant may be written as

$$k_2 = 4\pi N_A(D_c + D_s) (R_c + R_s) f \phi_s \quad [4-11]$$

where  $\phi_s$  is the encounter efficiency of the reactant pair and is a function of electron affinity of the scavenger and the solvation energy of the electron (116,118). When  $\phi_s = 1$ , the reaction is completely diffusion controlled (equations [4-2] and [4-6]). For a reaction of electrons with a specific scavenger in two different solvents with similar electron solvation energies, one might expect the values of R and  $\phi_s$  to be similar. Then

$$k_2' / k_2'' = (D_c + D_s)' f' / (D_c + D_s)'' f'' \quad [4-12]$$

$$\text{or} \quad (k_2' / f') / (k_2'' / f'') = (D_c + D_s)' / (D_c + D_s)'' \quad [4-13]$$

where the prime and double prime refer to different solvents.

The coulombic interaction factors,  $f$ , for the reaction of solvated electrons with nitrobenzene ( $M = 4.2D$  (158)) were calculated according to equations [4-7] and [4-9b], assuming an encounter distance of 0.5 nm. The values of  $k_2/f$  normalized to those in water are plotted against viscosity in Fig.4-8. In the water-rich mixtures, the dependence of the water normalized  $k_2/f$  on  $\eta^{-1}$  is observed, which means that in this region,

$$(k_2/f) / (k_2/f)_w = C / \eta \quad [4-14]$$

where  $C$  is a constant. From equation [4-7]

$$C = \eta_w (1/r_e + 1/r_s) / (1/r_e + 1/r_s)_w \quad [4-15]$$

Thus regardless of the change of dielectric properties of the solvent, the diffusion radii remain constant. This is consistent with the idea that the reactants are solvated in the clathrate-like microphases as discussed earlier.

The use of the dielectric correction factor ( $f$ ) in the Debye model however still does not provide a complete consideration of the solvent dielectric effects in the alcohol dominated region. The diffusion radius, for example, may also be related to the dielectric properties of the medium. The ratio of the effective diffusion radii ( $r_w/r$ ) in different solvents can be calculated from

$$r_w / r = (\eta / \eta_w) (k_2 / f) / (k_2 / f)_w \quad [4-16]$$

where  $1/r$  is defined as

$$1/r = 1/r_e + 1/r_s \quad [4-17]$$

The composition dependence of  $r_w/r$  for the reaction of nitrobenzene is shown in Fig.4-9. The values of  $r_w/r$  decrease with increasing alcohol content, which indicates that the diffusion radii increase towards the alcohol direction.



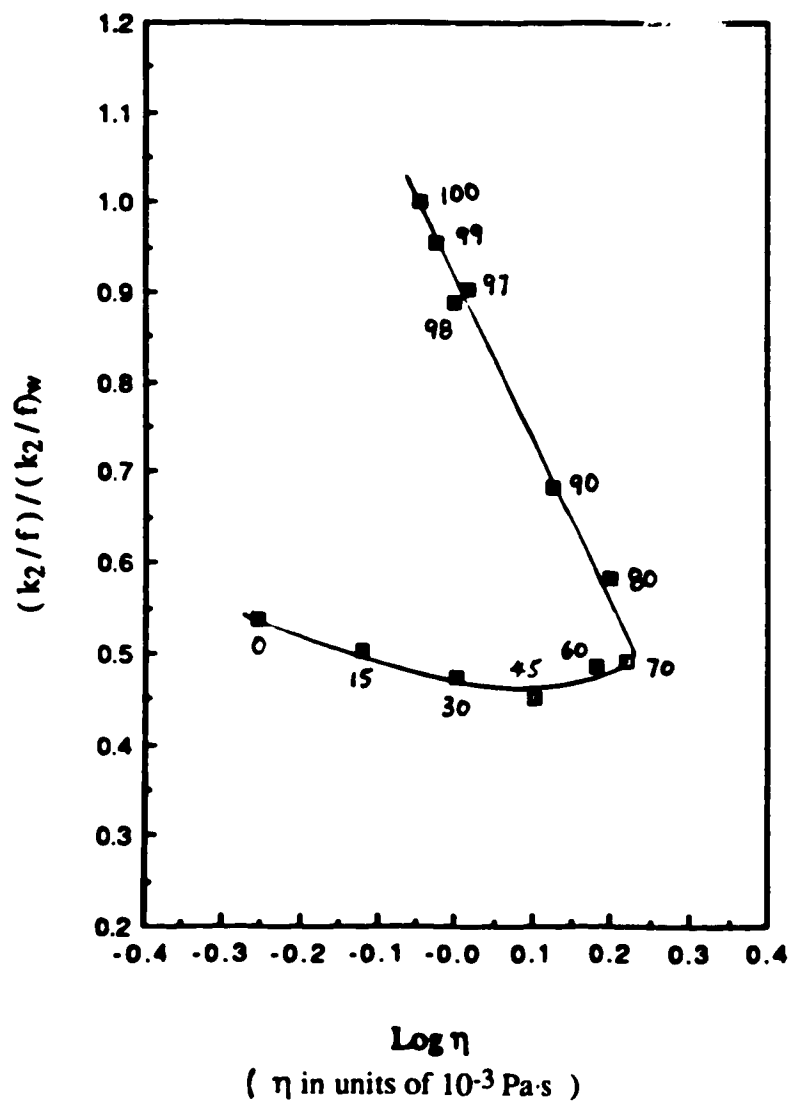
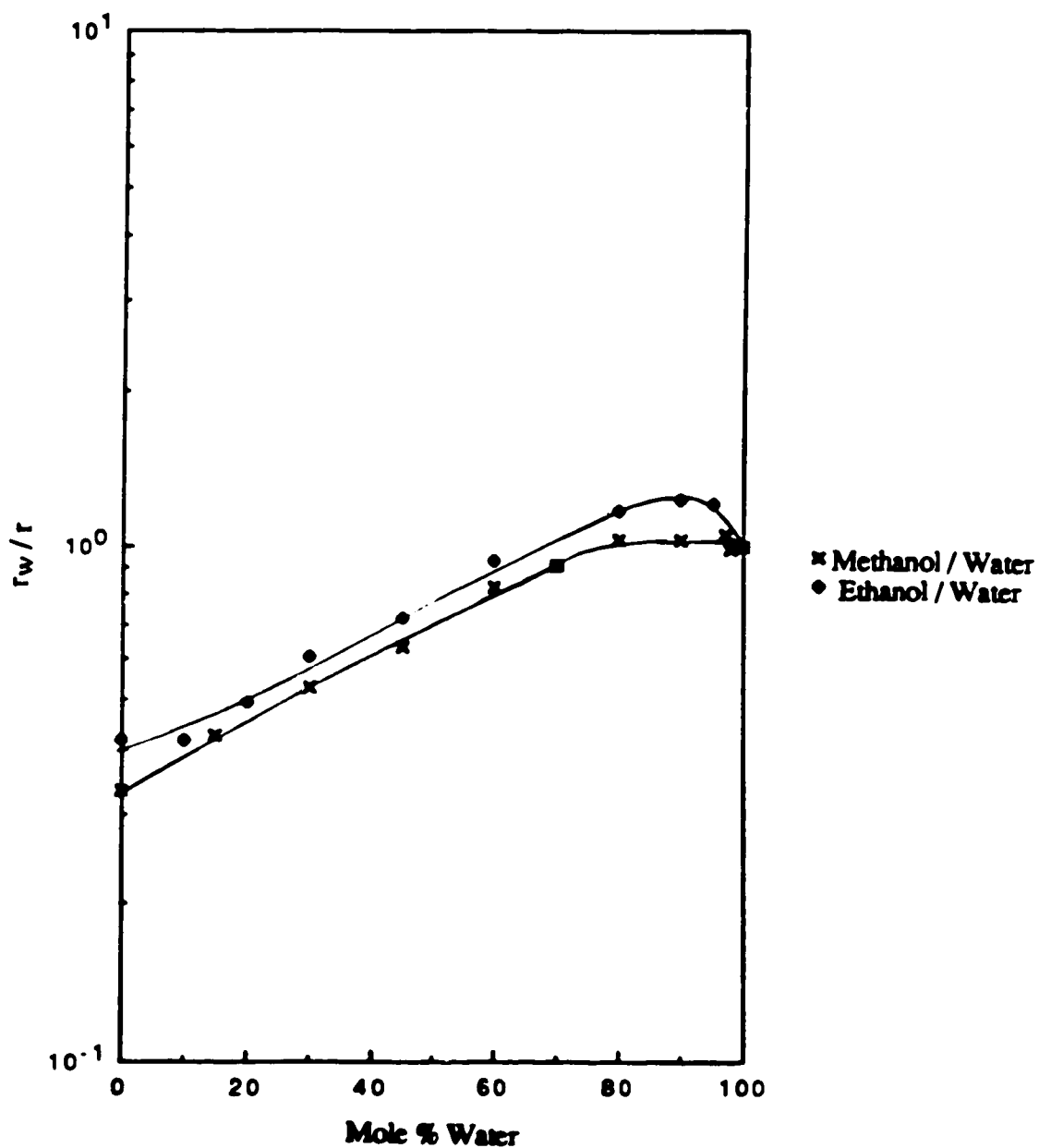


Fig.4-8 The viscosity dependence of the normalized  $k_2/f$  values for the reaction of solvated electrons with nitrobenzene in methanol/water mixtures at 298 K



**Fig.4-9** The composition dependence of the relative effective diffusion radii ( $r_w/r$ ) for the reaction of solvated electrons with nitrobenzene in methanol/water and ethanol/water mixtures at 298 K

**(b) Effects of Dielectric Constant**

The rate of the reaction of solvated electrons with nitrobenzene is only partially diffusion controlled (98,115). The probability of reaction per encounter is somewhat smaller in solvents where the electron solvation energy is greater, so the probability is smaller in primary and secondary alcohols than in tertiary alcohol (100,112-118,159). The fact that the reaction radii are much smaller than the physical radius of nitrobenzene suggest that the activation complex resembles a nitrobenzene anion. The dielectric properties of a polar medium therefore should also have an influence on the thermodynamic stability of this partially charged transition state. Whether this effect can manifest itself as rate will depend on its solvation energy relative to that of the ground state.

The composition dependence of the static dielectric constants in methanol/water and ethanol/water mixtures at 298K (148) are shown in Fig.4-10. The viscosity normalized rate constant,  $k_2\eta$ , for the reaction of solvated electrons with nitrobenzene and acetone are plotted against  $\epsilon^{-1}$  in Fig.4-11. Linear correlations are observed in the regions where  $0 \leq \chi_w \leq \chi_{\eta\max}$ . The composition dependence of the solvation energy of electrons in the water-rich solvents is small, as indicated by the small change of the optical absorption energies (23), so the linear correlations here indicate the effect of solvation on the transition state.

The solvation energy of an ion can be related to the dielectric constant of the medium. The Born equation (8,157) for electrostatic free energy of solvation ( $\Delta G_s^0$ ) is

$$\Delta G_s^0 = ( Z^2q^2 / 8\pi\epsilon_0r_i ) ( 1/\epsilon - 1 ) \quad [4-19]$$

where  $r_i$  is the radius of the ion. The change of the dielectric constant from one solvent to another will result in a change in the free energy of solvation ( $\Delta\Delta G_s^0$ ) of the ion

$$( 1 / \epsilon_2 - 1 / \epsilon_1 ) = \Delta\Delta G_s^0 ( 8\pi\epsilon_0r_i / Z^2q^2 ) \quad [4-20]$$

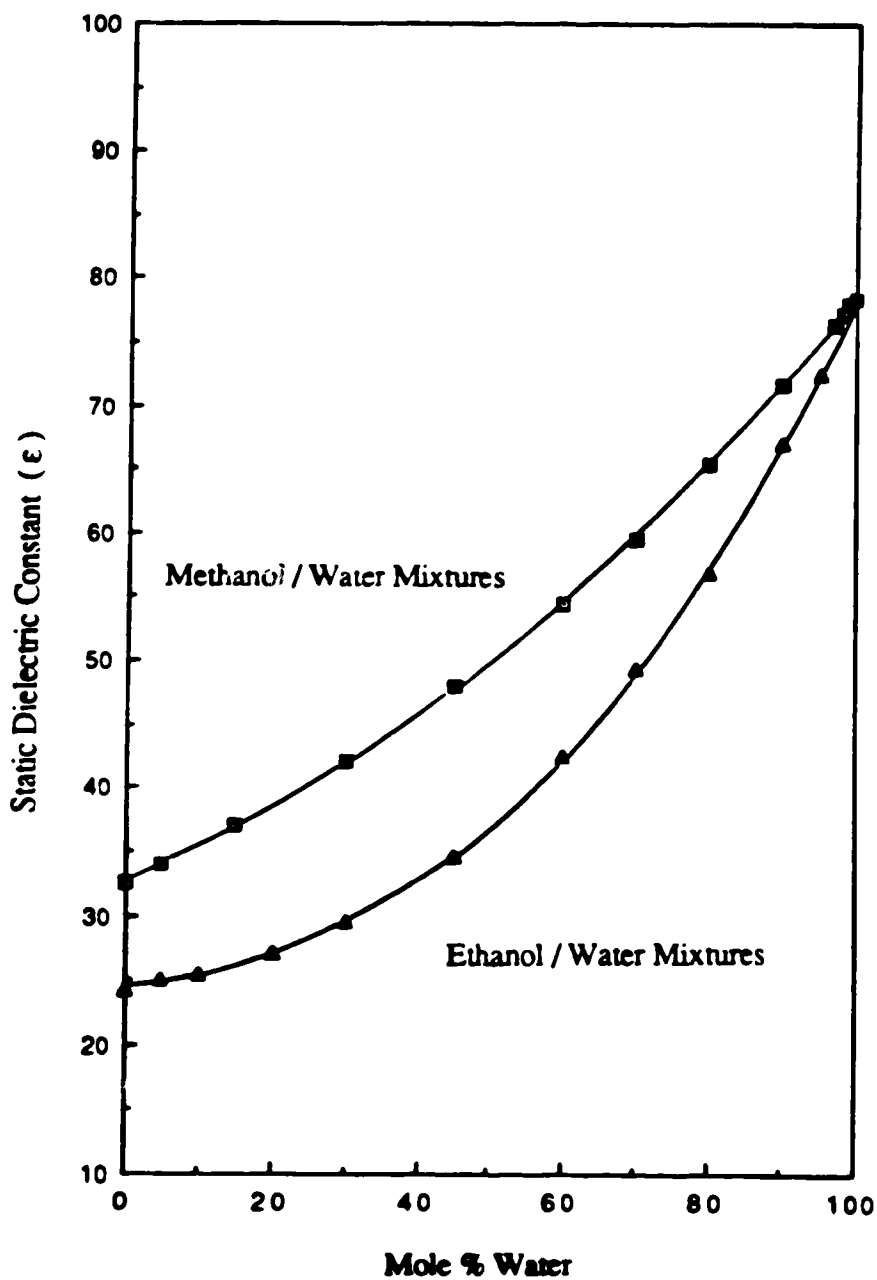


**Fig.4-10** The composition dependence of the static dielectric constants of solvated electrons in methanol/water and ethanol/water mixtures at 298K (Ref.148)

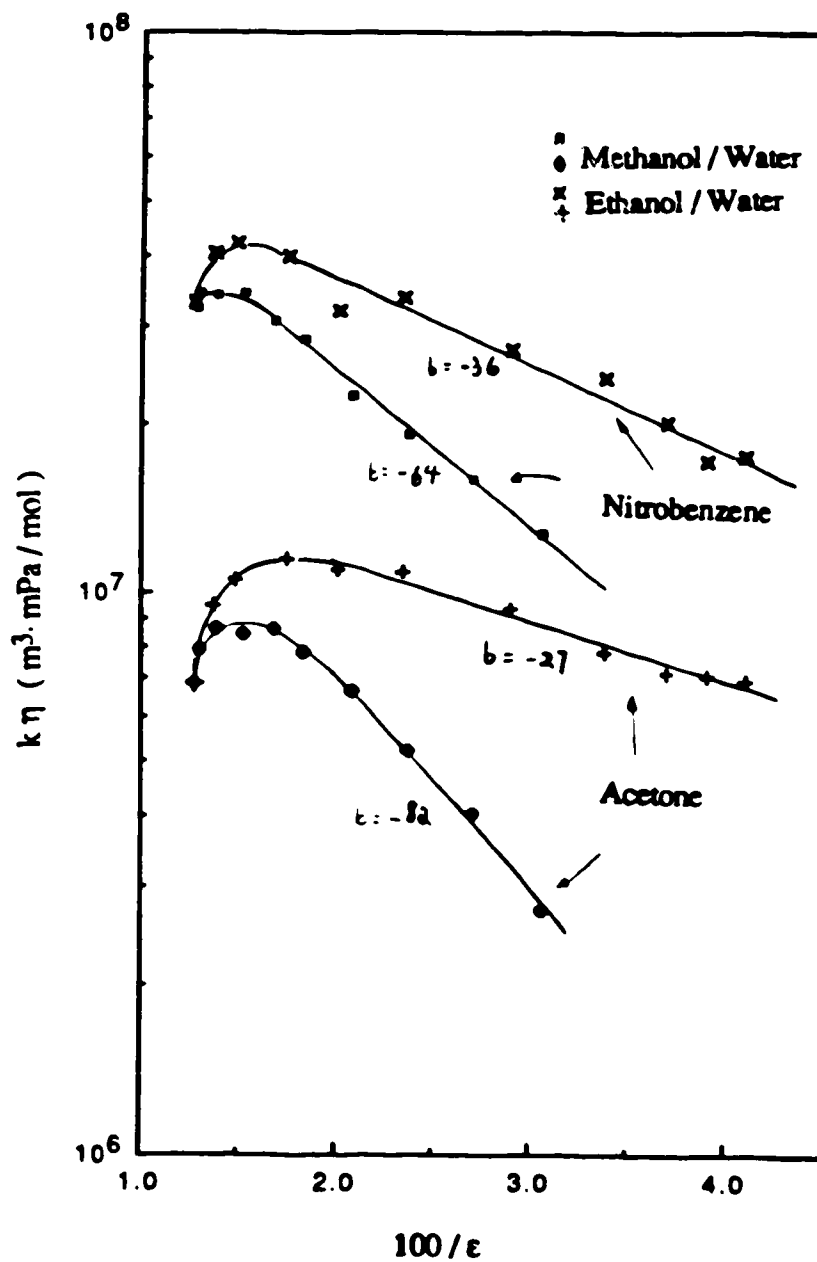


Fig.4-11 The viscosity normalized rate constants for the reaction of solvated electrons with nitrobenzene and acetone as a function of  $\epsilon^{-1}$  in methanol/water and ethanol/water mixtures at 298 K

From the transition state theory, the rate constant is related to the free energy of activation ( $\Delta G^\ddagger$ )

$$k = (k_B T / h) \exp(-\Delta G^\ddagger / RT) \quad [4-21]$$

where  $h$  is the Planck constant. The change of the viscosity normalized rate constant from one solvent to another will result in a change in free energy of activation ( $\Delta\Delta G^\ddagger$ )

$$\ln k_1 \eta_1 - \ln k_2 \eta_2 = \ln(\eta_1 / \eta_2) + \Delta\Delta G^\ddagger / RT \quad [4-22]$$

The slope of the line,  $b$ , in the  $0 \leq \chi_w \leq \chi_{\eta\max}$  region (Fig.4-11) is a measure of the sensitivity of change in free energy of activation to the change in free energy of solvation.

From equations [4-20] and [4-22]

$$\text{Slope} = b = -\left(\frac{Z^2 q^2}{8\pi\epsilon_0 r_i}\right) \left(\frac{1}{\Delta\Delta G_s^\circ}\right) \left[ \ln\left(\frac{\eta_1}{\eta_2}\right) + \frac{\Delta\Delta G^\ddagger}{RT} \right] \quad [4-23]$$

When  $b > 0$ , the change of the viscosity normalized rate constant ( $k_2 \eta$ ) is mainly due to the change of solvation of the reactants. When  $b < 0$ , the change of  $k_2 \eta$  is mainly due to the change of solvation of the transition state (activation complex).

Note that for reactions that take place in solvents of similar viscosity, an even more simple linear free energy relationship  $\Delta\Delta G^\ddagger \propto \Delta\Delta G_s^\circ$  can be obtained

$$\Delta\Delta G^\ddagger = -b \left( \frac{8\pi\epsilon_0 r_i RT}{Z^2 q^2} \right) \left( \Delta\Delta G_s^\circ \right) \quad [4-24]$$

Equation [4-25] indicates that in the case where reaction rates are only partially diffusion controlled, the inclusion of the viscosity term is required to satisfy the free energy relationship:

$$\ln \left( \frac{\eta_1}{\eta_2} \right) + \left( \frac{\Delta\Delta G^\ddagger}{RT} \right) = -b \left( \frac{8\pi\epsilon_0 r_i}{Z_i^2 q^2} \right) \Delta\Delta G_s^\circ \quad [4-25]$$

The lower values  $\ln\eta k_2$  and the greater  $1/\epsilon$  dependence in the methanol/water mixtures suggest that methanol/water mixtures can solvate the reactants better than the ethanol/water mixtures do. This agrees with the solvent effects on the optical absorption energies of solvated electrons. The  $E_{Amax}$  values of the solvated electrons in alcohol/water mixtures increase in the order of methyl > primary > secondary > tertiary (23). In alcohols, the values of  $\ln\eta k_2$  for the reaction of solvated electrons with nitrobenzene increase in the same order (Fig.4-12) (114). The negative slopes of the lines in Fig.4-11 indicate that within the same alcohol/water series, the change of free energy of activation ( $\Delta\Delta G^\ddagger$ ) is mainly due to the change of solvation of the transition state.

In the  $\chi_{\eta max} \leq \chi_w \leq 1$  region where the reactants are solvated in the microphases, the rate of the reaction is solely controlled by the rate of the diffusion of the microphases. The dielectric constants therefore have only small effect in this region. The correlation parameter  $1/\epsilon$  may also be related to the diffusion coefficients of ion in the alcohol/water mixtures (114).

The molar conductance  $\lambda_i$  of ions  $i$  is related to their mobility  $\mu_i$

$$\lambda_i = Z_i F \mu_i \quad [4-26]$$

where  $Z_i$  is the number of charges  $q$  on the ion,  $F=N_A q$  is the Faraday. The diffusion coefficient  $D_i$  is related to the mobility (eqn.[4-4]) and therefore to the molar conductance

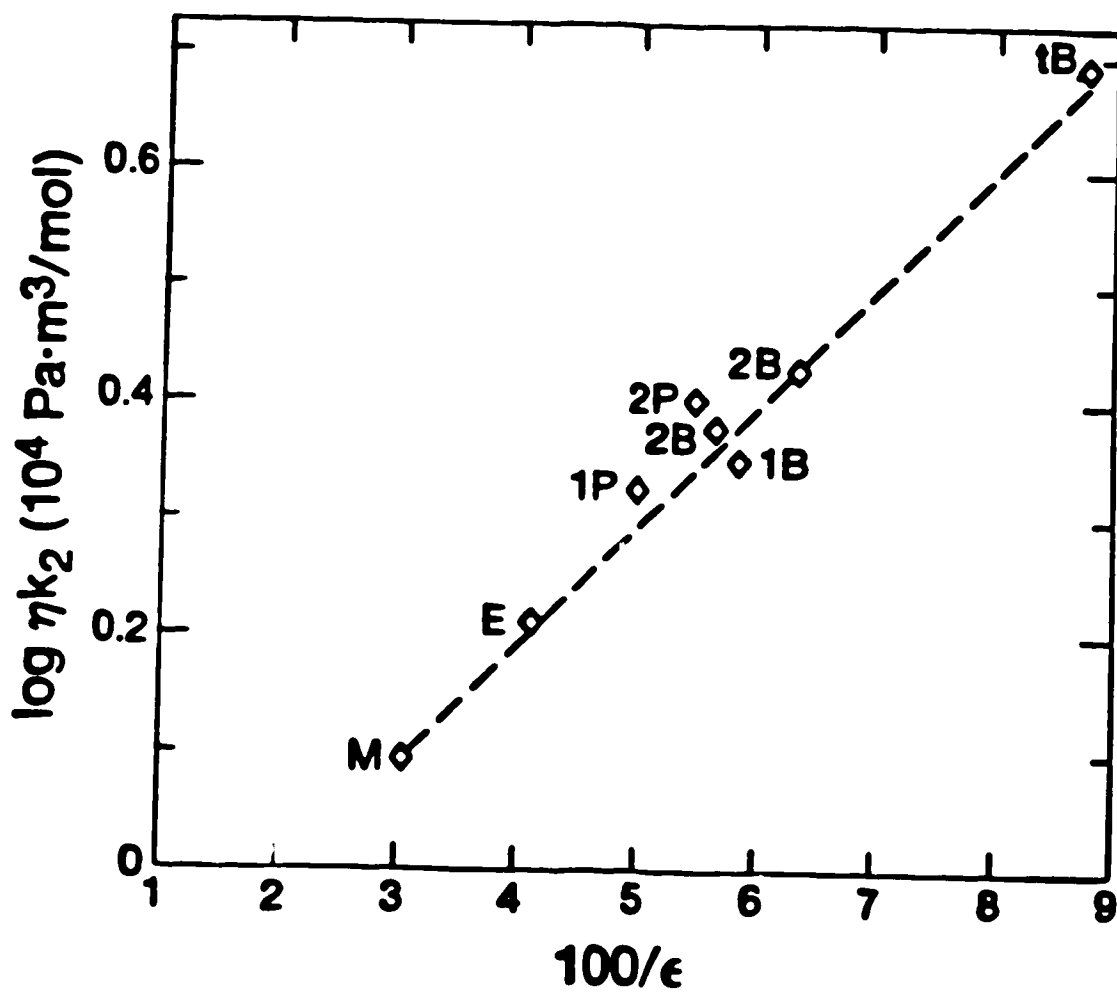


Fig.4-12 The viscosity normalized rate constants for the reaction of solvated electrons with nitrobenzene as a function of  $\epsilon^{-1}$  in alcohol at 298 K (Ref.114)

( M, methanol; E, ethanol; 1P,1-propanol; 2P, 2-propanol,  
1B, 1-butanol; 2B, 2-butanol; tB, t-butyl alcohol )



$$D_i = \frac{\lambda k_B T}{Z_i N_A q^2} \quad [4-27]$$

The solvation and diffusion of ions are influenced by the extent of solvent-solute interactions in the microenvironment. The similarity between the plots of  $\eta k_2$  against  $\epsilon^{-1}$  for the nearly diffusion controlled reactions (Fig. 4-11) and the plots of  $\eta \lambda_0$  against  $\epsilon^{-1}$  (Fig.4-13)(114) for a number of ions (including solvated electrons) in ethanol/water mixtures indicates that solvation and diffusion of ions may be related in a parallel manner. It is interesting to note that the values of  $\eta \lambda_0$  for ethoxide and electron in ethanol/water mixtures are identical, which indicates that solvated electrons diffuse like ethoxide ions in ethanol/water mixtures (29,114,160).

## 2. Inefficient Organic Electron Scavengers

The rate constants for phenol and toluene are three orders of magnitude lower than that of the nitrobenzene, therefore the kinetics of these reactions are not diffusion controlled. The viscosity of the medium however might still play some role to influence the course of the reaction. The protonation of the radical anion, for example, may involve molecular motions of the solvent molecules, which can be affected by the solvent viscosity. The negative slopes in the plots of  $\log k_2$  against  $\log \eta$  for the reaction of solvated electrons with phenol and toluene in methanol/water (Fig.4-14) and ethanol/water (Fig.4-15) mixtures may be partly due to this effect. The different viscosity dependences of rate constants for phenol and toluene in the alcohol/water mixtures illustrate that solute-solvent interactions are important.

The low rate constants for inefficient scavengers are due to the low probability of reaction of the encounter pair. When the electron affinity of the scavenger is low, a larger solvation energy of the electron decreases the probability that the electron would transfer from the solvent trap to the solute. The solvation energy of the electron (the electron trap

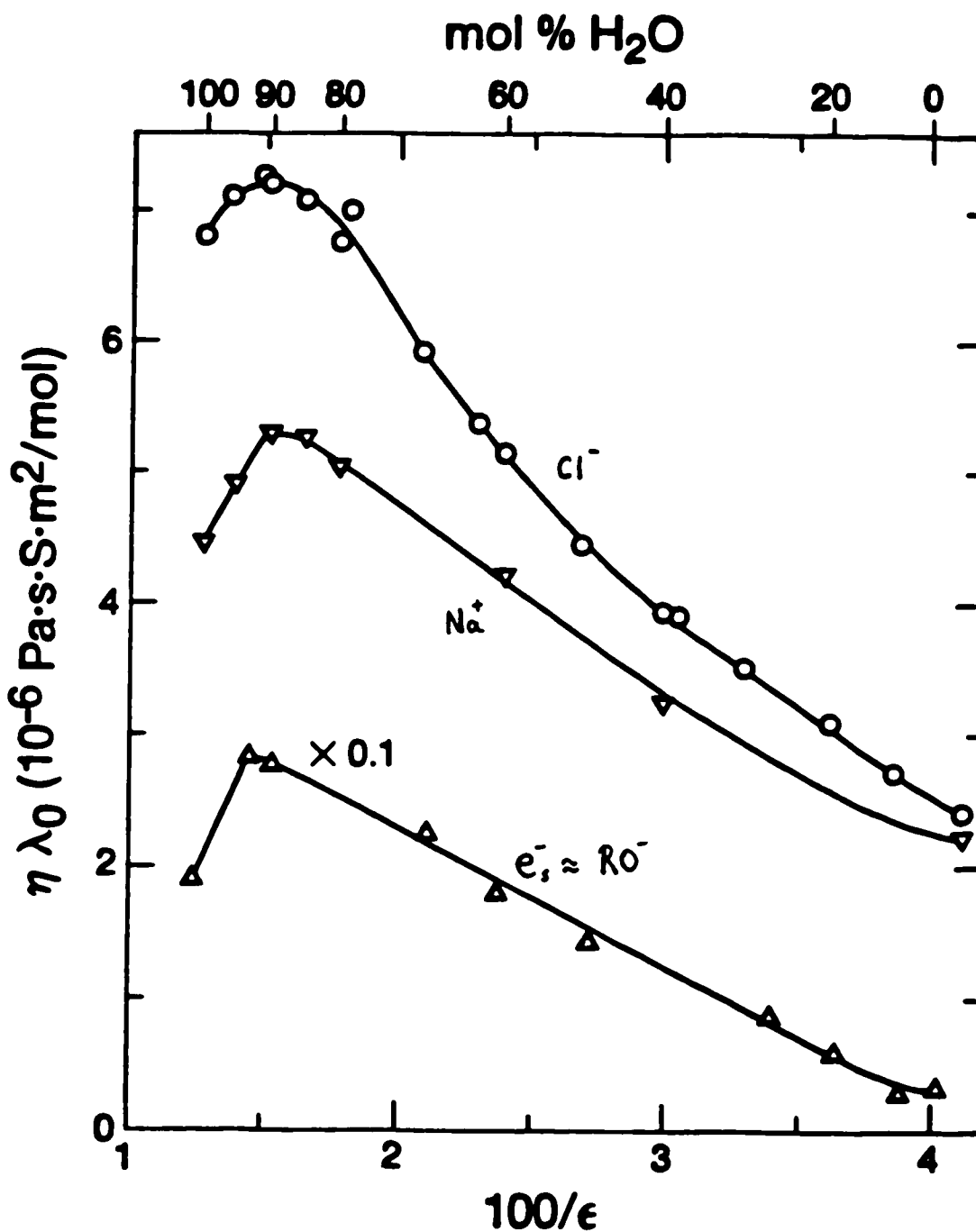


Fig.4-13 The viscosity normalized limiting molar conductance of some ions as a function of  $\epsilon^{-1}$  in ethanol/water mixtures at 298 K (Ref.114)

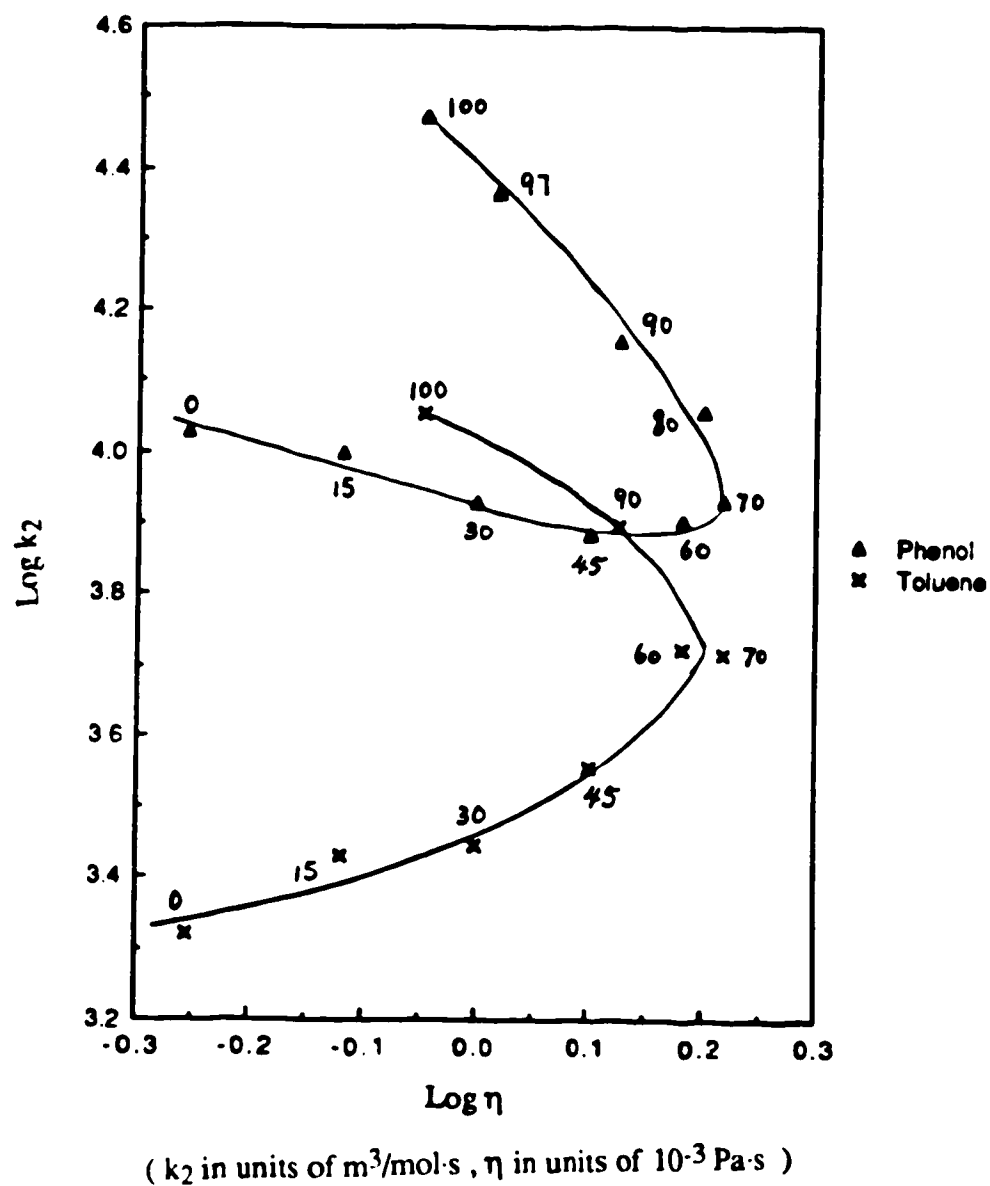


Fig.4-14 The viscosity dependence of the second-order rate constants for the reaction of solvated electrons with phenol and toluene in methanol/water mixtures at 298 K

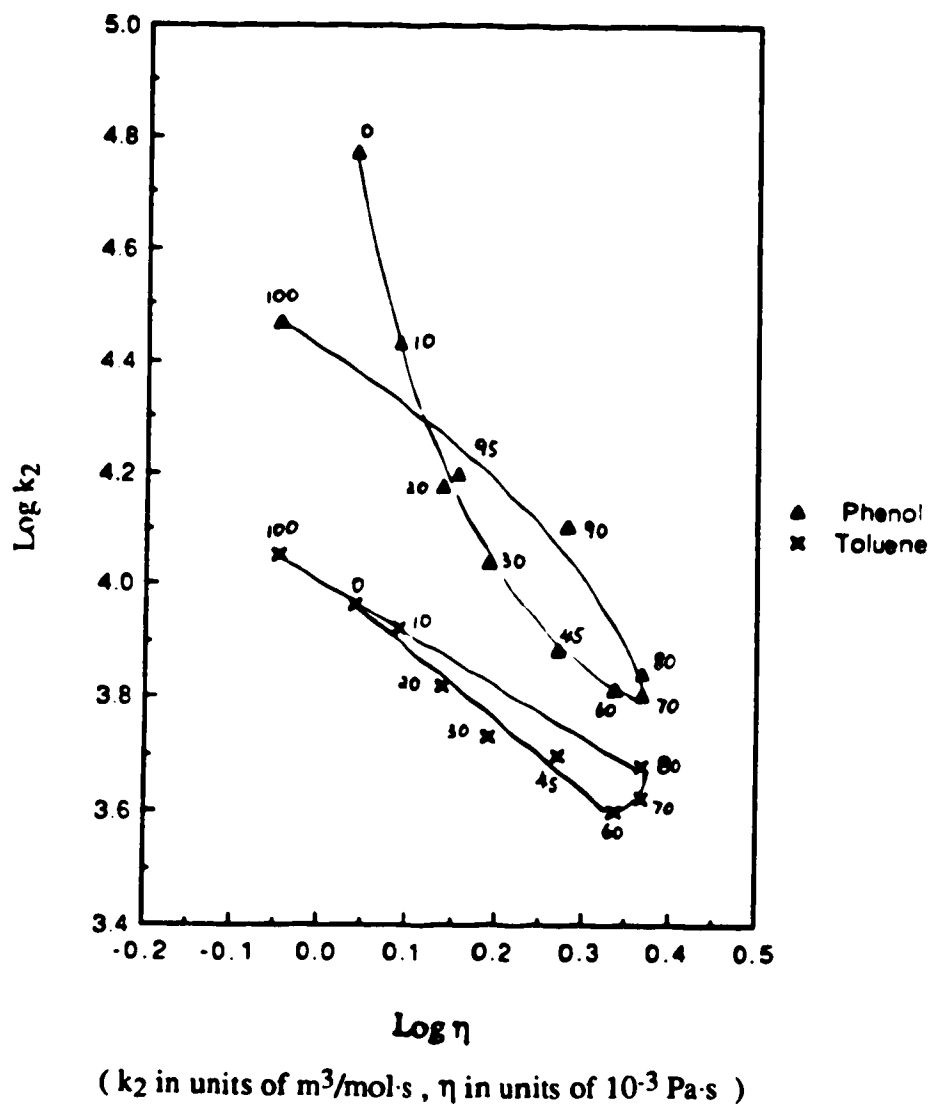


Fig.4-15 The viscosity dependence of the second-order rate constants for the reaction of solvated electrons with phenol and toluene in ethanol/water mixtures at 298 K

depth) therefore is important. The electron trap depth in the solvent is related to the optical absorption energy (12). The breadth of the optical absorption band indicates that all of the electrons are not in traps of the same depth. The electrons that have the lowest excitation energies have the greatest reactivity with inefficient scavengers (99,100). For kinetic purposes, the optical absorption energy at half-height ( $E_T$ ) has been used as an indicator of trap depth for the more reactive electron (26,52,99,161,162):

$$E_T = E_{Amax} - W_r \quad [4-28]$$

where  $E_{Amax}$  is the energy at maximum absorption and  $W_r$  is the width of the band on the low energy (red) side at half-height (Fig.4-16). The composition dependences of the optical absorption energies of solvated electrons for methanol/water and ethanol/water mixtures (52) are shown in Fig. 4-17 and Fig. 4-18, respectively.

Dividing  $k_2$  by the nearly diffusion controlled constant  $k_N$  of nitrobenzene displays the effect due to factors other than diffusion. The ratio  $k_2/k_N$  is an indication of the encounter efficiency of the reaction, assuming the encounter efficiency with nitrobenzene is unity. The logarithm of  $k_2/k_N$  can be related to the free energy of activation for the electron scavenging step. The reactants in an electron scavenging reaction first approach each other by diffusion (98) :



And then react together within the encounter complex :



The observed rate constant for electron capture is

$$k_2 = \frac{k_{29} k_{30}}{k_{-29} + k_{30}} \quad [4-31]$$

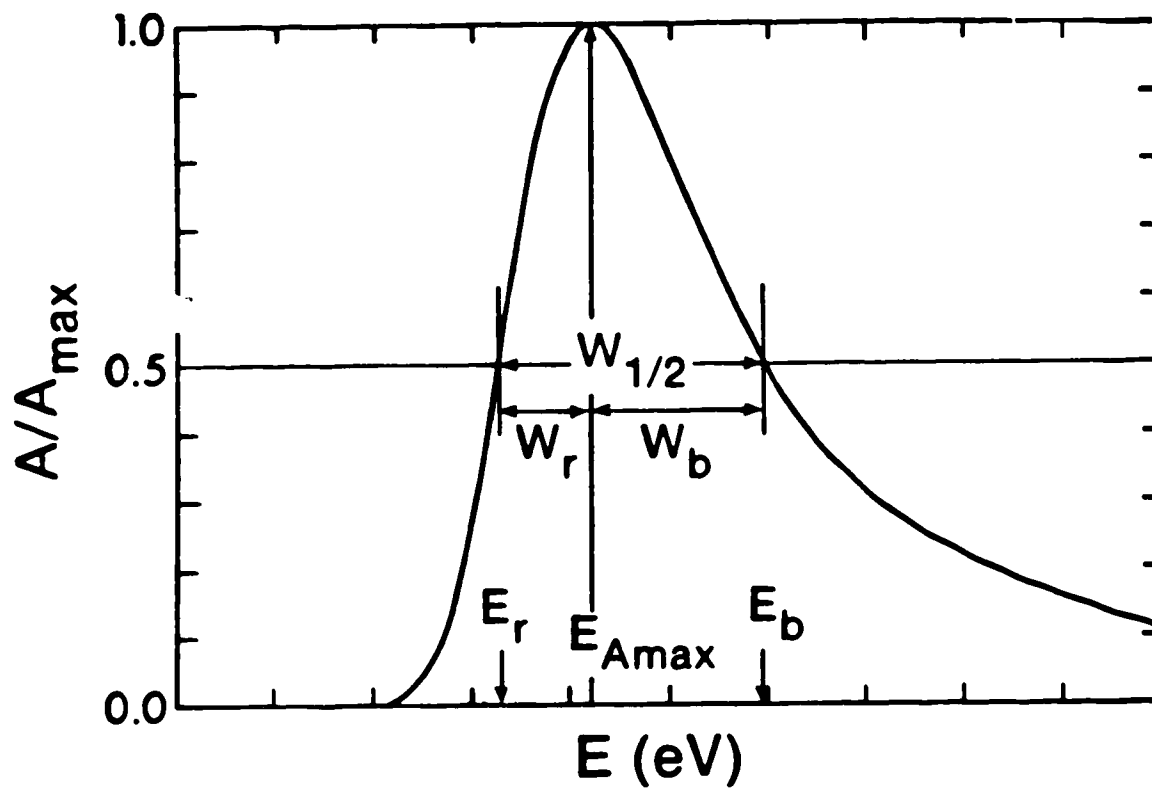


Fig.4-16 The relationship between  $E_{A_{\max}}$  and  $E_r$  in the optical absorption spectrum of solvated electrons

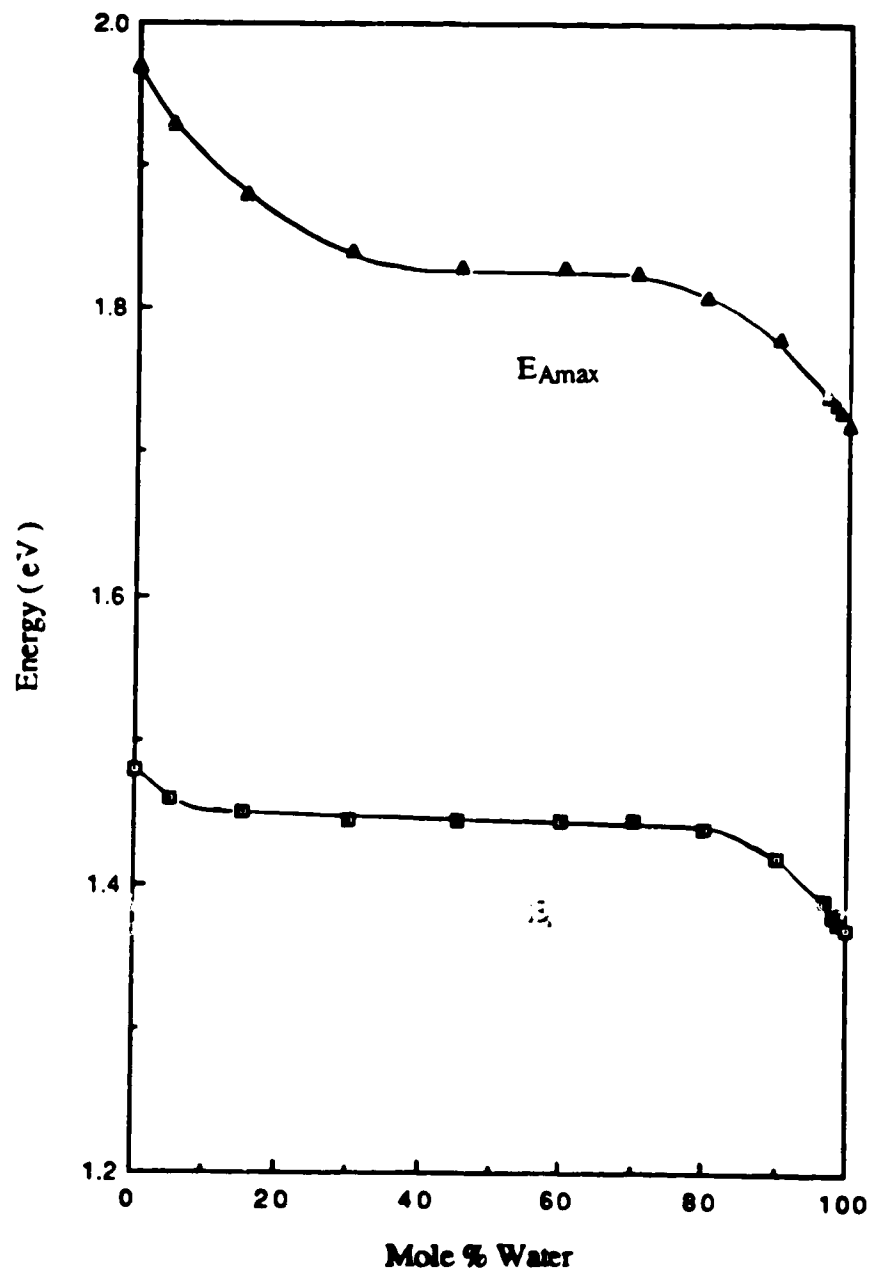


Fig.4-17 The composition dependence of the optical absorption energies of solvated electrons in methanol/water mixtures at 298K (Ref.52)

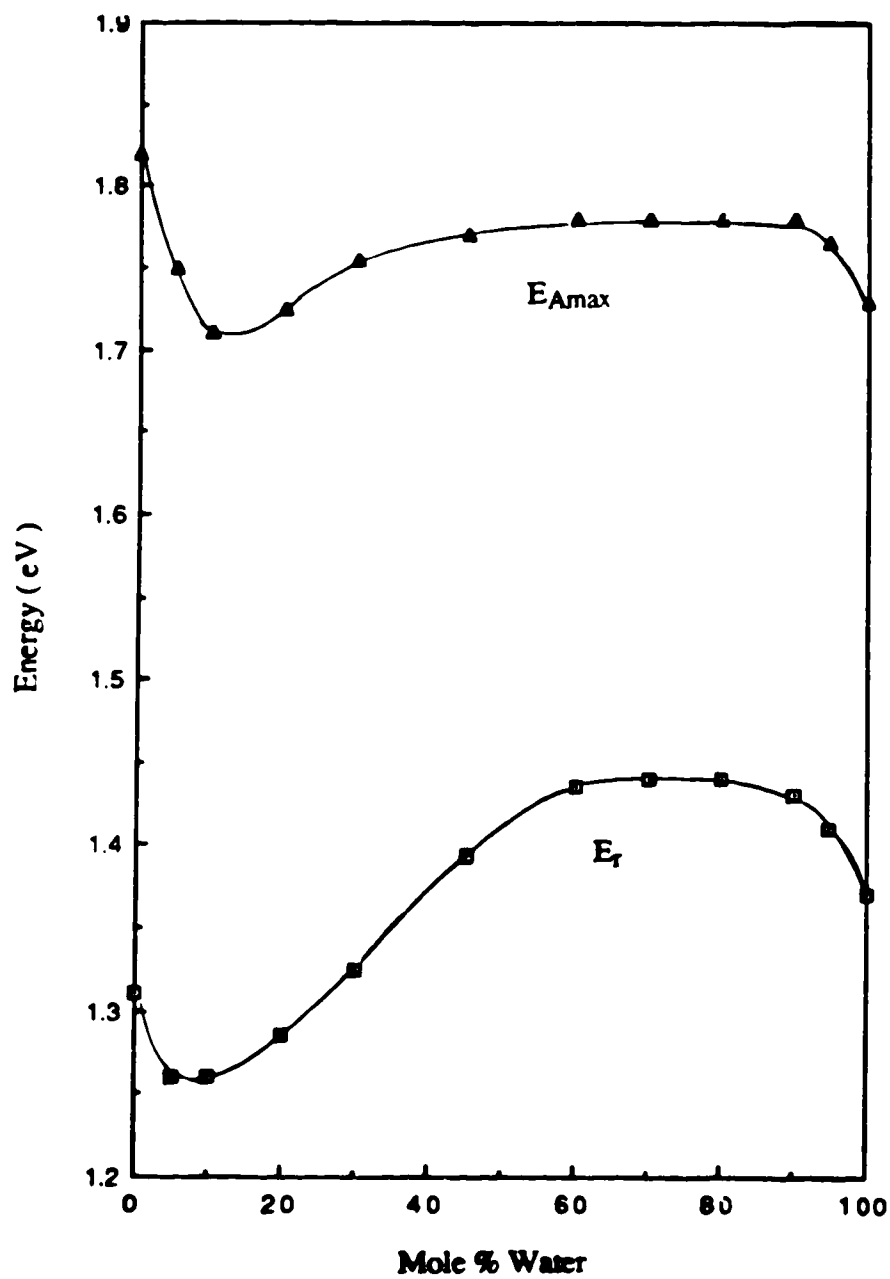


Fig.4-18 The composition dependence of the optical absorption energies of solvated electrons in ethanol/water mixtures at 298K (Ref.52)



Since the rate constant for nitrobenzene  $k_N$  is nearly diffusion controlled, in this case  $k_{30} > k_{29}$  and  $k_N \approx k_{29}$ . The rate constant  $k_2$  for an inefficient scavenger is mainly determined by factors which affect the step in equation [4-30]. Equation [4-31] can be rewritten as

$$\frac{1}{k_2} = \frac{1}{k_{29}} + \frac{k_{29}}{k_{29}k_{30}} \quad [4-32]$$

Since  $k_N \approx k_{29}$ ,

$$\frac{k_N}{k_2} = 1 + \frac{k_{29}}{k_{30}} \quad [4-33]$$

For the inefficient scavengers  $k_{29} \gg k_{30}$ , thus

$$\frac{k_2}{k_N} = \frac{k_{30}}{k_{29}} \quad [4-34]$$

According to the transition state theory

$$k = \frac{k_B T}{h} e^{-\Delta G^\ddagger / RT} \quad [4-35]$$

therefore

$$\ln \left( \frac{k_2}{k_N} \right) = \left( \Delta G_{29}^\ddagger - \Delta G_{30}^\ddagger \right) / RT \quad [4-36]$$

As  $k_{29} \gg k_{30}$ ,  $\Delta G_{30}^\ddagger \gg \Delta G_{29}^\ddagger$  and

$$\ln \left( \frac{k_2}{k_N} \right) = -\Delta G_{30}^\ddagger / RT \quad [4-37]$$

The logarithm of  $k_2/k_N$  of phenol and toluene is plotted against  $E_T$  for the ethanol/water mixtures (Fig.4-19). The inverse correlations between  $\ln(k_2/k_N)$  and  $E_T$  in the  $0.1 \leq \chi_w \leq 1.0$  region indicate that the decrease of the encounter efficiencies is due to the increase of electron trap depth. In the  $0 \leq \chi_w \leq 0.1$  region, the encounter efficiencies of phenol and toluene do not increase in spite of the decrease in  $E_T$ . This phenomenon has also been observed in the 1-propanol and 1-butanol/water systems and was interpreted in terms of solvent structure effects (112,113). In the primary alcohol/water mixtures, the addition of 10 mole % of water into alcohol produces hydrogen-bonded structures that make the hydrogens of the hydroxyl groups less accessible to the electron (23). Thus the  $E_T$  decreases. Since these protons are also needed to stabilize electro capture by phenol and toluene, by protonation of the anion:



The hydrogen-bonded structure makes the protons of the hydroxyl groups less accessible to  $S^-$ . The slow down of the protonation step therefore offsets the trap-depth effects on the encounter efficiency in this region.

In methanol/water mixtures, the  $E_T$  dependence of the encounter efficiency for phenol is different from that of the toluene (Fig.4-20). The encounter efficiency of phenol is inversely related to  $E_T$  in the water-rich region, whereas for toluene, this occurs in the alcohol-rich region. The stabilization of the activation complex may have a counter effect to neutralize the effect of  $E_T$ . This is evidenced from the  $E_T$  independence of the encounter efficiency in the alcohol-rich region for phenol, and in the water-rich region for toluene. When the trap-depth effects are small, as indicated by the same value of  $E_T$  in 70-30 mole % of water in methanol, the solvation effect on the activation complex can manifest itself as a large drop in encounter efficiency. This was observed in the case of toluene.

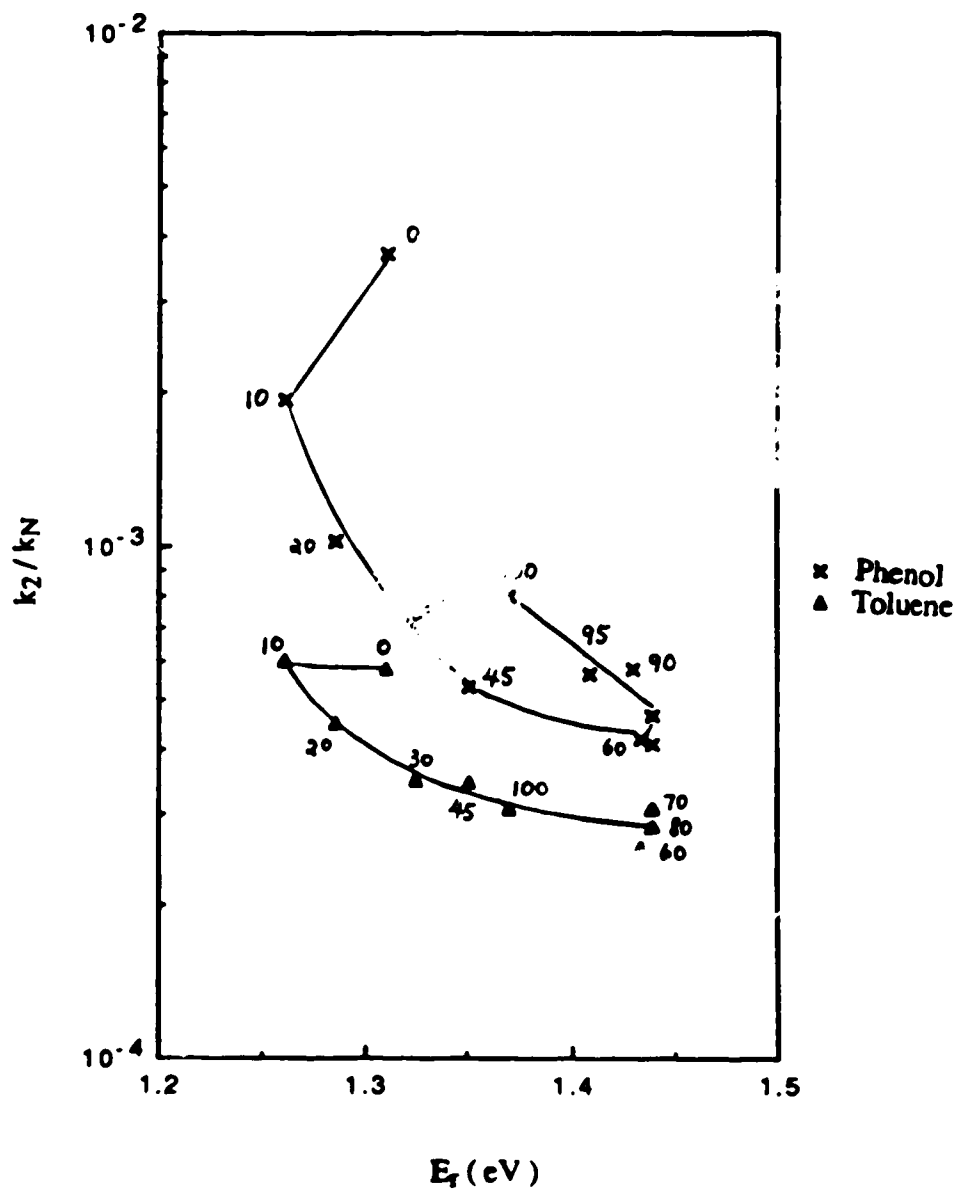


Fig.4-19 Encounter efficiency for inefficient scavenger against solvated electron trap depth in ethanol/water mixtures at 298K

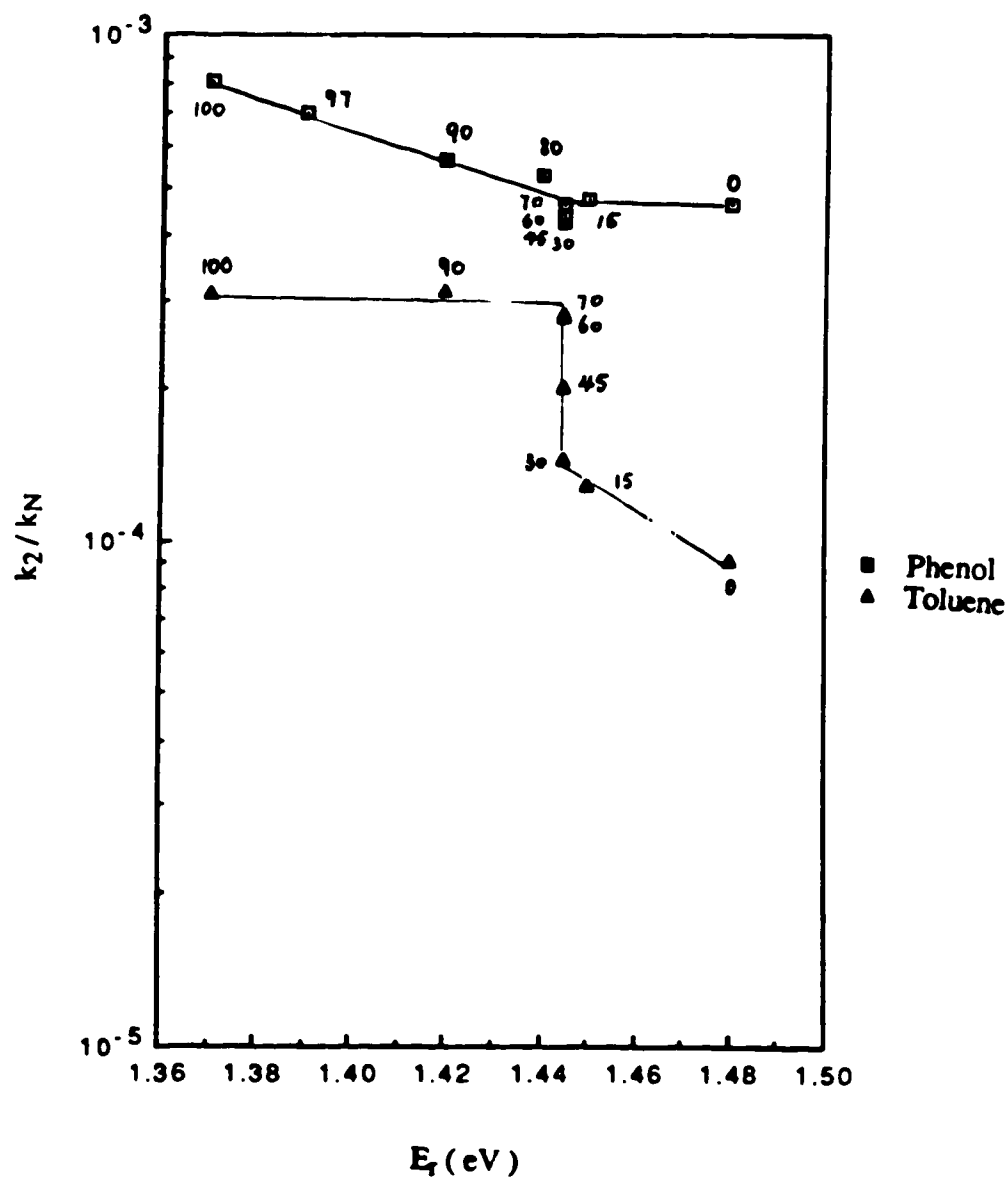


Fig.4-20 Encounter efficiency for inefficient scavenger against solvated electron trap depth in methanol/water mixtures at 298K

### 3. Energies and Entropies of Activation

The difference of reactivity between efficient and inefficient scavengers are generally due to changes of entropy rather than of energy. The composition dependence of the activation energy ( $E_a$ ) for the reactions with the efficient scavengers are different from that of the inefficient scavengers (Fig.4-21 and Fig.4-22). The similarity between the composition dependence of  $E_a$  for the efficient scavengers and the energy of viscous flow of liquid ( $E_\eta$ ) (Fig.4-23) emphasizes the importance of diffusion effects on the efficient reactions. The diffusion efficiency of the reactions therefore parallels the ease of liquid flow. The  $E_\eta$  values however are greater than the  $E_a$  values, which implies that the diffusion of the reactants is easier than the viscous flow. This is reasonable because the deformable solvated electron is more diffusive than normal molecules.

For the slower reactions, solvated electrons and the scavenger molecules diffuse together many times before a successful reaction can take place. The rate of the reaction therefore is not limited by the rate of diffusion. In the water-rich ethanolic solvents, the  $E_a$  values for phenol and toluene are lower or similar to that of the efficient scavengers. This suggests that the reaction between solvated electrons and inefficient scavengers might proceed within the encounter complex  $[e_s^-, S]$  (98).



The low values of  $E_a$  for the inefficient reactions in the water-rich solvents can be explained if the complex formation step is energetically favorable enough to compensate for the energy requirement for the electron capture step (Scheme I).

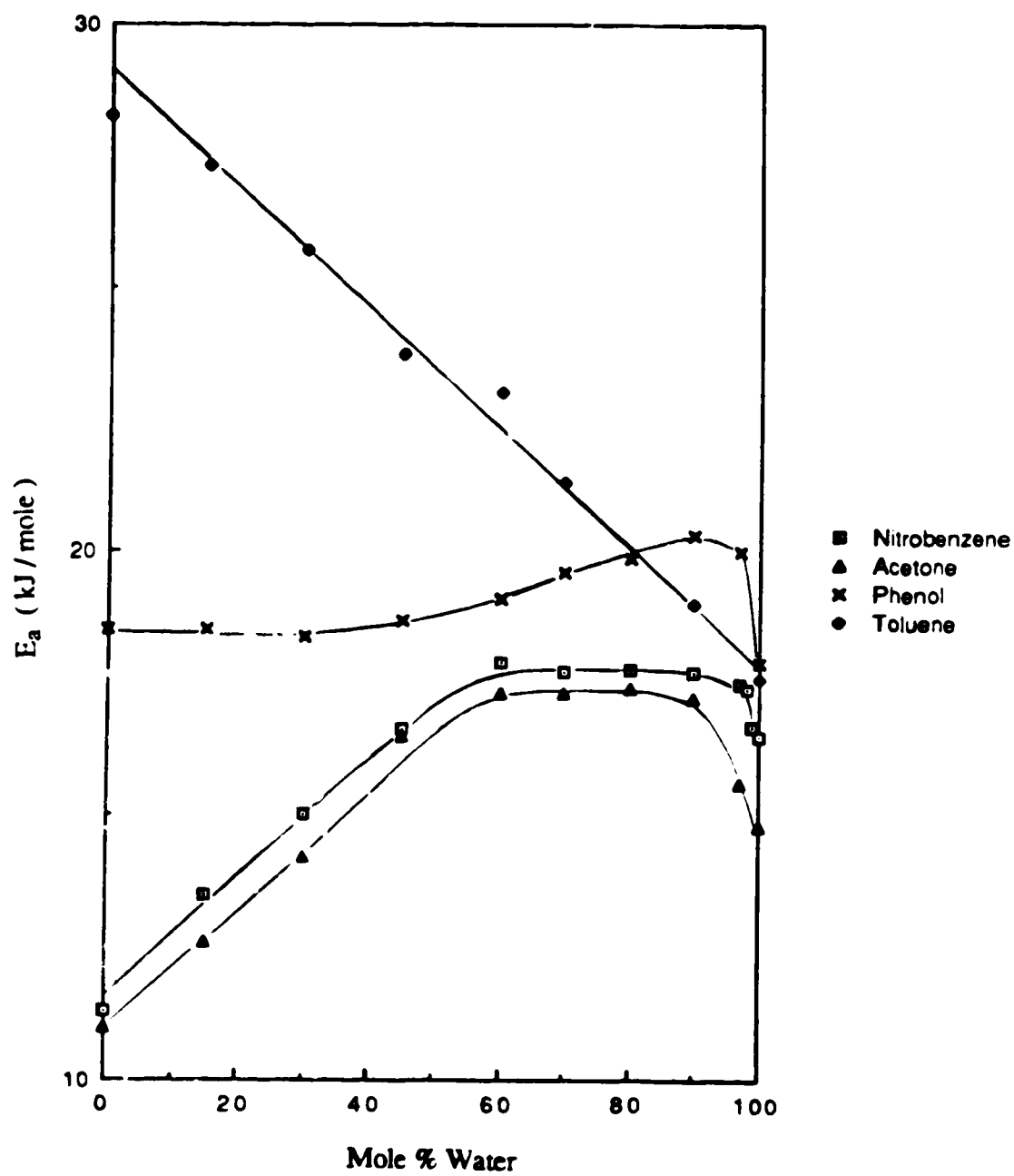


Fig.4-21 The composition dependence of the activation energies for the reaction of solvated electrons with organic electron-scavengers in methanol/water mixtures

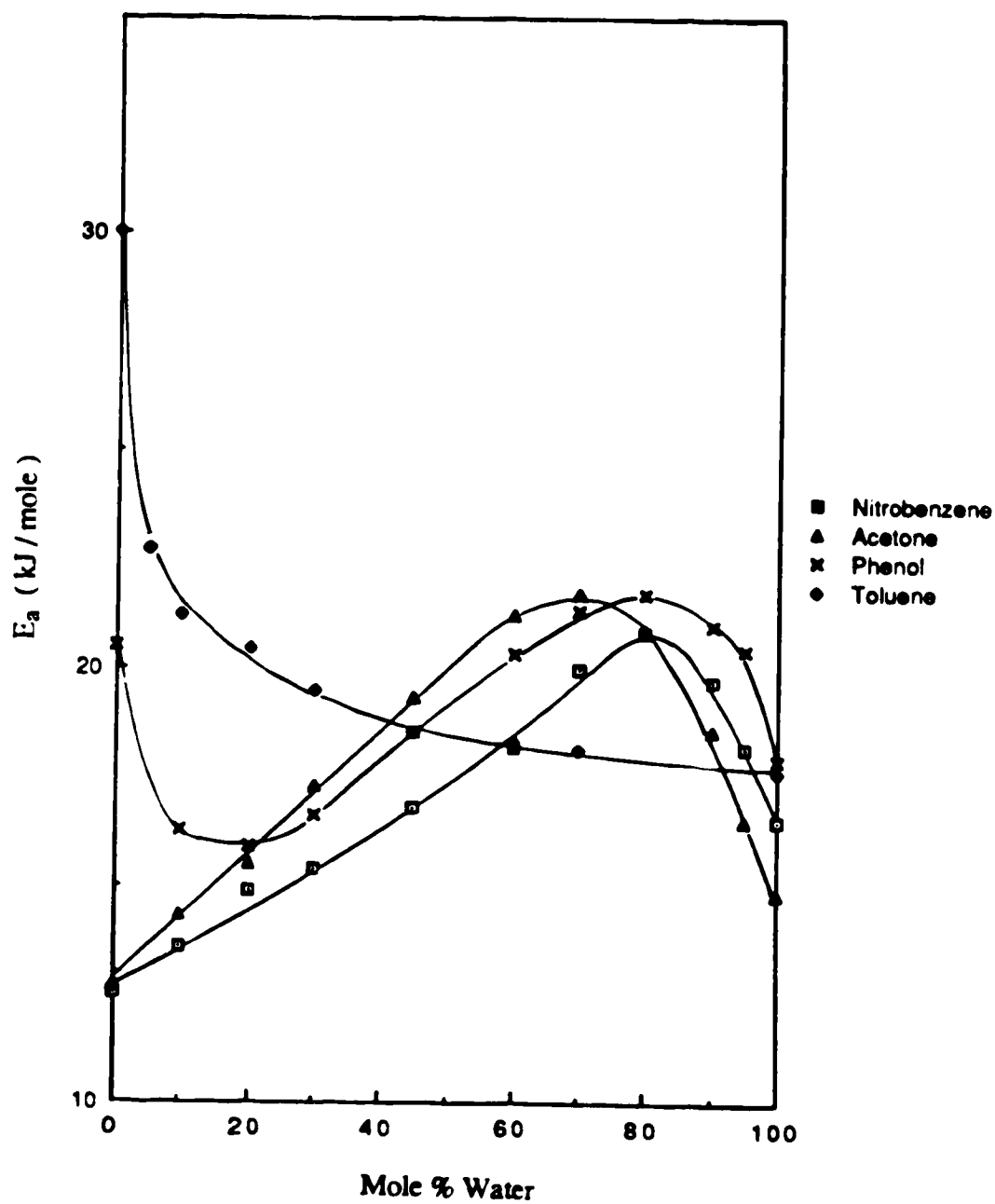


Fig.4-22 The composition dependence of the activation energies for the reaction of solvated electrons with organic electron-scavengers in ethanol/water mixtures

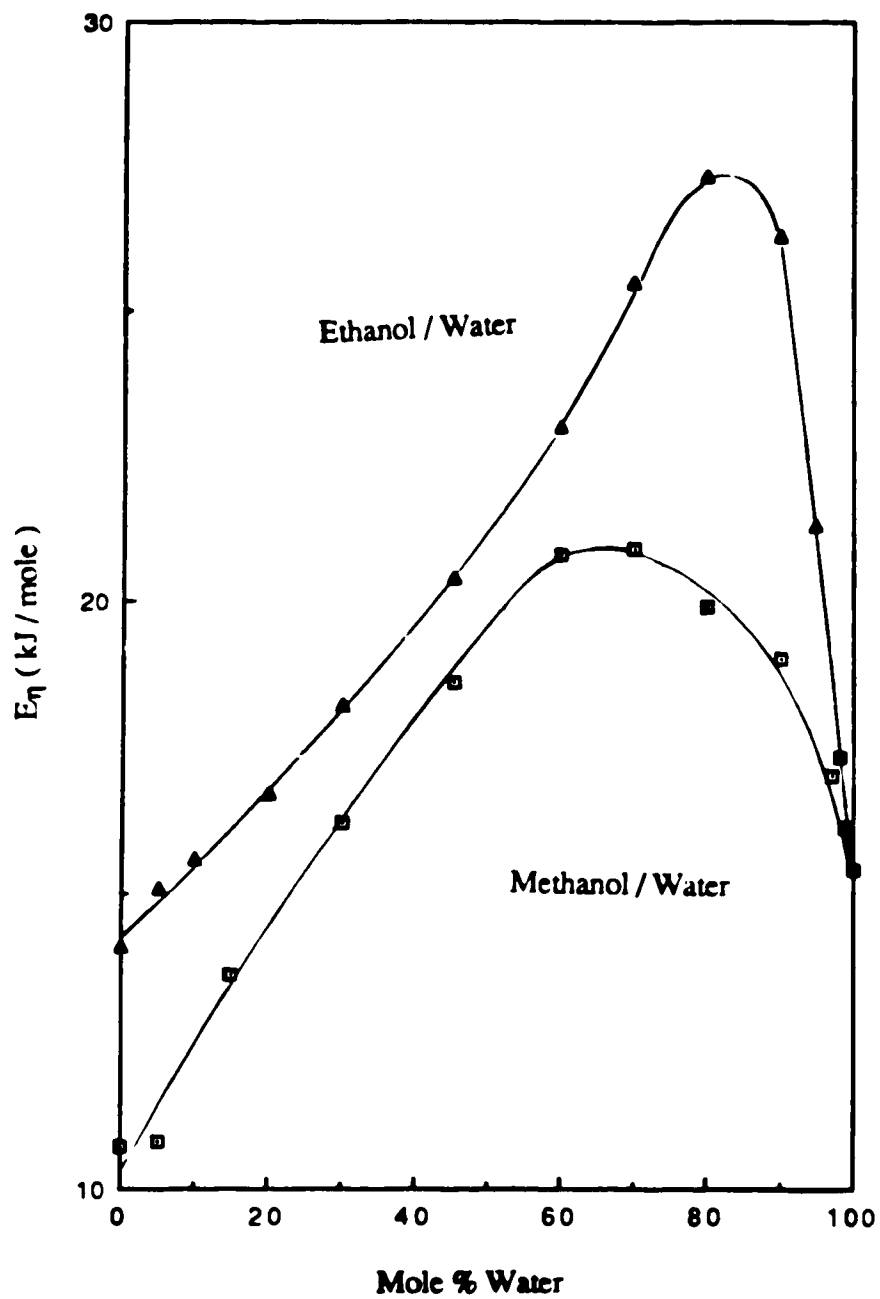
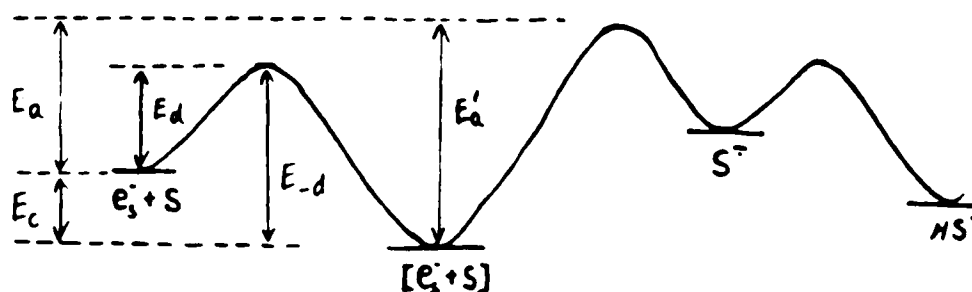


Fig.4-23 The composition dependence of the energies of viscous flow in methanol/water and ethanol/water mixtures at 298K (Ref.148)



## Scheme I



This mechanism not only allows the activation energy for the electron-capture step ( $E_a'$ ) to be much higher than that for the efficient scavengers (or the energy of diffusion of the reactants,  $E_d$ ), it also permits the apparent activation energy ( $E_a$ ) to be similar to that of the efficient scavengers. When  $E_a' \geq E_d$ , the apparent activation energy is given by

$$E_a = E_a' + E_c \quad [4-40]$$

where  $E_c$  is the enthalpy change for the  $[e_s^-, S]$  formation step.

In the alcohol-rich region, the  $E_a$  values for the reactions with inefficient scavengers are much higher than that with the efficient scavengers. This suggests that (i) the protonation step (equation [4-39]) is gradually becoming more important towards the alcohol direction and/or (ii) the exothermicity of the complex formation step decreases in the alcohol direction. Since toluene is only slightly soluble in water, the high exothermicity of complex formation in the water-rich region is mainly due to the solvation of the complex. In alcohol, the complex formation step is less exothermic (or even endothermic) when the ground state can be better solvated. The  $E_a$  for the reactions with toluene therefore increases in the alcohol direction.

The  $E_a$  values for the reaction of solvated electrons with toluene are higher in the methanol/water mixtures than in the ethanol/water mixtures. This suggests that the complex formation in the ethanol/water mixtures is energetically more favorable. The fact that the  $E_a$  values of toluene are lower than those of the other scavengers in the water-rich ethanol solvents indicates that in the hydroxylic solvents, the non-polar solute can diffuse more easily than the polar solutes.

The degree of exothermicity of the complex formation step depends on the interaction between scavenger and the solvent molecules. Phenol and its complex both have a hydroxyl group that can hydrogen bond with the solvent molecules. The variation of exothermicity with solvent composition for the complex formation step is therefore less extensive than that of the toluene.

The observation that some of the Arrhenius plots for the phenol (Figs.3-7,3-16) and toluene (115) reactions are curved downward at high temperatures is also consistent with this mechanism. At elevated temperatures, the equilibrium for  $[e_s^-, S]$  formation is driven to the reverse direction, the concentration of the complex is reduced, and results in a rate that is slower than predicted by the Arrhenius law for the temperature dependence of reaction rate constants.

The composition dependence of the entropy of activation ( $\Delta S^\ddagger$ ) is also similar to  $E_a$  (Fig.4-24 and Fig.4-25). Because diffusion is driven by the random motion of the liquid molecules, entropies of activation for the reactions with efficient scavengers are more positive. Entropies of activation are negative for the inefficient scavengers which indicates that the activation complex exerts more electrostriction on the surrounding solvent molecules than is exerted by the reactants. In the transition state, the electron is being absorbed by the scavenger molecule, so that the negative charge is more localized (and therefore more concentrated) than a ground state solvated electron where the charge can be spread over several solvent molecules.

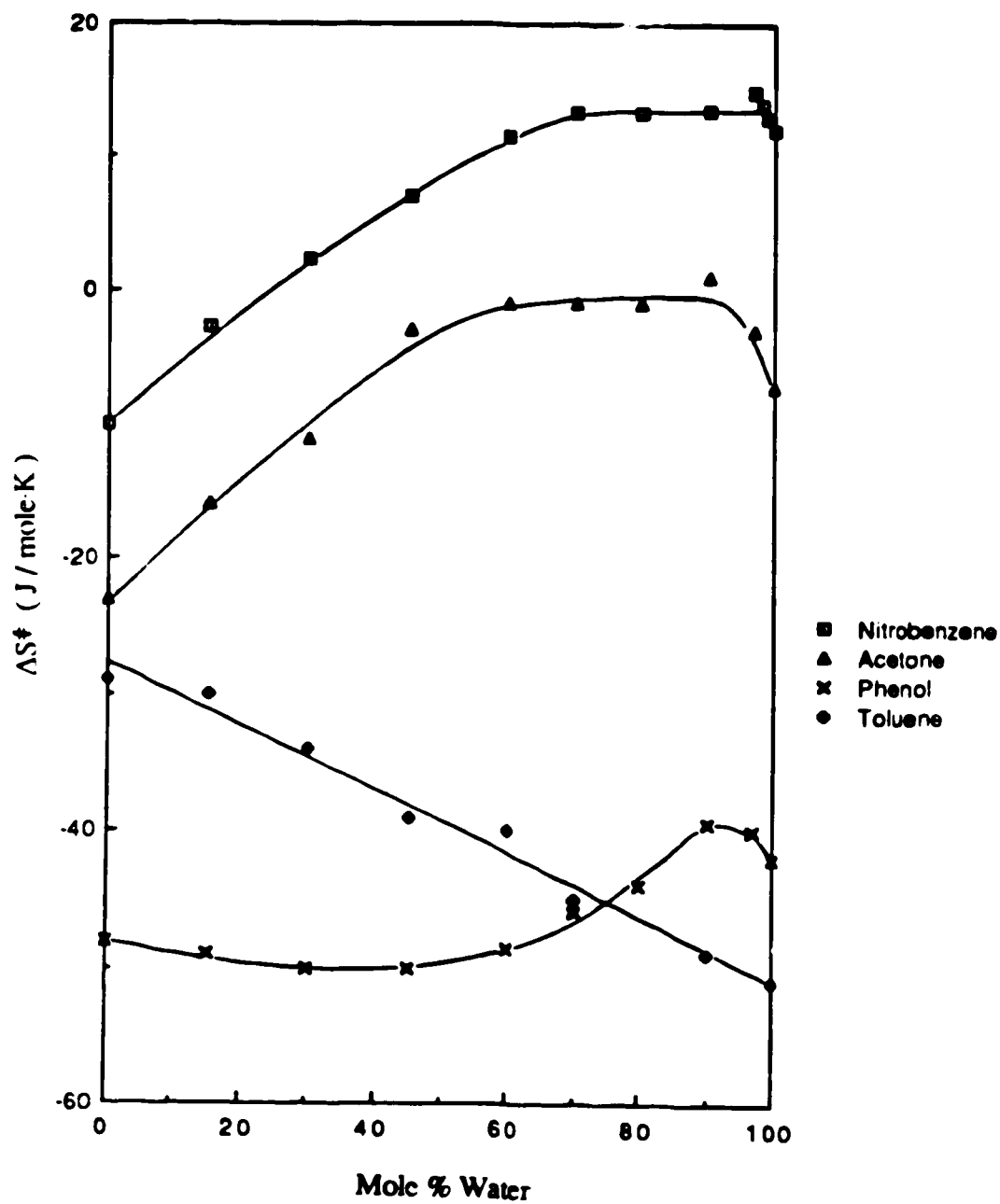
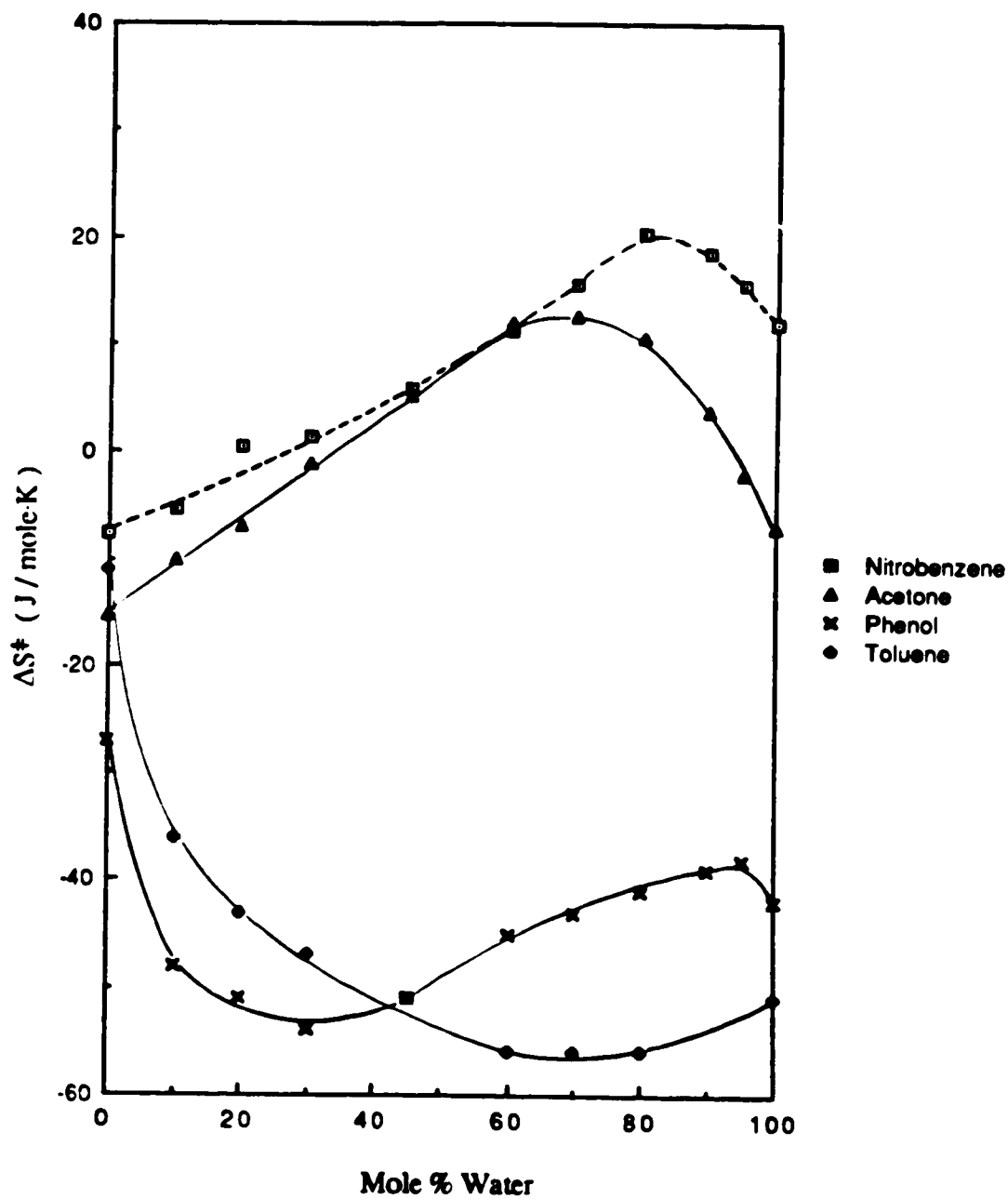


Fig.4-24 The composition dependence of the entropy of activation for the reaction of solvated electrons with organic electron-scavengers in methanol/water mixtures



**Fig.4-25** The composition dependence of the entropy of activation for the reaction of solvated electrons with organic electron-scavengers in ethanol/water mixtures

In the water dominated solvents, the difference of reactivity between efficient and inefficient scavengers in the water-rich region are due to changes of entropy rather than of energy. The  $\Delta S^\ddagger$  values for reaction between solvated electrons and inefficient scavengers are about 50 J/mol.K more negative than that for nitrobenzene. The  $E_a$  for the reactions of inefficient scavengers are within  $\pm 2$  kJ/mol of that for nitrobenzene. Therefore solvent rearrangement can make important contributions to the free energy of activation (163,164) in the slow electron-capture reactions.

The entropies of activation for the reactions with toluene are less negative towards the alcohol direction, which suggest that the gain in electrostriction on going from the ground state to the transition state decreases in that direction. This indicates that the encounter complex resembles the activation complex more closely in alcohol than in water. Toluene is different from the other scavengers in that it does not hydrogen bond with the solvent. It also has a low electron affinity. The capture of solvated electrons by such a scavenger depends upon the occurrence of a favorable configuration of solvent dipoles about the reaction site. The more negative entropy of activation in the water-rich region may also indicate a lower probability of this occurrence.

## II Reactions with Inorganic Electron Scavengers

The kinetics of the reaction of solvated electrons with silver perchlorate, copper(II) perchlorate, lithium nitrate and lithium chromate were also investigated in this study. From the conductivity measurements, it was found that the specific conductances increased linearly with the electrolyte concentration (Figs.3-36 to 3-39, 3-45 to 3-48), which indicates that these inorganic salts are completely dissociated under the experimental conditions. Since the second-order rate constants for the reactions of solvated electrons with perchlorate and lithium ions are less than  $10^5$  m<sup>3</sup>/mol.s (134), the observed rate constants of  $\sim 10^7$  m<sup>3</sup>/mol.s are due to  $\text{Ag}^+$ ,  $\text{Cu}^{2+}$ ,  $\text{NO}_3^-$  and  $\text{CrO}_4^{=}$ .

### 1. Positively Charged Scavengers

The reactivities of solvated electrons with the positively charged scavengers display smaller composition dependence than those with a negative charge (Figs.4-26 and 27).

The viscosity dependences of the rate constants for the reaction of solvated electrons with  $\text{Ag}^+$  are similar to that of the nitrobenzene (Figs.4-28 and 4-29). In the water-rich region where  $\chi_{\eta\text{max}} \leq \chi_w \leq 1$ , the  $k_2$  values for the nitrobenzene and  $\text{Ag}^+$  reaction are very similar. The inverse relationship between  $\log\eta$  and  $\log k_2$  can be interpreted in terms of the solvation of the reactants in the microphases that were discussed earlier. In the  $0 \leq \chi_w \leq \chi_{\eta\text{max}}$  region, the viscosity dependences of  $k_2$  for the nitrobenzene and  $\text{Ag}^+$  reactions are also similar. This suggests that the diffusion radii for nitrobenzene and  $\text{Ag}^+$  have similar composition dependence. The composition dependences of the relative effective radii of diffusion,  $r_w/r$ , calculated from [4-16] using a reaction radius of 1.0 nm for the reaction with  $\text{Ag}^+$  (118) in methanol/water and ethanol/water mixtures, are shown in Fig.4-30 and Fig.4-31, respectively. The nitrobenzene values are also included for comparison. The diffusion radii increase in the alcohol direction. The fact that the smaller  $\text{Ag}^+$  ion (149) has a similar or larger diffusion radius than that of the nitrobenzene indicates that  $\text{Ag}^+$  can drag a larger number of solvent molecules by electrostriction during its diffusion. The drag of a polar solvent upon ion diffusion in  $\text{CH}_2\text{Cl}_2$  is probably related to the solvent dipole reorientation time or dielectric relaxation time ( $\tau$ ). Unfortunately,  $\tau$  values for the alcohol/water mixtures are not available. At 298 K, the  $\tau$  values are 9ps in water, 50ps in methanol and 130ps in ethanol (165).

The composition dependence of the relative effective diffusion radii ( $r_w/r$ ) for the  $\text{Ag}^+$  and  $\text{Cu}^{2+}$  reactions are shown in Fig.4-32 and 4-33, respectively. The similar  $r_w/r$  values in the alcohol-rich solvents may suggest that (i) upon diffusion,  $\text{Ag}^+$  and  $\text{Cu}^{2+}$  can drag more solvent molecules in the methanol/water mixtures than in the ethanol/water mixtures or (ii) the cations are solvated mostly by the water molecules in the solvent mixtures. In the water-rich solvents, the diffusion radii in methanol/water mixtures are larger than those

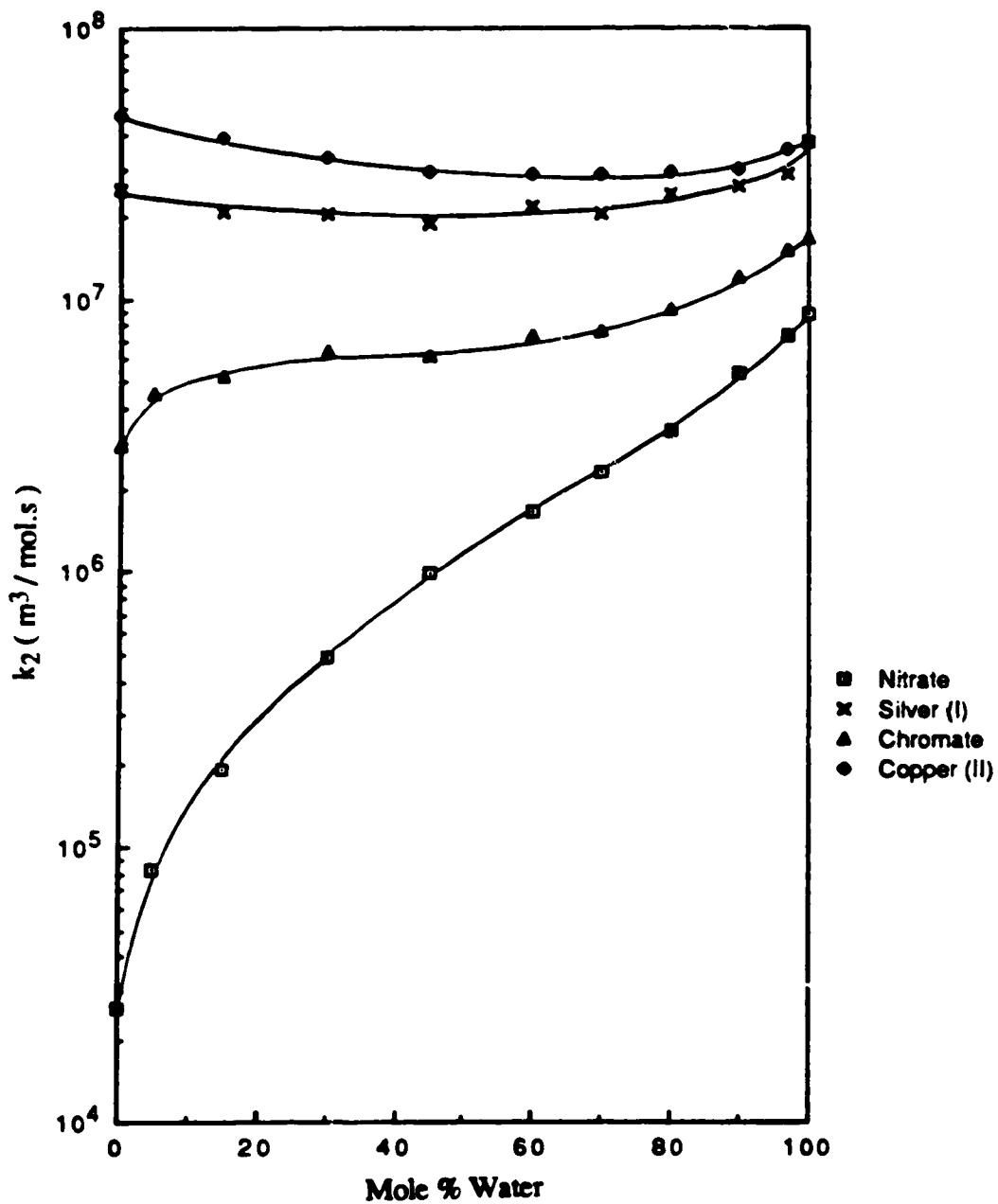


**Fig.4-26** The composition dependence of the second-order rate constants for the reaction of solvated electrons with inorganic electron scavengers in methanol/water mixtures at 298 K

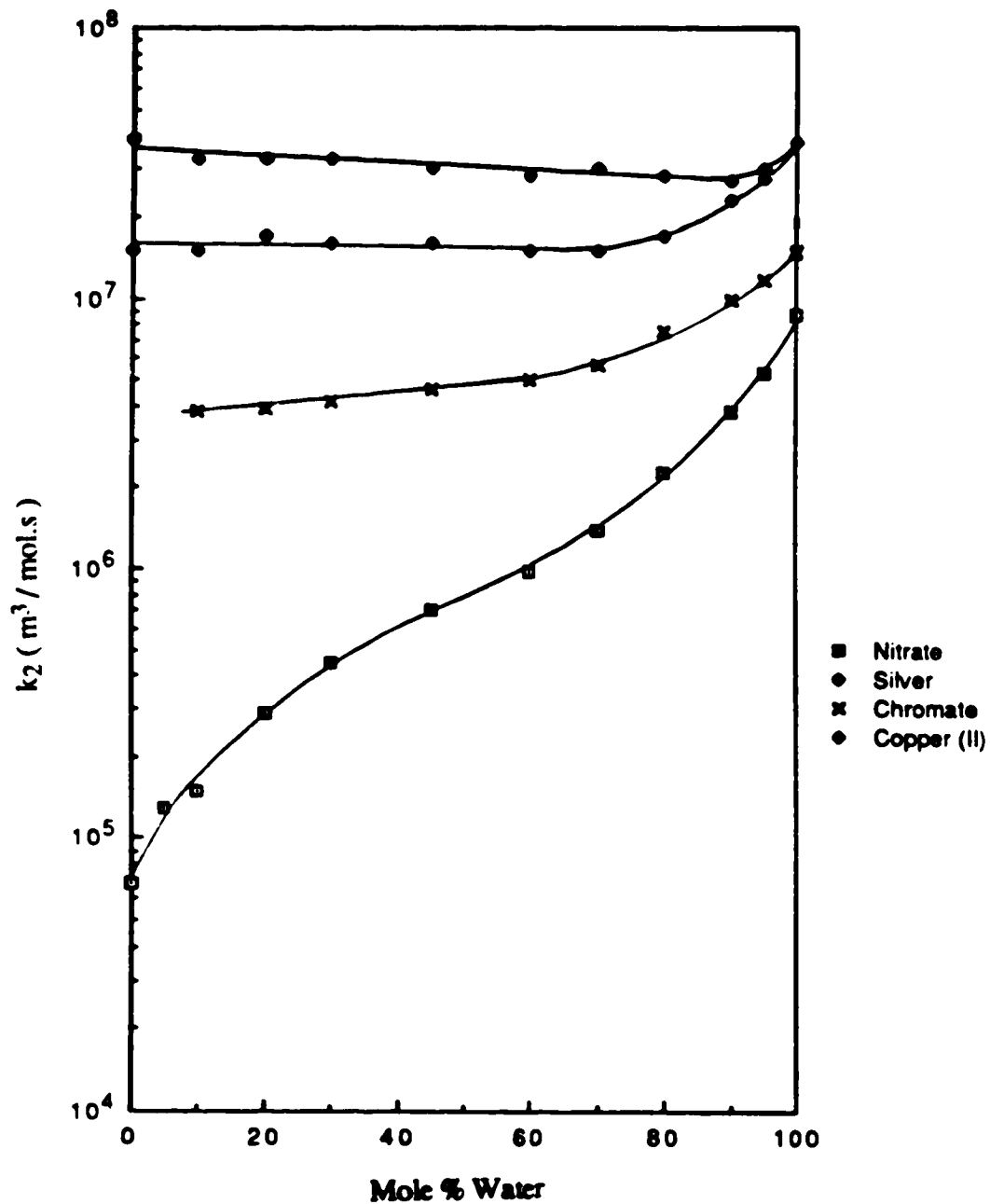


**Fig.4-27** The composition dependence of the second-order rate constants for the reaction of solvated electrons with inorganic electron-scavengers in ethanol/water mixtures at 298 K



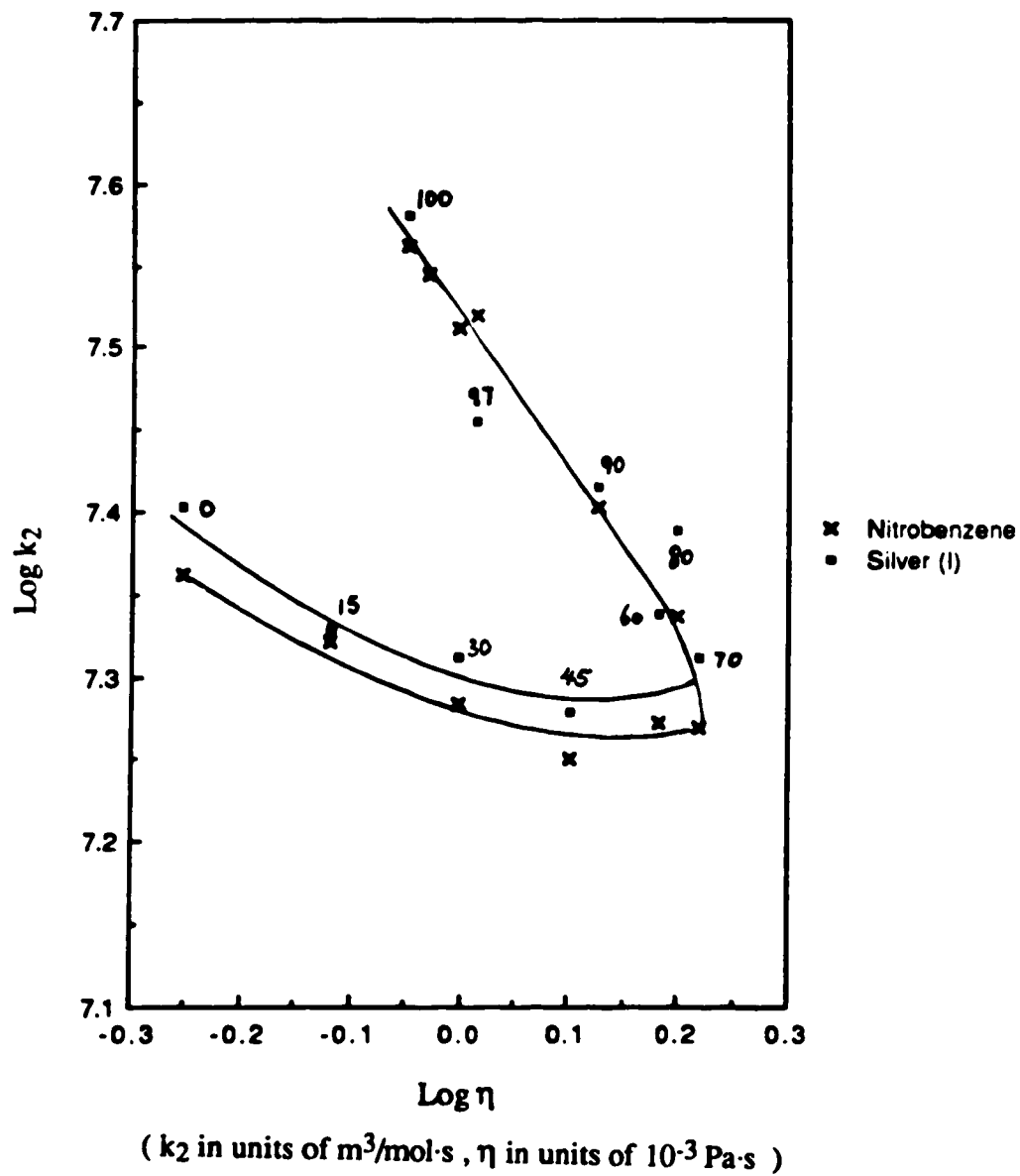


**Fig.4-28** The viscosity dependence of the second-order rate constants for the reaction of solvated electrons with silver ions and nitrobenzene in methanol/water mixtures at 298 K

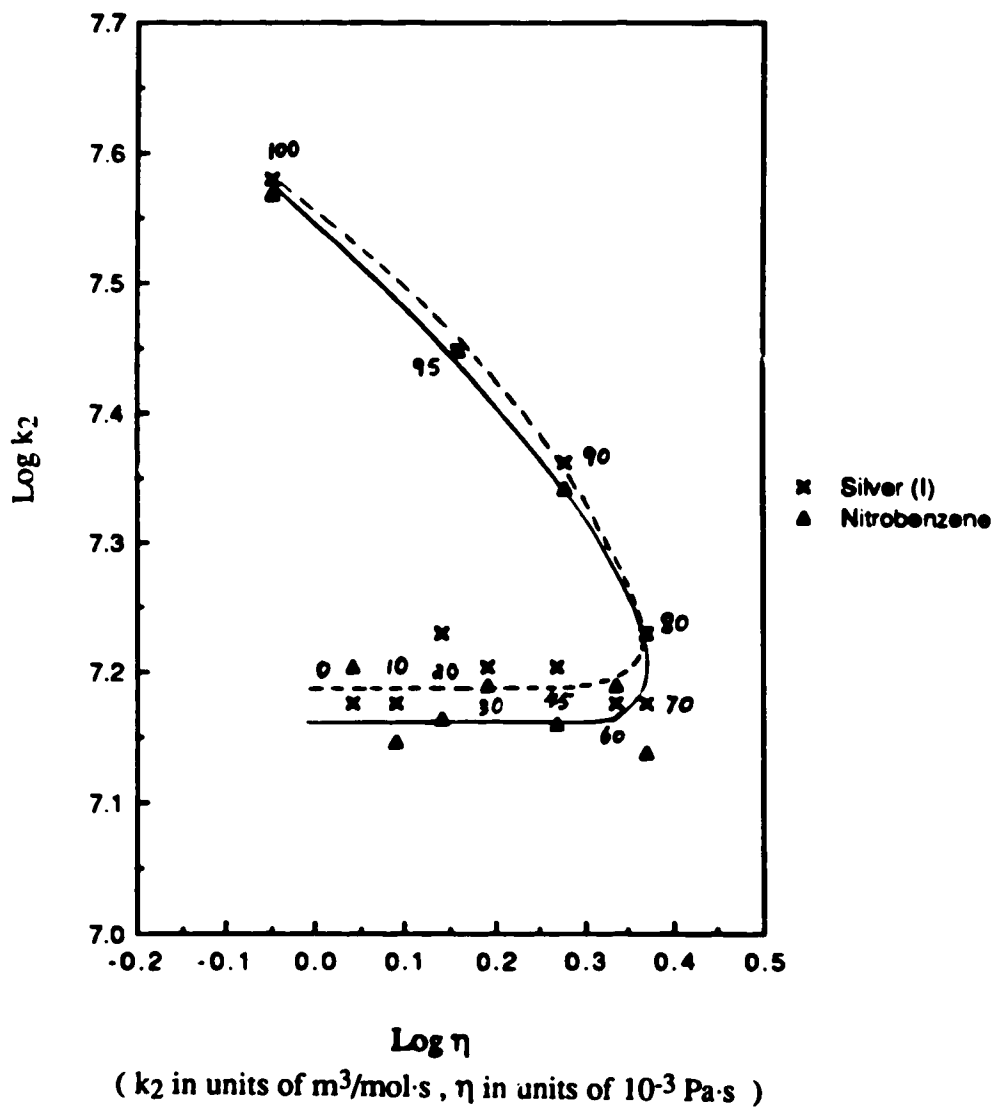


**Fig.4-29** The viscosity dependence of the second-order rate constants for the reaction of solvated electrons with silver ions and nitrobenzene in ethanol/water mixtures at 298 K

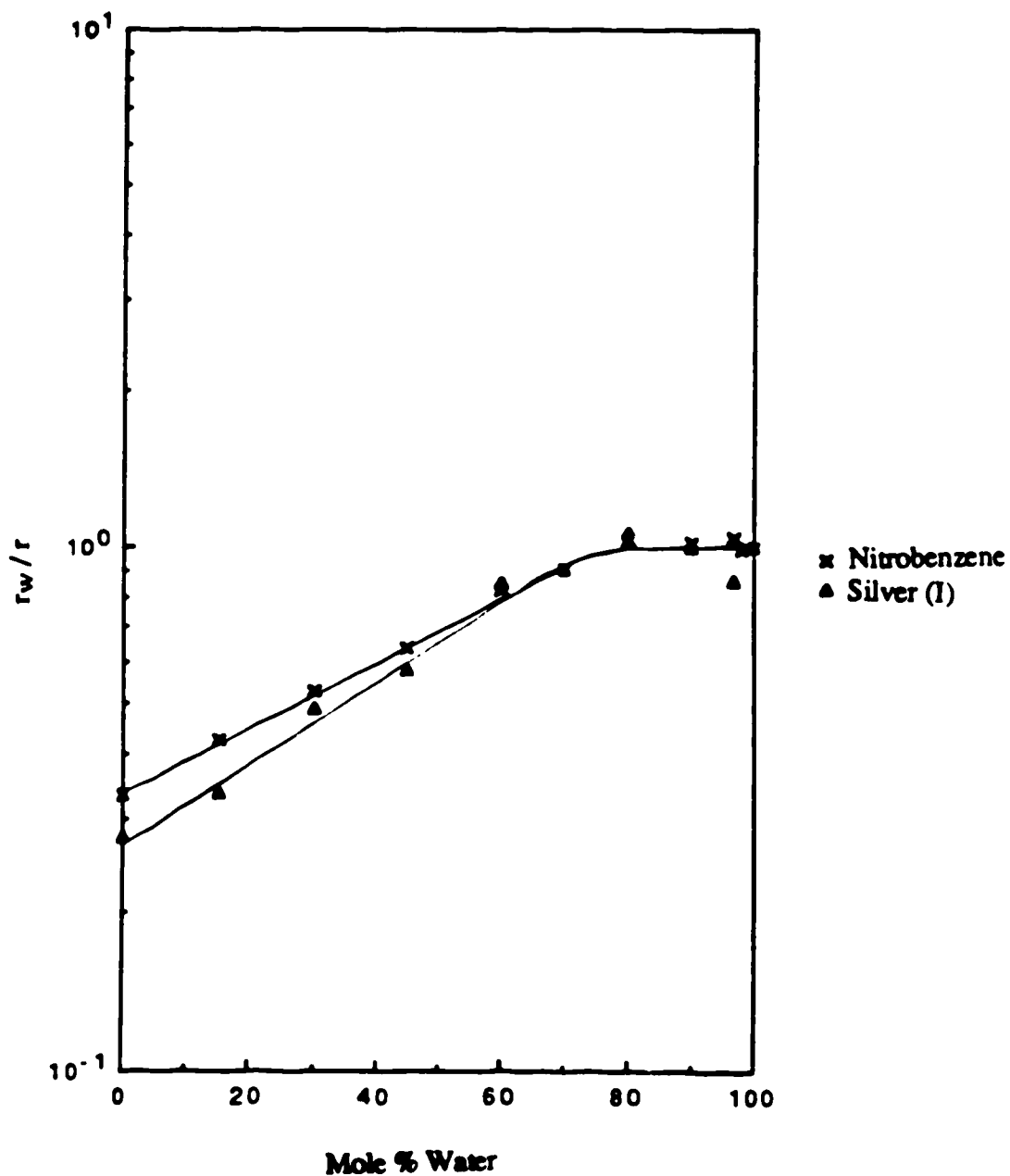


**Fig.4-30** The composition dependence of the relative effective diffusion radii ( $r_w/r$ ) for the reaction of solvated electrons with nitrobenzene and silver ions in methanol/water mixtures at 298 K

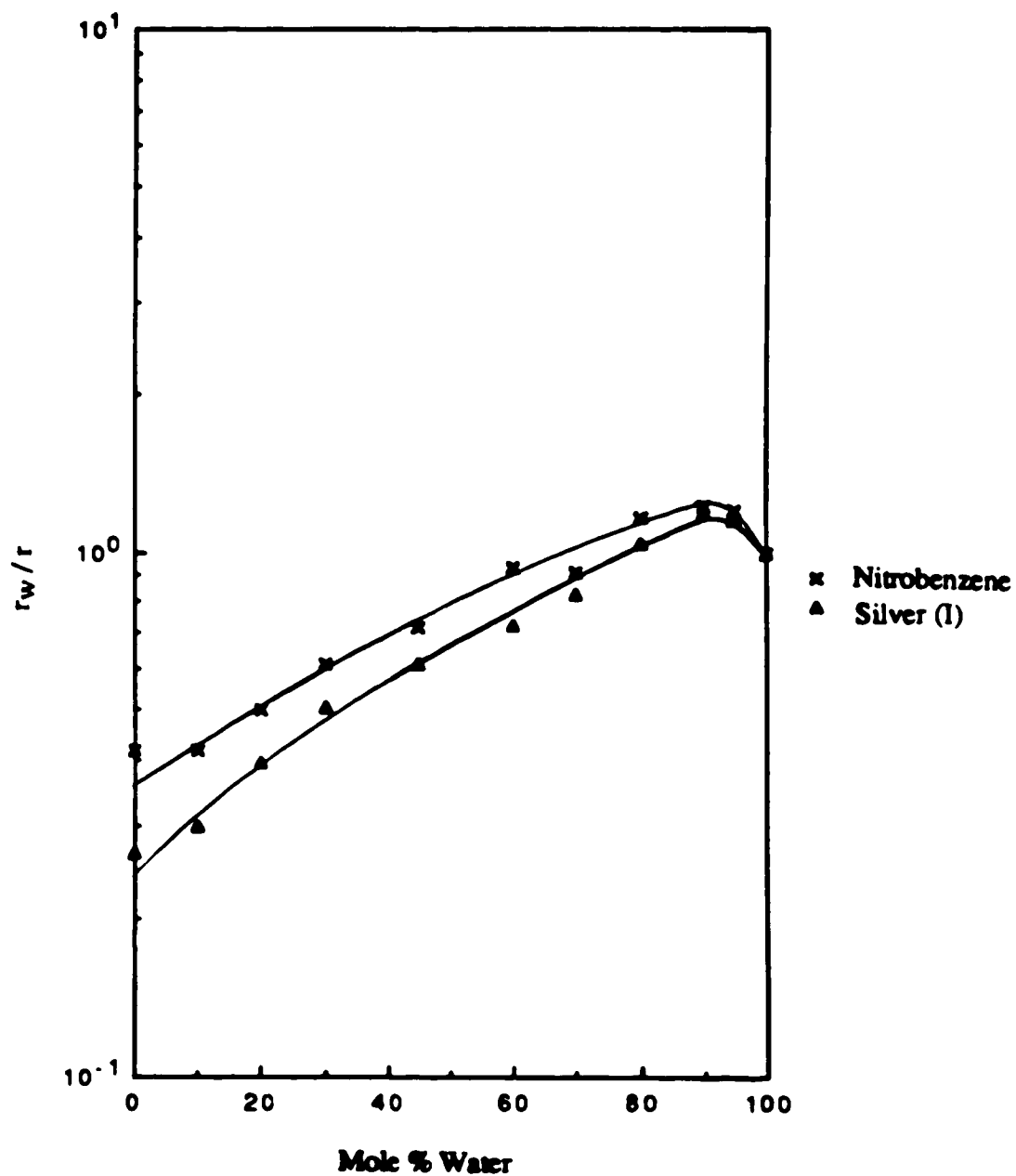
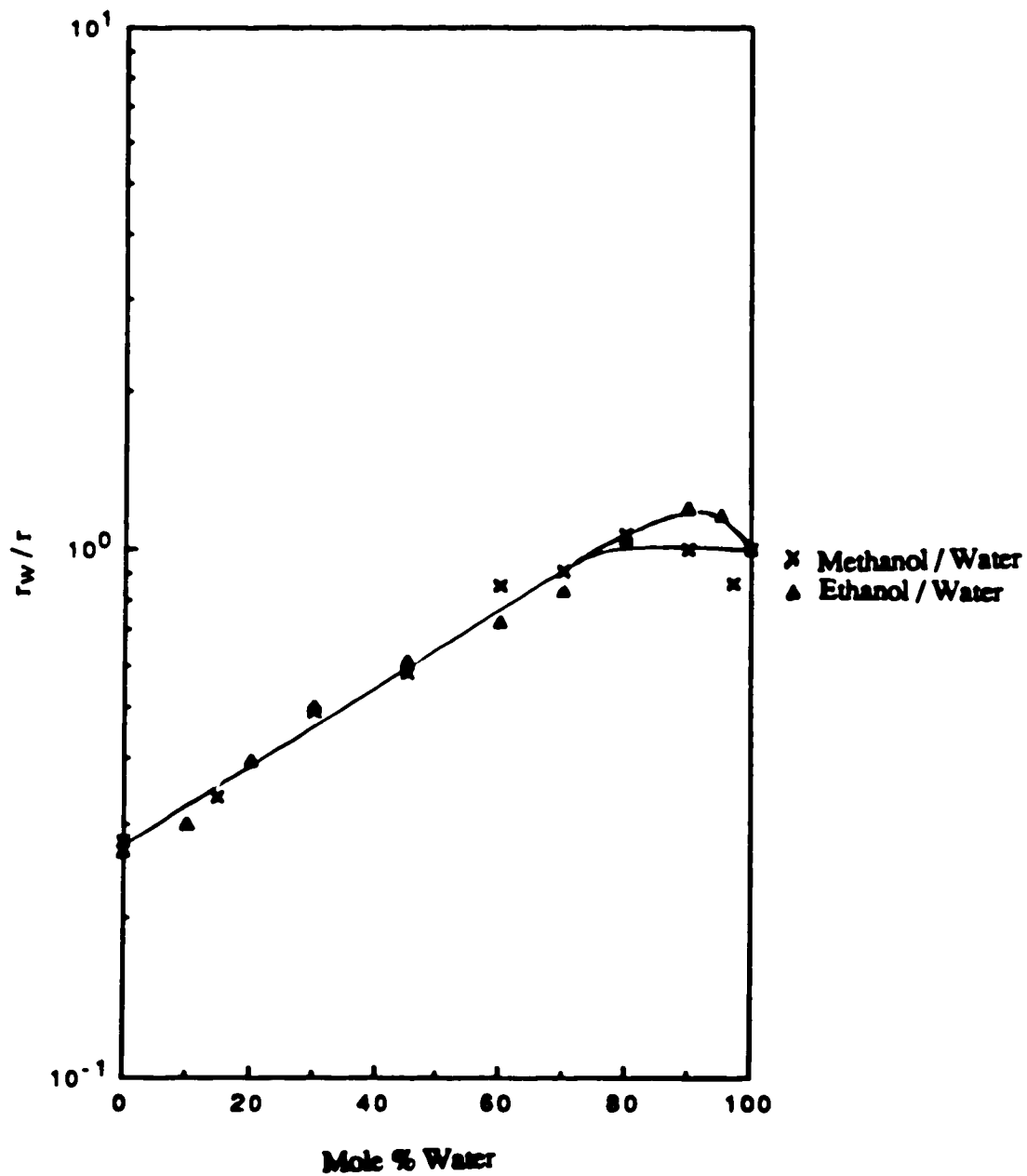
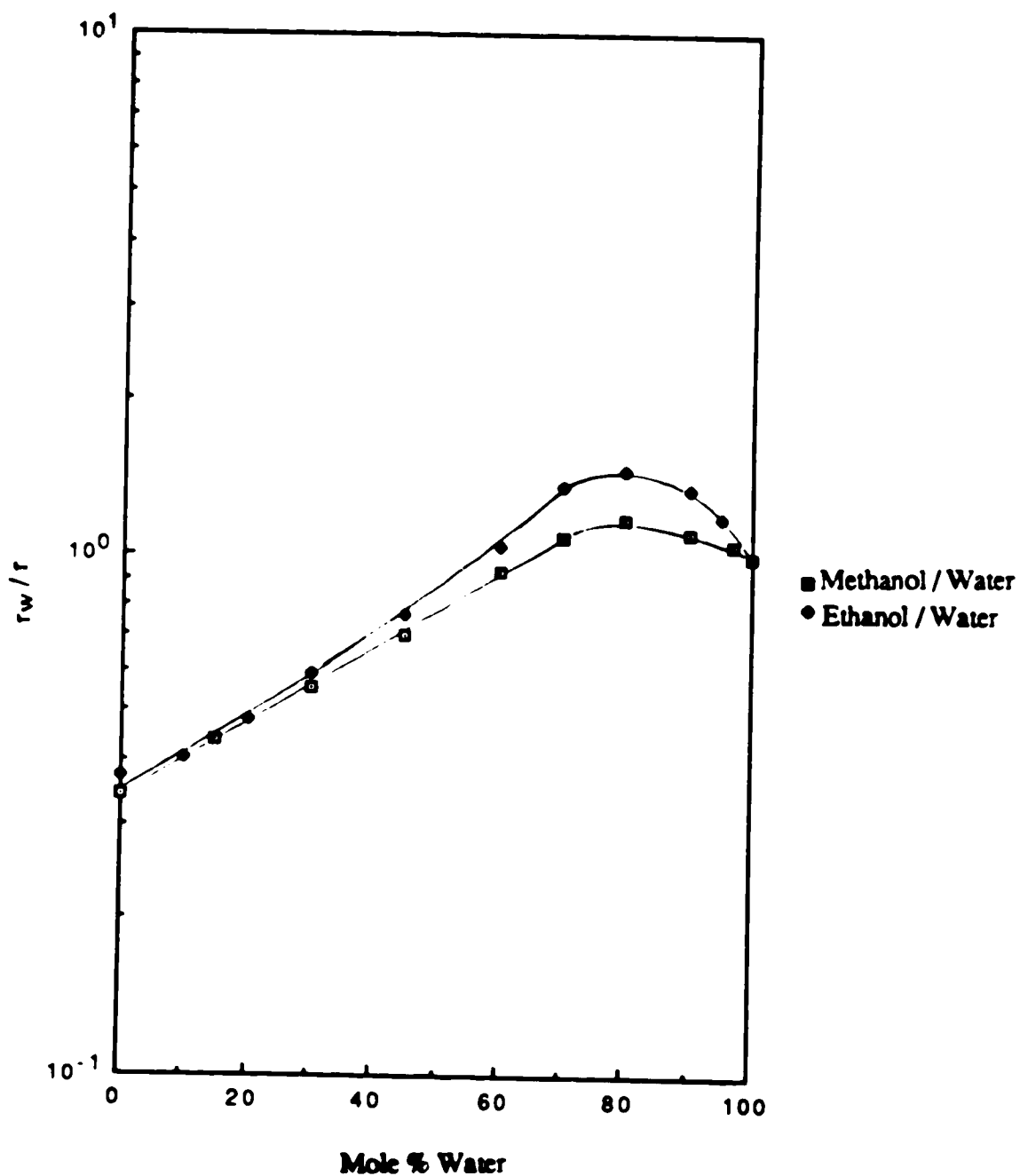


Fig.4-31 The composition dependence of the relative effective diffusion radii ( $r_w/r$ ) for the reaction of solvated electrons with nitrobenzene and silver ions in ethanol/water mixtures at 298 K



**Fig.4-32** The composition dependence of the relative effective diffusion radii ( $r_w/r$ ) for the reaction of solvated electrons with silver ions in methanol/water and ethanol/water mixtures at 298 K



**Fig.4-33** The composition dependence of the relative effective diffusion radii ( $r_w/r$ ) for the reaction of solvated electrons with copper (II) ions in methanol/water and ethanol/water mixtures at 298 K

in the ethanol/water mixtures, which gives further support to the idea that water structure strengthening effects are greater with the smaller alcohol.

## 2. Negatively Charged Scavengers

The rate constants for the reaction of solvated electrons with  $\text{CrO}_4^{2-}$  and  $\text{NO}_3^-$  are lower than those with a positive charge (Figs.4-26 and 4-27). The relative effective diffusion radii were calculated by assuming a reaction radius of 1.5 nm and 2.0 nm for the reactions with nitrate and chromate ions, respectively (118).

The higher rate constants for the reactions with  $\text{CrO}_4^{2-}$  in methanol/water mixtures are due to the smaller diffusion radii in these solvents (Fig.4-34). The smaller  $r_w/r$  values in the ethanol/water mixtures suggests that the anions are probably associated strongly with the alcohol molecules, so that the size of the alkyl group on the alcohol molecule has an influence on the diffusion of ions. The fact that the optical absorption energies of solvated electrons in these alcohol/water mixtures are dependent on the size of the alkyl group in the alcohol molecules (23) is also consistent with this view.

Among the electron-scavengers studied,  $\text{NO}_3^-$  displayed the greatest composition dependence. In going from water to alcohol, its reactivity decreases by two orders of magnitude. If the kinetics for the reaction of solvated electrons with  $\text{NO}_3^-$  are diffusion controlled, then it would require the effective radii ( $r_w/r$ ) to drop exceedingly rapidly on going from water to alcohol as shown in Fig.4-35. It is however difficult to rationalize why the diffusion radius of  $\text{NO}_3^-$  should be more sensitive to the change of solvent than that of the other ions. Since the rate constants for the reactions with nitrate in the alcohol-rich region are very low ( $< 10^5 \text{m}^3/\text{mol.s}$ ), the reactions of solvated electrons with nitrate are not diffusion controlled.

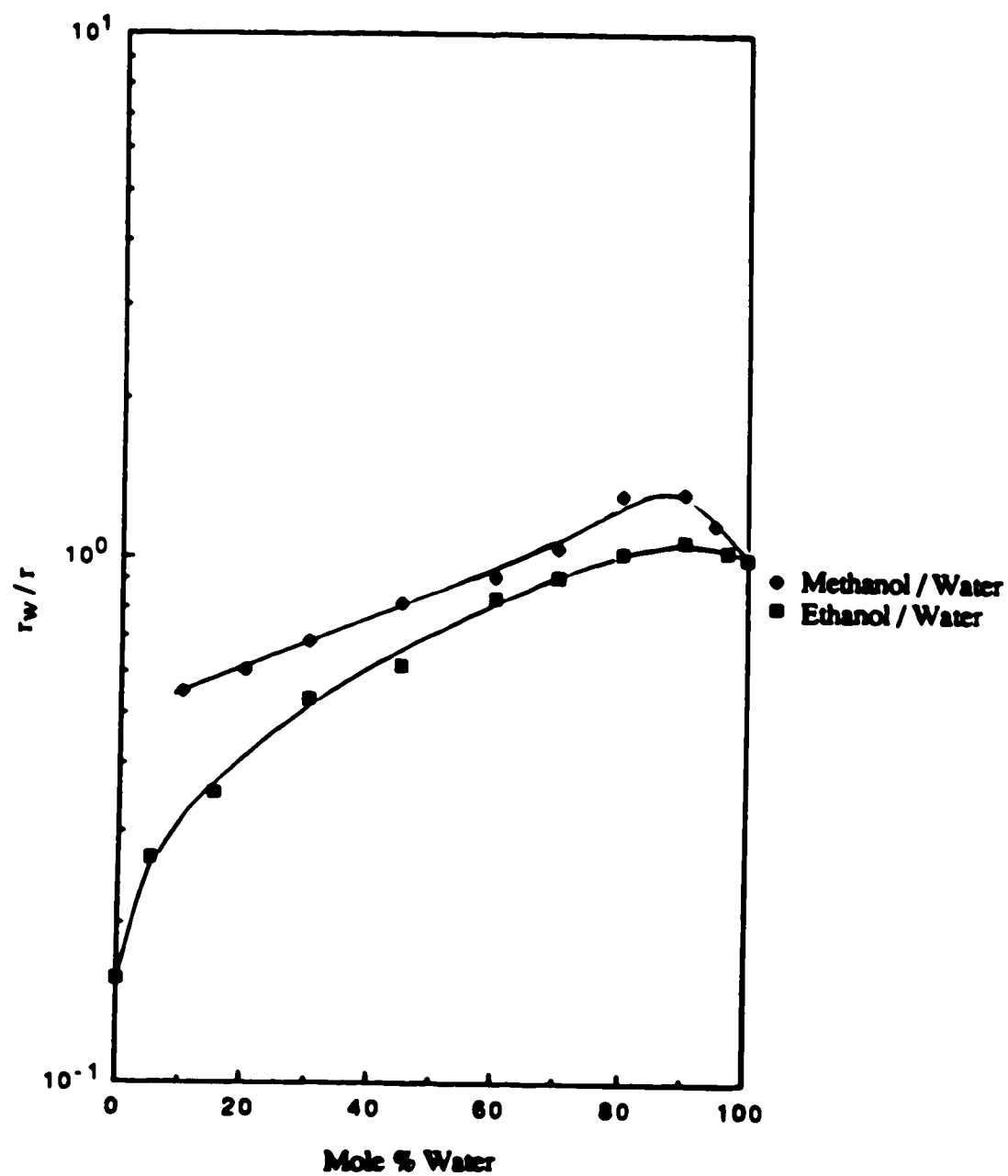


**Fig.4-34** The composition dependence of the relative effective diffusion radii ( $r_w/r$ ) for the reaction of solvated electrons with chromate ions in methanol/water and ethanol/water mixtures at 298 K



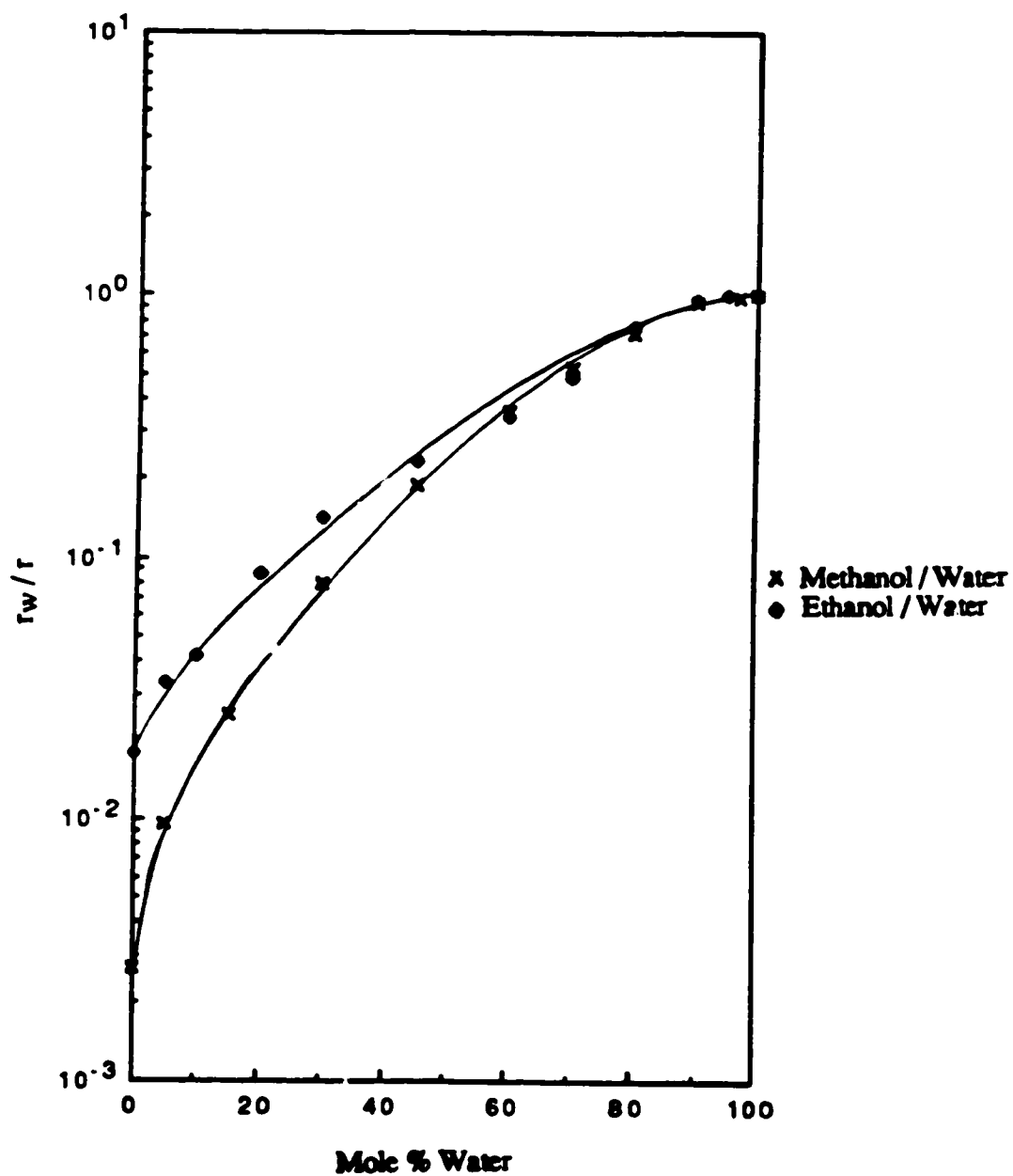


**Fig.4-35** The composition dependence of the relative effective diffusion radii ( $r_w/r$ ) for the reaction of solvated electrons with nitrate ions in methanol/water and ethanol/water mixtures at 298 K

### 3. Energies and Entropies of Activation

The activation energy of a diffusion controlled reaction is the energy of diffusion for the reacting species. The activation energies for the reactions of solvated electrons with the positively charged scavengers are generally higher than for the negatively charged scavengers (Figs.4-36 and 4-37). This could mean that the energies of diffusion for  $\text{Cu}^{2+}$  and  $\text{Ag}^+$  are higher than for the  $\text{CrO}_4^{=}$  and  $\text{NO}_3^-$  ions in these alcohol/water mixtures.

The entropy of activation for a nearly diffusion controlled reaction is related to the entropies of diffusion, and to the degree of solvent rearrangement on proceeding from the initial state to the transition state. The entropy of diffusion is always positive because the diffusion process is driven by the random motions of the liquid molecules. The degree of solvent rearrangement depends on the change of electrostriction at the reaction site. The reactions of solvated electrons with  $\text{Cu}^{2+}$  and  $\text{Ag}^+$  involve partial neutralization of the positive charge at the transition states. This causes the solvent molecules in the transition state to be less electrostricted than that in the initial state. The entropies of activation for the reactions with positively charged ions are therefore more positive (Figs.4-38 and 4-39). The transition states for the reactions of solvated electrons with  $\text{NO}_3^-$  and  $\text{CrO}_4^{=}$  involve the development of an additional negative charge, which enhances the electrostriction of the nearby solvent molecules. The entropies of activation for the anionic reactions are therefore more negative. For methanol/water mixtures and the water-rich ethanol/water mixtures, the difference of reactivity between the positively charged and negatively charged ions is due to changes of entropy rather than of energy.

The energies of activation for the reactions with the negatively charged electron-scavengers in the ethanol-rich mixtures ( $0 \leq \chi_w \leq 0.45$ ) increase sharply as the alcohol content increases. This perhaps can be interpreted by the encounter complex mechanism as described for the inefficient organic electron-scavengers. In the ethanol-rich mixtures, both the electron and the nitrate ion are solvated mainly by the hydroxyl ends of the alcohol molecules. The steric effects of the ethyl group on the ethanol molecule therefore not only

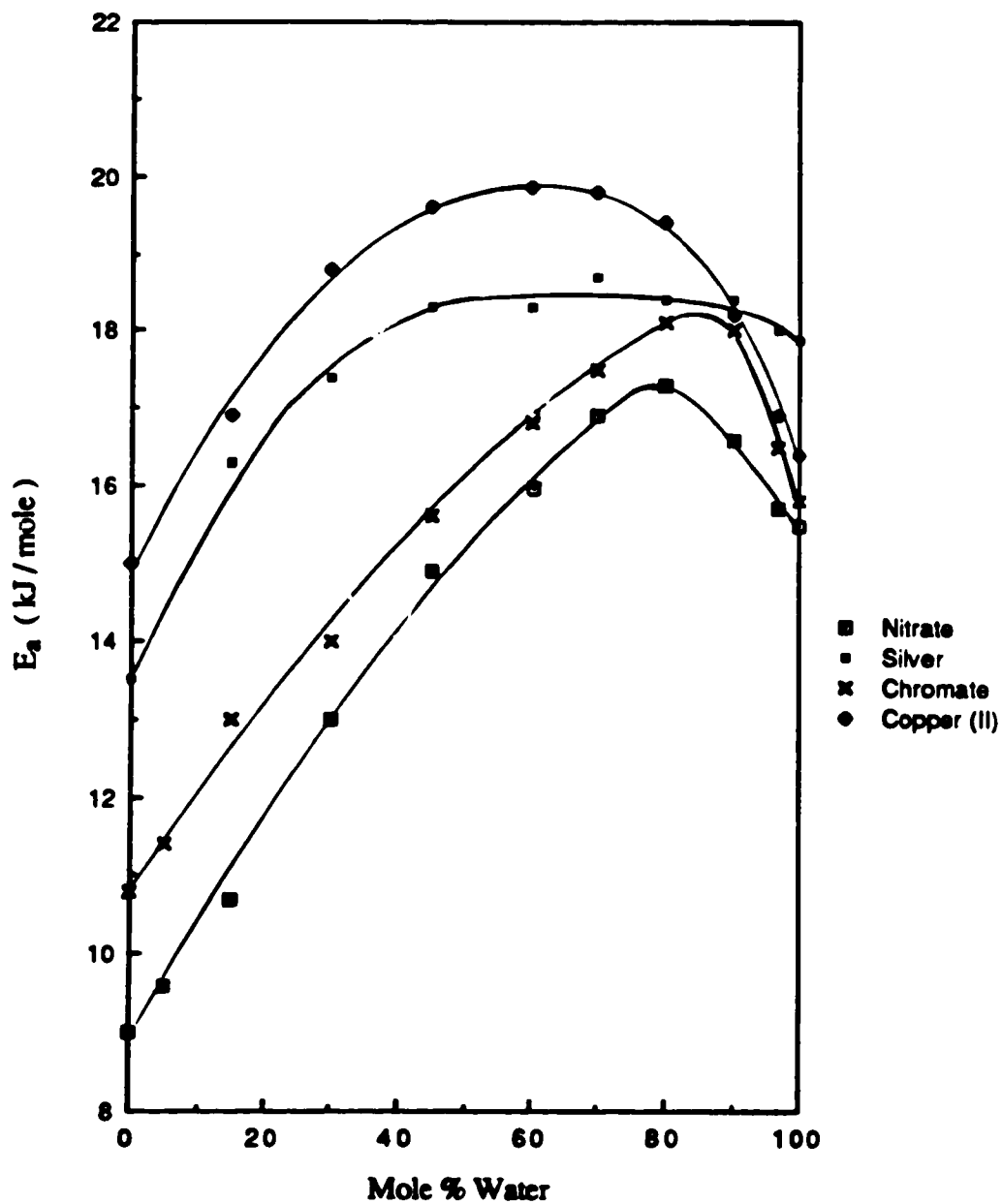


**Fig.4-36** The composition dependence of the activation energies for the reaction of solvated electrons with inorganic electron-scavengers in methanol/water mixtures

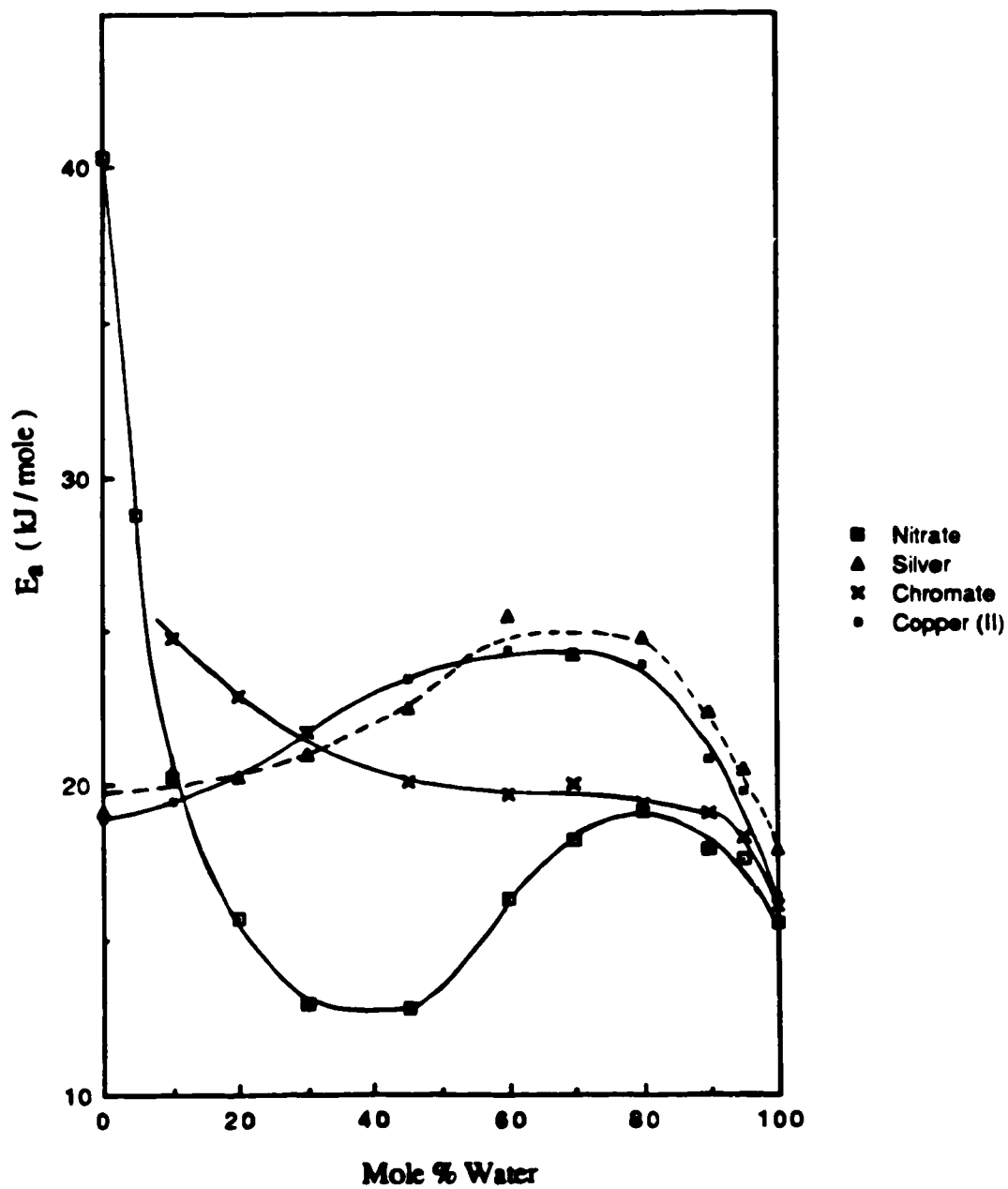


Fig.4-37 The composition dependence of the activation energies for the reaction of solvated electrons with inorganic electron-scavengers in ethanol/water mixtures

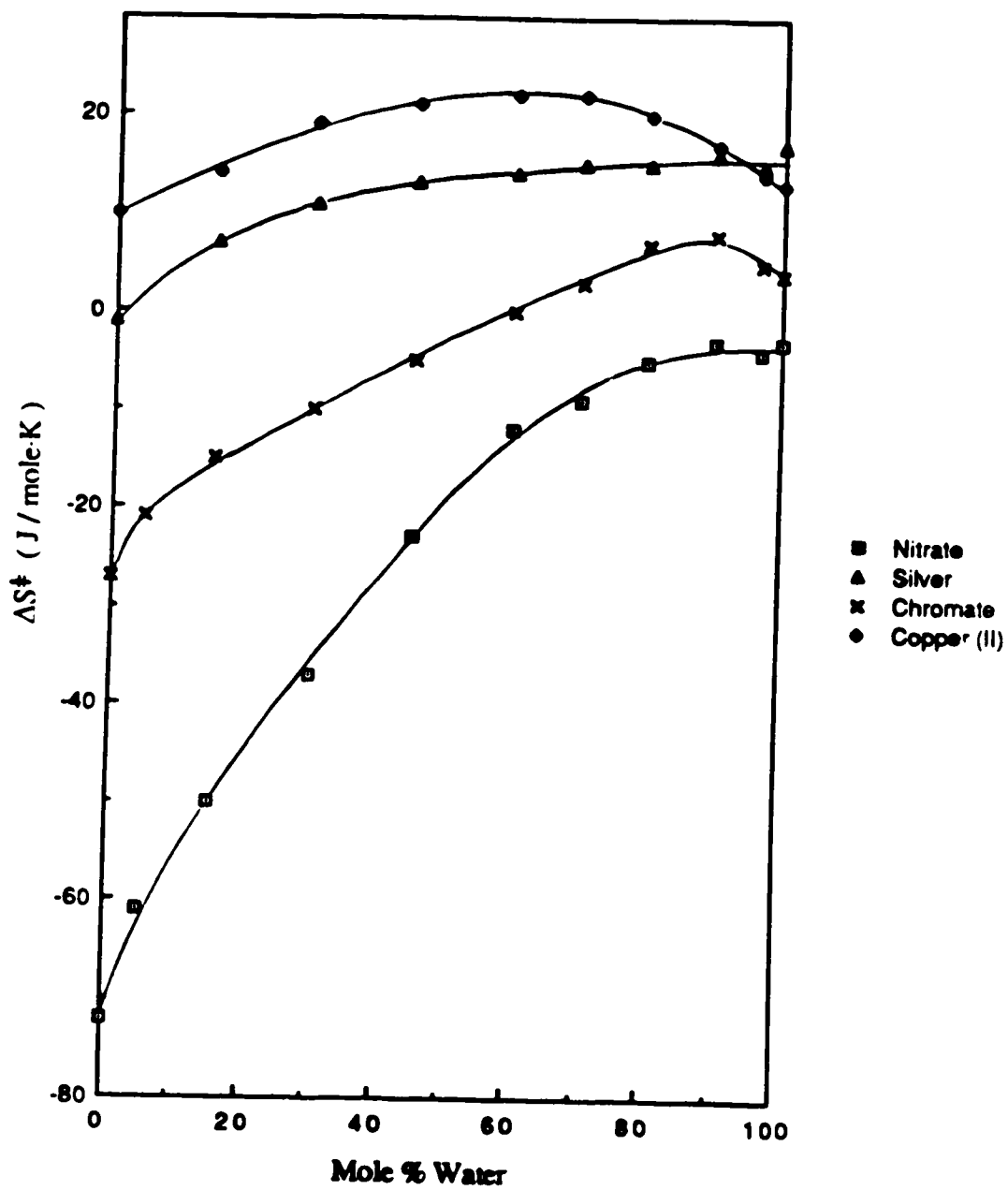
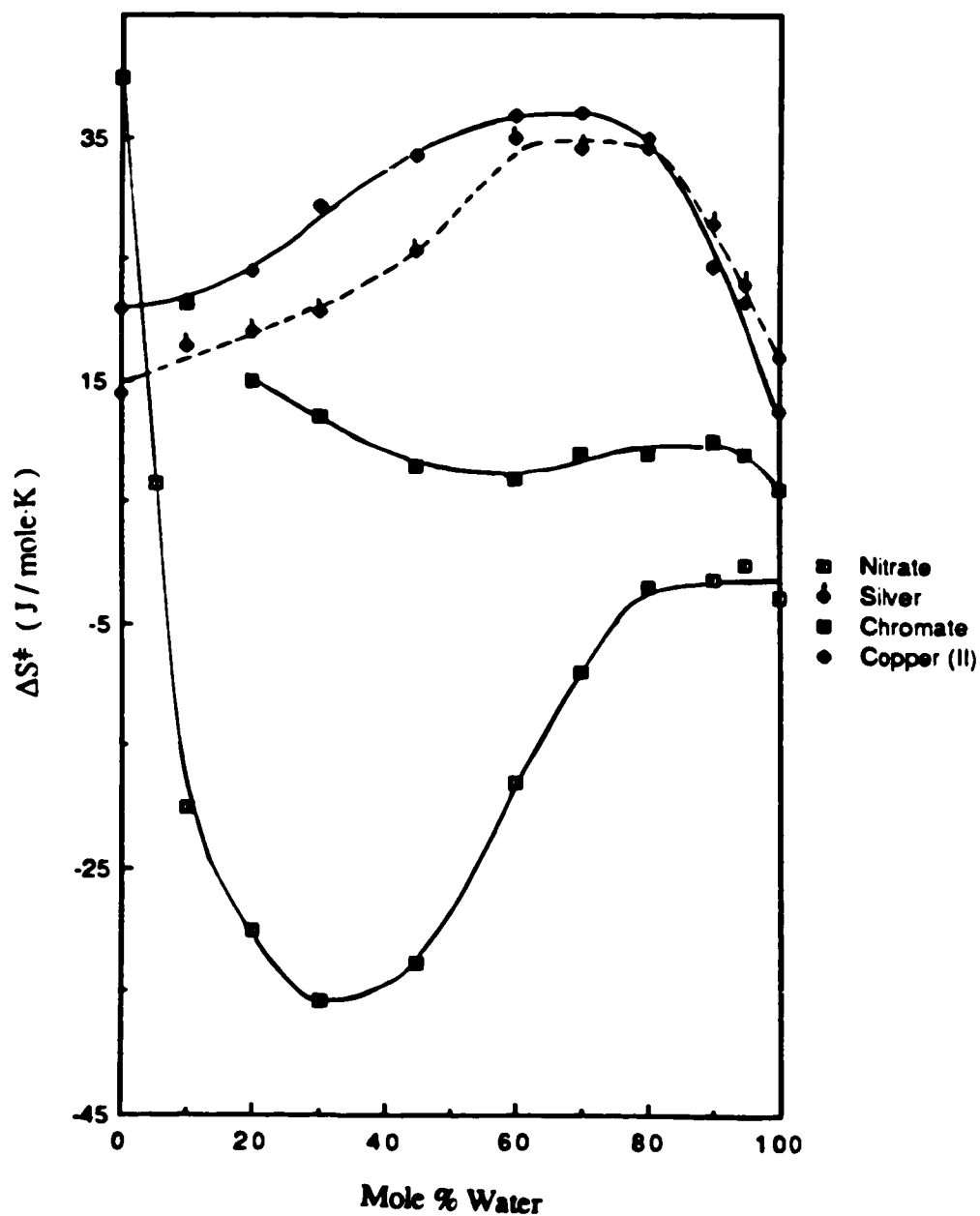


Fig.4-38 The composition dependence of the entropy of activation for the reaction of solvated electrons with inorganic electron-scavengers in methanol/water mixtures



**Fig.4-39** The composition dependence of the entropy of activation for the reaction of solvated electrons with inorganic electron-scavengers in ethanol/water mixtures

raise the energy of diffusion for the anionic species but also destabilize the encounter complex. This results in a large increase in the activation energy. Because of the steric effects of the alkyl group, the degree of solvent rearrangements on going from the encounter complex to the transition state are probably less extensive in ethanol than in water. This is indicated by the less negative entropy of activation towards the alcohol direction.

The composition dependences of  $E_a$  and  $\Delta S^\ddagger$  for the anionic reactions are more drastic with the ethanol/water mixtures than with the methanol/water mixtures. The size of the alcohol therefore has a large effect on the stabilization of the encounter and activation complexes. In ethanol-water mixtures, the  $E_a$  and  $\Delta S^\ddagger$  change more drastically with  $\text{NO}_3^-$  than with  $\text{CrO}_4^{2-}$ . This perhaps indicates that the steric crowding between the adjacent alkyl group of the alcohol in the cybotactic region of the encounter and activation complexes is more severe with the  $\text{NO}_3^-$  reactions. The volumes of the encounter and activation complexes presumably are larger in the  $\text{CrO}_4^{2-}$  reactions due to the greater electrostatic repulsion between the solvated electron and the dianion.

### III Conclusion

The reactivities of solvated electrons with solutes are dependent on the electron affinity of solute, the solvent structure, the electron-solvent and solute-solvent interactions.

The inverse relationship between  $k_2$  and  $\eta$  in the water-rich solvents indicates that electron and solute are solvated in water-rich microphases. For solutes with high electron affinity, the rate of the reaction is mainly controlled by the diffusion of the microphases.

In water-rich solvents, the  $k_2\eta$  values for the nitrobenzene reactions increase in the order of : methanol > ethanol > *t*-butyl alcohol, which indicate that the reaction radius also increases in that order.

As the alcohol content of the solvent increases, the diffusion coefficients of the nitrobenzene and ionic reactions decrease.

The solvent effects on the rate constants of the nearly diffusion controlled reaction are not only due to the changes in the transport properties (viscosity, diffusion coefficient) but also due to the change of dielectric constant of the medium. This is illustrated by the linear correlation between the viscosity normalized rate constant ( $\ln k_2\eta$ ) with  $\epsilon^{-1}$  for the reactions of solvated electrons with nitrobenzene and acetone.

The inverse correlations between the encounter efficiency ( $k_2/k_N$ ) and the optical absorption energy ( $E_T$ ) indicate that the free energies of activation for the phenol and toluene reactions in ethanol/water mixtures are governed by the solvation energy of the electron. In methanol/water mixtures, the encounter efficiencies are also governed by the solvation of the transition state.

For the  $\text{Ag}^+$  and  $\text{Cu}^{2+}$  reactions, the diffusion radii in the methanol/water ethanol/water are similar, which suggest that (i) upon diffusion,  $\text{Ag}^+$  and  $\text{Cu}^{2+}$  can drag more solvent molecules in the methanol/water mixtures than in the ethanol/water mixtures or (ii) the cations are solvated mostly by water.

The higher rate constants for the reactions with  $\text{CrO}_4^{2-}$  in methanol/water mixtures are due to the smaller diffusion radii in this these solvents. The larger diffusion radii in the



ethanol/water mixtures suggests that the anions are probably associated more strongly with the alcohol molecules. A larger alkyl group makes the diffusion of anions more difficult.

In the water-rich solvents, the differences in reactivity between efficient and inefficient scavengers are due to entropies of activation rather than energies of activation.

## **REFERENCES**

1. **W. Weyl, Ann. Phys. 121, 601 (1864).**
2. **C. A. Kraus, " The Properties of Electrically Conducting Systems ",  
Chemical Catalogue Co., New York, 1922, p.375.**
3. **A. J. Birch and G. Subba Rao, Adv. Org. Chem. 8, 1 (1972).**
4. **D. A. Copeland, N. R. Kestner and J. Jortner, J. Chem. Phys. 53, 1189 (1970).**
5. **J. Jortner, A. Gaathon, Can. J. Chem. 55, 1801 (1977).**
6. **D. Chandler, J. Chem. Phys. 81, 1975 (1984).**
7. **P. J. Rossky, J. Schnitker, K. Motakabbir and R. Friesner,  
Phys. Rev. Lett. 60, 456 (1988).**
8. **G. R. Freeman, " Kinetics of Nonhomogeneous Processes :  
A Practical Introduction for Chemists, Biologists, Physicists, and Materials  
Scientists ", Wiley-Interscience, New York, 1987, chapters 2 and 6.**
9. **W. J. Chase and J. W. Hunt, J. Phys. Chem. 79, 2835 (1975).**
10. **C. A. Hutchinson and R. C. Pastor, J. Chem. Phys. 21, 1959 (1953).**
11. **U. Schindewolf, Angew. Chem. Int. Ed. 7, 190 (1968).**
12. **J. Jortner and R. M. Noyes, J. Phys. Chem. 70, 770 (1966).**
13. **C. A. Kraus and W. W. Lucasse, J. Am. Chem. Soc. 45, 2551 (1923).**
14. **K. H. Schmidt and M. Anbar, J. Phys. Chem. 73, 2846 (1969).**
15. **W. J. Moore, " Physical Chemistry ", 3rd Edition, Prentice Hall,  
Englewood Cliffs, N. J. , 1962, p.337.**
16. **C. A. Kraus and W. C. Bray, J. Am. Chem. Soc. 35, 1315 (1913).**
17. **P. H. Tewari and G. R. Freeman, J. Chem. Phys. 51, 1276 (1969).**
18. **W. F. Schmidt and A. O. Allen, J. Chem. Phys. 52, 4788 (1970).**
19. **R. M. Minday, D. L. Schmidt and H. T. Davis, J. Phys. Chem. 76, 442 (1972).**
20. **J. P. Dodelet and G. R. Freeman, Can. J. Chem. 50, 2267 (1972).**

21. J. P. Dodelet, K. Shinsaka and G. R. Freeman, *J. Chem. Phys.* **59**, 1293 (1973).
22. J. Corset and G. Lepoutre, in "Metal-Ammonia Solution", G. Lepoutre and M. J. Sienko (Eds.), W. A. Benjamin, Inc., New York, 1964, p.187.
23. A. D. Leu, K. N. Jha and G. R. Freeman, *Can. J. Chem.* **60**, 2342 (1982).
24. G. R. Freeman, *Actions Chimiques et Biologiques des Radiations* **14**, 73 (1970).
25. L. Kevan, H. A. Gillis, K. Fueki and T. Kimura, *J. Chem. Phys.* **68**, 5203 (1978).
26. F. Y. Jou and G. R. Freeman, *Can. J. Chem.* **54**, 3693 (1976).
27. M. T. Lok, F. J. Tehan and J. L. Dye, *J. Phys. Chem.* **76**, 2975 (1972).
28. D. Huppert, P. Avouris and P. M. Rentzepis, *J. Phys. Chem.* **82**, 2282 (1978).
29. T. R. Tuttle, S. Golden, S. L. Wenje and C. M. Stupak, *J. Phys. Chem.* **88**, 3811 (1984).
30. D. C. Walker, *Can. J. Chem.* **55**, 1987 (1977).
31. N. Okabe, T. Kimura and K. Fueki, *Can. J. Chem.* **61**, 2199 (1983).
32. J. Jortner and N. R. Kestner, *J. Phys. Chem.* **77**, 1040 (1973).
33. A. Kajiwara, K. Funabashi and Naleway, *Phys. Rev. A* **6**, 808 (1972).
34. R. Lugo and P. Delahay, *J. Chem. Phys.* **57**, 2122 (1972).
35. G. L. Hug and I. Carmicheal, *J. Phys. Chem.* **86**, 3410 (1982).
36. K. Funabashi, I. Carmicheal and W. H. Hamill, *J. Chem. Phys.* **69**, 2652 (1978).
37. L. Kevan, D. P. Lin, T. Huang and I. Eisele, *J. Chem. Phys.* **57**, 4702 (1972).
38. J. K. Baird, L. K. Lee and E. J. Meehan, *J. Chem. Phys.* **83**, 3710 (1985).
39. T. Kimura, O. Hirao, C. Okabe and K. Fueki, *Can. J. Chem.* **62**, 64 (1984).
40. J. K. Baird and C. H. Morales, *J. Phys. Chem.* **89**, 774 (1985).
41. K. F. Baverstock and P. J. Dyne, *Can. J. Chem.* **48**, 2182 (1970).
42. T. Shida, S. Iwata and T. Watanabe, *J. Phys. Chem.* **76**, 3683 (1972).
43. K. Kato, S. Takagi and K. Fueki, *J. Phys. Chem.* **85**, 2684 (1981).
44. R. A. Ogg, *Phys. Rev.* **69**, 243 (1946).

45. J. Jortner, *J. Chem. Phys.* **30**, 839 (1959).
46. D. A. Copeland, N. R. Kestner and J. Jortner, *J. Chem. Phys.* **53**, 1189 (1970).
47. D. F. Feng, K. Fueki and L. Kevan, *J. Chem. Phys.* **58**, 3281 (1973).
48. A. Banerjee and J. Simons, *J. Chem. Phys.* **68**, 415 (1978).
49. D. Chandler, *J. Phys. Chem.* **88**, 3400 (1984).
50. L. Kevan, *J. Phys. Chem.* **84**, 1232 (1980).
51. G. R. Freeman, *J. Phys. Chem.* **77**, 7 (1973).
52. A. D. Leu, K. N. Jha and G. R. Freeman, *Can J. Chem.* **61**, 1115 (1983).
53. R. R. Hentz and G. A. Kenney-Wallace, *J. Phys. Chem.* **78**, 514 (1974).
54. G. E. Hall and G. A. Kenney-Wallace, *Chem. Phys.* **32**, 313 (1978).
55. F. Y. Jou and G. R. Freeman, *Can. J. Chem.* **57**, 591 (1979).
56. F. Y. Jou and G. R. Freeman, *Can. J. Chem.* **60**, 1809 (1982).
57. J. D. Bernal and P. H. Fowler, *J. Chem. Phys.* **1**, 515 (1933).
58. A. H. Narten, *J. Chem. Phys.* **56**, 5681 (1972).
59. A. H. Narten and H. A. Levy, *J. Chem. Phys.* **55**, 2263 (1971).
60. J. A. Pople, *Proc. Royal Soc. A* **222**, 498 (1954).
61. S. A. Rice and M. G. Sceats, *J. Phys. Chem.* **85**, 1107 (1981).
62. S. A. Rice and M.G. Sceats in "Water : A Comprehensive Treatise" **7**,  
F. Franks Ed., Plenum, 1982.
63. F. H. Stillinger and A. Rahman, *J. Chem. Phys.* **60**, 1545 (1974).
64. H. E. Stanley and J. Teixeira, *J. Chem. Phys.* **73**, 3404 (1980).
65. H. S. Frank and Y. W. Wen, *Discuss. Faraday Soc.* **24**, 133 (1957).
66. G. J. Safford, P. S. Leung, A. W. Neumann and P. C. Schaffer,  
*J. Chem. Phys.* **50**, 4444 (1969).
67. G. Nemethy and H. A. Scheraga, *J. Chem. Phys.* **36**, 3382 (1962).
68. A. T. Hagler, G. Nemethy and H. A. Scheraga, *J. Chem. Phys.* **76**, 3229 (1972).
69. M. S. Jhon, H. Eyring, J. Grosh and T. Ree, *J. Chem. Phys.* **44**, 1456 (1966).

70. Y. I. Naberukhin , *J. Struct. Chem.* **25**, 223 (1984).
71. P. J. Rossky, *Pure Appl. Chem.* **57**, 1043 (1985).
72. P. Huyskens, *J. Mol. Struct.* **100**, 403 (1983).
73. "The Hydrogen Bond", Edited by P. Schuster, G. Zundel and C. Sandorfy, Vol. 3, North Holland Publishing, 1976, p. 1070.
74. M. C. R. Symons and V. K. Thomas, *J. Chem. Soc. Farady Trans. I* **77**, 1883 (1981).
75. H. H. Eysel and J. E. Bertie, *J. Mol. Struct.* **142**, 227 (1986).
76. B. M. Pettit and P. J. Rossky, *J. Chem. Phys.* **78**, 7296 (1983).
77. W. L. Jorgensen, *J. Phys. Chem.* **90**, 1276 (1986).
78. J. G. J. Kirkwood, *Chem. Phys.* **7**, 911 (1939).
79. J. Liszi, L. Meszaros and I. Ruff, *Acta. Chim. Accad. Sci. Hung.* **104**, 279 (1980).
80. J. P. Hasted in "Aqueous Dielectrics" Chapman and Hall, London, 1973, p. 176.
81. F. Y. Jou and G. R. Freeman, *Can. J. Chem.* **60**, 1809 (1982).
82. A. D'Aprano, I. D. Donato, G. D'Arrigo, D. Bertollini, M. Cassettari and G. Salvetti, *Mol. Phys.* **55**, 475 (1985).
83. B. Marongin, I. Ferrio, R. Monaci, V. Solinas and S. Forraza, *J. Mol. Liq.* **28**, 229 (1984).
84. A. C. Brown and D. J. G. Ives, *J. Chem. Soc.* **1962**, 1608 (1962).
85. Y. I. Naberukhin and V. A. Rogov, *Russ. Chem. Rev.* **40**, 207 (1971).
86. H. Tanaka, K. Nakanish and H. Touhara, *J. Chem. Phys.* **81**, 4065 (1984).
87. T. M. Bender and R. Pecora, *J. Phys. Chem.* **90**, 1700 (1986).
88. H. Leiter, C. Albayrak and H. G. Hertz, *J. Mol. Liq.* **27**, 211 (1984).
89. M. C. R. Symons and G. R. Eaton, *Farad. Sympos.* **17**, 31 (1982).

90. **W. L. Jorgensen, J. Gao and C. Ravimohan, J. Phys. Chem. 89, 3470 (1985).**
91. **H. S. Frank and M. W. Evans, J. Chem. Phys. 13, 507 (1945).**
92. **A. H. Hafez and H. Sadek, Acta. Chim. Accad. Sci. Hung 89, 257 (1976).**
93. **A. D'Aprano, D. Donato, E. Caponetti and V. Agrigento, J. Sol. Chem. 8, 793 (1979).**
94. **M. Anbar, M. Bambenek and A. B. Ross, Natl. Stand. Ref. Data Ser., Natl. Bur. Stand., 43 (1973).**
95. **I. A. Taub, M. C. Sauer, Jr. and L. M. Dorfman, Discuss. Faraday Soc 36, 206 (1963).**
96. **I. A. Taub, D. A. Harter, M. C. Sauer, Jr. and L. M. Dorfman, J. Chem. Phys. 41, 979 (1964).**
97. **S. Arai and L. M. Dorfman, J. Chem. Phys. 41, 2190 (1964).**
98. **G. L. Bolton and G. R. Freeman, J. Am. Chem. Soc. 98, 6825 (1976).**
99. **K. Okazaki and G. R. Freeman, Can. J. Chem. 56, 2313 (1978).**
100. **A. M. Afanassiev, K. Okazaka and G. R. Freeman, J. Phys. Chem. 83, 1244 (1979).**
101. **A. M. Afanassiev, K. Okazaki and G. R. Freeman, Can. J. Chem. 57, 839 (1979).**
102. **M. S. Tunuli and Farhatziz, J. Phys. Chem. 90, 6587 (1986).**
103. **S. Farhatziz, Kalachandra and M. S. Tunuli, J. Phys. Chem. 88, 3837 (1984).**
104. **S. Kalachandra and Farhatziz, Chem. Phys. Lett., 78, 465 (1980).**
105. **M. A. Rauf, G. H. Stewart and Farhatziz, Radiat. Phys. Chem. 26, 433 (1985).**
106. **B. H. Milosavljevic and O. I. Micic, J. Phys. Chem. 82, 1359 (1978).**

107. O. I. Micic and B. Cercek, *J. Phys. Chem.* **81**, 833 (1977).
108. O. I. Micic and B. Cercek, *J. Phys. Chem.* **78**, 285 (1974).
109. F. Barat, L. Gilles, B. Hickel and L. Lesigne, *J. Phys. Chem.* **77**, 1711 (1973).
110. H. A. Schwarz and P. S. Gill, *J. Phys. Chem.* **81**, 22 (1977).
111. J. Cygler and G. R. Freeman, *Can. J. Chem.* **62**, 1265 (1984).
112. Y. Maham and G. R. Freeman, *J. Phys. Chem.* **89**, 4347 (1985).
113. Y. Maham and G. R. Freeman, *J. Phys. Chem.* **91**, 1561 (1987).
114. Y. Maham and G. R. Freeman, *J. Phys. Chem.* **92**, 1506 (1988).
115. P. C. Senanayake and G. R. Freeman, *J. Phys. Chem.* **91**, 2123 (1987).
116. P. C. Senanayake and G. R. Freeman, *J. Chem. Phys.* **87**, 7007 (1987).
117. Y. Maham and G. R. Freeman, *J. Phys. Chem.* (In Press).
118. P. C. Senanayake and G. R. Freeman, *J. Phys. Chem.* **92**, 5142 (1988).
119. G. Nemethy, H. A. Scheraga, *J. Chem. Phys.* **36**, 3401 (1962).
120. F. Franks and D. J. G. Ives, *Q. Rev. Chem. Soc.* **20**, 1 (1966).
121. F. Franks and D. S. Reid, in "Water, a Comprehensive Treatise " 2, F. Franks Ed., Plenum, 1973, p.323.
122. M. Yusz, G. P. Methur and R. A. Stager, *J. Chem. Eng. Data.* **22**, 32 (1977).
123. B. R. Hammond and R. H. Stokes, *Trans. Faraday Soc.* **49**, 890 (1956).
124. K. C. Pratt and W. A. Wakeham, *Proc. R. Soc. (London), Ser. A* **393**, 336 (1975).
125. M. S. Jhon and H. Eyring, *J. Am. Chem. Soc.* **90**, 3071 (1968).
126. F. X. Hassion and R. H. Cole, *J. Chem. Phys.* **23**, 1756 (1955).
127. J. B. Hasted, in "Water, a Comprehensive Treatise " 2, F. Franks Ed., Plenum, 1973, p.405.
128. D. Bertolini, M. Cassettari and G. Salvetti, *J. Chem. Phys.* **78**, 365 (1983).
129. O. N. Awasthi and S. Sathish, *Ind. J. Pure Appl. Phys.* **16**, 489 (1978).
130. M. V. Smoluchowski, *Z. Phys. Chem.* **92**, 129 (1917).

131. P. Debye, *Trans. Electrochem. Soc.* **82**, 265 (1942).
132. J. B. Hubbard and L. Onsager, *J. Chem. Phys.* **67**, 4850 (1977).
133. S. M. S. Akhtar and G. R. Freeman, *J. Phys. Chem.* **75**, 2756 (1971).
134. M. Anbar and E. J. Hart, "The Hydrated Electron", John Wiley & Sons, Inc., N. Y., 1970.
135. M. Anbar and E. J. Hart, *ACS Adv. in Chem.* **81**, 79 (1968).
136. J. H. Baxendale, E. M. Fielden and J. P. Keene, *Proc. Roy. Soc.* **A286**, 320 (1965).
137. P. C. Senanayake, Ph.D. Thesis, University of Alberta, 1987.
138. A. Peiris and G. R. Freeman, unpublished results.
- 139a. A. Einstein, "Investigations on the Theory of Brownian Movement", Dover, New York, 1956, p.75.
- 139b. R. C. Reid, J. M. Prausnitz and T. K. Sherwood, "The Properties of Gases and Liquids", 3rd edition, McGraw-Hill, Inc., New York, 1977, p.575.
140. K. R. Harris and L. A. Woolf, *J. Chem. Soc., Faraday Trans. 1*, **76**, 377 (1980).
141. "International Critical Tables", Edited by E. W. Washburn, McGraw-Hill, New York, **3**, 1928, p.388.
142. R. W. Gallant, "Physical Properties of Hydrocarbons", **1**, Gulf Publishing Co., Huston, TX, 1968.
143. A. D'Aprano, D. I. Donato and V. Agrigento, *J. Sol. Chem.* **10**, 673 (1981).
144. P. Fowles, *Trans. Faraday Soc.* **67**, 428 (1971).
145. A. V. Rudnev, A. V. Vanikov and N. A. Bakh, *High Energy Chem. (Engl. Transl.)* **6**, 416 (1972).
146. A. V. Vannikov, E. I. Mal'tzev, V. I. Zolotarevsky and A. V. Rudnev, *Int. J. Radiat. Phys. Chem.* **4**, 135 (1972).
147. J. A. Riddick and C. Carr, *Ind. and Eng. Chem.* **43**, 69 (1951).



148. J. Timmermans, "Physico-Chemical Constants of Binary Mixtures", Interscience, New York, 4, 1960.
149. "Handbook of Chemistry and Physics", Edited by R. C. Weast and M. J. Astle, 59th Edition, CRC Press, Inc., Boca Raton, Florida, 1978.
150. S. Okazaki, K. Nakanishi and H. Touhara, J. Chem. Phys. 81, 890 (1984).
151. J. E. Desnoyers, Pure and Appl. Chem. 54, 1469 (1982).
152. K. Nakanishi, K. Ikari, S. Okazaki and H. Touhara, J. Chem. Phys. 80, 1956 (1984).
153. A. Huidt, R. Moss and G. Neilsen, Acta Chem. Scand., Ser B 32, 274 (1978).
154. D. Roberts, G. Person and J. E. Desnoyers, J. Sol. Chem. 9, 629 (1980).
155. K. H. Schmidt and W. L. Buck, Science, 151, 70 (1967).
156. I. Carmichael, J. Phys. Chem. 84, 1076 (1980).
157. "Physical Chemistry", K. J. Laidler and H. M. Meisser Eds., Benjamin/Cummings, California, 1982.
158. R. D. Nelson, D. R. Lide and A. A. Maryott, "Selected Values of Electric Dipole Moments for Molecules in the Gas Phase", NSRDS-NBS 10, U.S. Government Printing Office, Washington, D.C., 1967.
159. K. M. Idriss-ali and G. R. Freeman, Can. J. Chem. 62, 2217 (1984).
160. H. F. Hameka, G. W. Robinson and C. J. Marsden, J. Phys. Chem. 91, 3150 (1987).
161. F. Y. Jou and G. R. Freeman, J. Phys. Chem. 81, 909 (1977).
162. F. Y. Jou and G. R. Freeman, J. Phys. Chem. 83, 1979 (1979).
163. R. A. Marcus, J. Chem. Phys. 24, 966 (1956).
164. R. A. Marcus, J. Phys. Chem. 67, 853 (1963).
165. F. Buckley and A. A. Maryott, "Tables of Dielectric Dispersion Data for Pure Liquids and Dilute Solution", NBSC 589, U.S. Department of Commerce, Washington, D.C., 1958.